THE SHELL STRUCTURE AND MINERALOGY OF THE BIVALVIA

INTRODUCTION. NUCULACEA—TRIGONACEA

BY

JOHN DAVID TAYLOR
WILLIAM JAMES KENNEDY
ANTHONY HALL

29 Plates, 77 Text-figs.

BULLETIN OF
THE BRITISH MUSEUM (NATURAL HISTORY)
ZOOLOGY Supplement 3
LONDON: 1969

THE BULLETIN OF THE BRITISH MUSEUM (NATURAL HISTORY), *instituted in* 1949, *is issued in five series corresponding to the Departments of the Museum, and an Historical series.*

Parts will appear at irregular intervals as they become ready. Volumes will contain about three or four hundred pages, and will not necessarily be completed within one calendar year.

In 1965 *a separate supplementary series of longer papers was instituted, numbered serially for each Department.*

This paper is Supplement No. 3 *of the Zoology series. The abbreviated titles of periodicals cited follow those of the World List of Scientific Periodicals.*

World List abbreviation
Bull. Br. Mus. nat. Hist. (Zool.) Suppl.

TRUSTEES OF
THE BRITISH MUSEUM (NATURAL HISTORY)

Issued 18 *July*, 1969 *Price* £4 10s.

THE SHELL STRUCTURE AND MINERALOGY OF THE BIVALVIA

INTRODUCTION. NUCULACAE—TRIGONACAE

By J. D. TAYLOR, W. J. KENNEDY & A. HALL

CONTENTS

SYNOPSIS

The bivalve shell consists of two valves made of crystalline calcium carbonate with an organic matrix and an organic ligament. The whole shell is covered by an outer organic layer, the periostracum. All parts of the shell are secreted by epithelial cells of the mantle. These are joined to the shell only at the outer fold of the mantle, by the periostracum, and at the points of attachment of the pallial, adductor, pedal and other muscles. Except at these points, the calcium carbonate and organic matrix of the shell are deposited from a solution, situated in a cavity between the mantle and the shell and called the extrapallial fluid. Little is known of the composition and properties of this fluid, but all the inorganic and organic constituents of the shell must be secreted into it by the mantle cells. The periostracum is secreted at the extreme margin of the mantle and serves as a substrate for subsequent deposition of calcium carbonate and organic matrix. Under normal conditions of calcification two polymorphs of calcium carbonate, calcite and aragonite, may be deposited. Some species contain aragonite alone and others a combination of calcite and argonite. The two polymorphs always occur in discrete layers. The carbonate and organic matrix aggregate together into a number of distinct but regularly occurring structures recognisable throughout the class. The shell may consist of several layers each formed from one of these structures, as well as characteristic structures secreted beneath the various muscle attachment areas.

The main factor controlling the distribution of structural types is undoubtedly genetic. Factors controlling the mineralogy are poorly known. Each polymorph, however, always occurs in separate, structurally distinct layers, so that the two polymorphs are never intimately mixed with each other, although they may occur in different layers of the same shell. In *some* genera where both calcite and aragonite are secreted, the proportion of aragonite increases with increasing temperature. Seven basic shell structure types may be recognised:

Nacreous structure is always aragonitic, consisting of euhedral or rounded plates, which join to form sheets lying subparallel to the shell surface, or columns normal to the surface. These grow as a mosaic crystal by a combination of epitaxis and spiral growth.

Prismatic structure may be aragonitic or calcitic, and consists of polygonal columns of carbonate usually separated by organic matrix, developing in a manner similar to spherulitic growth.

Foliated structure is always calcitic and consists of euhedral laths joined laterally to form sheets that are in turn arranged in larger units lying subparallel to the shell interior. It develops by a process similar to dendritic growth in inorganic systems.

Crossed-lamellar structure is always aragonitic and is built up of needle-like laths, arranged in two interpenetrant blocks with opposing inclination relative to one another and to the shell surface.

Complex crossed-lamellar structure is also aragonitic, and is similar to the last, but the laths are arranged in four or more (possibly radial) directions.

Homogeneous structure is always aragonitic, consisting of minute carbonate granules, all with a similar crystallographic orientation.

Myostracal layers—associated with muscle attachment areas, are always aragonitic, with a characteristic irregular prismatic structure. They occur in most, if not all, bivalves.

The fibrous part of the ligament in many bivalves is calcified, invariably with aragonite. The aragonite is in the form of fine needles.

Many calcified structures show banding of several orders, both of seasonal and on a finer scale, perhaps of diurnal origin.

Many shells are perforated by minute cylindrical holes—tubules—lying normally to the shell interior, with indications of both syn- and post-depositional origins. Their fine structure has been elucidated by scanning electron microscopy, although their origin remains obscure.

Among extant forms, the Palaeotaxodonta are wholly aragonitic. The Nuculacea have an outer prismatic and inner and middle nacreous layers. The Nuculanacea have inner and outer homogeneous lyers.

The Cryptodont Solemyacea are wholly aragonitic, with a unique outer ' prismatic ' and inner ' homogeneous ' layer.

The Pteriomorphia are complex in mineralogy. The Arcoida are wholly aragonitic; both the Arcacea and Limopsacea have an outer crossed-lamellar and inner complex crossed-lamellar layer, sometimes with pillar-like extensions of the myostraca (myostracal pillars) extending through the inner layer to the inner shell surface. Within the Mytiloida, the Mytilacea may be wholly aragonitic with nacreous and complex-lamellar structures, or may contain finely prismatic calcitic layers; some forms are tubulate. In the Pinnacea there is an outer prismatic calcitic layer and distinct middle and inner nacreous layers. The extant group of the Pterioida, the Pteriacea, show a similar distribution of structures and mineralogy to the Pinnacea.

In the Pectinacea, the shells of the Pectinidae are built mostly of foliated calcitic structure. Some forms possess an aragonitic middle crossed-lamellar layer; aragonite is of course present as myostraca and in the calcified part of the ligament. In the Spondylidae and Plicatulidae there is an outer foliated calcitic layer and middle and inner aragonitic crossed-lamellar layers, with tubulation throughout. The Anomiacea are built largely of foliated calcite, with an inner aragonitic crossed-lamellar or complex crossed-lamellar layer in some species. In the oysters (Ostreina, Ostreacea) the shell is almost entirely of foliated calcite, with a prismatic calcitic layer on the upper valve of some species. Aragonite is confined to myostraca, ligament and prodissoconch.

The Palaeoheterodonta are wholly aragonitic. The extant group of Unionoida, the Unionacea, have an outer prismatic layer and middle and inner nacreous layers. The cemented Etheriidae differ from them in lacking an outer prismatic layer. The extant group of Trigonoida, the Trigonacea, have an outer prismatic and middle and inner nacreous layers.

INTRODUCTION

Purpose

THE purpose of this work is to redefine the shell-structure types present in the Bivalvia, and to describe their mineralogy and distribution within the class. Standard palaeontological and zoological texts state that shells generally consist

of an outer prismatic layer and an inner nacreous, or lamellar layer (Moore *et al.* 1952 : 402 ; see also Shrock and Twenhofel 1953, Easton 1960, Buchsbaum 1951, Borradaile *et al.* 1963, Manigault 1960 etc.). This is an infrequent arrangement in bivalves, but even experienced molluscan workers have repeated this error. We hope to remedy this here.

In this account, mineralogical determinations have been carried out by Hall, sampling, optical and electron microscopy by Taylor and Kennedy, systematic determinations by Taylor, and final preparation of manuscript by Kennedy.

Historical

Early literature on shell structure and mineralogy of bivalves is extensive, and is listed and reviewed by Schenk (1934). Two workers in the third and fourth decades of this century made fundamental advances : Schmidt (1921–1925) and Bøggild (1930). Schmidt's unsurpassed light microscopy elucidated many details only recently redefined by electron microscopy. Bøggild, who was strictly a mineralogist, presented the first comprehensive summary of shell structure types, their mineralogy and distribution in bivalves and other molluscs. His work has been taken as the standard by many later workers (Deer *et al.* 1962, MacKay 1952, Barker 1964, Oberling 1964, MacClintock 1963, 1967, etc.). Unfortunately material supplied to Bøggild was misidentified in some cases, whilst the classification used (Zittel 1915) is now unacceptable. Bøggild used much fossil material which led to confusion due to problems of generic identification. In spite of these minor points, his is a classic piece of research.

The next major advances came from the use of electron microscopy, i.e. Grégoire *et al.* (1955), Grégoire (1957, 1959, 1960, 1961a, 1961b, 1967, etc.), Watabe (1955), Watabe and Wada (1956), Wada (1957, 1958, 1959, 1960a, b, 1961a, b, 1963d), Tsuji (1960), I. Kobayashi (1962), studies by Wilbur and his associates (references in Wilbur, 1964, see also below), Hare (in Degens 1965), Hubendick (1958) and Hudson (1968). Only a limited number of species and structures have so far been studied, the literature is dispersed, and the present knowledge of ultrastructure is still inadequate.

Oberling (1964) presents a list of microstructure distributions within the Bivalvia. Works by MacKay (1952) and Kado (1953) are based on rather limited data. MacClintock (1967) in a study of patelloid and bellerophontid archaeogastropods, (at optical level) has made observations on the shell structure types discussed below.

Methods

Mineralogy. During the present investigation we have made over 600 mineralogical determinations on shell layers and associated calcified structures, using standard X-ray diffractometer and powder photograph techniques.

Structure

1. Optical work. About 1000 acetate peels of surfaces and polished and etched sections (at various orientations) have been examined ; the techniques used are

reviewed by Kummel and Raup (1965). The length of the etching period and the concentration of the acid (usually dilute HCl) necessary to produce satisfactory peels vary between groups, apparently depending on the amount and distribution of organic matter in the shell. Acetate peels are more satisfactory for the identification of structural types than thin sections, but a limited number of these were also examined to study crystal optics and to elucidate poorly calcified and uncalcified structures. Surfaces and fractured sections of a large number of the species studied have also been examined.

2. Electron microscopy. Replicas of shell surfaces, fractured sections and polished and etched sections were prepared, using the Formvar two-stage or carbon single-stage methods (Kaye 1961). The replicas were shaded with gold/palladium or carbon, and examined with A.E.I., E.M. 6B, Phillips E.M. 75 and Akashi Tronoscope T.R.R. 50 microscopes. Specimens have also been examined using a Cambridge Instrument Company Scanning electron microscope.

THE BIVALVE SHELL

Introduction. Each valve of the bivalve shell grows as a close approximation to a logarithmic spiral (Raup 1966), and consists of a thin outer organic (' conchiolin ') layer, the periostracum, and within this the calcified shell. Both are secreted externally by the mantle, which is an enveloping outer fold of the tissues of the animal. The calcified shell consists of crystals of calcium carbonate in an organic matrix ; these crystals form a limited number of basic shell structure types that recur throughout the Bivalvia (and other molluscs). The calcified part of the shell consists of two or three discrete layers (see below) of these structures. A further characteristic crystalline aggregate is laid down beneath the muscle attachments to the shell.

Nomenclature

In naming the shell layers we speak of *inner, middle* and *outer* shell layers, these terms being simple and unambiguous. As entirely topographical divisions they imply no homology between groups.

The shell layer names introduced by Oberling (1964) are unduly complicated and carry questionable implications of homology. Oberling's scheme is summarised below.

Palliostracum	Periostracum		
	Ectostracum		Mesectostracum
	Mesostracum		Mesendostracum
	Endostracum		

We regard the word *Palliostracum*, which is synonymous with the word ' shell ' as unnecessary. The term *Periostracum* for the outermost conchiolin shell layer is well known and unambiguous ; *Ectostracum* is the outer major calcareous shell layer, *Mesostracum* the middle shell layer between ectostracum and the trace of the pallial line, *Endostracum* the innermost shell layer, bounded by the pallial trace.

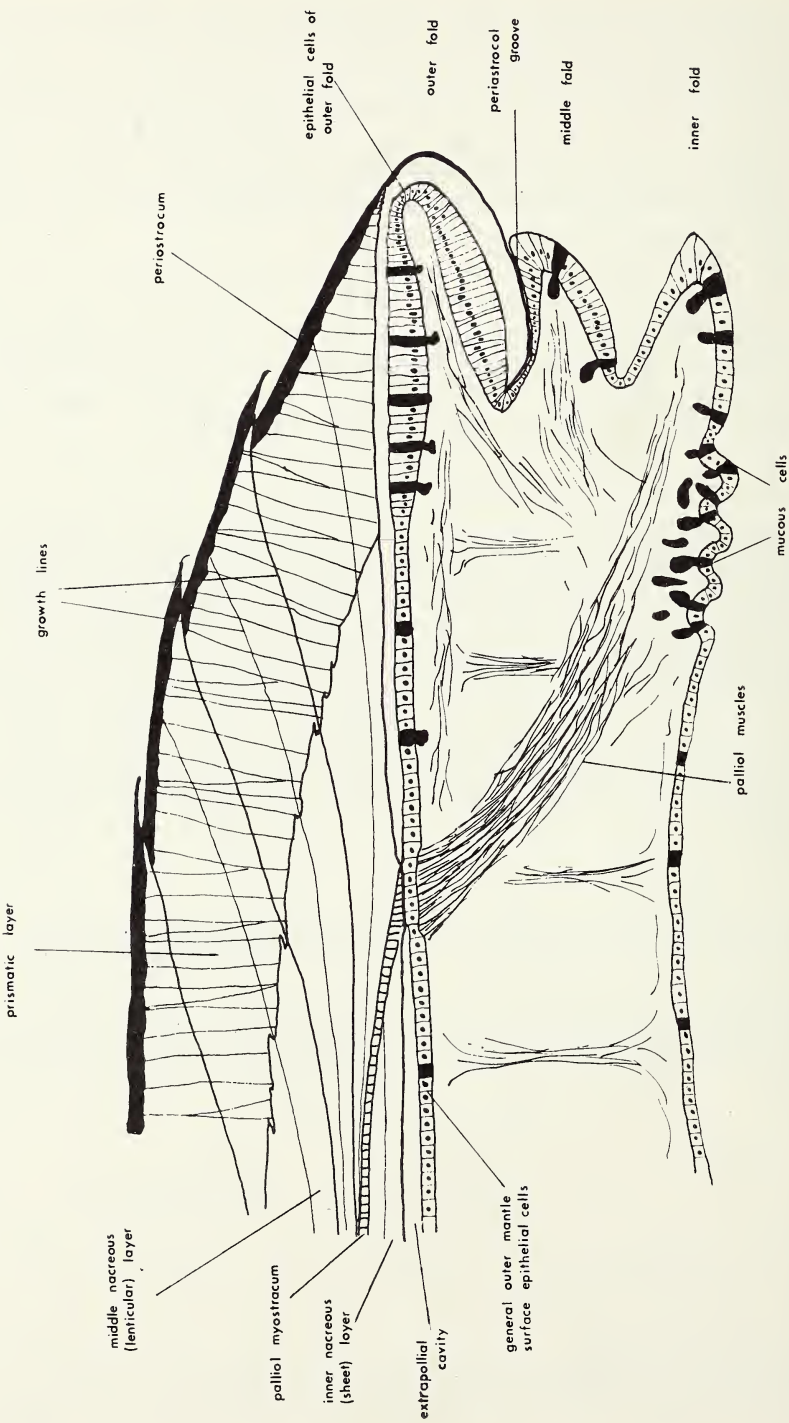

FIG. 1. Diagram of shell/mantle relations in the marginal region of *Anodonta cygnea* as seen in radial section, based on Beedham (1958a) with additions.

The terms *Mesendostracum* and *Mesectostracum* for combined layers are misleading. They imply homology of layers in various groups, and suggest that combination from an originally three-layered shell has taken place. Oberling's use of the term *Myostracum* for the calcareous deposits secreted beneath muscle attachment areas is preferable to the older use of such terms as ' hypostracum ' or ' Helleschicht '.

Numerous other terms for shell layers (listed in Oberling 1964), are ambiguous and superfluous and are rejected.

MacClintock (1962, 1967) has suggested that in gastropods the pallial myostracum be used as a datum for naming shell layers. We have not applied this usage to bivalves, as in the monomyarian Anomiacea, Ostreacea, Limacea and Pectinacea, pallial attachment is secondary, so that the homology of this position of the myostracum in the layers is uncertain.

Shell formation

Unlike some other phyla (Brachiopoda, Arthropoda), secretory cells of the molluscan epithelium producing the shell material are not in direct contact with the shell except at muscle attachment areas and in the periostracal groove (text fig. 1). Both carbonate and organic matrix are formed in a thin layer of *extrapallial fluid*, contained within the *extrapallial cavity*, between shell and mantle.

The components for shell formation are secreted into the extrapallial fluid from the mantle by the epithelial cells. The physico-chemical characteristics and composition of the fluid probably define the nature of the organic matrix, and the calcium carbonate polymorph deposited (Wilbur 1964). There is good evidence (based on regeneration studies) that organic matrix acts in the nucleation of calcium carbonate, and that the periostracum acts as the original support for both organic matrix and carbonate. However, the structural types developed in the calcareous parts of the shell show such a remarkable similarity to growth forms in inorganic systems that, beyond nucleation, the organic matrix may well behave passively during calcification.

Extrapallial fluid

Relatively little work has been done on the composition or physico-chemical properties of the extrapallial fluid of bivalves, and no distinction has previously been made between regions of the extrapallial cavity. In most bivalves, two regions of the cavity can, however, be recognised, an inner and an outer separated by the pallial line. Observations suggest that in forms where pallial attachment is secondary, or is well within the shell margins allowing deep withdrawal of the mantle (Pectinacea, Ostreacea, Pinnacea) extensive withdrawals of the mantle edge would sever the contact in the periostracal grooves so that the outer region of the extrapallial cavity would appear to come into direct contact with the water surrounding the shell. Simkiss (1965) has suggested that the extrapallial fluid of *Crassostrea virginica* is sea-water modified by mantle products, and that it is continuous with the surrounding seawater. However, Korringa (1951) has shown that active mantle movement and withdrawal in *Ostrea* may occur without severing the mantle from the thin elastic periostracum.

Electrophoretic studies on the protein content of extrapallial fluid by S. Kobayashi (1964) in eleven bivalve species show that where the shell is almost wholly calcitic the fluid contains only one protein fraction, but where the shell is of aragonite, or aragonite and calcite, three distinct protein fractions are present ; the blood of those species examined also contained mucopolysaccharides. The presence of mucopolysaccharides in shell matrix and regeneration products of bivalves (for references see Wilbur 1964 : 251) suggests that these too occur in the fluid.

De Waele (1930) records sodium, potassium, calcium, magnesium, manganese, chloride, sulphate and phosphate ions in both the blood and extrapallial fluid of *Anodonta cygnea*, in comparable amounts in each. S. Kobayashi (1961) records similar concentrations of calcium in both the blood and extrapallial fluid of *Chlamys nipponensis*.

Determinations of the pH of the fluid made by several workers range from pH 7·0 to pH 8·35, varying with method, time of sample, and interval between sampling and measurement. Watabe and Kobayashi (in Wilbur 1964) found that the summer values for *Mercenaria mercenaria* were 0·4 pH units in excess of the winter figure (water temperatures 2° and 9°C respectively). Wada (1961b) has found in *Pinctada martensii* that during the period of maximum shell deposition, pH increases as the concentration of calcium ions decreases, and that this inverse relationship extends to daily and seasonal changes in calcium metabolism.

Etching of inner surfaces of shells during hibernation and starvation, when carbonate secretion ceases, may be due to acidic conditions in the fluid.

Mantle

In bivalves the mantle edge is divided into three folds—an inner muscular, a middle sensory and an outer secretory fold (text fig. 1, Plate 4, fig. 3). Shell secretion begins with the formation of the periostracum by the epithelial cells on the inner side of the outer mantle fold, in the groove lying between the middle and outer folds. The first calcareous material is laid down from the epithelial cells of the outer part of the outer fold. The rest of the shell is laid down by the cells of the general outer surface of the mantle. Trueman (1949), Yonge (1953), Beedham (1958a), Dunachie (1963) and Kawaguti and Ikemoto (1962b) have all shown that the cells in these various parts of the outer mantle vary in shape and structure, and differ in histochemical properties (Beedham 1958a). All studies indicate that cells secreting the periostracum and outer layer are tall and slender, while those of the general outer surface of the mantle tend to be broad and short. The electron microscope work of Kawaguti and Ikemoto (1962a) on *Fabulina* shows that three types of cell are present, but intermediate forms exist between the types. Evidence suggests that there is a generative zone at the inner part of the periostracal groove, and cells produced there migrate around the mantle edge, changing their shape, chemistry and function as they do so. Each cell in turn secretes periostracum, outer shell layer, and middle shell layer in succession, becomes an attachment area at the pallial line, and then secretes inner shell layer, perhaps finally becoming adductor muscle attachment.

The periostracal, outer and inner layers of the ligament in bivalves are derivatives of the same regions of the mantle as the corresponding shell layers (Owen, Trueman and Yonge 1953). The cells of the epithelial region which secrete the inner and outer layers of the ligament, show different morphologies, sometimes paralleling those seen in cells secreting the rest of the shell. In *Anodonta cygnea* (Beedham 1958a) the cells beneath the inner layer of the ligament are short, with distally situated nuclei, while those beneath the outer layer are tall, with proximal nuclei, although similar in general appearance to the remainder of the mantle cells.

Periostracum

The outermost layer of the shell is the thin, entirely organic periostracum, which consists of quinone-tanned protein (Beedham 1958b, Degens *et al.* 1967). General reviews on the formation of the periostracum have been given by Haas (1929–1935) and Kessel (1944). In species where it has been investigated in detail, the periostracum may consist of several layers. Thus there are two layers in *Fabulina nitidula* (Kawaguti and Ikemoto 1962b), three layers in *Mytilus edulis* (Dunachie 1963), and four layers in *Solemya parkinsoni* (Beedham and Owen 1965). These layers differ in their structure and/or staining properties. The first, outer layer is laid down at the extreme base of the periostracal groove, and the other layers are secreted, in turn, along the inner edge of the outer mantle fold. In *Mytilus edulis*, as the outer periostracal layer is secreted it becomes temporarily attached to the outer surface of the middle mantle fold by adhesive epithelia, and blood pressure in the haemocoele of the outer mantle fold holds the secreting epithelium tight against the periostracum (Dunachie 1963).

Degens *et al.* (1967) have analysed the amino acid content of the periostracum in eight species of bivalves, and find that the same amino acid groups are present as in the organic matrix of the calcified shell, but that the relationship of the groups to each other is different. They consider that the purpose of the quinone tanning is to provide a rapid turnover from a soluble to an insoluble protein. Hare (1963) analysed the amino acids in *Mytilus californianus* and found that while similar amino acids were found in the periostracum as in the rest of the shell, the ratio of acidic to basic amino acids was low. This is apparently a characteristic of non-calcified components.

The periostracum plays a very important role in subsequent shell deposition ; it acts as the support and substrate for the initial nucleation and crystal growth of the outer shell layer, which is secreted by the outer surface of the outer mantle fold. Thus in *Anodonta cygnea*, rounded and sometimes polygonal spherules are seen in apparently random orientation upon the periostracum. These gradually grow together, forming the prismatic layer (text fig. 2). In some Unionacea and Trigonacea small bosses may be seen at the outer end of fully grown prisms, separated from each other by a conchiolin wall apparently continuous with the periostracum. These small bosses mark the site of original spherulite development (Plate 31, fig. 1).

The periostracum also has a protective function, especially in preventing the corrosion of the calcified shell by acidic waters, it is thick in freshwater forms,

those living in acidic interstitial waters and those secreting acid as an aid to rock borings.

In the Ostreacea, Pectinacea, Limacea and Anomiacea, where the structural changes associated with monomyarianism have resulted in pallial attachment being secondary, the mantle/periostracum contact is tenuous, and the periostracum thin and inconspicuous, as for example in *Ostrea edulis* (Korringa 1951).

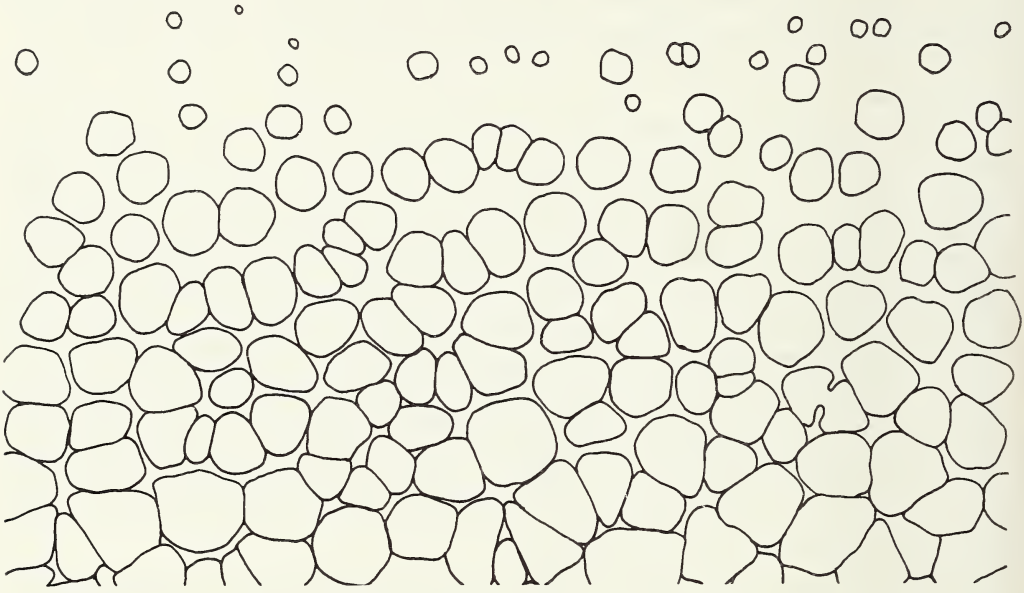

FIG. 2. Early stages of the formation of the outer prismatic layer on the inner surface of the periostracum at the shell margin of *Anodonta cygnea*. ×225.

The Organic Matrix

Grégoire (1955, 1957, 1961a & b, 1962) and Watabe (1965) have shown that the calcified crystalline components of the shell structures so far studied are intimately associated with a proteinaceous organic matrix. This usually consists of a " lace like " network structure which surrounds the crystals, is present within the crystals, and forms layers which alternate with crystal layers. Crystals of calcium carbonate are situated *within* and *upon* the organic matrix. Several workers have suggested that the organic matrix may influence crystal type, mineralogy, and orientation of the mineralised layers (Roche *et al.* 1951, Ranson 1952, Watabe and Wilbur 1960, Wilbur and Watabe 1963, Degens *et al.* 1967, Wada 1961b etc.). Although the actual process of mineralisation is poorly understood, any theory of calcification has to take into account the contemporaneous formation of the matrix. Watabe (1965) found in the nacreous layer of certain bivalves that even individual crystals had an *intracrystalline* matrix of organic fibrils, oriented in the same directions as the crystal axes (Towe and Hamilton 1968 have recently disputed this). The morphology of the organic matrix has only been studied in detail in nacreous,

prismatic and foliated structures, and is discussed under these headings below, together with further observations of our own in these and other types of shell structure.

Amino acid determinations on the organic matrices of individual molluscan shells have been made by Beedham (1958b), Tanaka *et al.* (1960), Hare (1963), Hare and Abelson (1964, 1965), Stegeman (1961, 1963) and Degens *et al.* (1967), who showed that organic matrices closely resemble the keratin-myosin-epidermin-fibrin group of proteins. They considered that the independent existence of basic amino acids was a crucial factor in the nucleation of the mineral phase, and demonstrate that shell proteins of each species react differently to environmental factors such as temperature and salinity.

Hare (1963) considered that certain side chains in the protein matrix may concentrate Ca^{++} and CO_3^{--} ions in specific positions, and thus provide an initial concentration of these ions prior to calcification. His view that aspartic and glutamic acid side chains attract Ca^{++} ions while basic chains attract carbonate or bicarbonate ions is supported by Degens *et al.* (1967).

Mineralogy

The mineralogy of bivalve shells is fairly well known, although no comprehensive modern survey has been produced. Limited determinations were given by early workers e.g. Carpenter (1844, 1848), Sorby (1879), Cornish and Kendall (1888), Kelly (1901), Loppens (1920) etc., and these were summarised and expanded by Bøggild (1930). Subsequent workers—Stolkowski (1951), MacKay (1952), Lowenstam (1954a, b, 1963, 1964), Chave (1954), Togari and Togari (1959), Turekian and Armstrong (1960), Wada (1961b), Dodd (1963, 1964), Keith, Anderson and Eichler (1964)—have used the only reliable technique : X-ray diffraction. None of these authors, however, approaches the degree of thoroughness of Bøggild's classic research.

Aragonite and calcite dominate bivalve shell mineralogy. They occur together consistently in the superfamilies Mytilacea, Pinnacea, Pteriacea, Pectinacea, Limacea and Ostreacea of the subclass Pteriomorphia, the remaining two superfamilies of this subclass, the Arcacea and Limopsacea being wholly aragonitic. The calcite and aragonite always occur in separate layers.

Calcite also appears in the shells of two heterodont superfamilies. Thus in the extant superfamily Chamacea we have found calcite in appreciable amounts in a single species, *Chama pellucida*, confirming Lowenstam's (1954b, 1963, 1964) determination. Lowenstam (1954) also reported calcite in *Chama semipurpurata*, in which, however, it forms only 4% of the shell and is possibly contamination. Aragonite and calcite also occurred together in shells of the extinct superfamily Hippuritacea—the rudists (Kennedy and Taylor 1968).

In the subclasses Palaeotaxodonta, Cryptodonta, Palaeoheterodonta and Anomalodesmata the shell is wholly aragonitic.

Some simple conclusions may be drawn on the occurrence of calcite. Calcite layers are generally outermost, and occur only in the subclass Pteriomorphia

(excepting the Arcacea and Limopsacea), and in the Chamacea and the extinct Hippuritacea. All these groups are epifaunal.

No bivalves are known with a shell wholly of calcite. The oysters, formerly regarded as such, have been shown to possess an aragonitic adductor myostracum and inner ligament (Stenzel 1962, 1963, confirmed here) and an aragonitic prodissoconch (Stenzel 1964).

Several other mineral species are known to occur in mollusc shells. Vaterite has been reported from regenerating shells of *Helix* (Mayer and Weineck 1932, Stolkowski 1951), *Viviparus intertexus* (Wilbur and Watabe 1963, Wilbur 1964) and *Elliptio complanatus* (Wilbur and Watabe 1963). However, the process of regeneration, discussed at length by Wilbur (1964), represents atypical calcification. *Viviparus*, normally wholly aragonitic, produces all three calcium carbonate polymorphs during regeneration, *Crassostrea*, usually largely calcitic, produces appreciable amounts of aragonite. Watabe (1956) and Wada (1961b) have also recorded dahllite from the prodissoconch I of *Pinctada martensi*. It is clear that the prodissoconch may differ considerably from the rest of the shell, as in *Ostrea* referred to above.

The factors controlling shell mineralogy are poorly understood, but three principal factors have been considered as influential : the organic matrix of the skeletal carbonate, the temperature during growth, and the salinity of water in which the bivalves live.

The possibility that the organic matrix may influence the polymorph of calcium carbonate deposited has been considered by many workers, and is strongly suggested by the recognition of differences in amino acid contents between aragonitic and calcitic shell layers, or aragonitic and largely calcitic species, (Roche *et al.* 1951, Tanaka *et al.* 1960, Hare 1963). The most direct evidence is seen in the influence of decalcified organic matrix on calcification under experimental conditions. When such matrix is inserted into the region between the mantle and shell of a bivalve it often induces crystallisation of a different form of calcium carbonate in that region to the normal crystal type formed *in vitro* (Watabe and Wilbur 1960, Wilbur and Watabe 1963, Wilbur 1964). Thus the organic matrix from *Elliptio* and the aragonitic layers of *Atrina* and *Pinctada* induce aragonite precipitation in aqueous solutions of calcium bicarbonate, whilst decalcified matrix from the prismatic layer of *Pinctada* produces calcite. Again, decalcified organic matrix from aragonitic shell when inserted between the mantle and calcite shell of *Crassostrea* induced aragonite deposition in 25% of the experiments. In criticism of this work Simkiss (1964, 1965) considered that natural water contains ions which not only favour formation of aragonite, but inhibit calcium carbonate precipitation as a whole. The influence of organic substances, including amino acids, on the precipitation of calcium carbonate polymorphs from aqueous solution has also been investigated experimentally by Kitano and Hood (1965).

The effect of temperature (at normal salinities) on the aragonite-calcite ratio of species secreting both minerals is clear from the work of Lowenstam (1954a, b ; 1964) and Wilbur and Watabe (1963). Lowenstam's work indicated that in families in which aragonite and calcite occur together, species living in warmer waters have a

higher aragonite content than those living in temperate conditions. The interpretation of Lowenstam's results requires caution, because in bivalves secreting both calcite and aragonite the two polymorphs are confined to different shell layers, and the proportions of these layers vary from species to species within a genus, and perhaps also with the age of the individual. Lowenstam's data for the mytilid '*Volsella*' (= *Modiolus*) can be disputed, as they relate to 3–4 species, varying in weight from 2·63–24·49 gms., with differences in aragonite content of 18%. Similar criticisms can be made of his data for *Pinna, Pteria, Lima, Anomia* and *Pecten*. (The last example was however, the subject of qualification in his 1964 paper.) In some cases minimum differences in aragonite : calcite ratios are of the order of 2%, while shell weights differ by factors of up to ten. An assemblage of *Pedalion* from a single locality varied by up to 30% in aragonite content (in part a result of size differences). The more recent work of Dodd (1963) has provided indisputable evidence of this temperature effect in *Mytilus californianus* populations, but only in individuals more than 15 mm. long ; it appears true, however, that tropical species of *Mytilus* are wholly aragonitic whereas temperate forms may contain calcite (J. D. Hudson, personal communication ; this paper, table 6). The degree to which calcite-aragonite ratios may vary in one family is shown in text figs. 55–57 which show the great differences in extent of the inner aragonite layer of the three genera *Pinna, Atrina*,and *Streptopinna* which can all occur at the same locality (see also page 86).

With regard to salinity, Lowenstam (1954b) with samples from the Baltic, and Dodd (1963, 1966a) with material from Washington (U.S.A.) present evidence that the percentage of aragonite in *Mytilus edulis* shells increases with decreasing salinity, as well as varying with temperature. Eisma (1966) on the basis of samples from the Dutch coast has demonstrated that in this region at least, there is no such relationship. Furthermore, he disputes the work of Lowenstam and Dodd, suggesting that the observed variation can be explained as a temperature effect. More work is needed, with growth of populations under controlled salinity-temperature conditions (in progress ; Dodd 1966a), and better documentation of the change in conditions experienced by individuals under natural conditions. The views of Togari and Togari (1959) are based on a limited and biased sample and do not withstand examination.

The calcium carbonate of bivalve shells invariably contains small amounts of trace elements isomorphously replacing calcium, particularly magnesium and strontium. The abundance of these and other trace elements in mollusc shells has been the subject of many investigations, the results of which have been summarised in standard works by Clarke and Wheeler (1922) and Vinogradov (1953). More recent studies include those by Chave (1954), Turekian and Armstrong (1960), Leutwein and Waskowiak (1962), Leutwein (1963), Lowenstam (1964), and Waskowiak (1962), the latter being particularly comprehensive. The trace element contents of shells, like the calcite-aragonite ratios, have been shown to vary with environmental conditions such as temperature and salinity (Chave 1954, Lowenstam 1964, Dodd 1965, Lerman 1965b).

The distribution of trace elements between coexisting calcite and aragonite in shells has been discussed by Lowenstam (1964). In general, magnesium is concentrated in calcitic shell layers and strontium in aragonitic layers.

The distribution of strontium between aragonite and calcite layers is variable, but less so than that of magnesium. This is probably explained by the fact that the Bivalvia show a strong physiologically determined discrimination against strontium relative to calcium in comparison with sea water (Odum 1951, Lerman 1965a).

The isotopic composition of carbon and oxygen in the shells of Bivalvia and other molluscs has been studied by Epstein and Lowenstam (1953), Keith, Anderson and Eichler (1964), Lloyd (1964), and Keith and Parker (1965). It has been found that C^{14} and O^{18} contents show appreciable variations which can be related to both temperature and salinity, as well as to additional factors such as diet. Keith, Anderson and Eichler found differences in isotopic composition between different shell layers, both in wholly aragonitic shells and in those containing both aragonite and calcite.

Mineralisation

During shell growth, the formation of the periostracum provides a substrate upon which deposition of the organic and inorganic constituents of the outer mineralised layers of the shell can take place. No data are available on the earliest stages of normal shell deposition, and the exact sequence of events at initiation is unknown. For instance it is not known whether the organic matrix is laid down on the periostracum before, or contemporaneously with the calcium carbonate.

Mineralisation can be divided into two related but different processes : firstly, *nucleation* ; and secondly, *subsequent crystal growth* (Glimcher 1960, Grigorev 1965).

Nucleation may be either : (1) *homogeneous*—where a new phase is formed in the absence of foreign inclusions by the spontaneous precipitation of carbonate from a supersaturated medium, sites of deposition being controlled only by local fluctuations in the concentrations of calcium and carbonate ions ; or (2) *heterogeneous*—where the introduction of foreign inclusions induces deposition of a crystalline phase. In vertebrate tissues the latter process is widely held to occur (Glimcher 1960, with references), and similar processes are thought to operate in molluscs (Wilbur 1964, etc.), with the organic matrix acting as a template for calcification.

The first step in mineralisation is that calcium ions, or compounds, are attracted to specific areas of the organic matrix, from which the embryo crystals develop. A number of agents have been thought to operate as nucleation sites. Wada (1964a–j, etc.) has suggested that certain acid mucopolysaccharides, bound with specific regions of amino acid side-groups in conchiolin protein, may offer appropriate sites. Hare (1963) and Degens *et al.* (1967), consider that certain side-groups in the protein matrix may concentrate Ca^{++} and CO_3^{--} in specific positions on the matrix, i.e. the aspartic and glutamic acid side chains attract calcium ions while the basic side chains attract carbonate or bicarbonate ions. Crystal growth after this, and the

subsequent development of the various shell structures are discussed below in relation to our observations on the morphology of shell structure types.

Metabolic aspects of shell formation are discussed at some length by Wilbur (1964) and Wilbur and Owen (1964). Work with Ca^{45} isotopes, particularly autoradiography, has given direct evidence of the path of calcium from uptake to deposition (Wada 1964d).

Regeneration

Although an atypical calcification process, notes on regeneration of the shell in molluscs are included here as they are the only available source of information on the early stages of mineralisation. Most of the work has been on terrestrial gastropods (Abolinš-Krogis 1958–1963, etc.). Recent work on bivalves is limited to that of Wilbur and Watabe (1963), Wada (1960b, 1961b, 1964b, g, h, j), Beedham (1965) and Kawaguti and Ikemoto (1962c).

After damage, mantle cells show the same sequences of morphological development and secretory activity as occur during normal shell formation at the mantle edge. Thus they first produce periostracum and then the normal sequence of shell-layers, often repeating this several times, until the damage is repaired, and the stimulus removed (Beedham 1965, fig. 3). We have seen similar, repeated sequences of shell layers in a number of naturally damaged shells of several superfamilies indicating great plasticity in function of mantle epithelial cells. A similar sequence is seen in pearl formation, where concentric periostracum-like conchiolin, prismatic and nacreous layers, often repeated several times, are deposited around the nucleus (Haas 1929–1935, Wada 1957 etc.).

Closely related to regeneration studies are the works of Wada (1961b, 1964b, c, h, j) on organic and inorganic deposition on glass slips inserted between the shell and mantle, or of mantle grafts sandwiched between glass slips, inserted into the adductor muscle of another individual of the same species. This work has been largely carried out on the pearl oyster, *Pinctada*.

Grafted tissues are reported to produce the same shell structure as that normally produced in the area they were taken from (Wada 1961b ; 718). Where nacre is being formed, there is said to be a parallelism between growth of grafted tissues, structure of the fenestrated sheets of organic matrix, and crystal orientation (Wada 1960b, 1961b ; 735, figs. 58, 59, 60).

The regeneration process, although important for the understanding of shell growth, is atypical. Products differ in mineralogy from those of normal growth. Also, workers on regeneration suggest that organic granules are important in calcification, whereas those studying normal shell growth stress the importance of organic matrix.

NACREOUS STRUCTURE

Plate 1, figs. 1–4 ; Pl. 2, figs. 1–4 ; Pl. 3, figs. 1–4 ; Pl. 4, figs. 4–5 ; Pl. 5, fig. 1 ; Pl. 7, figs. 2, 3, 4, 5 ; Pl. 8, fig. 2 ; Pl. 10, figs. 2, 3, 4 ; Pl. 11, fig. 5 ; text-figs. 3–13.

This is the best known and most widely studied shell structure. It is present in the Nuculacea, Mytilacea, Pinnacea, Pteriacea, Unionacea, Trigonacea, Pandoracea and Pholadomyacea. It is invariably aragonitic.

We have examined the fine structure of nacre in *Pinctada margaritifera, Nucula sulcata, Andonta cygnea, Margaritifera margaritifera, Quadrula metanevra, Potamides littoralis, Neotrigonia margaritacea, N. dubia, Inoceramus concentricus* (Cretaceous, Albian, Gault Clay), *Modiolus auriculatus, Stavelia horrida, Chamostrea albida* and *Anantina hispidula.*

As an introduction it will be convenient to summarise the organic matrix/calcium carbonate relationships, based on a study of surfaces and sections, both etched and unetched, and of decalcified thin sections (Grégoire 1957, 1959, 1962 ; Grégoire *et al.* 1955 ; Wada, mainly 1961b ; Watabe 1963, 1965 ; and our own work).

Layers of tablets are separated by an *interlamellar* organic matrix of fenestrate sheets (text-fig. 3). These sheets are made up of irregular beaded and tuberculate cords or trabeculae (Grégoire *et al.* 1955 etc.) (Plate 3, fig. 1). The pattern of perforations is distinctive for each of the molluscan classes so far studied (Bivalvia, Gastropoda, Cephalopoda).

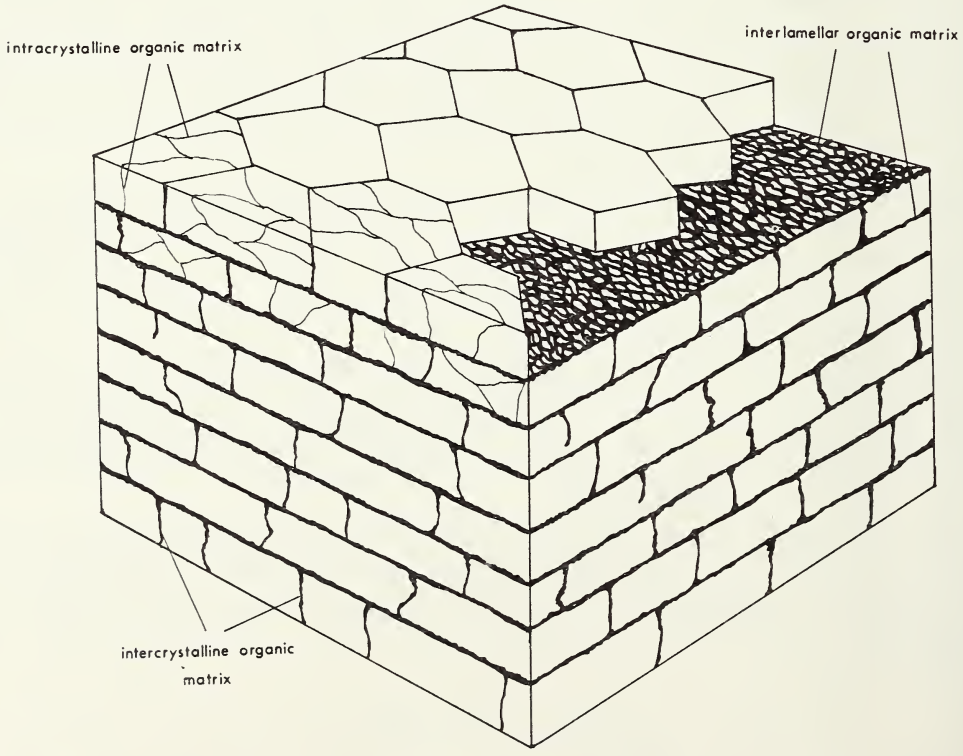

Fig. 3. Block diagram of carbonate and organic matrix relations in nacreous structure. ×10,000.

In bivalves the trabeculae are more slender and twisted than in the other classes, whilst the openings are irregular, smaller and unequally dispersed in the sheets (Grégoire 1959 : 4–5). In sections, the interlamellar matrix appears as straight bands, running between layers of nacre tablets, and varying in thickness from 0·02–0·3 microns (Wada 1961b, Watabe 1965). Fine structure is sometimes visible in these bands (Watabe 1965, figs. 5b, 9), and indicates that they are built up of fibrils 100–200 A in diameter, helically coiled, and arranged in bundles about 15000 A in diameter. Discontinuities and thickenings seen in sections represent the tubercles and perforations of the sheet as a whole.

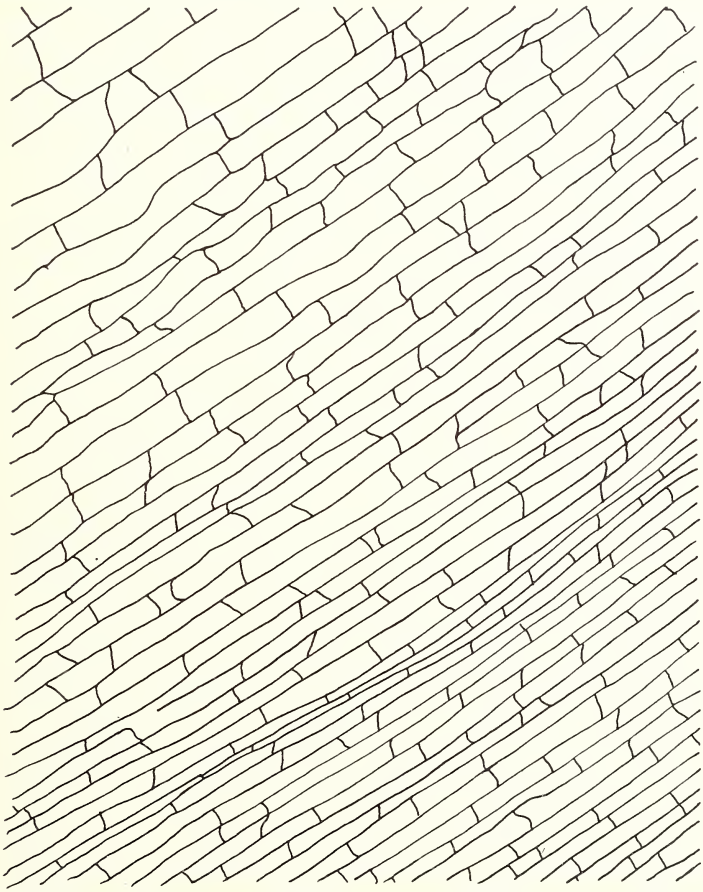

Fig. 4. Section of the middle nacreous layer of *Quadrula metanevra* showing a part of the cyclical changes in the thickness of the sheets of nacre tablets. (Based on an electron micrograph of an etched, radial section shell interior towards the bottom of the diagram.) ×3000.

Individual nacre tablets are separated and surrounded by an envelope of *intercrystalline* organic matrix, 300–1,000 A thick. This has a structure which is comparable to that of the *interlamellar* matrix, being built up of fibrils 100–200 A in

diameter, again helically coiled. The intercrystalline matrix appears in sections as vertical or diagonal bands running between the bands of *interlamellar* matrix. On the upper (001) and lower (00$\bar{1}$) surfaces of the nacre tablets, the interlamellar and intercrystalline matrices are sometimes distinct from each other, but usually cannot be separated. Plate 1, fig. 4 shows the normal appearance of replicas of sections of heavily decalcified nacre.

Each nacre tablet or crystal is made up of smaller blocks, each surrounded by *intracrystalline* matrix resembling the intercrystalline matrix in thickness and general structure, while further intracrystalline matrix is present within these smaller blocks.

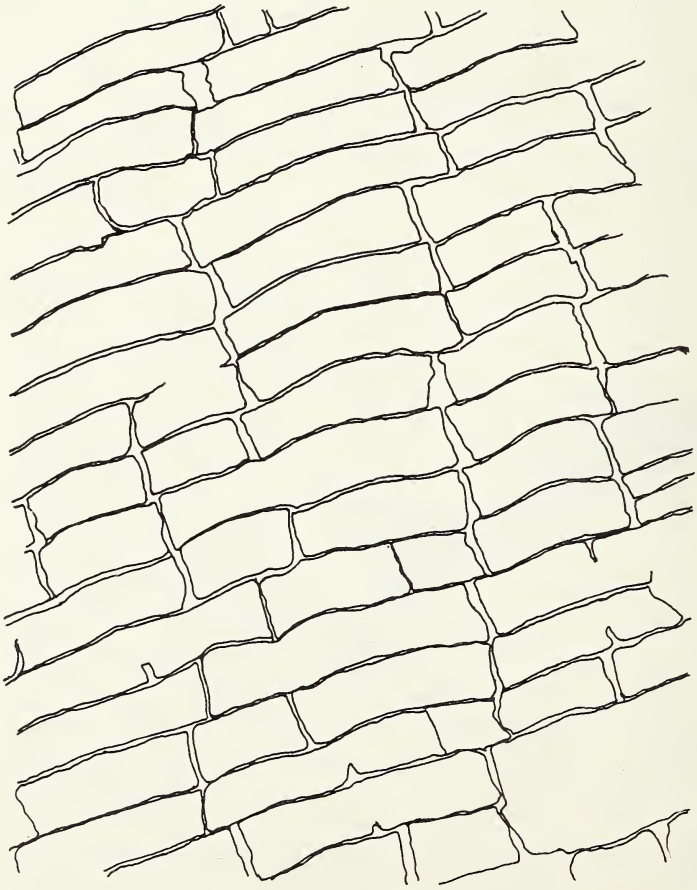

FIG. 5. Section of lenticular nacre in the middle shell layer of *Quadrula metanevra* showing the prominent columnar arrangement of the tablets. The irregular variation in the thickness of nacre tablets and the curvature of individual tablets is quite different from that seen in sheet nacre. The continuity of tablets in adjacent layers may indicate sites of screw dislocations. (Based on an electron micrograph of an etched, radial, section.) ×4500.

Towe and Hamilton (1968) have criticised the work of Watabe (1965), disputing his evidence for the presence of intracrystalline organic matrix within nacre tablets. Further work is needed to reconcile these opposing views.

Two distinct types of nacre can be recognised at optical and electron microscope level : *sheet nacre* (text fig. 4) in which tablets are arranged in regular layers parallel to the shell interior, and *lenticular nacre* (text fig. 5) where tablets are arranged in columns normal to growth lines.

Sheet nacre

Surfaces show a great variation in the size and shape of individual tablets, depending upon the rate of carbonate deposition (Wada 1961b). At times of rapid shell growth, tablets are small and rounded ; with slower growth they are larger and euhedral (usually hexagonal). Tablet size is very variable, depending on

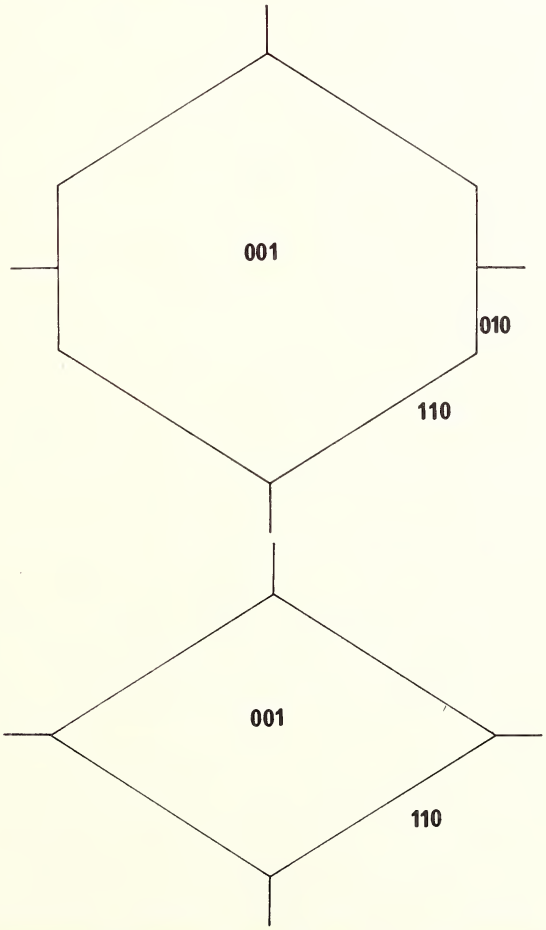

Figs. 6–7. Plan view of the commonly occurring forms of nacre tablets with the faces and crystallographic axes indicated.

species, area of shell and stage of growth. In *Pinctada martensi*, Wada (1960, 1961b) records crystals between 1 and 4 microns across near the shell margins, and 3–8 microns across in the central region of the shell ; most crystals are between 2 and 10 microns across.

Light microscopy and electron diffraction indicate that the flat horizontal surfaces of the tablets correspond to the basal pinacoid faces of aragonite {001}, and the sides to the {010} and {100} forms (text figs. 6 and 7). The {110} form is usually dominant, often giving rise to rhombic crystals.

One interesting feature seen on the {001} surfaces of single crystals is the presence of stepped dextral and sinistral spirals, with smooth, curved outlines in rounded crystals, and straight, polygonal outlines in euhedral crystals (Plate 7, fig. 3 ; text figs. 8–9). These successively higher layers are interpreted as being the result

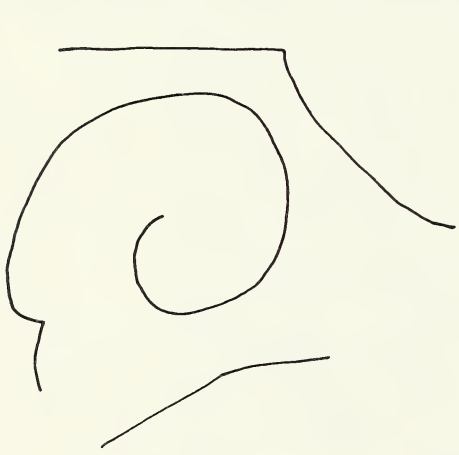

8

9

Fig. 8. Screw dislocation in a rounded nacre tablet in *Pinctada martensi*. (Based on Wada 1961b.) ×6500.

Fig. 9. Screw dislocation in euhedral nacre tablet of *Pinctada martensi*. (Based on Wada 1961b.) ×4250.

of screw dislocations within the crystals, a feature well known in inorganic crystal growth (Read 1953, Frank 1952, Dekeyser and Amelinckx 1955). The origin of these dislocations is largely speculative. They may be caused by the foreign inclusions which are abundant in nacre in the form of the inter- and intracrystalline organic matrix.

Development of sheet nacre begins with the appearance of minute, elongate, rounded aragonite seed crystals on, and in, an underlying interlamellar matrix, (Wada 1961b, fig. 6). The seeds are usually oriented parallel to one another and to the structure within the interlamellar matrix. The seeds grow and develop as rounded or euhedral tablets (Plate 1, fig. 2) or euhedral crystals, and with continued growth link up along parallel faces, often in chains, to form first a dendritic layer and then a continuous sheet. Intermediate stages show great variation in form,

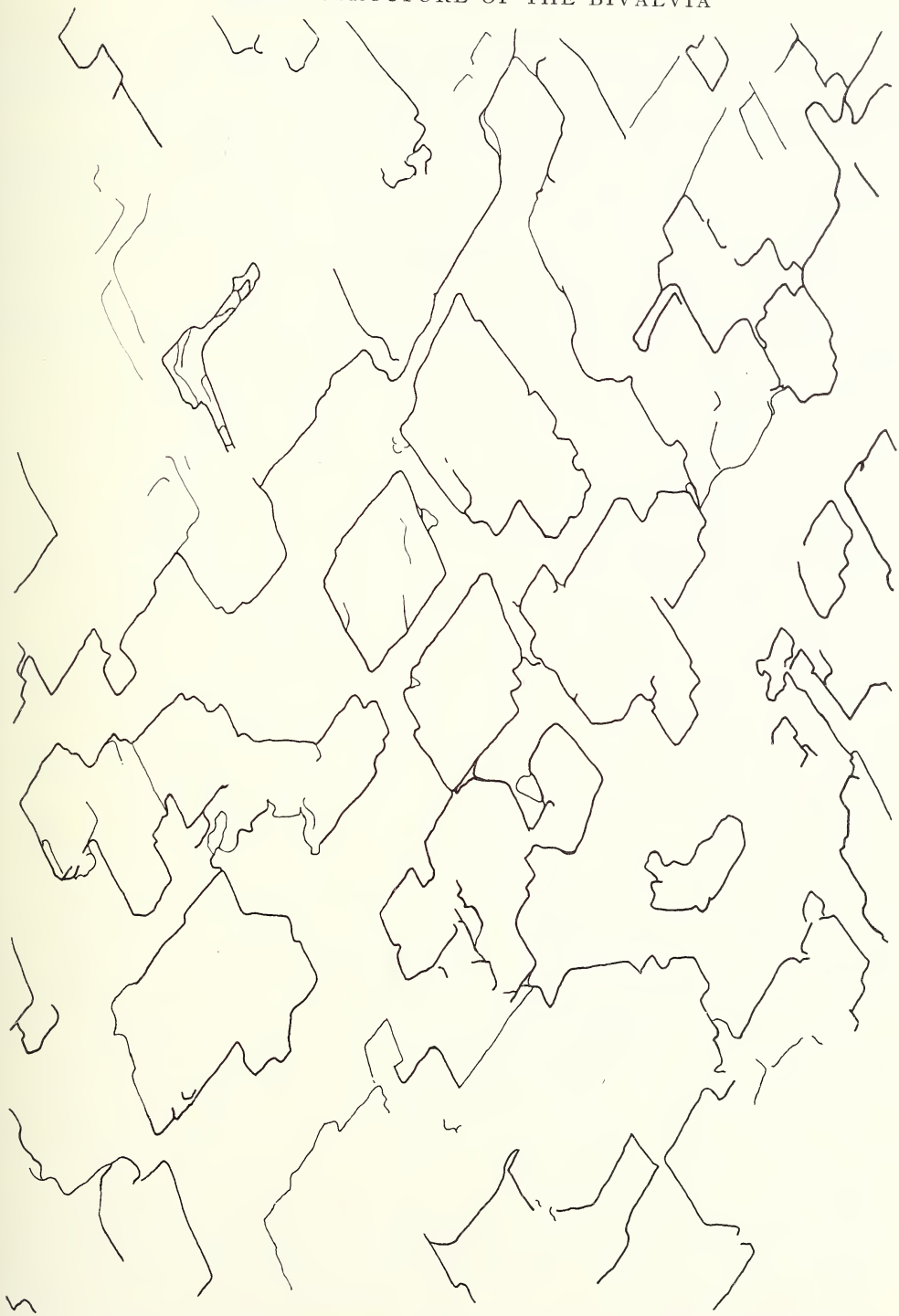

FIG. 10. Parallel growth of nacre tablets on the inner surface of the middle shell layer of *Pinctada margaritifera*. The long axes of the tablets are arranged normal to the shell margin. (Based on electron micrographs.) ×3000.

with a remarkable parallelism of crystals within any one field of observation (text fig. 10 ; see below). Sheets formed by fusion of euhedral crystals may retain traces of the original form of these crystals, faintly visible within larger masses, and picked out by their intercrystalline organic matrix envelopes (Plate 1, fig. 1).

Sheets of nacre formed by growth and fusion of rounded and euhedral tablets show modification of the original shape of the tablets into irregular, frequently five-sided polygons (Plate 3, fig. 2, text figs. 11–13). After the formation of one such sheet an interlamellar organic membrane is laid down and the succeeding sheet grows on this.

Autoradiographic studies on the inner surfaces of nacreous shell layers of bivalves injected with Ca^{45} (Wada 1964d) indicate that calcium carbonate is deposited

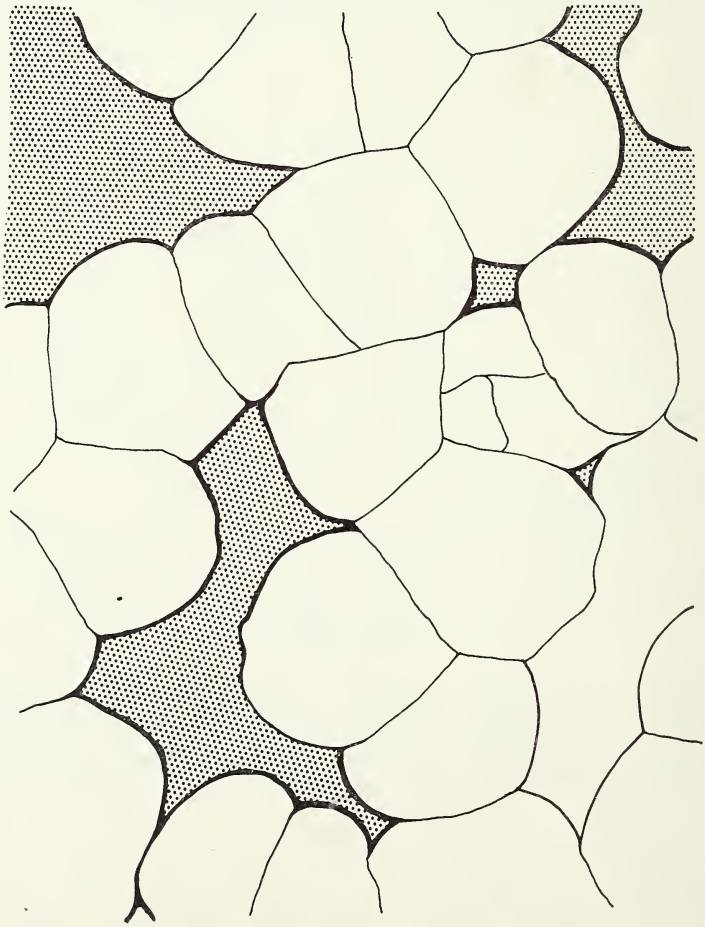

FIGS. 11–12. Inner surface of the nacreous layers of *Anodonta cygnea* showing the characteristic mosaic produced by the growth together of rounded nacre tablets. Growing edges of the nacre tablets are shown by heavy lines, the surface of underlying layer is shown stippled. The completed sheet consists of irregular polygons. (Based on electron micrographs.) Fig. 11 inside pallial line, ×4000 ; Fig. 12 inside pallial line, ×6000.

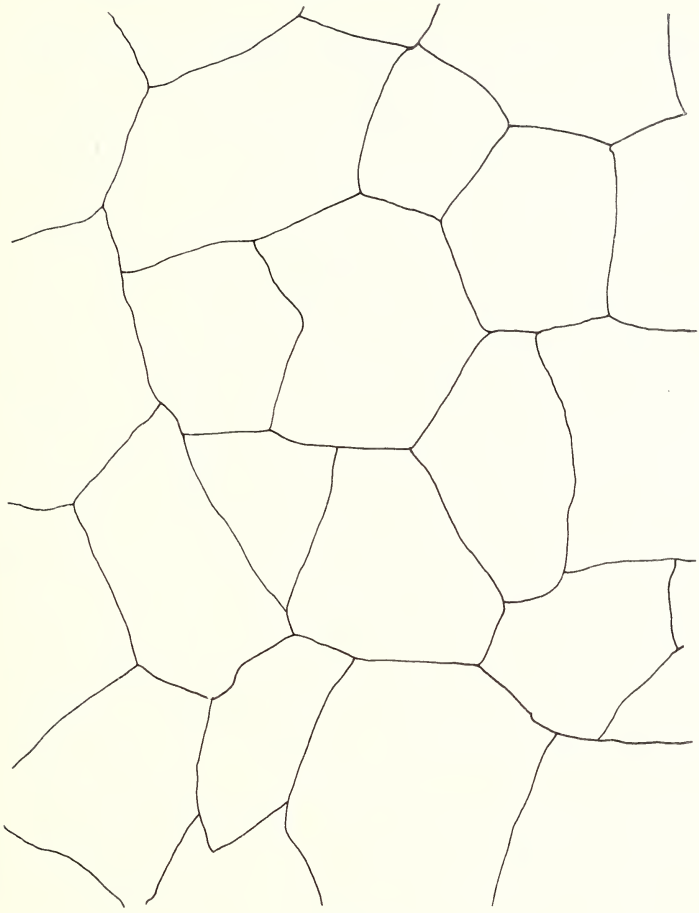

FIG. 12

over the whole surface of the layer, and that the sheets successively outcrop on the inner surface of the layer and accrete horizontally over one another. However, this picture is undoubtedly over-simplified. Thus tablets often bear small parasitic crystals on their {001} surfaces, growing in parallel with the host, while some tablets show thickening and overgrowths around the margins of the {001} faces. Yet other tablets show irregular surfaces (Plate 1, fig. 1), with the irregularities perhaps caused by the interlamellar or intercrystalline organic matrix, or perhaps even by outcropping intracrystalline matrix. Other features of the surfaces of nacre sheets have been interpreted as due to dissolution and corrosion (Plate 2, fig. 4, see also Wada 1961b, 762, figs. 118, 124). Seasonal variation in the surface morphology of nacre deposited by *Pinctada martensi* is discussed at length by Wada (1961b).

Sections of sheet nacre show the familiar ' brick wall ' appearance (Plate 1, fig. 4, Pl. 3, fig. 1 ; text fig. 4). Individual tablets vary in thickness by a factor of about two ; individual sheets sometimes pinch out completely (Fig. 4) while successive sheets also show great variation ; in a section of *Quadrula metanevra*

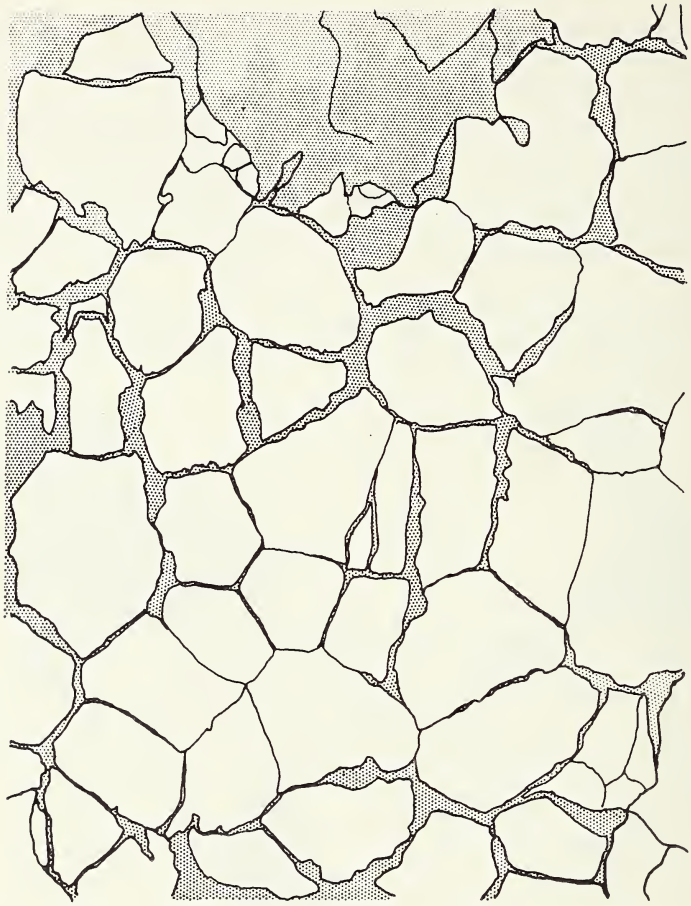

FIG. 13. Inner surface of the inner nacreous layer of *Margaritifera margaritifera* showing the irregular shapes of the nacre tablets. This may be the result of natural dissolution due to changes in pH of the extrapallial fluid. (Based on an electron micrograph.) ×4500.

tablets varied between 0·4 and 2 microns in thickness within an area of 40 × 30 microns. Other bivalve species show comparable variation. In general, our own observations suggest that tablets and crystals vary between 0·4 and 2 or 3 microns in thickness depending on both species and region of shell. In general, mytilid nacre is very finely layered compared with other forms. The nacreous layer of many species studied shows bands of nacre sheets with progressive increase or decrease in the thickness of successive sheets (text fig. 4).

In many sections there is an apparent irregularity in the spacing of the vertical walls of intercrystalline organic matrix, which sometimes fails to connect successive sheets of interlamellar matrix. The interlamellar matrix itself may be discontinuous, so that several tablets in successive layers are in direct continuity (Plate 1, fig. 4). Such sections are perhaps cut through screw dislocations within individual

nacre tablets, or through overgrowths, or even through a place where part of a nacre tablet has grown to fill a depression left unfilled in an underlying layer (see Plate 1, fig. 3).

Nacre probably develops by epitaxial growth, i.e. new layers are laid down on existing ones in such a way that the old and new layers are crystallographically, if not always physically, continuous. One type of epitaxial growth may occur if the interlamellar matrix is discontinuous, and tablets, or parts of tablets of an underlying layer project through it. Such projections could act as nucleation sites and determine the orientation of the layer above. It is known that epitaxial growth can occur in inorganic systems even when successive layers are separated by a film of some foreign substance, up to 1 micron thick.

The intimate relationship between the structure of the organic matrix and of the aragonite suggests that another type of epitaxial growth may occur, i.e. that the organic matrix may be acting as a substrate for the deposition of aragonite (the observations of Watabe (1965, see above) are very relevant here), and the aragonite may also perhaps act as a substrate for development of a regular structure in the organic matrix, indeed they may both act as substrates for one another. Whichever process or combination of processes operate, the preferred orientation is a result of the tendency of the crystals to approach the minimum free energy configuration, as in inorganic systems (Bauer 1964).

A comparison which may be of relevance is the development of a structure similar to nacreous layering in some inorganic systems, where impurities separate out into layers parallel with a crystalline front, as a result of incomplete liquid phase diffusion (Petrov and Kolacher 1958).

As already noted (p. 22), from seeding onwards, both euhedral and rounded tablets show a preferred orientation. From the results of grafting experiments (Wada 1916b etc.), studies of the growth and development of baroque pearls (Wada 1960a), and studies on orientation of tablets over the whole surface of the nacreous layer of shells (Wada 1961a, b), it appears that the *b* crystallographic axis of individual nacre tablets is parallel to the direction of growth and mantle movement over large areas of shell surface. The observed orientations may thus originate as a result of currents and concentration gradients set up in the extrapallial fluid by this movement. In inorganic systems, it is well known that crystals will tend to elongate in the direction of concentration gradients (Buckley 1951). A further parallelism is between the *b* axes of tablets and the structure of the organic membrane upon which they are growing ; Watabe (1965 : 369) also notes that intracrystalline matrix fibrils in the nacre of *Elliptio complanatus* are oriented in the same directions as the crystallographic axes of the tablets. The surface energy involved in this arrangement is lower than that for a random distribution of fibrils.

Spiral patterns are frequently seen on the inner, growing surface of nacre, particularly in the Pteriacea. These spirals have been studied intensively by Wada (1961b, with references ; more accessible is Wada 1966). Individual spirals, both dextral and sinistral, may be up to several millimetres in diameter, and may merge with their neighbours to form a complex surface pattern (Plate 2, figs. 2 and 3). The

spirals consist of successive steps descending outwards from the origin of the spiral. The height of each step is equivalent to the thickness of a single lamella. Step surfaces are like those of the sheet nacre already discussed, while individual tablets show parallelism related to the general orientation over the shell as a whole, rather than to individual spirals (Wada 1958, 1959, fig. 3, 1961b fig. 138, 139) ; the origin of the spiral is frequently a single screw dislocation.

These growth spirals closely resemble those seen on the faces of single inorganic crystals (see, for instance, Forty, 1954, Fulman 1955, Dekeyser and Amelinckx 1955, Sheftal 1958) where they arise from screw dislocations. In nacre, the whole mosaic rather than the individual tablet forms the spiral.

Lenticular nacre

This is particularly well developed in the middle shell layer of the Nuculacea, Unionacea, Trigonacea and Pandoracea.

Electron micrographs of surfaces of this type of nacre (Plate 3, fig. 3) show that tablets, either euhedral or rounded, grow in piles several tablets high, in marked contrast to sheet nacre, where surfaces usually expose only a single layer of tablets. Up to five superimposed tablets have been observed and each successive tablet shows a similar form to the one beneath it ; the {001} faces of tablets show a similar range of surface morphologies to those of sheet nacre. As a result of the piling up of tablets, their {110} and {010} side faces are well exposed and show fine terraces parallel to the (001) plane (Plate 3, fig. 3). Small seed crystals are present all over the surfaces of the tablets, and on the floor of the spaces between piles.

In section (Plate 5, fig. 1) the tablets are arranged in horizontal layers, but these are less regular than those in sheet nacre, as individual tablets are distorted, with wavy upper and lower surfaces (Plate 5, fig. 2 ; Figure 5). As well as this horizontal arrangement, there is a prominent stacking into columns of up to fifteen tablets, with the columns approximately 20–30 microns high. Within columns, tablets are of rather similar dimensions in the central part but decrease in size at either end to give the lenticular shape (Plate 5, fig. 1, Pl. 4, figs. 4–5 ; text fig. 5). Columns usually end in a single crystal, although the apparent size of this clearly depends on the relation of the plane of the section to the axis of the column. Adjoining columns vary in width sympathetically and form a solid structure. Sections show that there is a well developed envelope of intercrystalline organic matrix around each tablet, and a suggestion of intracrystalline matrix within the tablets (Plate 5, fig. 1). Thicker sheets of interlamellar matrix are sometimes developed.

In *Neotrigonia dubia* successive tablets first appear as rims to the (001) face of the tablet below. Electron micrographs of the surface of *Pinctada* nacre *outside* the pallial line show a similar mode of accretion ; see also Wada (1960, fig. 3 ; 1961b, figs. 104, 117, 118), who does not, however, specify the exact region of the shell.

A different build up is seen in *Anodonta* (Plate 3, fig. 3) where successive tablets usually appear centrally on the (001) face of the underlying tablet. Spaces between piles of tablets are gradually filled by lateral accretion, and the appearance and building up of new columns follows from random seeding.

The distribution of sheet and lenticular nacre may be related to shell geometry. In forms in which both types of nacre are present, lenticular nacre forms the middle shell layer of a shell with a high spiral angle and distinctly convex shell. In the Mytilacea and Pteriacea, where the spiral angle is low, and the shell flattened, sheet nacre is developed throughout. Sheet nacre represents growth parallel to the shell interior, lenticular nacre respresents growth normal to the marginal area, between the outer layer and the pallial line. It should be noted, however, that the *middle* layer of *Pinctada* shows a mode of accretion on surfaces like that seen in some lenticular nacres, as though the vertical component is only just appearing.

The regular alternation of layers of calcium carbonate tablets and thinner sheets of intercrystalline and interlamellar matrix may be the result of a periodic, perhaps diurnal secretory rhythm. The organic layer accumulates at times of non-deposition of calcium carbonate.

FOLIATED STRUCTURE

Plate 4, figs. 1, 2, 3, 6 ; Pl. 5, figs. 2, 3, 4; Pl. 6, figs. 1–4 ; text-figs. 14–16.

Foliated structure, which forms the calcitostracum or subnacreous layer of many authors, is present in the Ostreacea, Pectinacea, Anomiacea, and Limacea. It is always calcitic.

The morphology of foliated structure at optical level has been described by several early workers (see Korringa 1951) and particularly by Schmidt (1924) and Bøggild (1930 : 249). In section the structure is seen to be made up of fine sheets grouped in larger, lenticular folia (Plate 4, figs. 1, 2, 3, 6), which in turn form larger units. The folia are usually oriented parallel or sub-parallel to the inner surface of the layer built of this structure. In some shell layers, particularly in the Pectinacea, folia develop highly irregular orientations as seen in radial sections (Pl. 4, fig. 3) transverse sections show that part at least of this irregularity is due to the plane of the radial section cutting obliquely across folia which are in fact parallel or subparallel to rib surfaces. In umbonal regions, the folia show a concentric arrangement in section, since they follow shell, and hence mantle surfaces (Plate 4, figs. 2).

Sections parallel to individual folia show that these in turn are composed of small elongate tablets or laths (Plate 4, fig. 6) which join up laterally to form sheets. Foliated structure is easily recognisable in peels and sections by its characteristic colour variation, adjacent folia varying from straw coloured to reddish-brown, and showing marked pseudopleochroism. As discussed below under crossed-lamellar structure (p. 41), this is in part an effect of the varying proportions of organic matrix exposed in sections at different planes of intersection with the folia. This colour variation makes visible the build up of similarly oriented folia throughout a shell layer, forming what can be regarded as a three-dimensional dendritic system.

Detailed electron microscopic studies of foliated structure have been rather limited. The foliated layers of *Crassostrea virginica* have been investigated in detail by Tsujii *et al.* (1958), Watabe *et al.* (1958), Watabe and Wilbur (1961) and Watabe (1965). Short notes on *Anomia lischkei*, *Ostrea gigas*, and *Chlamys nobiliis* are given by Wada (1961b, 1963a, b, c and e, 1964a etc.). Except for the work of

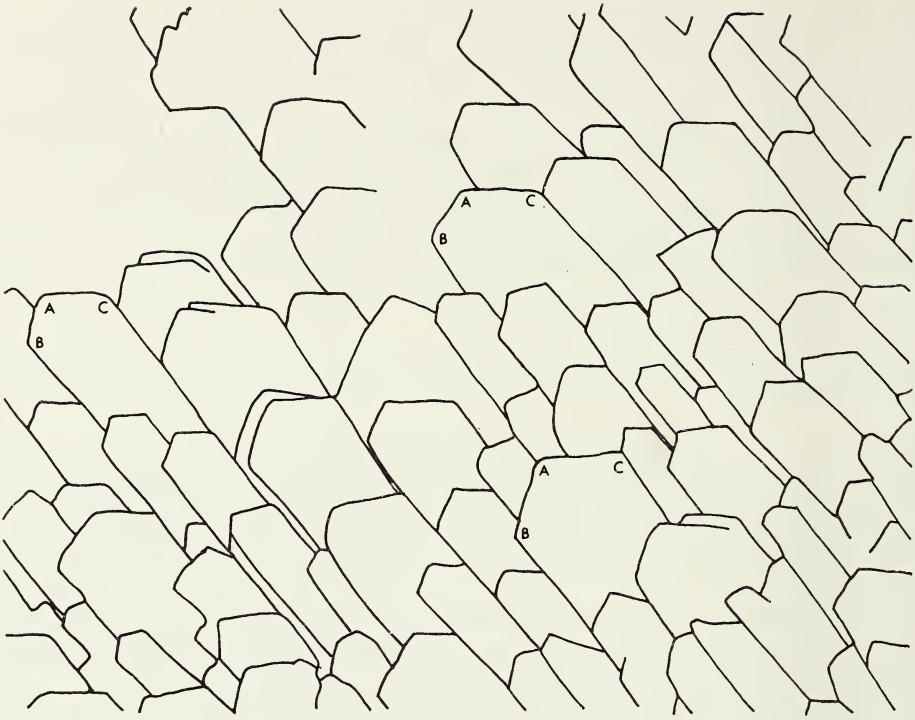

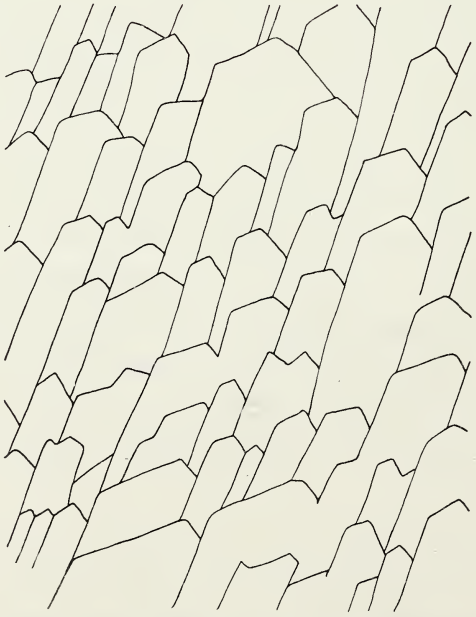

FIGS. 14–15. Inner surface of the foliated layer of *Ostrea hyotis* (based on electron micrographs) showing the characteristic build up of overlapping sheets of calcite laths joined together in side to side contact, direction of overlap is towards the top. Fig. 14, ×9700, (angles mentioned in the text are indicated); Fig. 15, ×6500.

Watabe (1965) on ultrathin sections, and Watabe and Wilbur (1961), only observations and figures based on an examination of shell surfaces have been published to date.

We have examined foliated structure in five species, *Ostrea edulis*, *Ostrea hyotis*, *Ostrea irridescens*, *Anomia ephippium* and *Placuna placenta*. On the inner surface of a shell, foliated structure appears to be built up of long, tabular, idiomorphic

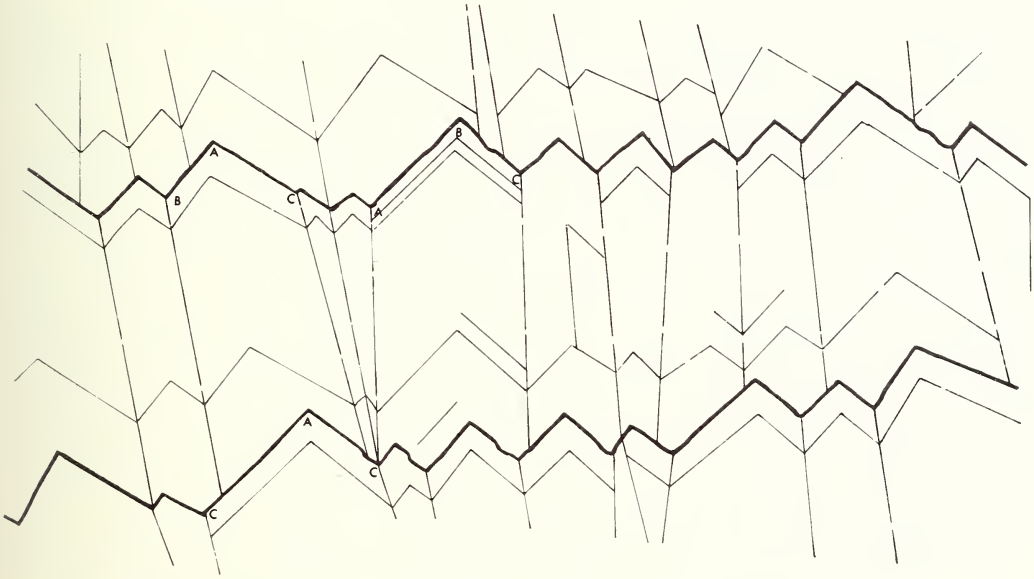

FIG. 16. Inner surface of the foliated layer of *Anomia ephippium* (based on electron micrographs) showing the form of sheets, lath boundaries, lath terminations, and growth halts. The angles indicated are those referred to in text (p. 32). ×4500.

laths, joined laterally to form sheets. The sheets are slightly inclined to the shell surface, and successively overlap in parallel, rather like tiles on a roof (Plate 5, fig. 4 ; Pl. 6, figs. 1, 3, 4 ; text figs. 14–16). These ' laths,' and ' sheets ' correspond to those seen at optical level. The rows of laths forming successive sheets show a marked parallelism of their long axes over limited areas of shell, but variations in direction in successive sheets are frequent (Plate 6, fig. 1 ; text figs. 14–16). When this occurs, laths of the overlying layer may bend round parallel to those in the underlying layer (Wada 1964a, fig. 4) ; branching of laths may also occur (Wada 1963c, fig. 3).

As a result of the successive overlap of sheets, only parts of laths are visible on the surface of a shell layer ; both the width and observed length of laths vary greatly between adjacent laths, between sheets, between different areas of shell, and between species.

On surfaces of *Crassostrea virginica*, Watabe and Wilbur (1961) estimated crystal (i.e. lath) length as at least twice the width (about 2 microns), and recorded lengths of up to 9 microns in section. Wada recorded a maximum exposed length of up

to 17 microns in *Anomia lischkei* (1963b), a length of up to 10 microns and width of 3·5 microns in *Chlamys nobilis* (1964a), while in *Ostrea gigas* (1963c) the ' particle size ' (*sic*) was said to be usually smaller than 8 microns. Recorded thicknesses of laths are between 0·2 and 0·5 microns (Watabe and Wilbur 1961, Wada 1963b, 1963c, 1964a).

Few determinations have been made of the crystallographic orientation of the calcite elements in the foliated structure. Optical measurements, made on a universal stage, show that in *Placuna placenta* the *c* axis of the carbonate lies consistently at an angle of 26° to the plane of the foliation. Information on crystallographic orientation may also be obtained by studying X-ray diffractometer patterns of shell fragments mounted on sample slides in such a way that the plane of the foliation is parallel to the plane of the slide. Patterns obtained from *Ostrea edulis*, *Placuna placenta* and *Anomia* sp. all reveal a strong preferred orientation of the crystallites. Peaks corresponding to lattice planes lying parallel to, or at a low angle to the *c* axis are eliminated, and those corresponding to lattice planes at a high angle to the *c* axis are enhanced. The peaks showing greatest enhancement are $10\bar{1}8$ (= morphological $\{10\bar{1}2\}$), 000,12 (= morphological {0001}), and especially $10\bar{1}$,10 (= morphological $\{20\bar{2}5\}$). The latter peak is not only enhanced relative to $10\bar{1}4$ (normally the strongest peak) by a factor of up to 150, but is also enhanced relative to $10\bar{1}8$ (morphological $\{10\bar{1}2\}$). This result is at variance with the optical observations, since the angle of 26° between the *c* axes and the plane of foliation in *Placuna placenta* corresponds exactly to the angle between the *c* axes and the morphological {1012}, but is too high for $10\bar{1}$,10 (morphological $\{20\bar{2}5\}$). It would be surprising if the plane of foliation were parallel to $\{20\bar{2}5\}$, which is not even known as a crystal form, in contrast to $\{10\bar{1}2\}$, which is both a common form of calcite and the composition plane of the ubiquitous polysynthetic twinning. On the other hand, the plane of foliation need not necessarily correspond to any particular crystallographic direction in calcite, since the constituent crystallites in foliated structure do not show any crystal faces parallel to the plane of foliation.

The actual faces developed on the constituent crystallites have been examined by electron diffraction (e.g. Wada 1964a), and the large flat exposed faces of the laths have been identified as {0001}, i.e. normal to the *c* axis. Beyond this, indexing of the faces forming sides and terminations of laths is difficult ; tablets are not always parallel sided, while the interfacial angles of the free faces are very variable within a species, between species, and even during the growth of an individual lath.

Details of interfacial angles that we have measured are as follows. In *Ostrea hyotis*, angle A (see text fig. 14) varies between 94° and 116°, usually lying between 105° and 113° ; angle B varies from 119° to 137°, usually between 125° and 131° ; angle C varies between 114° and 135°, usually between 124° and 127°. In *Anomia ephippium* the relevant figures are : A 85°–99° ; B 119°–138°, mostly 128°–134° ; C 128°–140°, mostly 133°–137°. If these are true interfacial angles, this is a remarakable variation. Other workers (Tsujii *et al.* 1958 etc.) have explained this variation as a result of differences in the attitudes of individual laths with respect

to the shell surface, so that the angle measured on a replica is the *apparent*, not the *true* angle. The angles as measured by these authors in *Crassostrea virginica* are as follows : A 81°–125°, mostly 96°–100° ; B 111°–145°, mostly 130°–135° ; C 116°–155°, which they relate to true angles of 90°, 120° and 150° respectively. They relate these angles, in turn, to the angles between $\{10\bar{1}0\}$ and $\{11\bar{2}0\}$ forms in calcite ; i.e. 90° for the angle $\{\bar{1}\bar{1}20\}$—$\{1\bar{1}00\}$, 120° for $\{\bar{1}\bar{1}00\}$—$\{10\bar{1}0\}$, and 150° for $\{10\bar{1}0\}$—$\{1\bar{1}20\}$. Wada (1963a, b, c, e, 1964a) has similar results showing an equally great variation in interfacial angle. We would prefer not to adopt this indexing for the present, as we can see no reason why these angles could not be related to some of the higher index forms developed in calcite.

Laths vary in their surface morphology. In *Anomia, Placuna* and *Ostrea irridescens* the surface is smooth (Plate 3, fig. 4 ; Pl. 6, fig. 3), and lath contacts are indicated by discontinuous lines. These lines may be due either to organic matrix projecting upwards or to grooves ; in electron photomicrographs these two structures are very difficult to distinguish (cf. Grégoire 1962). Former positions of crystal fronts, probably representing growth halts, are picked out in a similar fashion (Plate 5, fig. 4) ; the relative position of these fronts is closely similar in successive overlapping sheets (Plate 5, fig. 4 ; text fig. 16). Small areas of non-deposition are often present along terminal crystal faces, and with further growth these become incorporated into the lath as irregular, aligned pits (Plate 6, fig. 3) floored by the underlying sheet. Occasional small, rounded overgrowths may also be present.

Surfaces of *Ostrea hyotis* that we have examined (Plate 5, fig. 2 ; Pl. 6, fig. 4) show a stronger surface relief and ornament. Marked longitudinal grooves and ridges are present. Some of these were obviously produced by the coalescence of smaller laths, while others are probably related to the component lamellae within each lath (Plate 6, fig. 4 ; see Watabe 1965, discussed below). Other surfaces are mammillate, bearing small rounded seeds 0·5–0·75 microns in diameter (Plate 6, fig. 2). Over some areas of the shell, the pattern of successive outcropping laths is masked by what is probably a thick organic membrane (Plate 5, fig. 2). More definite evidence of organic matrix is very common, as when the surfaces of laths and sheets are covered in a reticulate network of fibres (Plate 5, fig. 2).

Detailed carbonate/organic matrix relations in the foliated layer of *Crassostrea virginica* have been studied by Watabe (1965) and are only summarised here. Thick interlamellar matrix, so prominent in nacre, (p. 19) is not developed. Intercrystalline matrix is present ; it is 120–200 A thick and lacks the granular structure of nacreous matrix. Sometimes two or three elemental layers, of the order of 50 A thick, can be resolved. The intracrystalline matrix completely surrounds each lath. Continuous with it are very thin sheets of intracrystalline matrix, which surround individual crystal blocks within laths. These blocks are vertical, parallel lamellae, 100–400 A wide and 150–2000 A high, running along the length of the laths. Traces of these blocks are shown in Plate 6, fig. 4.

In section the laths appear as elongate, tabular blocks. In *Ostrea edulis* these are 0·1–0·3 microns thick and have a maximum observed length of 13 microns, though they must in fact be much longer than this. Within any field the laths

have a comparable attitude but may show slight folding and buckling. Intercrystalline organic matrix is clearly visible.

Scanning electron-microscopy of fractured surfaces gives a better picture of general relationships in foliated structure, and shows groups of parallel laths, constituting individual folia, building up the whole shell. Laths in adjacent folia have slightly different orientations (Plate 5, fig. 3).

The growth and development of foliated structure is discussed by Watabe and Wilbur (1964) and Wilbur (1964), and is considered as three-dimensional dendritic growth, similar to that seen in inorganic systems (i.e. Gorodetsky and Saratovkin 1958). The branchings shown by Watabe and Wilbur (1961, figs. 3, 4, 5) are consistent with such an interpretation. Our results are inconclusive on this point since we have only observed the normal pattern of parallel overlapping sheets. What we take to be the initial seeding of a foliated layer on, and in, a thick organic membrane is shown as Plate 6, fig. 2 (cf. Wilbur 1964, p. 255).

Overall orientations of rhombohedral axes on the whole inner shell surface of *Ostrea* and *Anomia* have been studied by Wada (1963a), who also records spiral and mound-shaped structures on foliated shell-layer surfaces (Wada 1963b, c, e, 1964a, e).

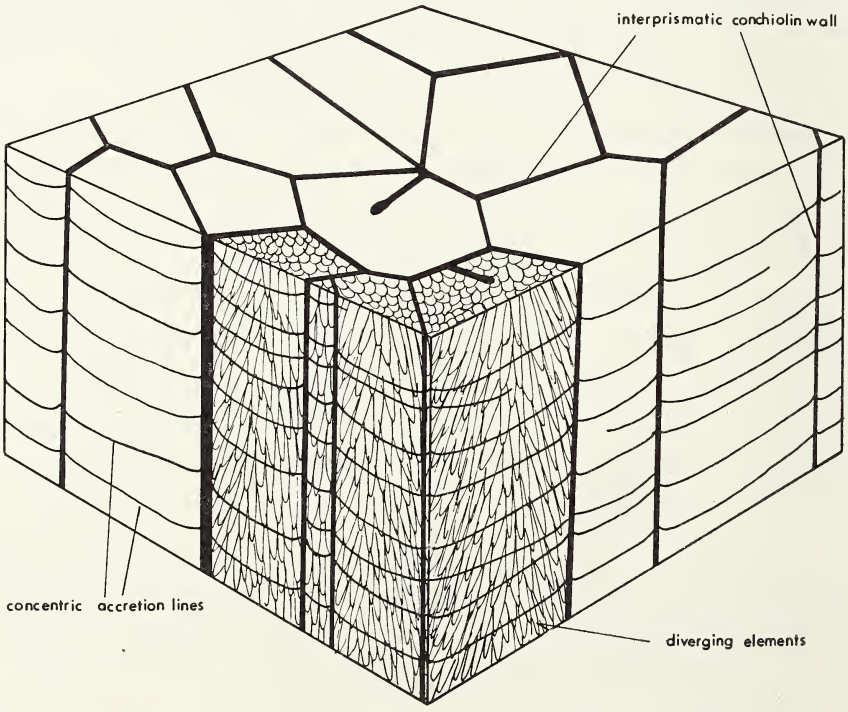

Fig. 17. Block diagram of part of the aragonite prismatic layer of *Unio pictorum*. Small scale like crystals are seen enclosed within the polygonal, columnar conchiolin sheaths. ×300. The inner surface of the shell is in the direction of the bottom of the diagram.

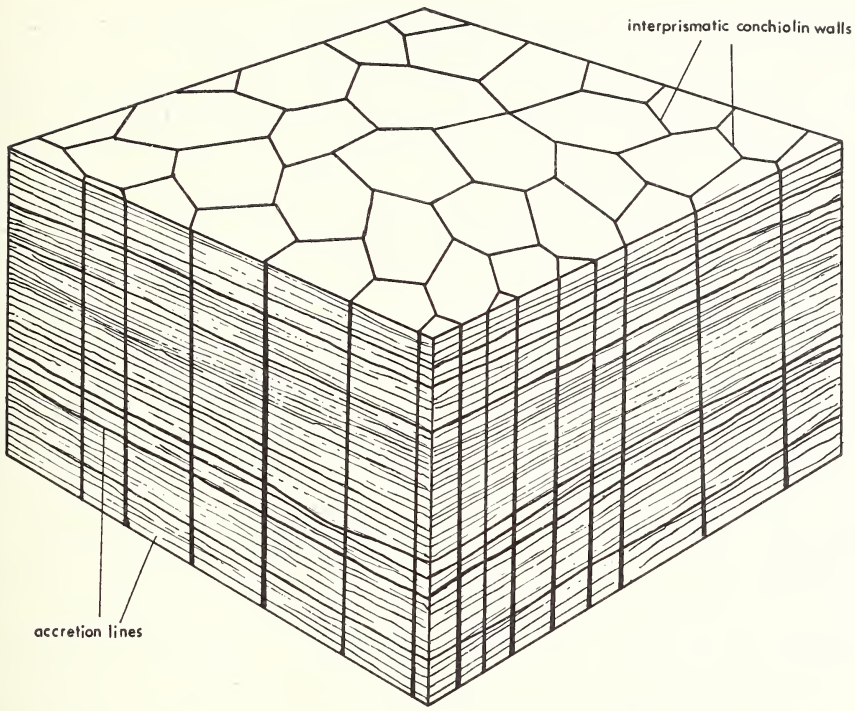

FIG. 18. Block diagram of part of the calcitic prismatic layer of *Atrina vexillum*. ×150.

PRISMATIC STRUCTURE

Plate 7, figs. 1, 2, 4, 5, 6 ; Pls. 8, 9, 10, 11, 12, 13 ; Pl. 26, fig. 5 ; text-figs. 2, 17, 18, 22, 75.

Together with nacre, prismatic structures are very well known, and descriptions of prisms have been given by many authors, notably Carpenter (1844, 1848), Rose (1858), Biederman (1901), Schmidt (1922, 1924, 1925), Bøggild (1930) and Haas (1929–1935). Two main types of prism are recognised here, i.e. *simple* prisms and *composite* prisms, and these are discussed, in turn, below. Prismatic layers of both types usually form the outer layers of shells in families where they occur. Simple prisms may be aragonite or calcite, but composite prisms are always aragonite. Many earlier workers have referred to prismatic layers in the inner and middle shell layers of bivalves (the dependent prismatic layer of Bøggild). We regard such layers as myostracal bands.

Simple prismatic structure

This is the best known type of prismatic structure and can occur as either aragonite (text-figs. 17 ; Plate 7, figs. 2, 4, 5 ; Pl. 10, Pl. 11, figs. 1, 2) or calcite (text-figs. 18 ; Plate 7, figs. 1, 6 ; Pl. 9), with only minor differences in form ; the most consistent such difference is that calcite prisms have transverse striations (Pl. 7, figs. 1, 6) while aragonite prisms have longitudinal, diverging striations as well as less con-

spicuous transverse ones. (Plate 10, fig. 1 ; Pl. 7, fig. 4). However, calcitic prisms sometimes show longitudinal striations which do not diverge.

Calcite simple prisms are found in the Pteriacea, Mytilacea, Pinnacea, Ostreacea and possibly in that anomalous member of the Chamacea *Chama pellucida*. Aragonite simple prisms are found in the Unionacea, Trigonacea, Pandoracea, Pholadomyacea and Poromyacea.

In surface view, simple prisms show the well known ' honeycomb ' structure pattern, with a thick wall of conchiolin separating the individual units of calcium carbonate. The prisms are usually irregular pentagons, although hexagons and four sided shapes also occur. The conchiolin wall may appear as a groove between chambers, as a low ridge, or may stand high above the surface as in Plate 9, fig. 1. It varies in thickness from 1–8 microns in *Pinctada martensi* (Watabe and Wada 1956), and from 0·5–3 microns in *Anodonta cygnea* ; in the latter species it was seen to vary from 0·8–1·6 microns along a wall length of 7 microns. It is generally thicker and more irregular at the junction with the middle nacreous layer. Prism walls are usually fairly straight, but occasionally they may be markedly curved ; walls of adjacent prisms usually meet at triple points, with interfacial angles of approximately 120°. The surface of the walls is usually smooth, but obliquely transverse ridges are sometimes present. Small granules, presumably of calcium carbonate, may be present. Sometimes the conchiolin wall between adjacent prisms is discontinuous, and appears as a thicknened flange, projecting into the carbonate (Plate 9, fig. 3 ; text-fig. 17). Decalcification shows that periostracum and interprismatic conchiolin walls are completely continuous. At optical level, the surface of the calcium carbonate of the prism is fairly homogeneous and structureless ; electron-microscopic studies of this surface show, however, that it is made up of very small, irregular, scale-like crystals, 0·3–2 microns in diameter in *Pinctada martensi* (Watabe and Wada 1956) and 0·2–1 microns in *Anodonta cygnea*. These small crystals usually lack any obvious orientation, but on some surfaces, concentric, arcuate patterns, or vague linear arrangements are seen. Tsujii *et al.* (1958) have shown that the surface of the prism chamber of *Crassostrea virginica* is divided by a series of parallel grooves of organic matrix, 0·28 microns apart, separating blocks of crystal. This same pattern is described by Grégoire (1961) in *Ostrea edulis*.

The diameter of prism chambers is very variable, but it usually increases inwards from the shell margin. In *Crassostrea virginica*, chambers at the margin average 9 microns in diameter, while at the centre they reach 44·6 microns (Tsujii *et al.* 1958).

In radial and transverse sections,[1] prisms are columnar, and more or less regular ; each prism is separated from its neighbour by a vertical wall of conchiolin. The length of the prisms increases from the outer edge of the prismatic layer to a maximum where growth is terminated by the development of the underlying shell layer. Prisms are narrower at their contact with the periostracum than at their inner

1. Radial sections are normal to the shell surface and run from umbo to margin. Transverse sections are normal to the shell surface and run in an antero-posterior direction.
Tangential sections are normal to the shell surface and tangential to growth lines. Planar sections are parallel to the shell surface.

ends. Close to the periostracum small prisms are numerous, but many of these wedge out inwards, so that surviving prisms appear to branch. This may explain the ' prism branching ' observed by Bøggild (1930 ; 247 ; see Pl. 7, fig. 5).

Calcitic prisms often have transverse striations that are meniscus-shaped and convex towards the inside of the shell. These striations are interpreted as accretion lines (Plate 7, fig. 6). Aragonite prisms show a typical feathery appearance, due to diverging longitudinal striations (Plate 7, fig. 4), but are also crossed by transverse striae. The studies of Grégoire (1961) have shown that prisms are made up of a pile of disc-shaped calcium carbonate lamellae, each separated by a thin sheet of organic matrix. Watabe and Wada (1956) show that in *Pinctada martensi* the horizontal carbonate lamellae may be from 0·7 to 7 microns thick, and the conchiolin sheets separating them between 0·04 and 0·5 microns thick. They also found that lamellae may be made up of more irregular subchambers. Our study of sections of prisms of *Margaritifera margaritifera* shows that each prism is divided longitudinally into blocks ; each block is about 2–3 microns wide, and is separated from adjacent blocks by a thin wall of organic matrix approximately 0·3 microns wide (Plate 11, fig. 3). The longitudinal blocks intersect the conchiolin prism wall obliquely, and probably represent the diverging striations seen in longitudinal section at optical level. Transverse divisions of the prisms were not seen. The calcium carbonate within each prism appears to be finely and irregularly granular, although this may be due to etching. The granules are sometimes aligned obliquely to the axis of the prism.

Grégoire (1961 a and b) has described the structure of the conchiolin wall and of the organic matrix within the prisms of 19 species of bivalves, with both aragonite and calcite prisms. He found that, except in *Mytilus edulis*, the organic matrix from the prismatic layer differs structurally from that of the underlying nacreous layer. The prism wall conchiolin is very rigid, and strongly resistant to mechanical dissociation. It consists of tightly reticulated sheets of fibrils which lack the regularity of the interlamellar matrix of the nacreous layer. In *Mytilus edulis* however, no difference could be seen between the conchiolin surrounding the calcite prisms and that associated with the aragonitic nacreous layer below.

Watabe and Wada (1956), using transverse thin sections of *Pinctada martensi* in polarised light, found that each prism extinguishes in several smaller blocks. It therefore appears that each prism consists of several crystallites in slightly different crystallographic orientation to one another. We have made the same observation in several other species with calcite prisms ; the aragonite prisms of the Unionacea show a characteristic extinction pattern, described by Bøggild (1930 : 248).

In the Unionacea and the Trigonacea a small boss is present at the periostracum end of each prism, and is especially well seen between ribs in *Neotrigonia*. The boss has concentric growth rings and appears to be the original spherulite, which developed on the periostracum substrate. Results so far obtained from examination of this feature (Plate 13, figs. 1, 2, 3) in the species *Neotrigonia margaritacea* show, rather surprisingly, an actual perforation in the periostracum at this point, while the original spherulite appears to have been removed.

Growth of simple prisms

The form of the prismatic layer in bivalves may be explained on the basis of the principles of the group growth of inorganic spherulites, as elaborated by Grigor'ev (1965).

Spherulites may be formed in one of three ways:—

1. By overgrowth of crystallites on a more or less spherical extraneous object.

2. By the spherical accumulation of crystallites. This entails the initial crystallisation, at certain points, of differently oriented crystallites. Only those crystal-

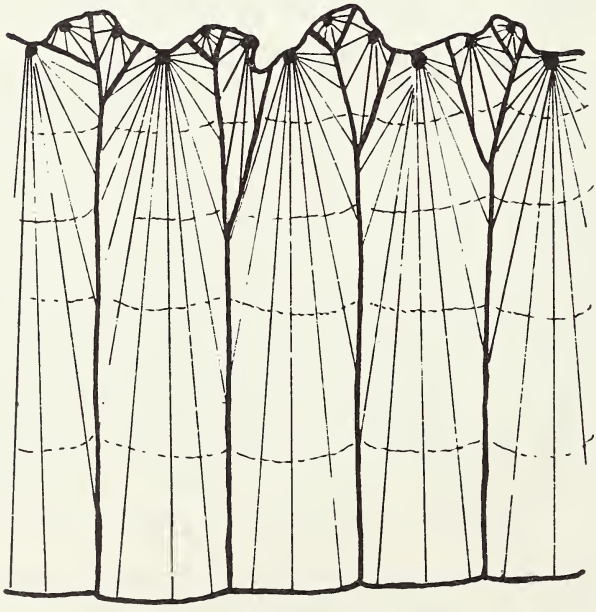

FIGS. 19–21. This series of diagrams, based on spherulitic growth in an inorganic system (Grigor'ev 1965) arising from an irregular surface, shows the internal structure of the spherulites and the development of prismatic structure. The structures are very similar to those seen in the prismatic layers of bivalves. The elimination of some spherulites and the increase in size of the remaining prisms as a result of geometric selection is also comparable to that of the bivalves.

lites with their elongation parallel to the radius of the accumulation, and situated on the periphery, will be able to grow freely, thus producing a roughly spherical aggregate.

3. By the split growth of a crystal, producing a bilobate formation within the crystal.

In bivalves, individual spherulites are present at the edge of the prismatic layer, where concentrically zoned, circular, or vaguely polygonal spherulites can be seen, isolated from each other (Plate 8, figs. 1, 5 ; text-fig. 2). Spherulites in bivalves may possibly form by the second of the methods listed above. However, the formation of the prismatic layer is a result of group growth of spherulites. As the initial spherulites grow, they eventually meet to form polygonal blocks, and subsequent growth can only be in one direction, so that the spherulites will become long and acicular.

Two different initial conditions can produce a similar end result : (1) the simultaneous group growth of spherulites on an uneven surface (text figs. 19–21), or (2) the growth of spherulites on an even surface with the individuals growing at irregular. rates. Under these conditions of growth some spherulites will be eliminated for lack of free space to grow, a process known as geometric selection. Text figs. 19–21 represent this process diagramatically.

Geometric selection may be observed in the prismatic layers of most bivalves, and explains the so-called branching observed by Bøggild near the outer side of such layers. In inorganic systems, concentric zoning in spherulites is probably due to changes in conditions within the mineralising fluid. In bivalves we would interpret it as a result of comparable changes in the extrapallial fluid. Voll (1960) has shown, in a discussion of mineral grain growth (seen also in foams), that the grain shapes developed are a compromise between space filling and the effect of the interfacial tension of the crystals ; the interfacial tension pulls the boundaries into equilibrium positions. Where three boundaries meet at a common edge, the triangle of forces determines this interfacial angle, which at a triple point is 120°, or for a corner of 4 edges 109° 28′ ; the commonest shape produced by this process is an irregular pentagon. Equilibrium is reached first at the triple point, and the faces and edges subsequently adapt by curvature. The size the crystals reach before they meet is determined by the number and spacing of the original nuclei. After crystals meet, growth in a lateral direction ceases due to locking mechanisms such as the accumulation of impurities at grain boundaries. The resulting honeycomb patterns are well known in metallurgy (Petrov and Kolachev 1958). Measurements of the triple angles occurring in *Pinctada margaritifera*, *P. martensi*, *Anodonta cygnea* and *Atrina vexillum* showed a close clustering around 120° (Plate 7, figs. 1, 6 ; Pl. 9). The accumulation of conchiolin around the polygonal crystals is thus thought to be due to the squeezing out of impurity to the boundary, where it acts as a locking mechanism to prevent further grain growth.

Composite prismatic structure

This structure was defined by Bøggild (1930 : 249) as consisting ' of larger prisms (prisms of the first order) each of them composed of fine prisms (of the second order)

arranged in a feathery manner . . . . the prisms of the first order are placed horizontally, in the radial direction, and form only one layer ; the prisms of the second order diverge towards the margin '. This structure is found typically in the Nuculacea but also occurs in some Lucinacea and Tellinacea. It is always aragonitic, and always forms the outer layer of the shell.

Seen at optical level, the first order prisms are arranged horizontally, and run parallel with the outer surface of the shell ; they are approximately square in tangential section, and lie in side to side contact. The first order prisms radiate from the umbo, becoming wider towards the shell margin. Each first order prism is present from the earliest observable growth stages, and branching or generation of additional first order prisms does not occur during normal shell growth. Each first order prism is separated from its neighbours by a distinct dividing line, which

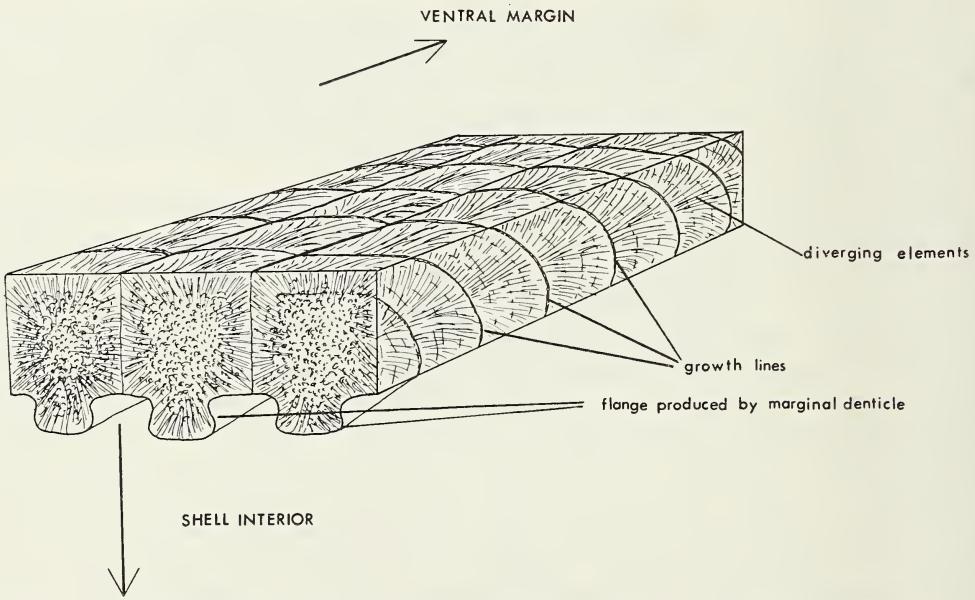

Fig. 22. Block diagram of the composite prismatic layer of *Nucula placentina*. ×50. The flanges on the lower surfaces of the prisms represent the trace of the marginal denticle present in this species. Except at the extreme ventral margin the flanges would normally be covered by the underlying middle nacreous layer. (See Pl. 11, fig. 5.)

is in some cases a thin wall of organic matrix ; thick walls of organic matrix, such as those separating simple prisms, do not occur. In the Nuculacea, the inner face of the first order prisms projects downwards into a flange, which represents the trace of the marginal denticle (Plate 11, fig. 5 ; text fig. 22).

Each first order prism is made up of smaller, second order prisms. These second order prisms are elongate, needle-like units, which in radial and horizontal sections are responsible for the feathery internal appearance of the first order prisms. The second order prisms diverge from the axes of the first order prisms ; they are curved, and are larger towards the outer and inner surfaces of the first order prisms

than near the central axis of the first order prisms. In tangential section, (Plate 11, fig. 5 ; text fig. 22) second order prisms towards the centre of each first order prism are cut at 90° to their long axes, while towards the margins of the first order prisms they are cut obliquely, producing a radiating appearance within each first order prism. Growth lines in this structure are strongly convex ventrally, and appear almost concentric in arrangement ; they may or may not disrupt the feathery structure of the second order prisms within each first order prism.

At electron microscope level, we have studied this structure in polished and etched sections of the lucinoid *Codakia punctata* and on inner surfaces and fractured sections of *Nucula sulcata*. In sections of *C. punctata*, the second order prisms are subcircular in cross section, varying in diameter from 5–6 microns near the contact with the underlying crossed-lamellar layer, to less than 1 micron towards the central axis of the first order prism. The maximum measured length of the second order prisms was 35 microns, but they are undoubtedly much longer than this. The second order prisms are relatively straight sided along their length, and each is enveloped in a sheath of organic matrix, approximately 0·2 microns thick (Plate 13, figs. 4, 5). Wedging out of smaller prisms was sometimes seen, but no obvious branching was noted. Some cross sections through the second order prisms show that an intracrystalline organic matrix is also present, dividing the prisms into smaller units, of variable size and irregular outline. Examination of the inner surface of *Nucula sulcata* shows that the second order prisms outcrop as small papillae, with irregular rounded terminations, producing a granular inner surface to the composite prismatic layer (Plate 26, fig. 5).

The growth of composite prisms can be envisaged as similar to that of the spherulitic growth of simple prisms (text figs. 19–21), but taking a horizontal rather than a vertical direction. The initiation and geometric selection cannot be seen, probably because they have taken place in early growth stages of the shell, which are not now visible.

The prismatic types present in the Trigonacea, Mytilacea and Solemyacea are discussed under these superfamilies.

CROSSED LAMELLAR STRUCTURE

Plates 14, 15, 16 ; Pl. 17, figs. 1–4, Pl. 18, figs. 1, 3, 4 ; text-figs. 23–28.

Crossed-lamellar structure is always aragonitic in extant bivalves. It is widely developed in heterodonts, and also occurs in the Arcacea, Limopsacea, some Pectenacea and Limacea. This structural type has been figured by many authors, notably Carpenter (1844, 1848), Rose (1858), Ehrenbaum (1885), Biedermann (1901), Schmidt (1924), and Bøggild (1930 : 251). Of these, Bøggild's interpretation has been taken as standard by many authors (Newell 1937, MacClintock 1963, 1967, McKay 1952, Cox 1960, Kobayashi, I., 1964 and Omari *et al.* 1962).

According to Bøggild, the shell-layer concerned is made up of two elements, i.e. larger, first order lamels, which in turn are composed of smaller, second order lamels. First order lamels have a more or less rectangular form. Their longest axes lie horizontally, parallel to the shell surface, and in bivalves are arranged

more or less concentrically parallel to the shell margin. The shortest axes of first order lamels are also parallel to the shell surface, but lie radially. The axes of intermediate length are more or less normal to the shell surface. Each first order lamel is made up of smaller, second order lamels which are oriented normally to the longest face of the first order lamel. Second order lamels of adjacent first order lamels are inclined in opposite directions, which intersect at angles of 82° and 98°.

This interpretation is correct in its essentials, if simplified in some respects.

Our own observations are as follows. Conventional light microscopy shows the inner surface of crossed-lamellar shell layers as a series of elongate, branching and interdigitating lenses, corresponding to the outcrop of the first order lamels (text-figs. 23–26). These are usually arranged concentrically, parallel to the shell or layer margin. They vary widely in their shape and size ; lengths of up to several millimetres and widths of about 0·5 mm. are common.

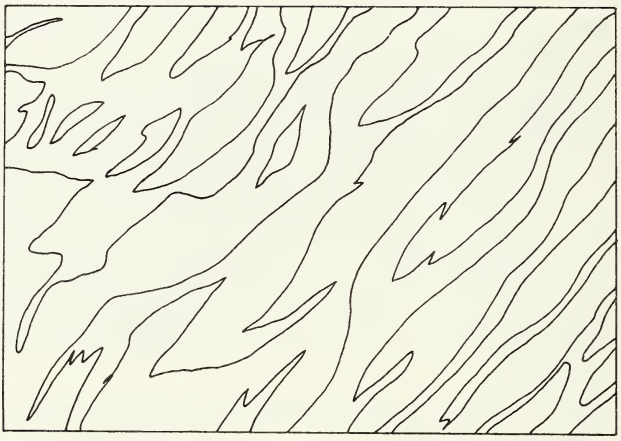

23

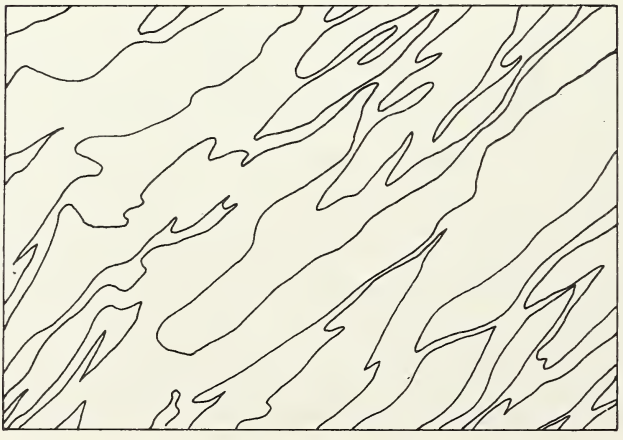

24

Becke line studies on a Universal stage reveal that the whole of a crossed-lamellar shell layer is an intergrowth of carbonate crystal in only two orientations, and alternate first order lamels represent regions of crystal in alternate orientation. Thin sections of crossed-lamellar structure in certain directions are symmetrically orientated with respect to both sets of first order lamels, and there is then no contrast in refractive indices between them ; in such orientations it is very difficult to see the boundaries between adjacent first order lamels, and they can only be distinguished by the orientations of their constituent second order lamels.

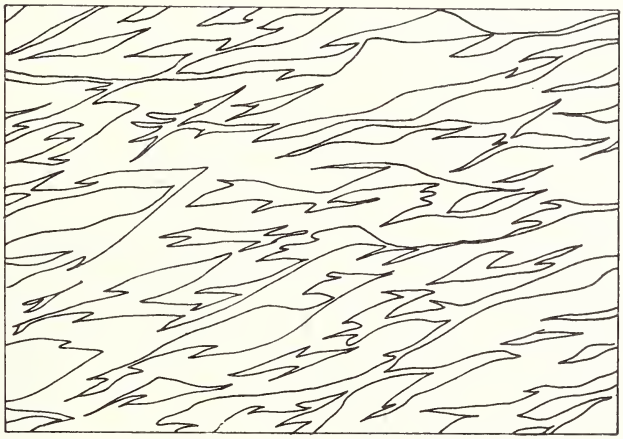

25

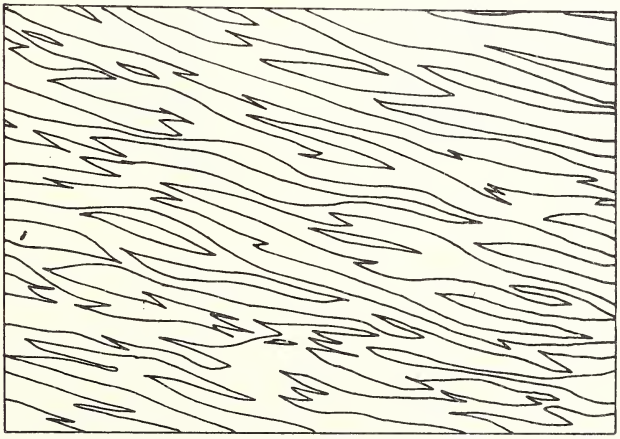

26

FIGS. 23–26. Planar sections of crossed-lamellar structure (based on acetate peels), to show the variation in shape of first order lamels. The long axis of the first order lamels are arranged concentrically to the shell margins. Figs. 23–24. *Hippopus hippopus* ×90. Fig. 25. *Glycimeris glycimeris* ×90. Fig. 26. *Spondylus calcifer* ×90.

In vertical, radial sections, crossed-lamellar structure shows very characteristic colour patterns, first order lamels being alternately straw or red-brown in colour. The first order lamels are usually normal to the inner surface of a shell layer, although they sometimes develop complex twists and turns when traced upwards through a shell layer towards the outside of the shell, being first curved and inclined, and eventually subparallel to the outer surface of the shell, or shell layer. Individual first order lamels frequently branch, lens out, and interdigitate (text-fig. 27). With such complexity of form, it is difficult to estimate the total height of first order lamels ; any one section may show every variation from short, isolated lenses to a continuous branched, twisting band, which in some cases extends for almost a centimetre, and perhaps even through the whole thickness of the shell layer. Variation

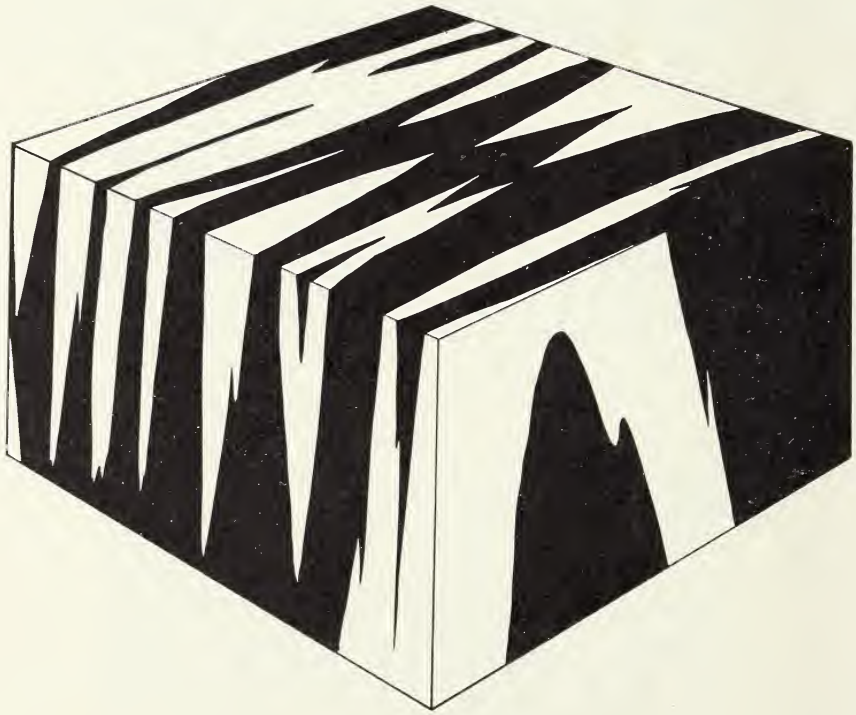

Fig. 27. Block diagram of crossed-lamellar structure based on *Lima squamosa*. Showing the relationship of first order lamels. ×150.

of form in section is very great between species ; compare for instance the complex form seen in *Hippopus hippopus* (Plate 14, fig. 5) with the relatively simple first order lamels, normal to the shell surface, of *Spondylus* (Plate 14, fig. 6).

Detailed accounts of variations in the attitude of first order lamels in various groups are given by Bøggild (1930) and are not discussed further here ; but in any one species they vary greatly as a result of slight differences in the angle of intersection of ribbing and the plane of the section examined. Radial sections of

umbonal regions built up of crossed-lamellar structure show a characteristic pattern of diverging primary lamels (Plate 15, figs. 1–2). An interesting and puzzling feature of crossed-lamellar structure is the correspondence of individual first order lamels across prismatic myostracal bands, as is seen in the Spondylidae (Plate 4, fig. 1).

Internal structures of first order lamels are difficult to resolve by the techniques of light microscopy which we have used, but the presence of second order ' lamels ', approximately 1 micron thick is indicated. Optical examination of radial sections (i.e. those across the first order lamels) show some indication that second order lamels are in turn composed of even smaller lath-like units (i.e. Plate 14, fig. 5). Other sections, cut close to the length of first order lamels (Plate 14, fig. 1) show that the second order lamels of adjacent first order lamels incline in opposite directions. We have, however, been unable to confirm precisely the conclusions of Bøggild (1930 : 251–2) concerning the relative attitudes of first order lamels and their constituent second order lamels, or of the relative attitudes of second order lamels of neighbouring first order lamels.

We have made electron microscopic studies of inner shell surfaces and sections of the crossed-lamellar layer of *Hippopus hippopus*, *Tridacna maxima*, *Trachycardium consors*, *Codakia punctata* and *Barbatia fusca*. The only previous work of which we are aware is a brief note by Kobayashi, I. (1964).

Surfaces of individual first order lamels, as they outcrop on the inner surface of the shell, show irregular, roughly parallel outcropping sheets, corresponding to the second order lamels seen at optical level (Plate 16, figs. 1–2). In striking contrast to euhedral forms so frequently seen in nacreous and foliated structures, no trace of crystal faces can be made out. The growth fronts of the second order lamels are highly irregular and indented, although roughly parallel. The surface of each second order lamel exposed on the inner shell surface is covered in irregular, flattened mounds (Plate 16, figs. 1–2). The maximum observed distance between successive growth fronts of second order lamels is 4 microns, whilst second order lamels sometimes ' lap out ' completely (Plate 16, figs. 1–2). Within each second order lamel, there is a poorly defined division into smaller component lath-like units, joined together in side to side contact (Plate 16, figs. 1–2). In some replicas of surfaces of crossed-lamellar structure that we have examined, differences in orientation and inclination of the second order lamels indicate the contact between adjacent first order lamels ; boundaries are irregular and very poorly defined (Plate 15, fig. 1).

Sections confirm that the second order lamels are made up of laths (Plate 16, fig. 3 ; Pl. 17, figs. 1–4 ; Pl. 18, figs. 1, 3) as is suggested by their surface morphology. The laths are parallel sided, with rather irregular, rounded or rectangular sections (Plate 16, fig. 3, Pl. 18, fig. 4), about a micron or occasionally more in diameter ; the greatest exposed length of a lath noted was 8 microns, in *Hippopus hippopus*.

Deeply etched sections (Plate 15, figs. 3–4) indicate that each lath is surrounded by a thin envelope of organic matrix. This is seen in transverse sections of the lath as a branching membrane (Plate 15, fig. 4) and in longitudinal section as a band between adjacent laths (Plate 15, fig. 3). Occasionally, lath surfaces are

covered by fine reticulations, which we believe to be replicas of the actual structures of the surrounding organic membrane. In some sections, the organic matrix separating adjacent second order lamels is much thicker and more conspicuous than that separating laths in the same second order lamel. Organic matrix is sometimes visible in fractured sections (Pl. 18, fig. 4).

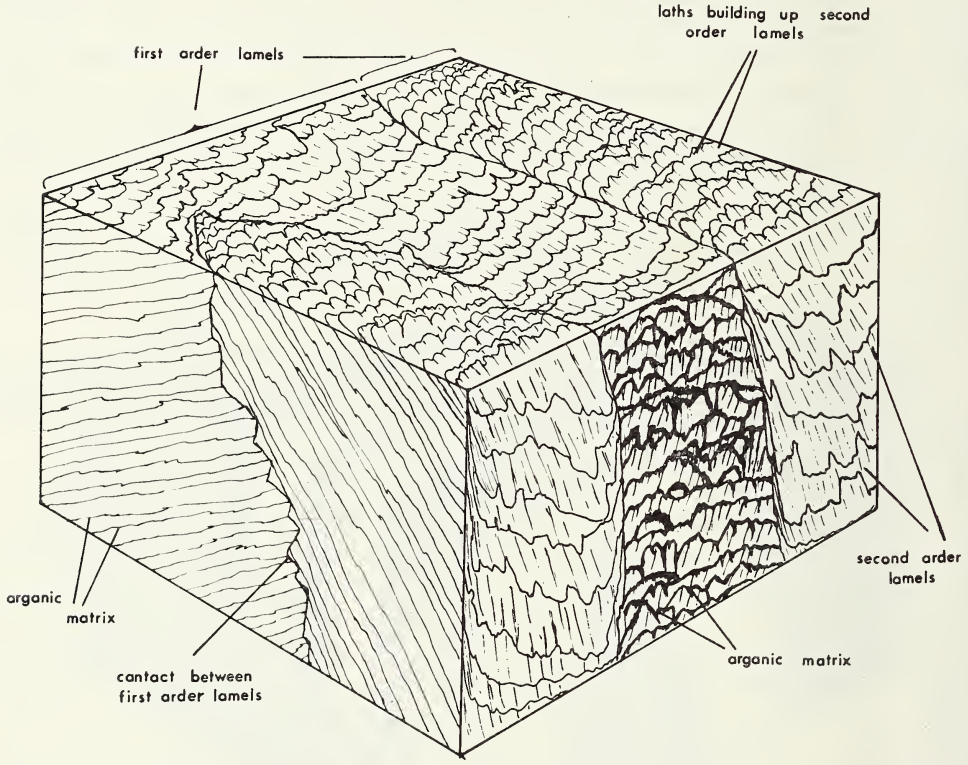

Fig. 28. Generalised block diagram of crossed-lamellar structure based on electron microscopy. Shown are three adjacent first order lamels with their constituent second lamels and laths. ×1500.

Longitudinal sections of laths (Plate 15, fig. 3 ; Pl. 17, figs. 1–3) sometimes show faint, parallel, longitudinal and transverse striations, which may possibly represent cleavages accentuated by etching. As on surfaces, boundaries between adjacent first order lamels are poorly defined and irregular, as suggested by light microscopy in certain instances (i.e. Plate 17, fig. 3). The general relationships in crossed-lamellar structure are summarised in text-fig. 28.

The relationships shown in this figure appear to explain the characteristic colour alternation seen in thin sections of crossed-lamellar structure. First order lamels cut approximately transversely to the second order lamels and laths are dark, and those cut approximately along second order lamels and laths are light. The amount of organic matrix intersected by the section is greater in the former case.

Refraction at the boundaries of first order lamels also causes the two sets of first order lamels to differ in brightness. The very striking pseudopleochroism, produced as a result of the presence of the organic inclusions (Hudson 1962, with references) accentuates this effect.

COMPLEX CROSSED-LAMELLAR STRUCTURE

Plate 14, fig. 3 ; Pl. 17, fig. 5 ; Pl. 18, fig. 2, Pls. 20, 21, 22 ; text-figs. 29.

The terms ' Complex ' structure and ' complex crossed-lamellar ' structure were introduced by Bøggild (1930 : 254), and have had a rather confused usage.

Complex crossed-lamellar structure, as originally defined, referred to a structure which is essentially built up of lamels corresponding to those of the second order in crossed-lamellar structure.

Complex structure (Bøggild 1930 : 254) refers to alternation of layers of complex-crossed lamellar structure with layers of a finely prismatic structure.

Oberling (1964 : 16), however, takes the view that the prismatic part of complex structure is " probably in most cases adductor and other myostraca ", and uses the term complex structure " whenever complex crossed-lamellar units predominate ".

This change in usage is confusing, and we have preferred to use complex crossed-lamellar structure in its original sense, and have abandoned ' complex ' structure as a term.

Complex crossed-lamellar structure is built up of the same structural elements as crossed-lamellar structure, with slightly different form and arrangement ; laths are arranged together in side-to-side contact to form second order lamels. Blocks of second order lamels build up the structure. The second order lamels are inclined in opposite directions in adjacent blocks. Complex crossed-lamellar structure shows the same straw-red/brown colour and pseudopleochroism as crossed-lamellar structure. It differs, however, in that the largest units are not concentrically elongate first order lamels but are much less regular, and more variable in form ; the whole of a shell layer often appears to be built up of a few large blocks of interpenetrant second order lamels only, as is shown in text-fig. 29.

Complex crossed-lamellar structure varies greatly, depending on the form and arrangement of the larger elements. At optical level it can best be described by reference to some commonly occurring forms.

In the Arcacea for instance (Plate 19, fig. 3), the outer part of the inner, complex crossed-lamellar layer, next to the pallial line, is seen in radial section as large, distinct, triangular or rhombic blocks made up of second order lamels, inclined in opposite directions in adjacent blocks. Traced downwards, towards the interior of the shell, these two inclinations can be traced as much smaller, elongate feathery patches (Plate 19, fig. 3) extending throughout the whole layer (text-fig. 29). Between these patches are areas with a much darker, honey-brown colour, lacking lath-like form and appearing minutely granular. These suggest a transverse section across the laths building up second order lamels.

In transverse section, the outer part of the layer is again seen to be built up of large, elongate blocks of differing colours, usually with a granular appearance, although sometimes showing traces of lamels inclined in opposite directions in adjacent blocks. In the inner part of the layer, patches of lamels are inclined in opposite directions and darker, granular patches are again visible between them.

The pattern produced is very complicated in sections taken in whatever direction ; a possible interpretation is to consider the layer to be built up of large blocks of second order lamels, inclined in several different directions. In the outer part of the layer these are discrete, but they become increasingly interpenetrant when traced downwards towards the inside of the shell.

Another type of arrangement, present in the inner ' complex ' layer of the Limopsacea, was described by Bøggild (1930 : 255) in a Miocene ' *Isocardia* '. In radial section, much of the layer is again built up of groups of second order lamels, inclined

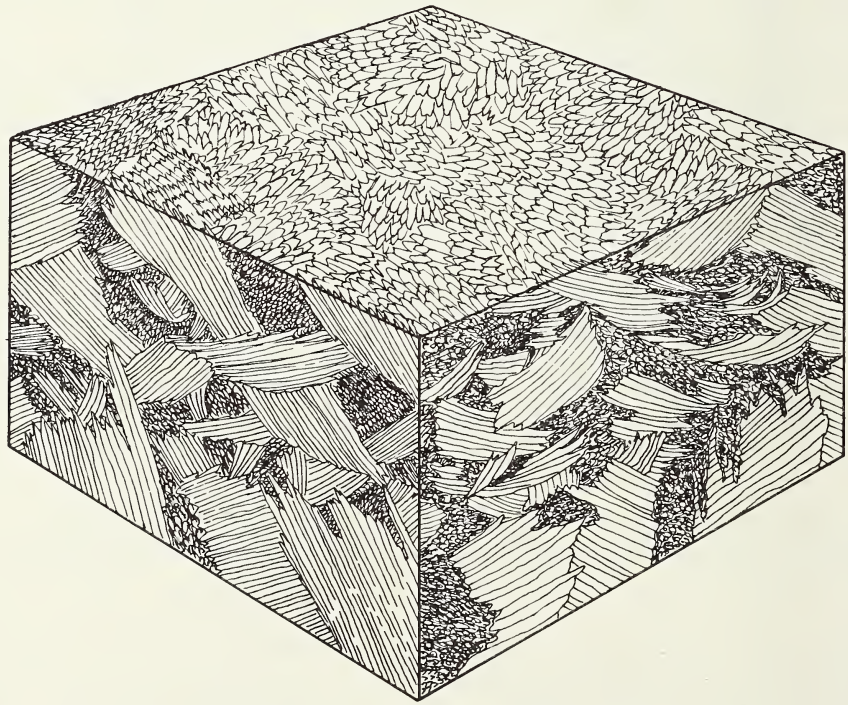

Fig. 29. Block diagram of complex crossed-lamellar structure based upon electron micrographs. Lath size in section exaggerated for clarity. The inner surface of the shell is indicated.

in opposite directions ; groups of lamels in this case have a distinctive columnar arrangement, normal to the shell surface (Plate 19, fig. 2). Transverse sections show a rather similar pattern (Plate 19, fig. 6), Bøggild (1930) suggested that there is in fact a radial arrangement of lamels in this sort of structure. A similar view is expressed by MacClintock (1967).

A common occurrence of complex crossed-lamellar structure is alternation with bands of prisms (Plate 20, figs. 3, 4). The complex crossed-lamellar part is usually similar to that seen elsewhere in the class. The prisms are very like those secreted beneath areas of muscle attachment, and also resemble the peculiar pillars of prisms occurring in the Chamidae, Carditacea and some Aracea and Limopsacea. Their origin is quite unknown, but may result from some periodic secretion of a myostracal layer caused by temporary attachment of the mantle over the whole of its surface within the pallial line.

In some genera, notably *Hippopus, Tridacna* and *Glossus,* this type of structure is on a very fine scale, and locally resembles a homogenous structure. In such cases the distinct prismatic and complex crossed-lamellar layers are recognisable over limited areas only.

We have examined the ultrastructure of complex crossed-lamellar structure in several species, i.e. *Trisidos tortuosa, Stavelia horrida, Trachycardium consors, Codakia punctata, Anadara antiquata, A. grandis, Arca scapha, Barbatia fusca, Glycimeris glycimeris, Tridacna maxima* and *Caryocorbula amethystina.* As at optical level, there is variation in the morphology of both surfaces and sections.

The surface of the complex crossed-lamellar layers of most of the species we have examined show that they are built up of small, elongate laths, dipping down into the shell-surface. The laths join in side-to-side contact to form sheets, corresponding to second order lamels (Plate 17, fig. 5 ; Pl. 20, figs. 1–2 ; Pl. 21, fig. 1 ; Pl. 22, figs. 1, 2, 4). Each lath, as in crossed-lamellar structure, is surrounded by a thin organic membrane. The second order lamels vary in attitude over any particular specimen, and are arranged in patches of similar orientation, which we take to correspond to the outcrop of the blocks seen at optical level. The laths are very small. In *Trachycardium consors* they appear to be 0·5–1·0 microns wide, and are very poorly defined, with a resultant confused surface pattern. A similar arrangement is seen in *Tridacna maxima,* where we have been able to decipher little other than a mass of laths with highly irregular terminations, arranged into second order lamels, which in turn form patches with a similar orientation ; the exposed surfaces are highly uneven.

A very different pattern is seen in the arcid *Anadara antiquata* (Plate 21, fig. 4 ; Pl. 22, fig. 1). In this species the surface relief of the complex layer is much more subdued than in most other species examined. It is built up of successively overlapping laths with well formed terminal faces (Plate 21, fig. 4) ; the laths are usually 0·5 to 1·0 microns wide, and may be exposed for lengths of up to about 4 microns. The laths are again joined in side-to-side contact to form second order lamels. Orientation of the laths is parallel over patches of shell surface, but varies between adjacent patches. The boundaries between these patches are rather poorly defined.

The surfaces of laths are very smooth, with no trace whatsoever of any organic matrix, unless the darker blobs seen on replicas at the point of lath terminations are a replica or pseudoreplica of an organic membrane.

Sections confirm the complicated arrangement of laths seen at optical level. The etched surfaces appear as a complex of laths cut at all angles. Some areas

show longitudinal sections of laths, inclined in opposing directions in adjacent areas (Plate 18, fig. 2 ; Pl. 21, figs. 2–3). Laths in these discrete areas have a similar, parallel attitude. Separating these areas are patches of a much more irregular structure which are interpreted as sections across laths (Plate 21, fig. 3) ; the contacts between areas of laths with similar orientation are highly irregular and complicated.

Sections also reveal details of carbonate/organic matrix relations. Each lath is surrounded by a membranous envelope. Minute dimples within the carbonate of laths are interpreted here, as elsewhere, as traces of intracrystalline organic matrix. Plate 18, fig. 2 shows the relation of complex crossed-lamellar structure to bands of myostracal-type prisms, in a section of *Ensis siliqua*.

A previously unrecorded occurrence of what we have taken to be a complex crossed-lamellar structure is seen in some mytilids, notably the genera *Modiolus* and *Stavelia*. In some species of these two genera, the inner layer of the shell is built up of interpenetrant sets of second order lamels. These are seen in radial section as elongate, branching, or triangular areas, which are normal to the shell interior and which show the characteristic colour and pseudopleochroism. Electron microscopy has confirmed this layer in both *Stavelia horrida* and *Modiolus auriculatus*.

Scanning electron microscopy has confirmed our conclusions on the nature of complex crossed-lamellar structure. Surfaces of this layer of *Caryocorbula amethystina* are built up of laths with quite irregular, pointed terminations, with a much higher relief than is suggested by conventional electron microscopy. These laths do not show a distinctive arrangement into second order lamels, but rather into blocks of similarly orientated laths, which must correspond to those seen at optical level, the orientation and attitude varying from block to block.

The surface of the complex crossed-lamellar layer of *Barbatia fusca* has a much more subdued relief. The laths have well-formed terminal faces and are arranged in blocks of uniform orientation ; the pattern is identical with that found in *Anadara antiquata*. In sections this structure has a distinct ' fibrous ' appearance. Fibres correspond to the laths building up second order lamels. The laths are long, extending across the whole field of view and probably across the blocks that they form. As on surfaces, the contacts between blocks are quite irregular. The whole structure appears as a mass of interpenetrant laths with a limited number of attitudes. (Plate 21, fig. 2).

HOMOGENEOUS STRUCTURE

Plates 23, 24.

Homogeneous structure was defined by Bøggild (1930 : 245), and the term has been used by subsequent authors (MacKay 1952, Oberling 1964). It is always aragonitic.

In peels and sections this structure is very difficult to decipher. Between crossed polars it shows a parallel extinction over wide areas of shell, usually with the crystallographic *c* axis normal to the shell surface. As used by Bøggild (1930), homogeneous structure includes structures which contain traces of other structural types, and

may pass into a crossed-lamellar, prismatic or foliated layer. The term ' homogeneously grained structure ' is used by Bøggild where there is a homogeneous groundmass consisting of many small carbonate grains. This is clearly a term of convenience for any fine-grained shell structures, and indeed in the Limidae we would regard the ' homogeneous ' outer layer as finely foliated, while in the Mytilidae we regard the ' homogeneous ' outer layer as finely prismatic.

In several other groups, however, notably the Nuculanacea, Arcticacea and Glossacea, there is a strong case for recognising homogeneous structure as a distinct structural type, although each individual group in which this name is used requires investigation at electron microscope level. Oberling's definition of homogeneous structure (1964 : 42) as ' A structure wherein there is no recognisable pattern ' reflects the difficulties of interpretation of this structure at the level of ordinary optical microscopy. We have taken *Arctica islandica* for a detailed examination of this structure and have also examined the nuculanacean *Adrana*.

In *Arctica*, as in several other forms (*Nuculana*, *Yoldia*, *Glossus*), the shell is dense and porcellaneous. In peels and sections of the inner layer, within the pallial line there is a marked colour banding, in greys and browns. The only fine structure that can be resolved is a suggestion of minute grains, which are most conspicuous in the translucent, grey-colourless parts of the shell. These grains are arranged in sheets parallel to the shell interior. In the outer layer grains can also be resolved, but are arranged in sheets parallel to the margin of the shell and growth lines. There is also an indication of an arrangement of grains normal to the shell interior.

These features can be seen more clearly in the umbonal region, where the arrangement of grains normal to layering is conspicuous. This arrangement of grains into layers corresponds to a very fine banding in the internal ligament, which suggests that the layering is a reflection of a repeated (? diurnal) deposition of carbonate. Another feature of the umbonal region (to be discussed later) is the presence of very thin (2–3 micron) prismatic bands parallel to the layering.

Outside the pallial line, the outer shell layer is very dense and opaque. The most obvious features are, again, the suggestion of fine grains arranged in sheets, giving the layer a very finely banded appearance.

This general picture, agreeing well with Bøggild's observations, is confirmed by electron microscopy. We have examined unetched inner surfaces, unetched fractured sections, and polished and etched sections of both shell layers.

Inner surfaces of the outer layer show a complicated pattern, lacking the regularity seen in so many other shell structure types. The structure is built up of minute, irregular, rounded granules, arranged in rows across the shell surface. In general, the granules are about 1·5 to 2 or 3 microns across, although their size is quite variable, depending in part on the degree to which granules are overlapped by their neighbours. The granules have highly irregular contacts with their neighbours, from which they are separated by an envelope of organic matrix. Sometimes, when a granule has been torn out in cleaning, these envelopes lie on the surface as pseudoreplicas. The surfaces of individual granules are rounded, with an irregular

terraced appearance. Minute bosses 0·2 microns in diameter are scattered all over the surface.

Inside the pallial line the structure is similar. It is built up of small, irregular granules, which sometimes outcrop in rows, although they usually appear as more continuous sheets. The surfaces of the granules inside the pallial line are much flatter than those outside, although they are still terraced. In some cases the larger granules appear to contain sheets of organic matrix, and are either built up of smaller blocks or are subdivided into compartments by the sheets of organic matrix.

These observations are confirmed and extended in replicas of polished and etched sections (Plate 24, fig. 4). Here the granules appear as elongate, lenticular or irregular blocks of carbonate, usually 1–3 microns long and 0·5–0·7 microns thick, with a poorly defined horizontal and sometimes vertical stacking. Each granule is surrounded by an organic membrane. This is seen on replicas as flaps, which are either replicas or pseudoreplicas of the actual membrane (Plate 24, fig. 4). In some cases, these membranes extend into the grains, dividing them into compartments. Etching also reveals minute ' dimples ' and filaments within granules ; these too seem to be traces of organic matrix. A rather poorly defined variation in the grain size of successive layers can sometimes be observed. This corresponds to a similar variation seen at optical level. Some replicas from the umbonal region of *Arctica* show a peculiar rhomboidal pattern (Plate 23, fig. 3). This may be due to a modification of the granule arrangement associated with the curvature of the layering in this region of the shell.

Electron microscopy reveals that virtually the whole of the *Arctica* shell is built up of carbonate granules set in organic matrix. It is difficult to reconcile this with Bøggild's (1930) comment that ' the homogeneousness is obscured . . . by the existence throughout the whole mass of so many small grains that the extinction is in many places difficult to see '. It is certainly not true that the inner layer, with its prominent banding, is a ' representative of the common complex structure '.

In *Adrana* examination of the inner surface failed to reveal any structure whatsoever at magnification of less than × 2000. At higher magnifications the surface appears granular. In *Clavagella* the inner surface of the tube is built up of small, irregular, flattened granules, up to 4 microns in diameter, of similar form to those seen in *Arctica* (Plate 24, fig. 2). The same features are seen in *Thracia* (Plate 24, fig. 3).

MYOSTRACAL LAYERS

Plate 4, fig. 1 ; Pl. 14, figs. 1, 2, 6 ; Pl. 18, fig. 2 ; Pl. 19, figs. 3, 4 ; Pl. 20, figs. 3, 4 ; Pl. 25 ; Pl. 26, figs. 1–4 ; Pl. 37 ; text-figs. 30–33.

We have adopted the general term ' myostracum ' for that part of the bivalve shell substance which is laid down beneath the areas of muscle attachment. This term is partly equivalent to the ' helle Schicht ' of many authors, or to the hypostracum of Thiele (1893), Jameson (1912), Lowenstam (1964) and others, or to the

' pellucid layer ' of Japanese workers (Kobayashi, I., 1964). Individual myostraca may be differentiated, for example, as pallial, pedal or adductor myostraca. Of these myostraca, the pallial myostracum, the adductor myostracum or myostraca, and those myostraca associated with Quenstedt's muscles in the oysters (Stenzel 1963) are the most conspicuous.

Very little work has been carried out on the mode of attachment of muscle tissues to the shell. We have examined normal histological preparations of several species (*Glycimeris glycimeris*, *Scapharca clathrata* and *Chama jukesi*) and have commenced a study of the fine structure of the mantle and muscle region of the unionid *Anodonta cygnea*.

The attachment of muscle fibres to the shell appears to be by modified outer mantle epithelium cells, which constitute what is known as the myo-adhesive epithelium (Mutvei 1964). These fibres are *not* attached directly to the shell ; in the species we have examined there is a sheet of short, cuboidal epithelial cells between the fibres and the shell. These cells resemble those of the general outer mantle surface, but appear to contain ' collagen ' fibres. The actual mechanism of attachment of these cells to the shell is quite unknown. Hubendick (1958) has described the manner of attachment of muscle to shell in the gastropod *Acroloxus lacustris* (Müller) at ultrastructure level. He found that the cells of the myo-adhesive epithelium bear numerous microvilli 0·05–0·1 microns in diameter, and

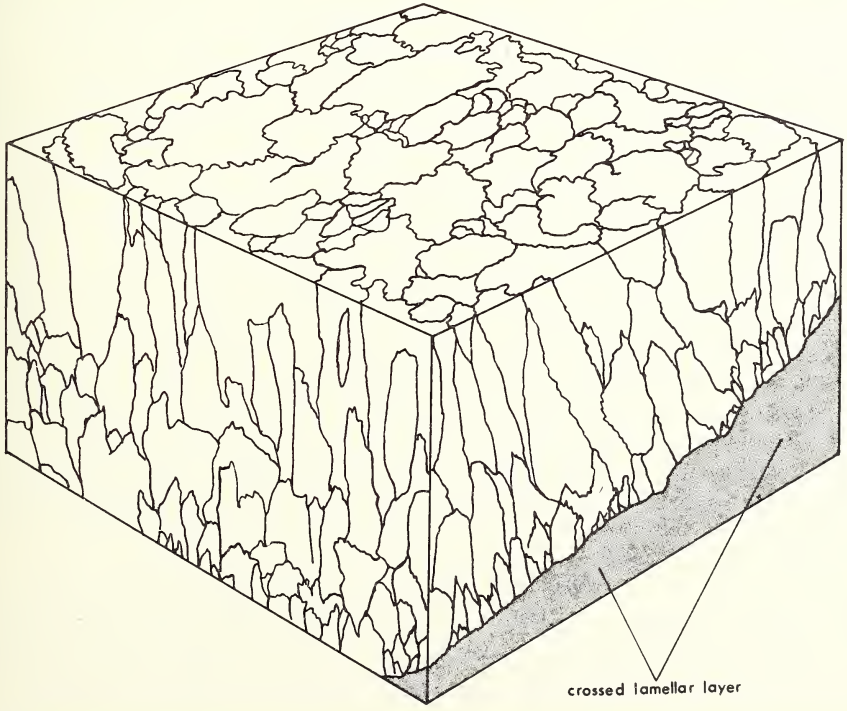

Fig. 30. Generalised block diagram of the fine structure of adductor myostracum based on electron microscopy. ×3000.

that these penetrate the shell substance. Our studies of the cells of *Anodonta cygnea* and those of Kawaguti and Ikemoto (1962b) on *Fabulina nitidula* show that even the mantle surface remote from any myostracal region bears microvilli in large numbers.

From studies on several hundred species of bivalves, two extremes can be recognised. The first extreme is where the myostracum is represented by a thick

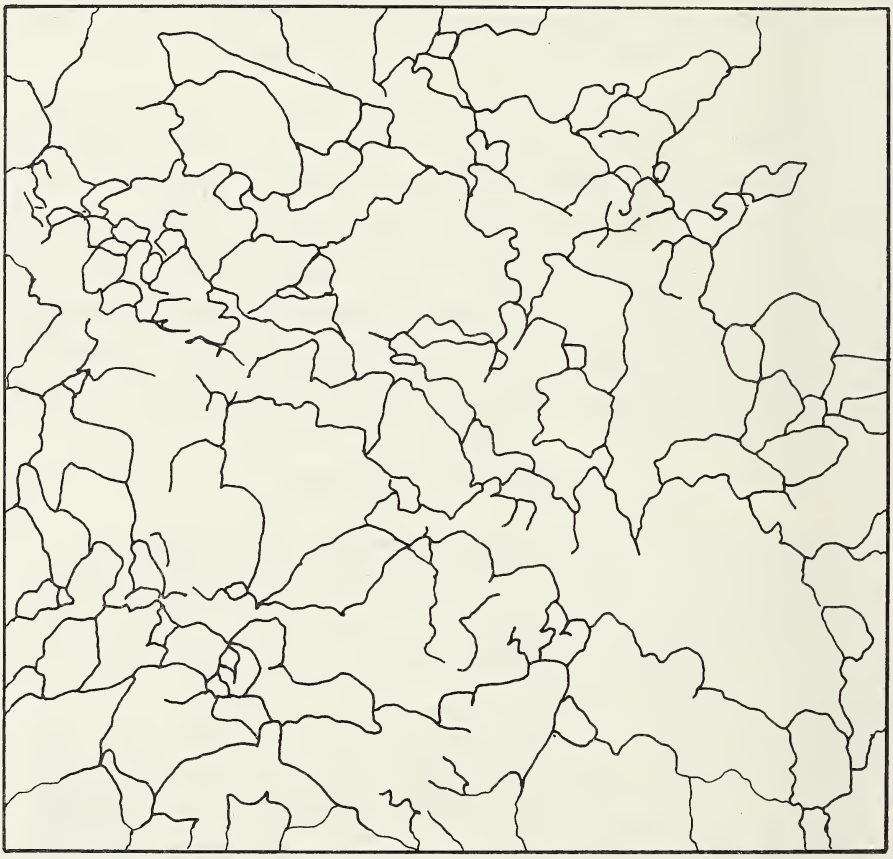

FIGS. 31–32. Fig. 31. Surface of the adductor myostracum of *Ostrea irridescens*. Showing irregular 'cells' enclosed by organic matrix. (Based on an electron micrograph.) ×5000. Fig. 32. Surface of the adductor myostracum in *Arctica islandica* (based on electron micrographs). ×5000.

carbonate layer or sheet within the shell. This sheet is invariably aragonite, and has a characteristic prismatic structure. The other extreme is where the myostracal trace can be followed through the shell, but where the myostracum is so thin as to appear as a line, with no definite associated sheet of prisms. Every intermediate exists between these two extremes, and sections may often show the pallial myostracum as a series of discontinuous lenses of prisms. In other cases,

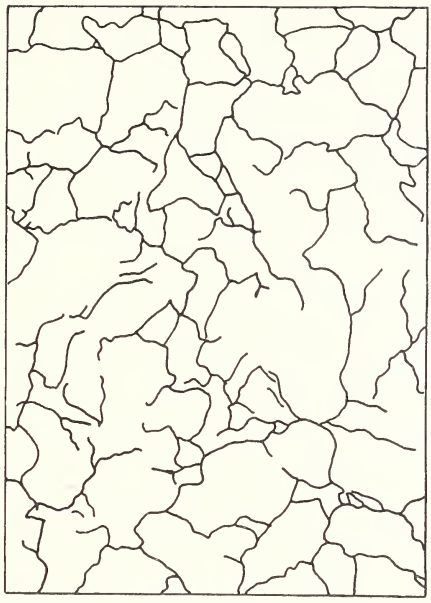

32

a distinctive prismatic pallial myostracum may be developed in the umbonal region only, as in some members of the Pectinidae.

When well developed, myostracal layers have a very characteristic appearance ; in peels and thin sections they are colourless, or appear light grey in contrast to the surrounding shell layers. On surfaces, thick myostraca are transparent, in contrast to the translucent or opaque aspect of the surrounding shell layers. Myostracal layers have a prismatic structure. The prisms are usually between 10 and 50 microns in diameter but vary greatly. They are oriented normal to the surfaces of the layer, with their crystallographic *c* axes oriented in the same direction. Horizontal sections show that the prisms differ greatly from those in the ' prismatic ' type of shell layer. There is no indication of a thick conchiolin wall surrounding each prism, while the prism outlines are highly irregular, with re-entrant angles. These outlines are sometimes rounded and may intrude into neighbouring prisms (text-figs. 31–32 ; Plate 25, fig. 3). Prisms vary greatly in both shape and size in different parts of the myostracal layer.

In general, the pallial myostracum lies between layers of differing in structural type (but see p. 95 : Spondylidae and Plicatulidae). In many cases growth lines are discordant between the inner and outer parts of the shell at this level, and where there is no very obvious prismatic layer, this separation of growth lines serves to indicate the position of the pallial myostracum. A thin prismatic band can then often be detected at high magnifications.

The pallial myostracum outcrops around the whole shell in most bivalves, forming a hollow cone of aragonite. This is thickened locally into the adductor myostraca which are detached from the pallial myostracum within the shell and have the form of distorted solid cones. Where there is no obvious continuity at the surface, the myostraca often join in the early parts of the shell.

We have examined the fine structure of the adductor myostracum in a number of species, e.g. *Arctica islandica, Modiolus auriculatus, Stavelia horrida, Ostrea irridescens, Trachycardium consors, Ostrea hyotis* and *Pseudochama corrugata,* and we have studied the pallial myostracum in *Margaritifera margaritifera, Trachycardium consors, Codakia punctata* and *Hippopus hippopus.*

The surfaces of adductor myostraca vary from species to species, but they all appear to be covered in irregular, polygonal " cells " (text-fig. 30). These " cells " correspond to the surface outcrop of the individual prisms building up the myostracum. The " cells " are marked out by thin, often discontinuous bands of organic matrix.

In *Ostrea irridescens* (Plate 27, fig. 2) the " cells " (text-fig. 31) vary between 0·5 and 8·0 microns in diameter over the surface of the adductor muscle pad. The outlines of the cells are highly irregular ; they may be polygonal or elongate, and have sharp, rounded or re-entrant angles. The surfaces of the " cells " show a very variable morphology. Some surfaces are smooth, while others have a slight relief of low, parallel, rounded ridges. The orientation of these ridges varies from " cell " to " cell ". The ridges are sometimes interrupted by minute elongate or rounded pits. Small irregular protuberances, sometimes seen as filaments, are present. We interpret these as organic matrix outcropping within the prisms.

" Cell " boundaries are marked by irregular, ragged, beaded lines, which we interpret as the inter-prismatic organic matrix. This matrix appears to be about 0·1 to 0·2 microns thick. Replicas suggest that it is rather variably developed ; the line separating cells may be discontinuous, or degenerate into a series of beads, so that some of the larger " cells " may be composite. Little information can be gained about the form of this organic matrix, although it sometimes appears on replicas as short filaments projecting upwards from the myostracum surface.

In *Arctica islandica* there is little trace of a prismatic layer associated with either the pallial or the adductor myostraca, even at high magnifications. The trace of the pallial attachment is indicated in section only by a change in the appearance of the shell structure and a change in the attitude of the growth lines between the inner and outer layers of the shell. However, electron micrographs of the surface of the adductor myostraca reveal a similar pattern to that seen in forms such as oysters, where a well-developed prismatic layer forms the muscle pad. Thus the surface of the *Arctica* myostracum is covered in minute " cells ", usually about 1·5 to 8 microns across. The outline of the " cells " is variable (Plate 27, fig. 1 ; text-fig. 32). They may be rounded, polygonal, elongate or even highly irregular. Individual cells are separated by thin, discontinuous, irregular lines, which at high magnifications can be seen to be replicas or pseudoreplicas of membranous sheets of organic matrix lying between the " cells " (Plate 27, fig. 3). These sheets sometimes appear as lines, which are often beaded, or they may disappear altogether. Traces of rather similar sheets of organic matrix are occasionally present within " cells " (Plate 27, fig. 3). The whole myostracal surface is covered in minute irregularities ; these may be pits, ridges and bosses, all of which are aligned in parallel within the limits of a single " cell ", although their direction of alignment varies between

neighbouring " cells ". On some areas of the myostracum surface minute elongate beads or fibrils are present. These are identical with the beads into which the sheets of organic matrix between cells sometimes breaks down (Plate 27, fig. 3). Problematic structures present on some parts of the myostracum are minute rings of projecting organic matrix between 0·1 and 0·3 microns in diameter (Plate 27, fig. 1).

The surface of the adductor myostracum of a specimen of *Ostrea hyotis* that we have examined showed some rather unusual features which are possibly associated with the gerontic condition of the specimen. Some areas of the myostracum are covered in minute rings. These are much smaller than those noted in *Arctica* ; they are up to approximately 0·025 microns in diameter (Plate 27, fig. 4). Some of these rings are associated with long filaments. These are either fibres projecting *from* the surface of the myostracum or replicas of tubes penetrating *into* the surface. Thus they might be fibres embedded in the shell substance. Alternatively, they may be pits in the myostracum surface, for insertion of the microvilli attaching the muscle to the shell. The " cells " seen on the myostracal surface of other forms are missing in this specimen. The surface of the myostracum is covered in minute rounded bosses ; these are about the same size as the possible fibres or pits.

Sections of myostraca show that they are built up of irregular prisms (text-fig. 30). In sections parallel to their long axes, the prisms are separated by thin irregular walls of organic matrix. Etching reveals traces of a longitudinal structure internal to the prisms. Rather more information is gained from oblique sections, where etching shows that each prism is surrounded by an organic envelope (Plate 26, figs. 1, 2, 4), which is usually seen as a ragged replica or pseudoreplica. There is sometimes a suggestion of fine structure within this organic envelope, which appears as sheets or reticulate networks of very thin fibres. There are sometimes indications of intra-prismatic matrix within the prisms.

There is also a progressive increase in prism size and decrease in the total number of prisms present in the myostracum when traced from the outer to the inner part of the myostracal layer. This represents geometric selection away from the point of initiation of the myostracal prisms similar to that noted in prismatic shell layers.

The surface of the pallial myostracum has been examined in one species only, i.e. *Margaritifera margaritifera*. In this species the surface is covered in " cells " with irregular rounded outlines. These " cells " are approximately 4 to 6 microns in diameter. Each " cell " is surrounded by a sheath of organic matrix. Within the sheath the surfaces of the " cells " appear as irregular, sometimes terraced mounds. There are definite indications of organic matrix within the " cells".

Sections through the pallial myostracum show features rather similar to those seen in sections of adductor myostracum. In the species we have examined to date, i.e. *Hippopus hippopus, Trachycardium consors, Codakia punctata* and *Margaritifera margaritifera*, the pallial myostracum consists of a single layer of prisms about 4 microns thick. Individual prisms have variable apparent diameters of up to 1 micron. The prisms are separated by thin bands of organic matrix, each of which

appear as a series of ragged flaps or as a beaded line. The termination of individual prisms against adjacent shell layers is irregular and this produces an undulating boundary to the myostracum.

As well as forming definite myostracal layers, the very distinctive myostracal prisms occur in two other ways : as ' pillars ' within the inner shell layer of some species of bivalve, and as sheets, alternating with complex crossed-lamellar structure (as already discussed) or alternating with sheets of nacre, as in some mytilids.

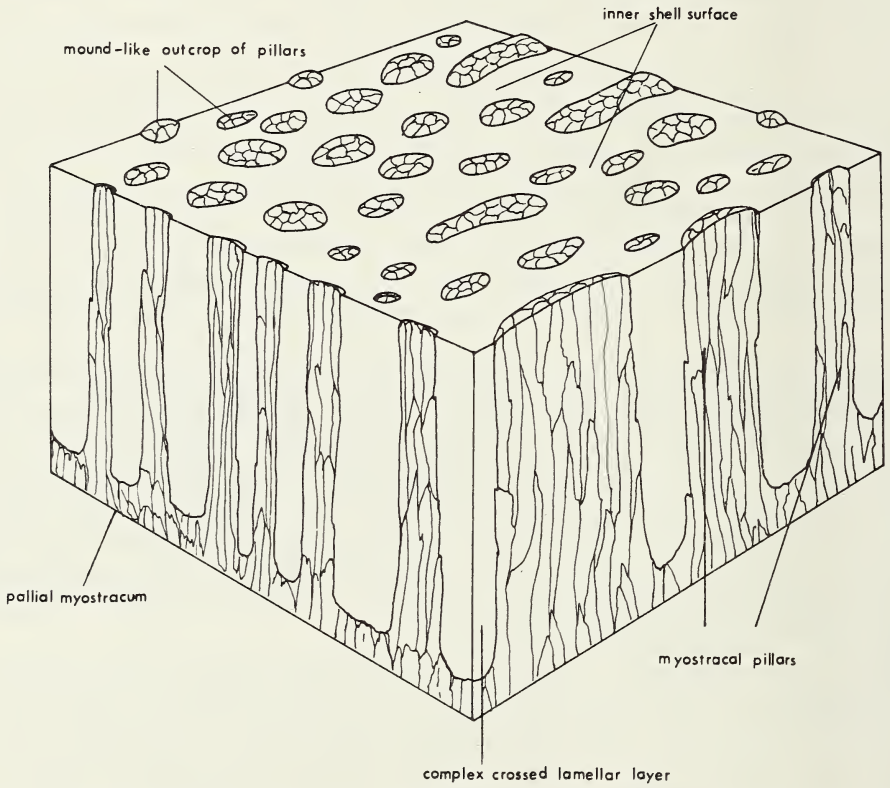

Fig. 33. Block diagram of myostracal pillars in the inner complex crossed-lamellar layer of *Chama nubea*. ×50. Details of the structure of the complex crossed-lamellar layer are ommitted. The top of the diagram represents the inner surface of the shell.

Myostracal pillars occur in several groups, and they are very prominent in the Chamidae, Carditidae and some Arcacea and Limopsacea. These pillars appear in peels and thin sections as elongate blocks of myostracal type prisms which are quite distinct from the surrounding structure (Plate 25, figs. 1, 5 ; text-fig. 33). Myostracal pillars are usually about 0·1 to 0·5 mm. across, although their size varies from species to species.

Most sections show the myostracal pillars as elongate ovals, with the long axis of the oval normal to the inner shell surface. When a section intersects the pillars

at the inner surface of the shell, they can be seen to project above the surface as distinct bosses (Plate 25, fig. 1). Other sections show that many of the myostracal pillars arise from the pallial myostracum, so that it seems reasonable to interpret these as pillar-like outgrowths which are continuous with the pallial myostracum. On inner surfaces of shells the myostracal pillars outcrop as circular, oval or elongate bosses. These are sometimes arranged in rows which radiate from the apex of the shell.

If myostracal prisms indicate attachment areas, as they appear to, it seems reasonable to interpret myostracal pillars as a result of continued attachment of the soft body of the animal to its shell in small patches and bands all over the general outer mantle surface as well as at the usual attachment sites.

Sections were made of the appropriate areas of mantle of *Chama jukesii*. These show that the outer mantle surface is locally modified into small papillae which are produced by elongation of the normal mantle cells. These papillae agree in size and general outline with the myostracal pillars present in the shell of this species, and we regard them as the actual points of mantle attachment to the myostracal pillars.

THE CONTACTS BETWEEN LAYERS

Plate 4, fig. 1 ; Pl. 2, figs. 2, 4, 5 ; Pl. 8, fig. 2 ; Pl. 10, figs. 1, 2 ; Pl. 11, fig. 5 ; Pl. 12, figs. 3, 4 ; Pl. 14, figs. 1, 2, 3, 6 ; Pl. 17, figs. 1, 2 ; Pl. 19, figs. 3, 4 ; Pl. 20, figs. 3, 5 ; Pl. 25, fig. 4 ; Pl. 26, figs. 4, 5.

The contacts between layers are, because of replication problems, difficult to study by conventional electron microscopy. Where we have been able to study them, there is always a transitional zone, which although distinct in structure has certain features in common with the structures of the layers both above and beneath (cf. Wilbur 1964).

The contact between prismatic and foliated layers has been studied in detail by Watabe and Wilbur (1961). It is characterised by abundant deposition of organic matrix upon which small regular hexagonal or rounded crystals have been deposited.

At the junction of the prismatic and nacreous layers in *Margaritifera margaritifera* and *Anodonta cygnea*, the surface of the conchiolin walls of the prismatic layer becomes irregular and the conchiolin spreads over the surface of the calcium carbonate of the prisms. Layers of small rounded crystallites are deposited on this irregular conchiolin, which gradually becomes more regular and nacre-like further away from the contact. In *M. margaritifera* (Plate 8, fig. 2), some sections show that the development of the sheets of interlamellar matrix and the regular tablets characteristic of the nacreous layer, begins intermittently. Traces of interlamellar matrix and patches of nacre are mixed with the granular calcium carbonate of the prismatic layer. These become stronger and more continuous inwards, developing into a wholly nacreous layer.

The junction of the composite prismatic layer and the crossed lamellar layer in *Codakia punctata* is a narrow zone 2 to 3 microns wide. This has an irregular structure, with an indistinct horizontal lamination.

Scanning electron microscope studies of the junction of the prismatic layer and the lenticular nacre layer of *Neotrigonia* also show the gradual development of regular nacre tablets and columns of nacre from the granular carbonate of the prismatic layer. The junction of the prismatic adductor myostracum and the nacreous layer in *Modiolus auriculatus* is relatively sharp with no apparent transition zone, for the prisms terminate against a sheet of the interlamellar matrix of the nacreous layer.

The contact between the adductor myostracum and the crossed-lamellar layer of *Trachyardium consors* appears to be transitional (Plate 26, fig. 4). The laths building up the second order lamels of the crossed lamellar layer gradually increase in size and shape across the boundary and are intimately related to the prisms in the myostracum. The organic matrix surrounding the calcium carbonate in each layer *appears* continuous with that of the other layer, no definite breaks being recognisable.

A common feature of the contact between crossed lamellar layers where these are cut or separated by a myostracal layer is a correspondence of first order lamels across the myostracum. This feature is very conspicuous in the Spondylidae and Plicatulidae. At contacts of crossed-lamellar and complex crossed-lamellar layers there is a comparable correspondence, but in this case it is between first order lamels of the crossed-lamellar layer and blocks of laths in the complex crossed-lamellar layer.

LIGAMENT

(Plate 28, figs. 1–3 ; text-fig. 58)

The ligament is an almost uncalcified part of the shell which joins the two calcified valves dorsally, and functions as part of the opening and closing mechanism of the shell. The ligament usually consists of three layers, i.e. the periostracum, the lamellar layer and the fibrous layers. These layers are formed by mantle epithelial cells in the periostracal groove, in the outer part of the outer mantle fold, and in the mantle isthmus. The mantle isthmus is the dorsal part of the general outer mantle surface.

The dark brown lamellar layer of the ligament is formed of quinone-tanned conchiolin. The fibrous layer of the ligament is usually somewhat calcified, although the extent of the calcification is quite variable from species to species.

X-ray identifications of the calcium carbonate in the fibrous layer of the ligament of many bivalves show that it is always aragonitic. The aragonite is present as irregular fibres which are arranged with their long axes normal to the growth surface at the point of secretion of the ligament. Electron microscopy of the fibres in the calcified part of the resilium of *Chlamys*, (work in progress) shows that these fibres occur in bundles.

TUBULATION

(Plate 14, figs. 4, 6 ; Pl. 18, fig. 1 ; Pl. 19, figs. 1–6 ; Pl. 20, figs. 1–2; Pl. 22, fig. 2 ; Pl. 29.)

A prominent feature of many bivalve superfamilies, notably the Arcacea, Limopsacea, Pectinacea (Spondylidae) and Chamacea is the presence of minute cylindrical perforations known as tubules (Oberling 1964). These tubules are usually only a few microns in diameter and are open to the interior of the shell and penetrate through the shell layers including the periostracum.

The interpretation of tubules, which are certainly original features of the shell, is complicated by the presence of other perforations ; most similar are the tubes of boring algae which, however, form irregular, often branching, networks whereas tubules are relatively straight and regular and do not branch. Tubules are developed consistently within a species, genus or larger taxonomic group. We cannot agree with Kobayashi, I. (1964) who appears to regard tubules in *Barbatia obtusoides* and other species as possibly produced by external agents.

Tubules are developed to varying extents in different groups of bivalves. They may occur throughout the whole of the shell or may be restricted to the inner layer or layers. They may also vary in concentration over the shell interior. In general, the tubules are oriented approximately normal to the shell interior over the whole of the inner surface.

At optical level, tubules appear on shell interiors as minute perforations. In section tubules appear as straight, hollow, cylindrical perforations, cutting the fine observable units of shell structure of all types although not, in general, distorting the structures (Plates 29, figs. 1, 2).

Little more information on the detailed form of tubules can be gained from conventional microscopy. Tubules often have a well-defined margin in section, but we have seen no definite indication of any lining wall or any trace of an organic filling.

We have examined tubule/shell relations in the following species at electron microscope level ; *Trisidos tortuosa, Anadara grandis, A. antiquata, Barbatia fusca, Glycimeris* sp., *G. glycimeris, Stavelia horrida* and *Modiolus auriculatus.*

Conventional replication methods are rather unsatisfactory as in most cases the replicating fluid enters the tubule, and when finally examined the replica surfaces are covered in thick sock-like replicas of the tubule interior which obscure both the tubule opening and the details of the surrounding shell surface.

A much better picture of the structure and of the relationship between tubules and other parts of the shell is gained from scanning electron microscopy. At low magnifications, tubules appear as randomly distributed holes in the shell interior (Plate 29, fig. 3). At higher magnifications the opening of the tubule is seen as a distinct conical pit. The opening may show a distinct elongation in one direction so that the tubule lies assymetrically " off-centre ". There is no major modification of structure of the shell layer around the tubule. Thus the main trend of the second order lamels of complex crossed-lamellar structure remains undisturbed, while successive layers of lamels building the structure can be seen outcropping down the sides of the opening of the outer part of the tubule.

Fractured sections show tubules as straight-sided cylindrical perforations cutting through the shell structure (Plate 29, figs. 1, 2), again without disturbing or modifying the structure. The walls of the tubules are very smooth, with little trace of the surrounding structure in some cases. This may perhaps suggest the presence of a lining, although we have been unable to establish this definitely.

Little is known of the function and origin of tubules, although some information can be gained from their distribution within individual shells. Where tubules are present throughout the whole of the shell, including the marginal region, this could be the result of deposition *around* some extension of the outer mantle epithelium. Thus they would be an original feature of the shell accompanying shell deposition, like the punctae of brachiopods (Williams 1956, 1965).

In many bivalves, however, the actual abundance of tubules in a layer *increases* inwards from the margin of the shell and reaches a maximum in the region bounded by the pallial line. As this distribution is seen in individuals of different sizes and is a common feature in tubulate bivalves, it must result from the formation of *some* tubules at least subsequent to shell deposition, i.e. as a secondary, perhaps resorptive feature. Rather similar conclusions are drawn by Oberling (1964) on the basis of somewhat different considerations.

In order to determine whether soft tissues, presumably extensions of the mantle, are present in tubules, we have examined large numbers of serial sections of mantle and decalcified shell preparations of *Scapharca clathrata, Glycimeris glycimeris* and *Chama jukesii,* in all of which tubules are prominent. In no case have we seen any well defined structure which could be associated with tubules or extensions of the mantle, although some of our sections of *Scapharca* show traces of what appear to be cytoplasmic filaments shell.

A few comparable features have been described in other molluscs ; amphineuran aesthetes penetrate the shell, but these are much larger and have a very different form (Beedham *et al.* 1967). Rather more closely comparable to tubules are the epithelial papillae which fill the shell canals of the freshwater bivalve *Musculium lacustris* (Schröder 1907, Mutvei 1964). Schmidt (1959) records tubules in the monoplacophoran *Neopilina*).

Very small tubule-like structures of about 0·1 microns diameter (Plate 20, fig. 1) occur in mytilids, and extend throughout the whole shell. We have observed these definitely in *Stavelia horrida* and *Modiolus auriculatus* ; Dr J. D. Hudson (personal communication) is preparing a more detailed account of these structures, whose significance is unknown. They are of the same order of size as the microvilli of the outer mantle epithelium, so far as is known.

BANDING

Banding of some sort is present in almost every bivalve that we have examined in peel or thin section. Large bands correspond to annual or seasonal growth (Merrill *et al.* 1966) and can be linked to obvious growth lines on the outside of the shell. A much finer type of banding, with the bands usually about 5 to 10 microns thick, is present, and often conspicuous in prismatic, crossed-lamellar, complex

crossed-lamellar and homogenous structures (Plates 7, 14 etc.). This fine banding is also present in myostracal layers (Plate 14, fig. 2). Both types of banding can be traced into the ligament, whether this is calcified or uncalcified.

We have not investigated banding in detail, but it seems likely that the very fine banding is a diurnal phenomenon, produced by a secretory rhythm. This type of banding in molluscs is at present under investigation in the Geology Department, Yale University (Dr G. Panella, personal communication, Panella *et al. in litt.*). Similar fine banding is commonly present in many other invertebrate and vertebrate groups (Neville 1967).

Barker (1964) (on the basis of an examination of four species) has claimed recognition of a hierachy of five orders of banding in the Bivalvia.

Our only observation on banding is to suggest the possibility that alternate layers of complex-crossed lamellar structure or nacreous structure with layers of myostracal-type prisms is perhaps in some way related to normal banding.

SUMMARY OF STRUCTURAL TYPES

1. Nacreous structure	Rounded or euhedral tablets arranged either in thin sheets, separated by sheets of organic matrix (sheet nacre), or in columns (lenticular nacre). Invariably aragonitic.
2. Foliated structure	A dendritic aggregate of folia built of lath-shaped elements with euhedral terminations, joined in side-to-side contact to form sheets.
3. Prismatic structure	Columnar, usually polygonal blocks of carbonate, which may be simple or composite. Simple prisms are oriented normal to the shell surface, with each prism separated by a thick conchiolin wall. Simple prisms may be aragonitic or calcitic. Composite prisms lie parellel to the shell surface and are built up of fine acicular elements, which usually lack a thick conchiolin wall. Composite prisms are invariably aragonitic.
4. Crossed-lamellar structure	Elongate, interdigitating sheets oriented with the major and minor axes in the plane of the shell surface. These sheets are the first order lamels. They are built of inclined sheets (second order lamels) which in turn are built up of fine laths joined in side-to-side contact. Crystal orientation is uniform within a lamel but different in adjacent lamels. Invariably aragonitic.

5.	Complex crossed-lamellar structure	Blocks built up of laths arranged into second order lamels, as in crossed-lamellar structure, but with several different attitudes of lamels in the various blocks. Invariably aragonitic.
6.	Homogeneous structure	A very fine aggregate of granules with uniform optical orientation over wide areas of shell. Invariably aragonitic.
7.	Myostracal prisms	A ' prismatic ' aggregate laid down under areas of muscle attachment. Invariably aragonitic.

SYSTEMATIC DESCRIPTIONS

The mineralogy and distribution of shell structure types and other structural features of the living superfamilies of the Bivalvia are described below.

The classification adopted here is that of Newell (1965). This is to be used in the forthcoming Treatise on Invertebrate Palaeontology, part N, Mollusca 6 (Bivalvia), and is the most complete and up to date classification of the class.

The present account describes the superfamilies Nuculacea to Trigonacea ; the Chamacea to Poromyacea will be described in a subsequent account, which will also include comments and conclusions on the distribution of the various structural types, and the possible significance of this distribution in relation to problems of classification and evolution.

Sub Class *PALAEOTAXODONTA*
Order NUCULOIDA
NUCULACEA

(Plate 3, fig. 4 ; Pl. 11, fig. 5 ; Pl. 26, fig. 5 ; text-figs. 22, 34)

Thirteen species of Nuculacea were examined mineralogically and five optically. All species had completely aragonitic shells.

The outer shell layer is always formed of composite prismatic structure (see text-fig. 24 and Plate 11, fig. 5). This consists of large first-order prisms arranged with their long axes parallel with the spiral growth direction of the shell. These first-order prisms are discrete even at the earliest observable growth stages of shells, and they gradually increase in diameter during growth of the shell. Each first order prism appears to be separated from the neighbouring first order prisms by a thin organic wall. No branching or formation of new first-order prisms has been seen. Each first-order prism is made up of smaller thin and needle-like second order prisms. These are arranged in a feathery pattern, so that groups of second order prisms diverge from the central axis of each first-order prism, towards the prism margin, and towards the ventral margin of the shell away from the umbo. Concentric growth lines cut the first order prisms, and sometimes disrupt the continuity of the second order prisms. In section, the inner edge of each first-order

prism of the composite prismatic layer shows a well defined flange, projecting into the underlying middle nacreous layer (text-fig. 34 ; Plate 11, fig. 5). Each flange represents the trace of one of the internal marginal denticles present in nuculids. Near the umbo, the composite prismatic layer is thin, and it is frequently corroded and worn off from many specimens.

The middle shell layer is situated between the inside of the outer composite prismatic layer on the one hand and the pallial trace on the other. It has a very distinctive lenticular nacreous structure. The tablets are large and clearly visible, even on peels and thin sections at low magnifications (Plate 11, fig. 5). The lenticles are oriented normal to the growing edge of the layer at any one time. Intercrystalline and interlamellar organic matrix is conspicuous in this layer.

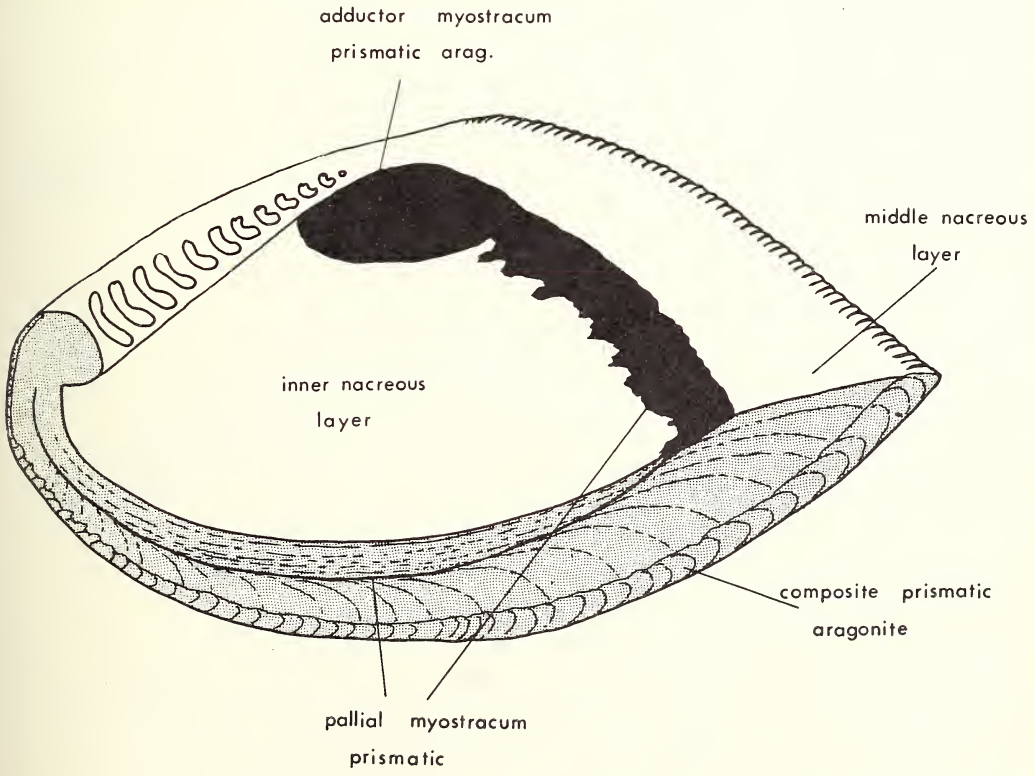

FIG. 34. Block diagram of the distribution of the shell layers in the Nuculidae (based on *Nucula placentina*).

In transverse section, the lenses of nacre tablets are arranged normal to the surface of the lower flange of each first order prism of the outer shell layer close to the contact with the outer layer, but when traced inwards towards the inside of the shell they come to lie in parallel. This change in attitude produces the apparent radiating effect present in the outer part of the middle layer, as is seen in Plate 11, fig. 5. Within the pallial line and within the trace of the pallial line lies the inner

TABLE 1

NUCULACEA

NAME	LOCALITY	COMPOSITION	OUTER LAYER	MIDDLE LAYER	INNER LAYER	MYOSTRACA	
						Pallial	Adductor
Nucula convexa (Sowerby)	Mombasa	Aragonite	Composite prisms	Lenticular nacre	Sheet nacre	Thin prismatic	
Nucula laevigata (Sowerby)	Pleistocene, Britain	Aragonite	Composite prisms	Lenticular nacre	Sheet nacre		
Nucula nucleus (Linnaeus)	Britain	Aragonite	Composite prisms	Lenticular nacre	Sheet nacre		
Nucula placentina (Lamarck)	Pliocene, Italy	Aragonite	Composite prisms	Lenticular nacre	Sheet nacre	Prismatic	
Nucula sulcata (Bronn)	Scotland	Aragonite	Composite prisms	Lenticular nacre	Sheet nacre		
Acila cobboldiana (Sowerby)	Pleistocene, Britain	Aragonite	Composite prisms	Nacreous	Nacreous		

Specimens of the following have been examined mineralogically, and were aragonitic throughout : *Nucula castrensis* (Hind), British Columbia ; *Nucula* sp., Greenland ; *Nucula sulcata* (Bronn), Pliocene, Sicily ; *Nucula pectinata* (Sowerby), Cretaceous, (Albian), Britain.

shell layer, which is also nacreous, although it consists of sheet nacre and is quite distinct from the middle nacreous layer. The nacre tablets are large, and again are clearly visible in peels and thin sections. There is a thick interlamellar matrix separating the layers of nacre tablets. The growth lines in this layer lie approximately parallel to the inner surface of the shell. The hinge and hinge teeth are both formed from the nacreous layers.

In *Nucula placentina*, a very thin prismatic myostracal band is present, but in most of the species examined the pallial myostracum is represented by a line only.

Electron microscopic studies have been carried out on the prismatic and nacreous layers of *Nucula sulcata*, and confirm the observations that we have made at optical level.

NUCULANACEA

(Plate 23, fig. 4 ; text-fig. 35)

Twelve species of Nuculanacea were examined mineralogically and six optically. All the species examined had completely aragonitic shells.

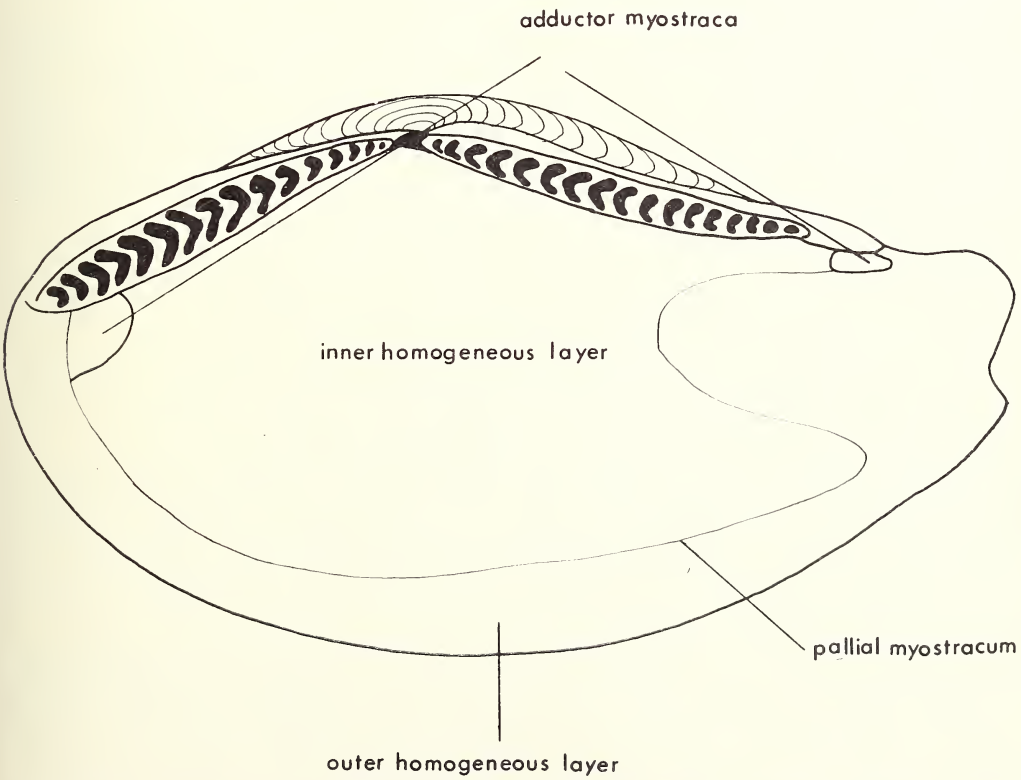

FIG. 35. Nuculanidae : View of the interior of *Nuculana emarginata* showing the distribution of shell layers and myostraca.

In the six species examined optically the shell consists of fine-grained homogeneous structure throughout (Plate 23, fig. 4). Only in *Nuculana crassa* and *Yoldia limatula* was any differentiation into inner and outer shell layers clearly seen, and in these two cases both layers were homogeneous.

The thickness of the shell in this superfamily is very variable. *Nuculana crassa* and *Nuculana oblongoides* are thick shelled, and here the homogeneous structure shows a distinct banded appearance similar to that seen in *Arctica* (p. 51). Thinner shells, such as those of *Yoldia eightsii*, are also banded which appears to be due to the development of thin conchiolin sheets within the homogeneous structure. Traces of pallial or adductor myostraca were indefinite. In *Nuculana crassa*, the position of the pallial trace and the contact between the inner and outer shell layers is marked by a discontinuity of growth lines and banding. The banding in the inner part of the outer layer is inclined to the shell surface, but when traced outwards it becomes quite strongly recurved and passes up into the concentric plicae on the outer surface of the shell. The banding in the inner layer, in contrast, lies parallel to the inner surface of the shell. A small wedge of prisms is present beneath the hinge plate of *Yoldia eightsii*. These prisms mark either the position of dorsal pallial attachment or of a pedal muscle.

Cox (1959) states that early fossil members of the Nuculacea and Nuculanacea are not easily distinguished, and that some Jurassic species of *Nuculana* have a nacreous layer. Inspection of specimens of *Nuculana* (*Ryderia*) *graphica* Tate (Jurassic—Lias—Britain) show that this species indeed has an inner nacreous layer. A study of shell structure changes in well preserved fossil material of this group, tracing the appearance of homogeneous structure in geological time would be of great interest.

Sub Class *CRYPTODONTA*
Order SOLEMYOIDA
SOLEMYACEA

(Plate 12 ; text-figs. 36–39)

Five species were examined mineralogically and two optically. The shell was aragonitic in all cases. Examination of members of this group is rather difficult, because the shell is very thin and brittle in museum specimens. The shell has a high organic content, which also makes examination difficult, especially the preparation of peels and thin sections.

The shell of members of this group is covered by a thick brown periostracum which may be up to 100 microns thick. In life this extends far beyond the calcareous valves, and radial pleats are developed around its margins. The calcified part of the valves consists of two layers, an outer prismatic layer and an inner homogeneous layer. At optical level, the prisms forming the outer layer have a form not seen in any other bivalves. On the inner shell surface the prisms are seen end-on as polygonal, elongate or irregular chambers. Each prism is surrounded

TABLE 2

NUCULANACEA

NAME	LOCALITY	COMPOSITION	OUTER LAYER	INNER LAYER	MYOSTRACA	
					Pallial	Adductor
Yoldia eightsii (Couthay)	Orkneys	Aragonite	Homogeneous		Prismatic	
Yoldia limatula Say	Lofoten, Norway	Aragonite	Homogeneous	Homogeneous		
Yoldia myalis Couthoy	St. Lawrence	Aragonite	Homogeneous			
Nuculana crassa auct.	Unlocalized	Aragonite	Homogeneous	Homogeneous	Trace	
Nuculana oblongoides Wood	Pleistocene, Britain	Aragonite	Homogeneous			
The following specimens were all aragonitic :—						
Adrana sowerbyana (d'Orbigny)	Ecuador ;					
Nuculana clavata (Calcara)	Pliocene, Nice ;					
Nuculana eburnea (Sowerby)	Ecuador ;					
Nuculana ensicula Angas	Tasmania ;					
Nuculana nitida (Brongiart)	Pliocene, Sicily ;					
Nuculana pella (Linnaeus)	Mediterranean ;					
Nuculana rostrata (Gmelin)	Arctic ;					

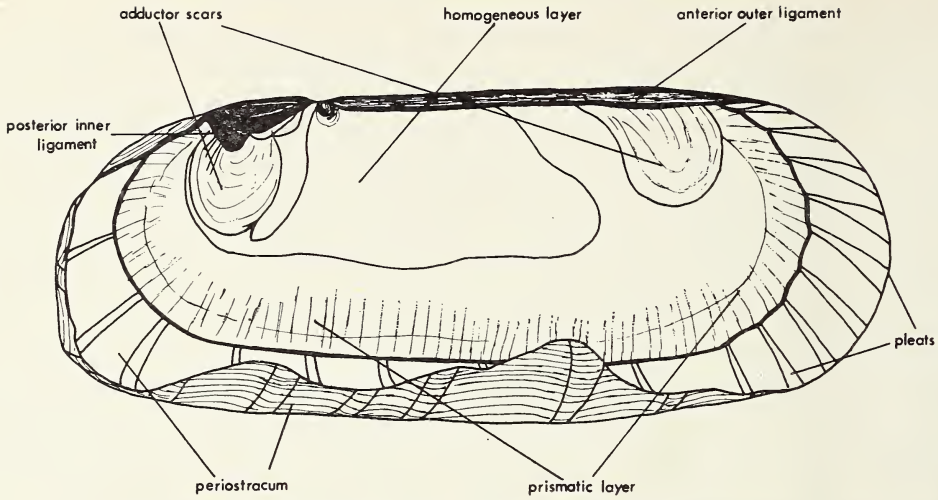

FIG. 36. Solemyacea : View of the interior of *Solemya australis* showing the distribution of the shell layers. The periostracum extends far beyond the shell margins, is pleated and infolded.

by a thick upstanding conchiolin wall usually about 8 microns thick (Plate 12, fig. 5). The prisms are very variable in shape, sometimes with re-entrant angles, but over much of the inner surface of the shell they are elongate with rounded terminations ; the direction of elongation is normal to the shell margins. Chambers are very variable in size, and in many areas the conchiolin walls are meandrine, while in other areas the polygonal pattern has broken down. In these areas the interprismatic conchiolin walls appear on the surface as short discontinuous lines and dots (text-fig. 38).

In section, the outer ends of the prisms lie normal to the inner surface of the periostracum, and are separated by thick, dark brown, conchiolin walls. Transverse banding is conspicuous within the prisms, and there is also a less prominent longitudinal banding ; geometric selection is seen, with small prisms, present near the periostracum, wedging out inwardly. In sections of *S. togata* the prisms branch, and bend ventrally when traced down towards the inner shell surface. At first they are inclined, and then bend sub-parallel to the inner surface of the shell. A complex branching and linking of conchiolin walls in this area produces a spongy appearance in sections.

The inner shell layer varies in extent from species to species, and within the same species. On the inner surface of the shell it appears as a dull, granular layer which spreads over the inner surface of the prisms of the outer layer, although there is no sharp boundary line between the two layers. In *Solemya parkinsoni*, Beedham and Owen (1965) record that the inner layer is restricted to an area immediately surrounding the posterior and anterior adductor scars. In section the inner layer has a finely laminated homogeneous structure. It is thickest in the dorsal areas beneath the umbone and thins ventrally.

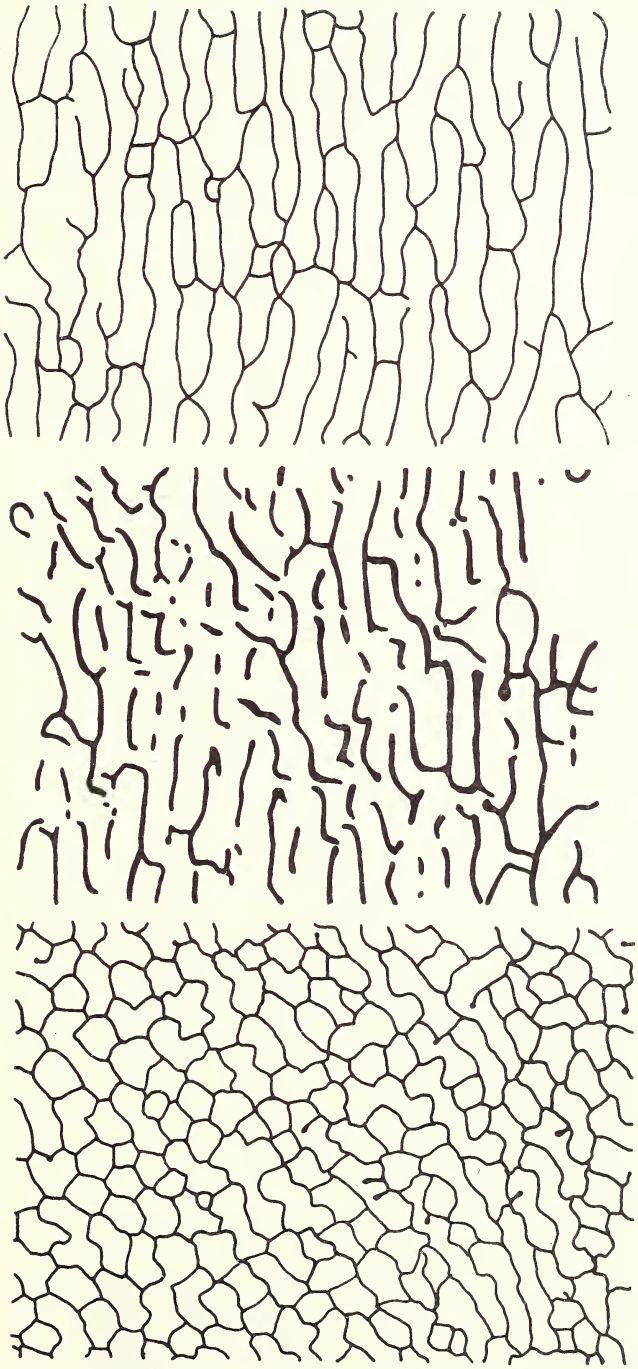

FIGS. 37–39. Variation of prism shape and the distribution of the conchiolin interprismatic walls on the inner surface of *Solemya australis*. ×100. The direction of elongation of the prisms is towards the shell margin.

TABLE 3

SOLEMYACEA

NAME	LOCALITY	COMPOSITION	OUTER LAYER	INNER LAYER	MYOSTRACA
Solemya australis (Lamarck)	South Australia	Aragonite	Prismatic	Homogeneous -laminated	
Solemya parkinsoni Smith	New Zealand	Aragonite	Prismatic	Homogeneous -laminated	
Solemya togata Poli	Italy	Aragonite	Prismatic	Homogeneous -laminated	
Solemya velum Say	Massachusetts, U.S.A.	Aragonite	Prismatic		
Solemya (*Acharax*) *winkworthi* Prashad	Seychelles	Aragonite			

We have examined *Solemya australis* by scanning electron microscopy, and find that within the conchiolin prism walls the aragonite is deposited as irregular plates and grains, apparently without any regular orientation in some chambers, although in others the grains seem to be deposited as a more regular surface (Plate 12, figs. 1–4).

The calcareous parts of the shell of *Solemya* have a high organic content, and the amino acid composition and histochemistry have recently been investigated by Beedham and Owen (1965). According to these authors, the non-calcareous organic matrix of the shell is made up of two types of conchiolin which they term ' A ' and ' B '. The outer layer contains their type ' A ' conchiolin which makes up 4·5% by weight of this part of the shell, and forms the prism walls. The organic matrix of the inner shell layer is mostly type ' B ' conchiolin. The two conchiolins have different amino acid compositions and the conchiolin in the outer layer is appreciably tanned, whereas the conchiolin of the inner layer is only lightly tanned.

Sub Class *PTERIOMORPHIA*
Order ARCOIDA
ARCACEA

(Plate 15, fig. 1 ; Pl. 18, fig. 1 ; Pl. 19, figs. 3, 4, 5 ; Pl. 21, fig. 4 ; Pl. 22, figs. 1, 2 ; Pl. 29 ; text-figs. 40–42)

Nineteen species of the group have been examined mineralogically and twelve optically (Table 4). The shell is aragonitic throughout.

Two main shell layers are present, i.e. an outer crossed-lamellar layer which forms the hinge and teeth, and an inner complex crossed-lamellar layer which is bounded by the trace of the pallial myostracum. In the outer crossed-lamellar layer, the first order lamels are arranged concentrically over the whole shell, except

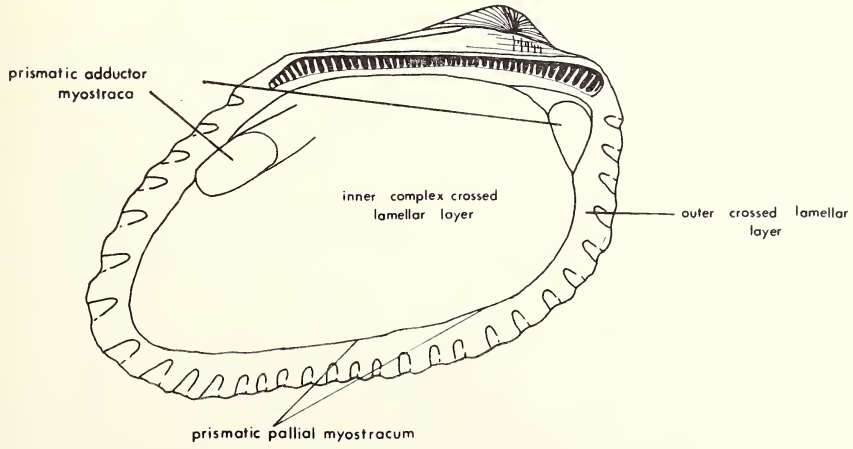

Fig. 40. Arcacea : General view of the interior *Anadara scapha* auct. showing the distribution of the shell-layers etc.

Table 4

ARCACEA

Name	Locality	Composition	Outer Layer	Inner Layer	Myostraca		Observations
					Pallial	Adductor	
Arca avellana Lamarck	Mombasa	Aragonite	Crossed-lamellar	Complex crossed-lamellar	Prismatic		Tubules in all layers, pillars of myostracal prisms in inner layer
Arca tetragona Poli	Britain	Aragonite	Crossed-lamellar	Complex crossed-lamellar	Prismatic	Prismatic	Tubules in all layers
Anadara antiquata (Linnaeus)	Seychelles	Aragonite	Crossed-lamellar	Complex crossed-lamellar	Prismatic		Tubules in all layers
Anadara grandis (Broderip & Sowerby)	W. Panama	Aragonite	Crossed-lamellar	Complex crossed-lamellar	Prismatic	Prismatic	Tubules in all layers
Anadara obesa (Sowerby)	Ecuador	Aragonite	Crossed-lamellar	Complex crossed-lamellar	Prismatic	Prismatic	Tubules in all layers
Scapharca subcrenata (Lischke)	Japan	Aragonite	Crossed-lamellar	Complex crossed-lamellar	Prismatic		Tubules in all layers
Trisidos tortuosa (Linnaeus)	Mombasa	Aragonite	Crossed-lamellar	Complex crossed-lamellar	Prismatic, in umbo only		Tubules in all layers : scarce
Barbatia barbata (Linnaeus)	Italy	Aragonite	Crossed-lamellar	Complex crossed-lamellar	Prismatic	Prismatic	Abundant tubules in all layers
Barbatia complanata (Bruguière)	Mombasa	Aragonite	Crossed-lamellar	Complex crossed-lamellar	Prismatic	Prismatic	Tubules in all layers
Barbatia lurida (Sowerby)	Columbia	Aragonite	Crossed-lamellar	Complex crossed-lamellar	Prismatic	Prismatic	Tubules in all layers
Barbatia reeveana (d'Orbigny)	Ecuador	Aragonite	Crossed-lamellar	Complex crossed-lamellar	Prismatic	Prismatic	Tubules in all layers
Barbatia fusca (Bruguière)	Seychelles	Aragonite	Crossed-lamellar	Complex crossed-lamellar		Prismatic	Tubules in all layers
Cucullaea labiata (Lightfoot)	Indian Ocean	Aragonite	Crossed-lamellar	Complex crossed-lamellar			Tubules in all layers, no pallial myostracum observed

Name	Locality	Composition	Outer Layer	Inner Layer	Myostraca		Observations
					Pallial	Adductor	
The following specimens were all aragonitic :							
Arca navicularis (Bruguière)	Seychelles ;						
Acar plicata (Dillwyn)	Seychelles ;						
Scapharca clathrata (Reeve)	Seychelles ;						
Barbatia helblingi (Bruguière)	Seychelles ;						
Cucullaea decussata Parkinson	Eocene, (Thanetian) Kent, England ;						
Trinacria media (Deshayes)	Tertiary. Sables de May, I. de Meldeuse, France						

in the hinge area. Here, the first order lamels are arranged concentrically in the lower part of the hinge plate, while the teeth are built up of obliquely aligned lamels.

A very thin, discontinuous, prismatic, pallial myostracum is present in ten of the species examined. In *Trisidos tortuosa*, myostracal prisms are present in the dorsal part of the pallial line only. In *Cucullaea labiata*, no pallial myostracum has been seen and the boundary between the layers is rather poorly defined. A thick pallial myostracum is present throughout all the umbonal part of the pallial line in *Anadara antiquata* and *A. grandis*. Sections through, or close to, the adductor muscle scars show a pad of myostracal prisms which is overlapped by the complex crossed-lamellar layer towards the umbonal region in the six species in which this region was examined. *Arca avellana* has thin, prismatic myostracal pillars in the inner, complex crossed-lamellar layer. These pillars arise from the pallial myostracum, and form small protuberances on the inner surface of the shell. A few of these pillars are connected to tubules in the outer complex crossed-lamellar layer of the shell.

We have examined the ultra-structure of several members of this superfamily, namely *Anadara antiquata*, *A. grandis*, *Arca scapha*, *Barbatia fusca* and *Trisidos tortuosa*. Details are given in the introductory sections : pp. 41–50 Kobayashi, I. (1964) has described the shell of *Barbatia obtusoides* with some observations on the ultrastructure.

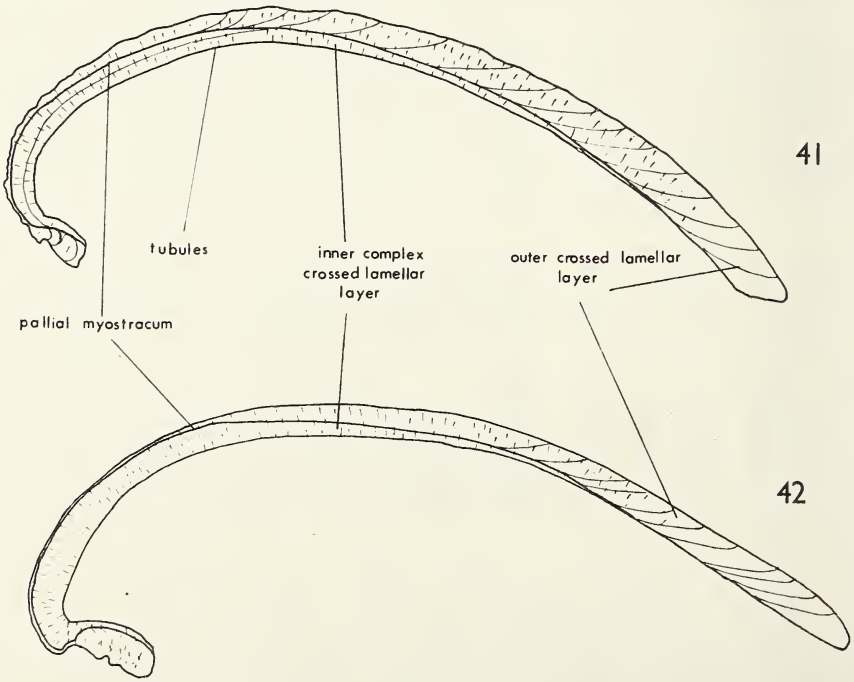

FIGS. 41–42. Radial section of *Anadara antiquata* (40) and *Barbatia complanata* (41) showing the distribution of the shell layers, myostraca etc.

All the species of Arcacea examined show tubules, passing through all shell layers, with diameters of several tens of microns. The tubules are most abundant in the area of the shell interior that lies within the pallial line. They also occur in the umbo and hinge, but appear to be absent from the adductor myostracum.

It is interesting to record that the fossil genus *Parallelodon*, which is considered to be the ancestor of *Cucullaea* and modern arcids (Cox 1954) shows, in specimens of *Parallelodon reticulata* (Blake) (Jurassic—Kimmeridgian—Britain), an outer, crossed-lamellar layer and an inner complex crossed-lamellar layer.

LIMOPSACEA

(Plate 14, fig. 4 ; Pl. 19, figs. 2, 6 ; text-figs. 43–47)

This superfamily shows great similarities in shell structure to the Arcacea. Eleven species belonging to this group have been examined mineralogically and five optically.

The shell is aragonitic throughout ; two main shell layers are present, i.e. an outer, crossed-lamellar layer and an inner, complex crossed-lamellar layer which is bounded by the trace of the pallial myostracum. In the outer layer the first order lamels are arranged concentrically over the whole of the shell except for the hinge region. Here, as in the Arcacea, the teeth are formed of obliquely aligned lamels, while the ventral part of the hinge plate is formed of concentrically arranged lamels (text-fig. 47). A very thin, discontinuous, prismatic, pallial myostracum was present in all species examined. Sections through the adductor regions of *Axinactis*

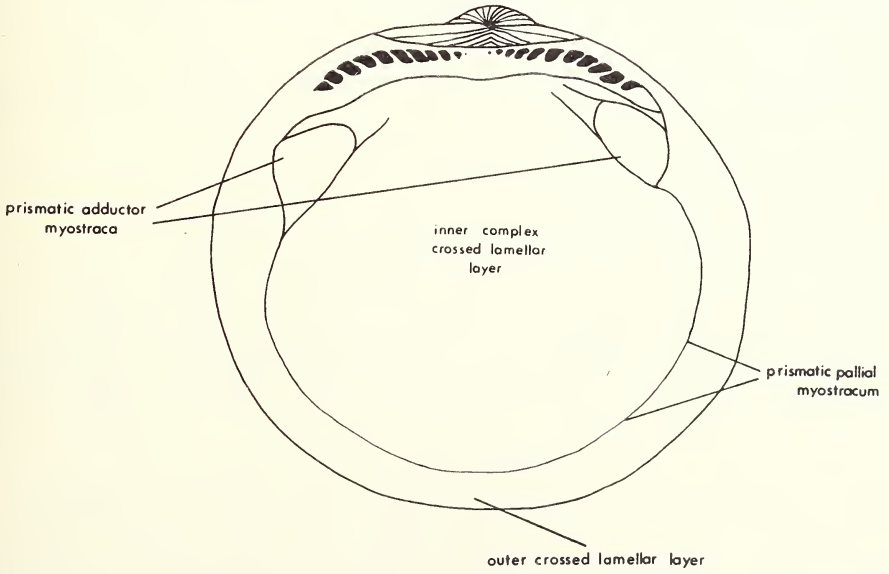

Fig. 43. Limopsacea : General view of the interior *Glycimeris glycimeris* showing the general distribution of shell layers etc.

TABLE 5

LIMOPSACEA

NAME	LOCALITY	COMPOSITION	OUTER LAYER	INNER LAYER	MYOSTRACA		OBSERVATIONS
					Pallial	Adductor	
Glycimeris glycimeris Linnaeus	Britain	Aragonite	Crossed-lamellar	Complex crossed-lamellar	Prismatic	Prismatic	Tubules in both layers
Glycimeris lintea Olsson	Ecuador	Aragonite	Crossed-lamellar	Complex crossed-lamellar	Prismatic	Prismatic	Tubules in both layers
Glycimeris violascens Lamarck	Pliocene, Sicily	Aragonite	Crossed-lamellar	Complex crossed-lamellar	Prismatic		Tubules in both layers
Glycimeris sp.	Pliocene, Italy	Aragonite	Crossed-lamellar	Complex crossed-lamellar	Prismatic		Tubules in both layers
Axinactis inaequivalvis (Sowerby)	Ecuador	Aragonite	Crossed-lamellar	Complex crossed-lamellar	Prismatic	Prismatic	Tubules in both layers
Limopsis aurita (Broc.)	Pliocene, Italy	Aragonite	Crossed-lamellar	Complex crossed-lamellar	Prismatic		Tubules in both layers, thin prismatic pillars in inner layer
The following specimens were aragonitic :—							
Glycimeris delta (Solander)	Eocene, Bartonian, England ;						
Glycimeris flammeus (Reeve)	Japan ;						
Glycimeris glycimeris (Linnaeus)	Pliocene, Essex, England ;						
Glycimeris pilosa (de Roissy)	Unlocalized ;						
Limopsis aurita (Broc.)	Pliocene, Nice, France.						
Limopsis granulata (Lamarck)	Pliocene, France ;						
Limopsis granulata (Lamarck)	Pliocene, Antibes, France ;						
Limopsis scalacor (Sowerby)	Eocene, Bartonian, England ;						

inaequivalvis, Glycimeris lintea and *Glycimeris glycimeris* show the development of a relatively thick lens of prismatic adductor myostracum.

Tubules of the order of 10 microns in diameter are present in all species examined. They are usually oriented normal to the shell interior, but may be inclined in some cases. The tubules are developed in both shell layers, and are usually most abundant in the area of shell interior bounded by the pallial line, but can occur outside this line, towards the margin, as in the species *Axinactis inaequivalvis* and *Glycimeris lintea*. Omari *et al.* (1962) have described the tubules of *Glycimeris vestita*. According to these authors the tubules are between 3·7 and 4·0 microns in diameter with densities of 8–13 per 100 sq. microns of inner shell surface.

We have examined the ultrastructure of one species only, i.e. *Glycimeris glycimeris*.

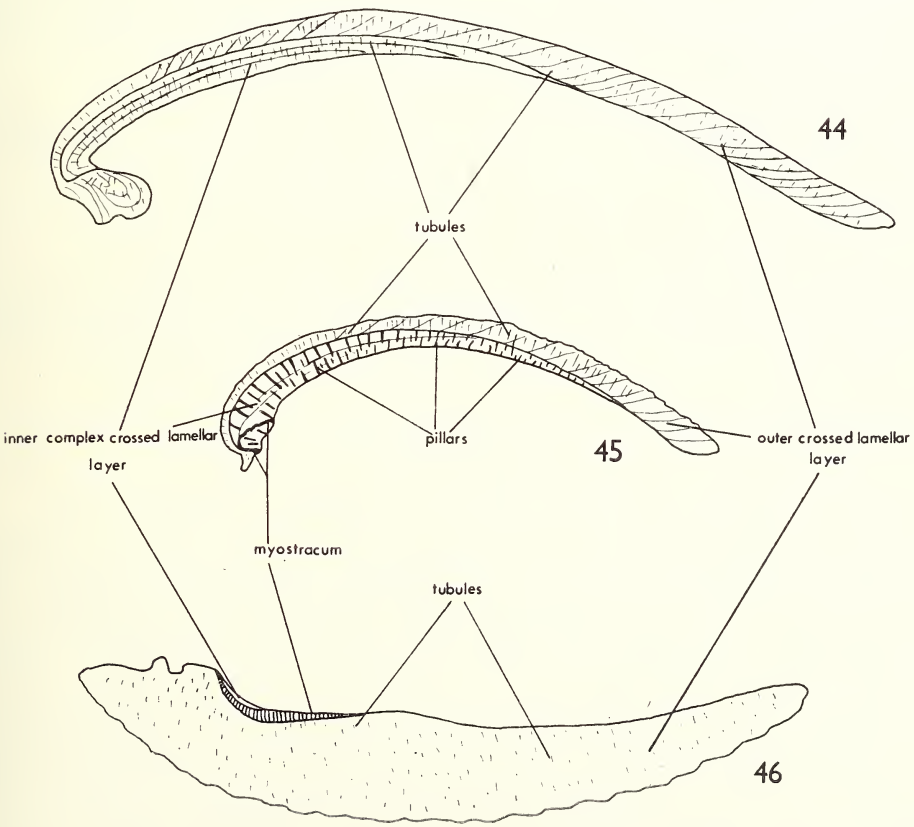

FIGS. 44–46. Limoposacea : radial sections showing the distribution of the shell layers etc. Fig. 44. *Glycimeris lintea*. Fig. 45. *Limposis aurita*. Fig. 46. *Glycimeris* sp. through adductor scar.

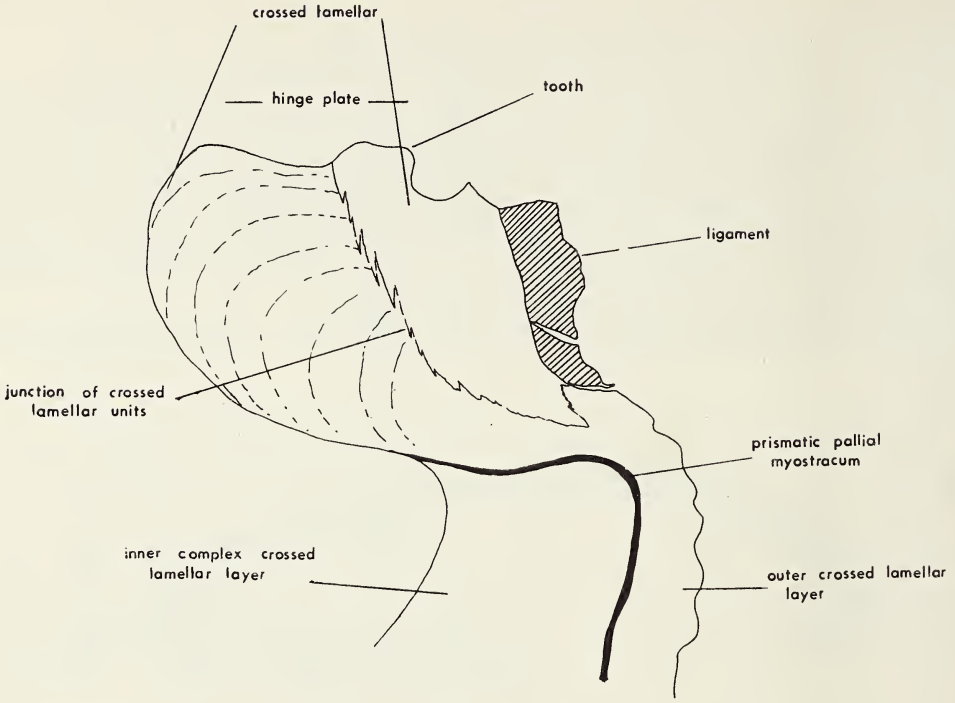

FIG. 47. Radial section of the hinge area of *Glycimeris lintea ;* detail showing the form of and contact of the crossed-lamellar regions building the hinge plate and ligamental ridge.

Order MYTILOIDA
MYTILACEA

(Plate 20, figs. 1–2 ; Pl. 22, fig. 4 ; Pl. 25, fig. 2 ; text-figs. 48–49)

Because of their considerable interest, and because of the problems raised by previous work on their shell mineralogy (Lowenstam 1954a, b, Dodd 1963, Eisma 1966) we have examined an especially large number of species belonging to the Mytilacea. Nineteen species have been examined mineralogically and eighteen optically.

In *Mytilus* (s.s.) and closely related genera, two groups can be recognised, i.e. a two-layered, wholly nacreous, wholly aragonite, warm-water group including *M. smaragdensis, M. viridis, Perimytilus purpuratus* and *Choromytilus palliopunctatus* and a two- or three-layered aragonitic and calcitic, temperate group including *Mytilus edulis* and *Mytilus californianus*. Within the latter group, the calcite occurs in an outer, finely prismatic layer in *M. edulis,* and as both an outer and inner finely prismatic layer in *M. californianus* (cf. Dodd 1964). The aragonite occurs as inner and middle nacreous layers respectively in these two species. The prisms of the calcitic layers are much smaller than in any other bivalve family.

The prismatic layer consists of extremely thin calcite needles 1–3 microns in diameter and up to 50 microns long. These needles are frequently inclined towards the shell margin and appear to be almost horizontal in some sections. In some cases the prisms are arranged into larger units, which appear to be broadly triangular in section but which have a conical form in three dimensions. Within these conical units, the needles radiate from the apex of the cone, which points outwards towards the exterior of the shell. These broader units are developed quite sporadically in any one shell. This arrangement of calcite needles in the prismatic layer of mytilids appears to be what Oberling (1964) refers to as *flabellate* structure, which he records from the outer layers of *Mytilus edulis*, *Mytilus californianus* and *'Volsella'* (= *Modiolus*) *capax*.

The species of *Brachiodontes* which we have examined have a wholly aragonitic shell and examination of *B. citrinus* shows that it occurs as both inner and outer nacreous layers. *Septifer bilocularis* is also wholly aragonitic ; the outer layer is nacreous, but most of the inner layer is built up of myostracal-type prisms.

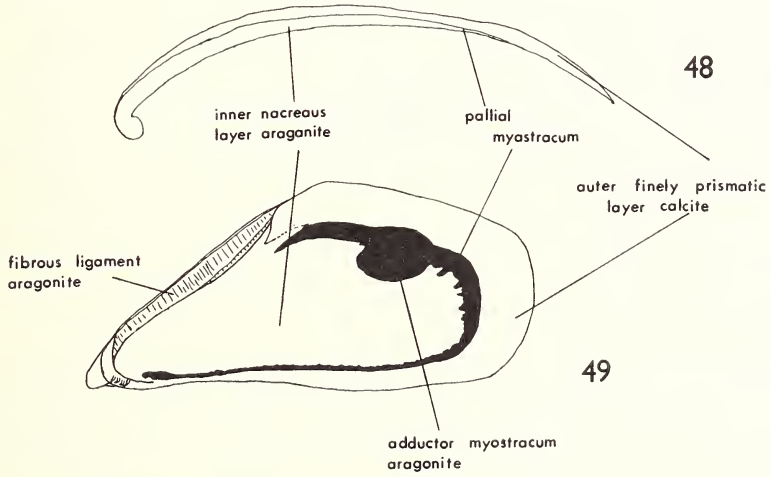

Figs. 48–49. Mytilacea : *Mytilus edulis*. Fig. 47. Radial section showing the distribution of the shell layers. Fig. 48. General view of the shell interior.

The mineralogy of *Modiolus* is complex. In the tropical species that we have examined, the shell is either wholly aragonite or contains a very small percentage of calcite in the outer layer of a few species. The origin and exact mode of occurrence of this calcite is at present uncertain. Temperate species of *Modiolus*, like temperate species of *Mytilus*, have a finely prismatic calcitic outer layer while tropical species have a nacreous outer layer, again like the corresponding species of *Mytilus*. In some species, both tropical and temperate, an inner layer of alternating sheets of aragonitic myostracal prisms and nacre (Plate 25, fig. 2) is developed. The sheets of prisms may possibly represent periodic mantle attachment over the whole inner shell surface. A similar alternation of myostracal prisms and complex crossed lamellar structure is seen in *Stavelia horrida*.

TABLE 6

MYTILACEA

NAME	LOCALITY	MINERALOGY	OUTER LAYER	MIDDLE LAYER	INNER LAYER	MYOSTRACA		OBSERVATIONS
						Pallial	Adductor	
Mytilus arciformis (Dall)	Ecuador	Aragonite	Nacreous aragonite		Nacreous aragonite	Prismatic aragonite	Prismatic aragonite	Several determinations.
Mytilus californianus Conrad	California	Calcite and aragonite	Finely prismatic calcite	Nacreous aragonite	Finely prismatic calcite	Prismatic aragonite		Fibrous ligament aragonite. Tubules in nacreous layer only.
Mytilus edulis (Linnaeus)	Britain	Calcite and aragonite	Finely prismatic calcite		Nacreous aragonite	Prismatic aragonite	Prismatic aragonite	Many specimens examined. Fibrous ligament aragonite.
Mytilus smaragadensis Gmelin	Mangalore, India	Aragonite	Nacreous aragonite		Nacreous aragonite	Prismatic aragonite	Prismatic aragonite	
Mytilus viridis (Linnaeus)	India	Aragonite	Nacreous aragonite		Nacreous aragonite	Prismatic aragonite	Prismatic aragonite	
Perimytilus purpuratus (Lamarck)	Pacific coast, S. America	Aragonite	Nacreous aragonite		Nacreous aragonite	Prismatic aragonite	Prismatic aragonite	
Choromytilus palliopunctatus (Carpenter)	Mazatlan, Mexico	Aragonite	Nacreous aragonite		Nacreous aragonite	Prismatic aragonite	Prismatic aragonite	
Brachiodontes citrinus (Röding)	Jamaica	Aragonite	Nacreous aragonite		Nacreous aragonite	Prismatic aragonite	Prismatic aragonite	
Brachiodontes variabilis (Krauss)	Seychelles	Aragonite						
Botula cinnamomea (Lamarck)	Seychelles	Calcite and aragonite						
Lithophaga teres (Philippi)	Seychelles	Calcite and aragonite	Finely prismatic calcite	Nacreous aragonite	Nacreous aragonite	Prismatic aragonite	Prismatic aragonite	The inner layer consists of complicated alternations of nacre and myostracal prisms with additional conchiolin sheets.

Name	Locality	Composition	Outer Layer	Middle Layer	Inner Layer	Myostraca		Observations
						Pallial	Adductor	
Septifer bilocularis (Linnaeus)	Singapore	Aragonite	Nacreous aragonite		Prismatic aragonite	→	→	Inner layer built up of myostracal type prisms apparently contiguous with the pallial and adductor myostraca, with traces of nacre in the umbonal region.
Septifer bilocularis (Linnaeus)	Mombasa	Aragonite	Nacreous aragonite		Prismatic aragonite	→	→	
Modiolus adriaticus (Lamarck)	Britain	Aragonite and calcite	Finely prismatic calcite	Nacreous aragonite	Complex crossed-lamellar, aragonite	Prismatic aragonite	Prismatic aragonite	Numerous specimens examined.
Modiolus auriculatus (Krauss)	Seychelles	Aragonite	Nacreous aragonite		Complex crossed-lamellar, aragonite	Prismatic aragonite	Prismatic aragonite	Small tubules seen by electron microscopy.
Modiolus auriculatus (Krauss)	Seychelles	Aragonite and calcite						Trace of calcite in outer layer.
Modiolus auriculatus (Krauss)	Tanzania	Aragonite and trace calcite						Trace of calcite in outer layer
Modiolus americanus (Leach)	E. Coast, Central America	Aragonite and trace calcite						Trace of calcite in outer layer.
Modiolus australis (Sowerby)	E. Africa	Aragonite and trace calcite						
Modiolus capax (Conrad)	Ecuador	Aragonite	Nacreous aragonite		Nacreous aragonite	Prismatic aragonite	Prismatic aragonite	Fibrous ligament, aragonitic.
Modiolus capax (Conrad)	Ecuador	Aragonite and trace calcite						Trace calcite in outer layer

TABLE 6 (*Contd.*)

NAME	LOCALITY	MINERALOGY	OUTER LAYER	MIDDLE LAYER	INNER LAYER	MYOSTRACA		OBSERVATIONS
						Pallial	Adductor	
Modiolus auriculatus (Krauss)	Phillippines	Aragonite and trace calcite	Nacreous aragonite		Complex crossed-lamellar aragonite	Prismatic aragonite	Prismatic aragonite	Trace of calcite in outer layer. Subsequent determinations showed only aragonite.
Modiolus modiolus (Linnaeus)	Hunstanton, Norfolk	Calcite and aragonite	Finely prismatic calcite	Nacreous aragonite	Nacreous with prismatic bands, aragonite	Prismatic aragonite	Prismatic aragonite	Inner layer built up of alternating sheets of nacre and myostracal prisms. Fibrous ligament aragonitic.
Modiolus pseudotulipus (Olsson)	Ecuador	Aragonite	Nacreous aragonite		Nacreous with prismatic bands, aragonite	Prismatic aragonite	Prismatic aragonite	Inner layer built up of alternating sheets of nacre and myostracal prisms.
Stavelia horrida (Dunker)	Queensland	Aragonite	Nacreous aragonite		Complex crossed-lamellar and prismatic bands aragonite	Prismatic aragonite	Prismatic aragonite	Inner layer contains many very thin sheets of myostracal prisms. Small tubules seen by electron microscopy.
Musculus lateralis (Say)	West Indies	Aragonite						

In the tropical, rock boring mytilids *Lithophaga teres* and *Botula cinnamomea*, the shell consists of both calcite and aragonite. *L. teres* has a complicated shell structure ; there is a thin, calcitic, outer layer, formed of fine needles which strongly incline towards the shell margin, producing a feathery appearance in sections. Inside this is a middle, aragonitic nacreous layer. Beneath this, there is a complex alternation of layers or nacre and aragonitic myostracal-type prisms. In the older parts of the shell of this species thin sheets of conchiolin are laid down within the shell. This feature, and the thick periostracum of this species may be adaptations to protect the shell from the acid secreted during rock boring.

The fine structure of *Mytilus edulis* prisms has been investigated by Grégoire (1961a), who describes the prisms as thin, elongate needles which are polygonal in cross section and have blunt, pyramidal terminations. Each prism is surrounded by a sheath of organic matrix which is in the form of tightly reticulated sheets. Grégoire was unable to detect any difference between the organic matrix surrounding the prisms and the inter-lamellar matrix of the underlying nacreous layer.

We have examined the fine structure of both surfaces and sections of *Stavelia horrida* and *Modiolus auriculatus*. This examination reveals the presence of very small tubule-like structures ; these are also present in many other mytilids, and are at present being investigated by Dr J. D. Hudson (personal communication).

Our observations on the mineralogy of mytilids agree with the general conclusions of Lowenstam (1954b, 1964), stressing the tendency for tropical Mytilacea (excepting *Lithophaga* and *Botula*) to be wholly aragonitic, and for temperate species to contain both calcite and aragonite. The results of Lowenstam's work and those of Dodd (1963) are discussed elsewhere (p. 13).

PINNACEA

(Plate 8, fig. 3 ; text-figs. 18, 50–52)

The superfamily Pinnacea is today represented by three extant genera, i.e. *Pinna*, *Atrina*, *Streptopinna*. Representatives of each of these were investigated—six species mineralogically and four optically. The shell consists of both calcite and aragonite.

In all species the thick outer layer of the shell is composed of simple calcite prisms, arranged with their crystallographic *c* axes normal to the layer surfaces. The prisms are larger than in any other family, reaching diameters of about 1 millimetre, and the prismatic layer as a whole can be several millimetres thick. Beneath this outer layer there is an inner aragonitic nacreous layer. This layer mainly occupies the area between the adductor muscle scars, and throughout its whole thickness it is sheet nacre.

No trace of pallial myostracum was seen in any species of this group, for as Yonge (1953b) has shown in *Pinna carnea*, there is no line of primary pallial attach-

ment between the adductor muscle scars. Only a secondary attachment is present, in the form of anterior and posterior pallial retractor muscles, which are attached to the shell at small areas near the anterior adductor muscle scars. Sections through the adductor muscle scars show pads of typical aragonitic myostracal prisms.

The inner, calcified ligaments of *Atrina vexillum* and *Pinna rugosa* were found to be aragonitic.

The extent and shape of the inner, nacreous layer is of considerable systematic importance in the Pinnacea. Of the three living genera, *Atrina* first appeared in the Carboniferous, *Pinna* in the Jurassic and *Streptopinna* in the late Tertiary ; these three genera show a progressive reduction in the area of the inside of the shell occupied by the nacreous layer (text-figs. 50–52). Thus the nacreous layer occupies almost half the area of the inside of the shell in *Atrina*, but is reduced to a tiny area near the anterior adductor muscle scar in *Streptopinna*.

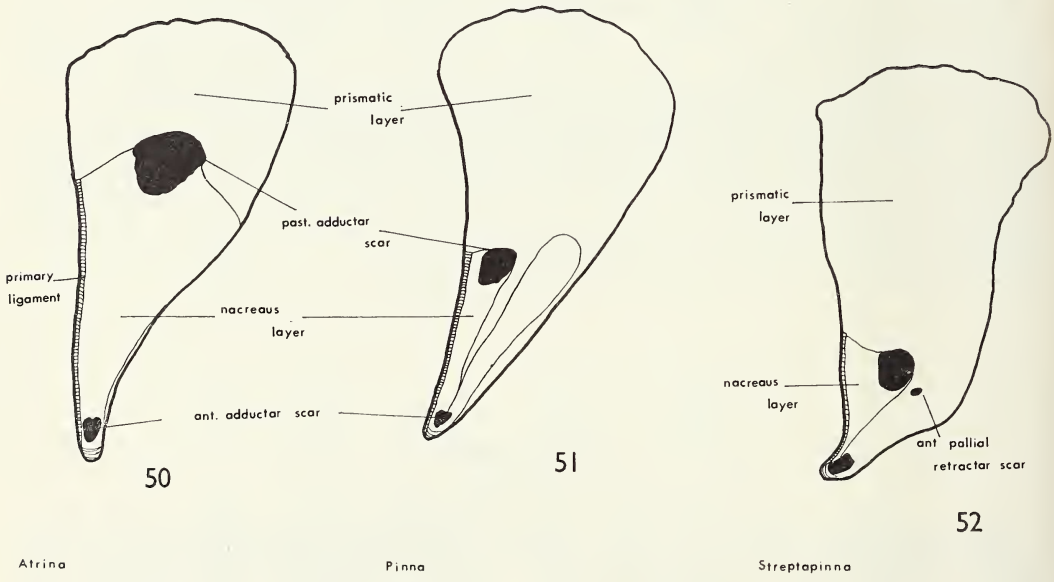

Figs. 50–52. Pinnacea ; diagram showing the variation in extent of the outer prismatic calcite layer and the inner nacreous aragonitic layer in *Pinna*, *Streptopinna* and *Atrina*.

Lowenstam (1954b) has suggested that calcite/aragonite ratios in the Pinnacea show the usual dependence of temperature during growth. However, the three genera described above have widely different calcite/aragonite ratios, but may all occur at the same locality in some Indo-Pacific areas ; moreover, *Streptopinna*, which has the lowest aragonite content, is exclusively tropical, whilst *Atrina* and *Pinna* with higher aragonite contents range into temperate waters.

TABLE 7

PINNACEA

NAME	LOCALITY	COMPOSITION	OUTER LAYER	INNER LAYER	ADDUCTOR MYOSTRACUM	OBSERVATIONS
Pinna muricata Linnaeus	Mombasa	Calcite and aragonite	Simple prisms, calcite	Sheet nacre aragonite	Prismatic aragonite	
Pinna rugosa Sowerby	Ecuador	Calcite and aragonite	Simple prisms, calcite	Sheet nacre aragonite	Prismatic aragonite	Fibrous ligament aragonitic
Atrina vexillum (Born)	Mombasa	Calcite and aragonite	Simple prisms, calcite	Sheet nacre aragonite	Prismatic aragonite	Fibrous ligament aragonitic
Streptopinna saccata (Linnaeus)	Seychelles	Calcite and aragonite	Simple prisms, calcite	Sheet nacre aragonite		

Order PTERIOIDA
PTERIACEA

(Plate 1, fig. 2 ; Pl. 2, fig. 3 ; Pl. 7, figs. 1, 6 ; Pl. 9, fig. 1 ; text-figs. 8–10, 53–55)

This superfamily consists of three living families, i.e. Pteriidae, Isognomonidae and Malleidae. Ten species were examined mineralogically and eight optically. The shell consists of both calcite and aragonite.

There is an outer prismatic layer, with middle and inner nacreous layers (figs. 53–55). The outer layer in all cases consists of simple prisms, always calcitic, with prominent, transverse accretion lines. It is often worn and corroded near the umbo, and is generally thin. In *Malleus malleus*, however, this layer is very thick, and most of the thickness consists of spaces between overlapping layers of prisms, giving a foliated appearance to the outer part of the shell. On the inner surface of the shell the margin is frequently very irregular, but the prismatic layer is rather wide (text-figs. 53–55). The prismatic layer is frequently dark brown in colour but in the Isognomonidae is usually black. In sections, the prismatic layer shows evidence of extensive geometric selection, i.e. many small prisms are present at the contact with the periostracum, but these wedge out downwards and become fewer in number and larger in size.

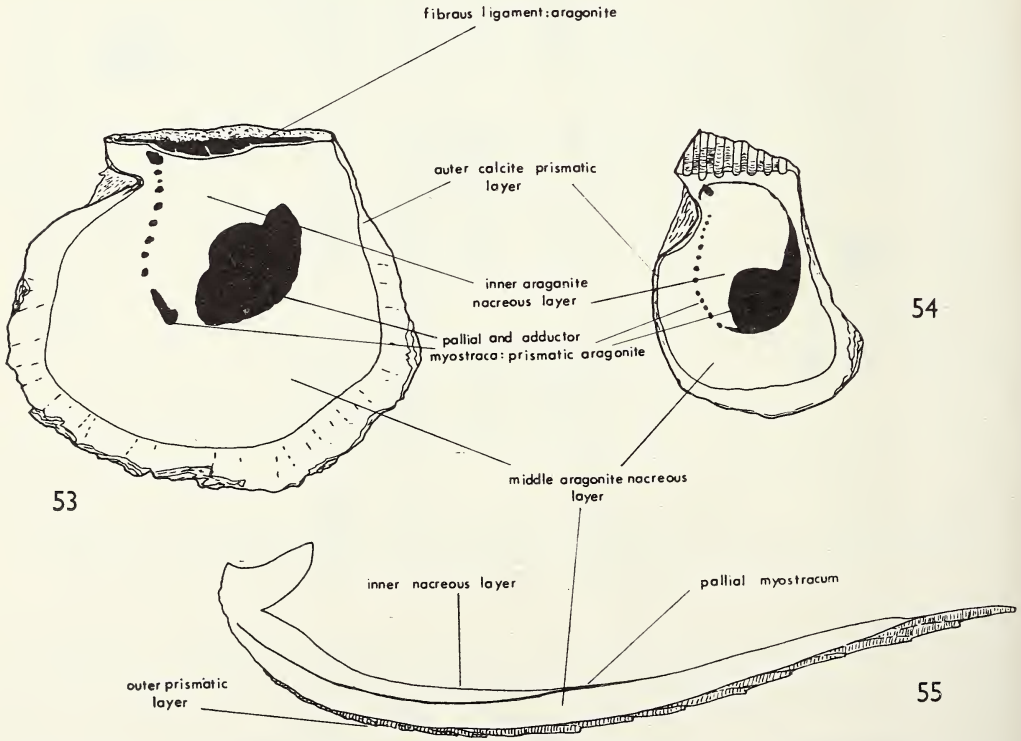

Figs. 53–55. Pteriacea ; Distribution of the shell layers and other features. Fig. 53. *Pinctada margaritifera*. Fig. 54. *Isognomon dentifer*. Fig. 55. Radial section of *Pinctada margaritifera*.

TABLE 8

PTERIACEA

NAME	LOCALITY	COMPOSITION	OUTER LAYER	MIDDLE LAYER	INNER LAYER	MYOSTRACA		OBSERVATIONS
						Pallial	Adductor	
Pteria sterna (Gould)	Ecuador	Calcite and aragonite	Simple prisms calcite	Nacreous aragonite	Nacreous aragonite	Prismatic aragonite	Prismatic aragonite	
Pinctada margaritifera (Linnaeus)	Seychelles	Calcite and aragonite	Simple prisms calcite	Nacreous aragonite	Nacreous aragonite	Prismatic aragonite	Prismatic aragonite	Fibrous ligament aragonitic
Electroma alacorvi (Dillwyn)	Seychelles	Calcite and aragonite	Simple prisms calcite	Nacreous aragonite	Nacreous aragonite		Prismatic aragonite	Fibrous ligament aragonitic
Isognomon attenuatus (Reeve)	Red Sea	Calcite and aragonite	Simple prisms calcite	Nacreous aragonite	Nacreous aragonite		Prismatic aragonite	
Isognomon chemnitziana (d'Orbigny)	Ecuador	Calcite and aragonite	Simple prisms calcite	Nacreous aragonite	Nacreous aragonite		Prismatic aragonite	
Isognomon dentifer (Krauss)	Seychelles	Calcite and aragonite	Simple prisms calcite	Nacreous aragonite	Nacreous aragonite	Prismatic aragonite	Prismatic aragonite	Fibrous ligament aragonitic. Complex crossed-lamellar patch in umbonal region.
Isognomon isognomon (Linnaeus)	Mombasa	Calcite and aragonite	Simple prisms calcite	Nacreous aragonite	Nacreous aragonite		Prismatic aragonite	
Malleus malleus (Linnaeus)	East Indies	Calcite and aragonite	Simple prisms calcite	Nacreous aragonite			Prismatic aragonite	
Perna maxillata (Lamarck)	Pliocene, Asti, Italy	Calcite and aragonite						

The contact of the outer prismatic layer with the underlying middle nacreous layer is well defined, but often oscillates back and forth over the areas in which nacre has been deposited, which produces interfingering of the layers. The middle layer is aragonitic, thick and wide, extending inwards to the discontinuous line of pallial muscle scars. Within this discontinuous pallial line there is a further, thinner, inner aragonitic nacreous layer. Although there is no apparent difference in the nacres on either side of the pallial line on the inner surface of the shell, sections show that growth lines are discontinuous across it, and have different attitudes. Wada (1961) has shown that the orientation of the crystallographic *b* axes of the nacre tablets is far less regular in the inner shell layer within the pallial line.

One of the species we have examined, *Isognomon dentifer*, shows an additional structure. There is a small area of complex crossed-lamellar structure, identical with that seen in some species of *Modiolus*, interdigitating with the inner nacreous layer in the umbonal region below the hinge.

The sites of muscle attachment (the single adductor and the separated pallial muscles) are areas of aragonitic myostracal prisms. The traces of these myostraca run through the shell, separating the middle and inner nacreous layers. The pallial muscles are attached to the shell as a series of isolated bundles. The trace of this attachment is seen as scars extending in an arcuate line from the adductor scar to the umbo, where there is a further scar marking the insertion of the pedal retractor muscle.

Two species, *Pinctada martensi* and *Pinctada margaritifera*, have received a great deal of attention from Japanese workers, because of their importance in the pearl and mother-of-pearl industries. As a result, the ultrastructure of shell and body, and the processes of calcification, are better known in these species than in any other molluscs. Details of the growth and development of prisms and nacre in these species have been included in the introductory sections of this work, but particular reference should be made to the work of Wada (1961b, with bibliography). We have examined the ultrastructure of the prisms and nacre of *Pinctada margaritifera* and *Pteria sterna* and well preserved aragonitic nacre of the fossil pteriacean *Inoceramus concentricus* (Cretaceous, Albian, Gault Clay).

In the three species in which it has been examined, the internal calcified ligament was found to be aragonitic.

PECTINACEA

The three extant families of Pectinacea (Pectinidae, Spondylidae and Plicatulidae) are considered separately.

PECTINIDAE

(Plate 4, figs. 2, 3, 6 ; Pl. 25, fig. 4 ; Pl. 28, figs. 1–3 ; text-figs. 56–58)

The shells of thirteen species have been examined mineralogically and nine optically. The calcified ligaments of twelve species have been examined mineralogically.

The shell contains both calcite and aragonite. In all the species examined, the bulk of the shell is made up of an outer, calcitic, foliated layer which also forms the hinge. Within this outer layer, the folia are arranged radially. They show little variation in attitude (but see Bøggild, 1930, p. 265), lying either parallel or sub-parallel to the shell surface, approximately following the topography of the ribs (both additive and non-additive), so that sections cut slightly oblique to the ribbing show steeply inclined elements. An aragonitic prismatic pallial myostracum is present in most species, although it may be very thin. No myostracal band was

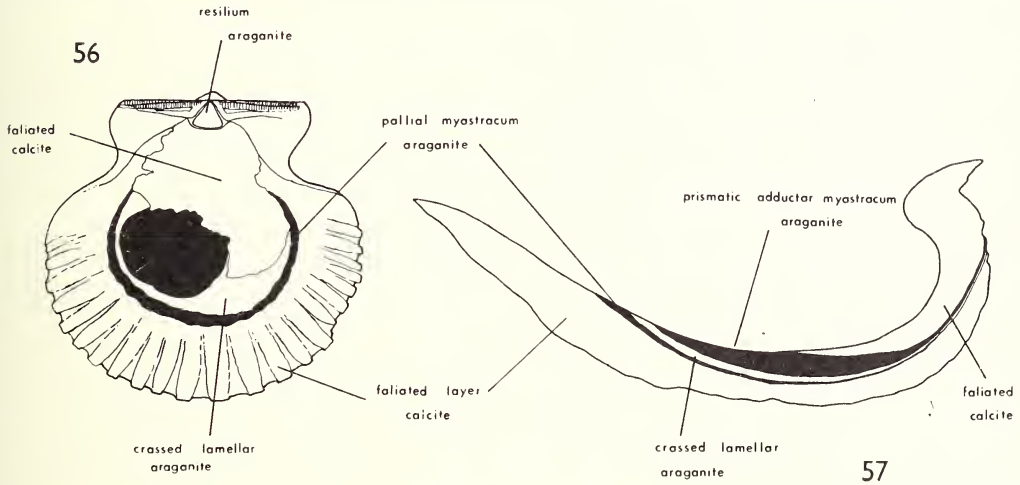

FIGS. 56–57. Pectinacea—Pectinidae—*Aequipecten circularis*. Fig. 56. General view of the interior of the shell. Fig. 57. Radial section showing distribution of the shell layers etc.

seen in *Pecten jacobeus* or *P. perulus* ; here the pallial trace is marked by a sharp discontinuity in both growth layers and shell structure. All species examined possess a single, relatively thick, irregularly prismatic adductor myostracum. A thin myostracal band is present in the umbonal region of several species (*Chlamys senatoria, C. varia, Hinnites distorta, Pecten jacobeus, P. maximus*). This band outcrops just below the hinge, and indicates the trace of the mantle attachment in this region.

The most variably developed element in the shell of the Pectinidae is the middle shell layer. This layer is limited to the region within the pallial line and is a thin sheet of aragonitic crossed-lamellar structure. This layer is present in the species of *Amusium, Aequipecten, Chlamys* and *Hinnites* that we have examined, but is absent in *Pecten maximus, P. jacobeus* and in the upper valve of *P. perulus*.

In addition to the foliated and crossed-lamellar layers, all species examined have an inner layer of irregularly oriented, calcitic foliated structure. This layer is thickest beneath the umbo and extends towards the margin to a variable extent, depending upon the species concerned and the age of the individual. This layer appears to be a secondary feature, produced late in the life of the individual, and

TABLE 9

PECTINIDAE

NAME	LOCALITY	COMPOSITION	OUTER LAYER	MIDDLE LAYER	INNER LAYER	MYOSTRACA		FIBROUS LIGAMENT	OBSERVATIONS
						Pallial	Adductor		
Pecten jacobeus (Linnaeus)	Mediterranean	Calcite and aragonite	Foliated calcite		Foliated calcite		Prismatic aragonite	Aragonite	Thin band of myostracal prisms outcropping beneath hinge
Pecten maximus (Linnaeus)	Britain	Calcite and aragonite	Foliated calcite		Foliated calcite	Prismatic aragonite	Prismatic aragonite	Aragonite	Thin band of myostracal prisms outcropping beneath hinge
Pecten perulus Olsson	Ecuador	Calcite and aragonite							
Upper valve :—			Foliated calcite		Foliated calcite		Prismatic aragonite		
Lower valve :—		,,	Foliated calcite	Crossed-lamellar aragonite	Foliated calcite		Prismatic aragonite		
Aequipecten circularis (Sowerby)	Ecuador	Calcite and aragonite	Foliated calcite	Crossed-lamellar aragonite	Foliated calcite	Prismatic aragonite	Prismatic aragonite		
Chlamys lentiginosus (Reeve)	Mollucas	Calcite and aragonite	Foliated calcite	Crossed-lamellar aragonite	Foliated calcite	Prismatic aragonite	Prismatic aragonite	Aragonite	
Chlamys senatoria (Gmelin)	Seychelles	Calcite and aragonite	Foliated calcite	Crossed-lamellar aragonite	Foliated calcite	Prismatic aragonite	Prismatic aragonite	Aragonite	Thin band of myostracal prisms outcropping beneath hinge
Chlamys varia (Linnaeus)	Britain	Calcite and aragonite	Foliated calcite	Crossed-lamellar aragonite	Foliated	Prismatic aragonite	Prismatic aragonite		Thin band of myostracal prisms outcropping beneath hinge
Amusium pleuronectes (Linnaeus)	Madras	Calcite and aragonite	Foliated calcite	Crossed-lamellar aragonite	Foliated calcite	Prismatic aragonite discontinuous	Prismatic aragonite		Internal ribs formed by thickening of outer jointed layer. A thin myostracal layer developed in the middle of the crossed lamellar layer

Name	Locality	Composition	Outer Layer	Middle Layer	Inner Layer	Myostraca		Fibrous Ligament	Observations
						Pallial	Adductor		
The following species were examined mineralogically and all had both calcite and aragonite in the shell.									
Aequipecten tumbezensis (d'Orbigny)	Ecuador ;								
Aequipecten opercularis (Linnaeus)	Mediterranean ;								
Chlamys glabra (Linnaeus)	Tunis ;								
Chlamys multistriata (Poli)	N. Italy								
In addition the fibrous layer of the ligaments of the following species wereexamined, all were aragonite.									
Pecten hericeus Gould	Puget Sound ;								
Pecten latus Gould	Japan ;								
Pecten novaezelandicus Reeve	New Zealand ;								
Aequipecten opercularis (Linnaeus)	Britain ;								
Chlamys aperrima (Lamarck)	Australia ;								
Chlamys varia (Linnaeus)	Britain ;								
Amusium pleuronectes (Linnaeus)	East Indies ;								

serves as a supporting and a strengthening device for the umbonal area at what would otherwise be a structurally weak point.

Amusium pleuronectes shows several interesting modifications. Generally considered as the most actively swimming pectinid, the shell of this species is largely made up of an extremely thin and flexible foliated layer, strengthened by thin, additive ribs which are developed from this layer. Where these ribs are covered by the crossed-lamellar inner layer, there is a reciprocal thickness variation, so that the relief of the central part of the shell is greatly reduced. An additional thin prismatic myostracal layer is present in the thin middle crossed-lamellar layer, between the pallial and adductor myostraca ; we are uncertain of its significance.

Lowenstam (1964) has noted that the resilium of the Pectinidae is calcified, and records the presence of aragonite in two species, i.e. *Pecten grandis* and *Hinnites*

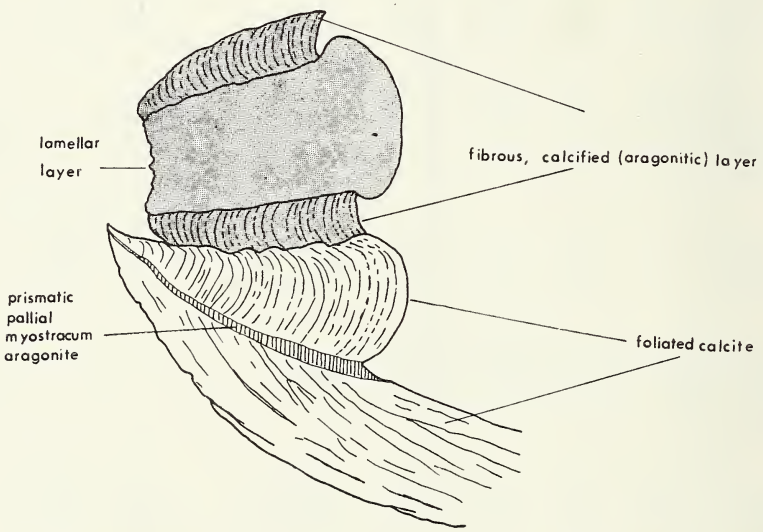

Fig. 58. Pectinacea : Pectinidae. Radial section of the innerligament (resilium) and hinge area of *Chlamys senatoria*. Inner ligament stippled.

gigantheus. The structure and function of the ligament in this superfamily have been described by Trueman (1953a and b). It has an elongate outer layer which extends along the hinge line, and an inner layer, the resilium, which consists of a brown, elastic, stout, conchiolin pad with laterally calcified areas which cement the ligament into a triangular pit, the resilifer, in each valve (text-fig. 58). The calcified area consists of fibres of aragonite, the presence of which has been confirmed in the twelve species listed below (Table 8). Merrill *et al.* (1966) have shown that in *Pleuropecten*, annual growth bands are easier to distinguish on the calcified ligament than on the shell surface, and are an aid in determining the age of populations.

The structure of the Pectinidae is of interest in that the inner layers bounded by the pallial line are greatly reduced, as a result of pallial attachment well within the margins. Pallial attachment is secondary in pectinids ; Newell (1937) has

suggested that the factors responsible for its establishment so far from the shell margin are associated with the active habits of the family, and specialisation of the mantle edge. Increased distance of mantle attachment from the margin of the shell would enable the development of long, more efficient muscle fibres, and thus rapid withdrawal of the mantle edge.

We have examined the fine structure of the inner calcified ligament of *Chlamys senatoria*, the details of which will be published at a later date. Wada (1964a) has briefly mentioned the foliated structure of *Chlamys nipponensis*.

SPONDYLIDAE

(Plate 4, fig. 1 ; Pl. 14, figs. 2, 6 ; text-figs. 26, 59–60.)

Four species have been examined, both optically and mineralogically. The shell contains both calcite and aragonite.

There is, in all the species that we have examined, an outer, foliated calcite layer. The folia are arranged in a similar fashion to the Pectinidae. A middle aragonitic,

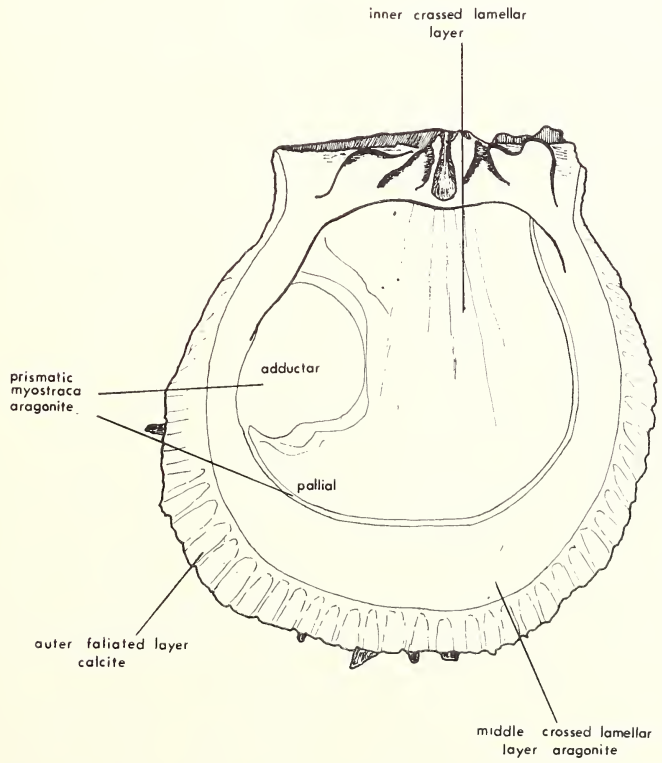

Fig. 59. Pectinacea : Spondylidae. *Spondylus gaederopus*. General view of the interior of the shell.

TABLE 10

SPONDYLIDAE

Species	Locality	Composition	Outer Layer	Middle Layer	Inner Layer	Myostraca		Observations
						Pallial	Adductor	
Spondylus gaederupus (Linnaeus)	Tunis	Calcite and aragonite	Foliated calcite	Crossed-lamellar aragonite, forming hinge	Crossed-lamellar aragonite with lenses of myostracal type prisms, breaking down into pillars	Prismatic aragonite	Prismatic aragonite	Tubules present throughout all shell layers, most abundant within pallial line.
Spondylus hystrix (Bolten)	Mombasa	Calcite and aragonite	Foliated calcite	Crossed-lamellar aragonite, forming hinge	Crossed-lamellar aragonite	Prismatic aragonite	Prismatic aragonite	Tubules present throughout, as above. myostracum in umbo, outcropping beneath hinge, the trace of pallial attachment in this region.
Spondylus nicobaricus Schreibers	E. Indies	Calcite and aragonite	Foliated calcite	Crossed-lamellar aragonite, forming hinge	Crossed-lamellar aragonite with lenses of myostracal prisms etc. as in *S. guaderupus*	Prismatic aragonite	Prismatic aragonite	Tubules present throughout, inner layer complicated by layers and lenses of prisms and pillars. 9
Spondylus calcifer Carpenter	Ecuador	Calcite and aragonite	Foliated calcite	Crossed-lamellar aragonite, forming hinge	Crossed-lamellar aragonite with thin sheets of myostracal prisms	Prismatic aragonite	Prismatic aragonite	Tubules present throughout, as *S. gaederapus*. Thin prismatic myostracum in umbo, outcropping beneath hinge, the trace of pallial attachment in this region.

Species	Locality	Composition	Outer Layer	Middle Layer	Inner Layer	Myostraca		Observations
						Pallial	Adductor	
In addition the fibrous layer of the ligament was examined in the following species, it was aragonitic in all cases.								
Spondylus americanus Hermann	Cuba ;							
Spondylus barbatus Reeve	E. Indies ;							
Spondylus gaederupus (Linnaeus)	Mediter-ranean ;							
Spondylus leucacantha Broderip	W. Coast, Central America ;							
Spondylus princeps Broderip	Columbia.							

crossed-lamellar layer, with concentrically arranged first order lamels, forms the hinge and teeth, while the pallial and adductor myostraca are prismatic aragonite. There is also an innermost, aragonitic layer, which is rather complicated and varied ; a crossed-lamellar structure with concentrically arranged lamels is dominant, but this is interrupted by lenses or patches of myostracal type prisms in two of the species that we have examined, i.e. *Spondylus gaederopus* and *S. nicobaricus*. These lenses of prisms break up laterally into prismatic myostracal pillars, and may give rise to them towards the shell surface. In all the species examined, the myostraca may give rise to short, pillar-like extensions ; those arising from the pallial myo-

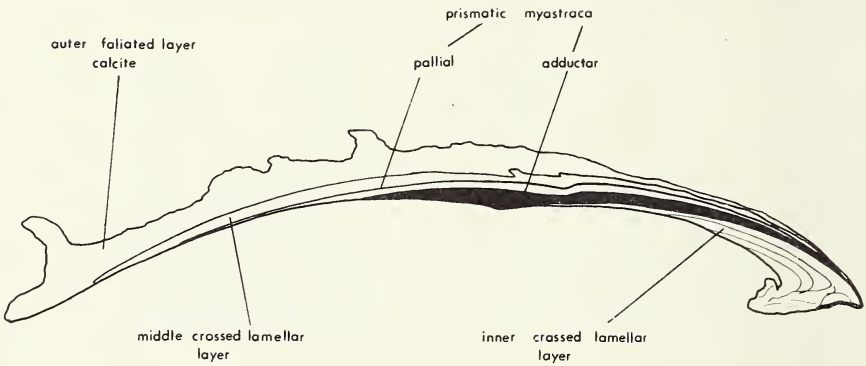

FIG. 60. Radial section of *Spondylus calcifer* showing the general distribution of the shell layers etc.

stracum are directed only inwards, but those arising from the adductor myostracum pass in both directions. Thin, prismatic myostracal bands are developed in the umbonal region of the crossed-lamellar layers, outcropping just below the hinge. These are the trace of the mantle attachment in this region. The first order lamels of the middle and inner shell layers show a striking correspondence and continuity across the pallial myostracum (Pl. 4, fig. 1).

In all the species examined, tubules are present in all shell layers and throughout the whole shell, although they are most abundant within the area bounded by the pallial line.

The calcified portions of the resilium of seven species of *Spondylus* were examined and found to be aragonitic in all cases.

PLICATULIDAE

(Family text-figs. 61–62)

Two species were examined, both mineralogically and optically. The shell consists of both calcite and aragonite and the shell structures greatly resemble those of the Spondylidae.

The outer shell layer is foliated and calcitic throughout. Beneath this layer there are middle and inner crossed-lamellar layers. In the crossed-lamellar layers the first order lamels are arranged concentrically, and are parallel to the shell margin over wide areas of the shell. The contact between the outer and middle layers is rather irregular, with an interfingering of wedges of folia and lamels. The two crossed-lamellar layers are separated by a thin, aragonitic, prismatic, pallial myostracum, which, in the last formed part of the shell, zig-zags up to the inner surface, as it does in many other cemented bivalves such as the Chamacea. Sections

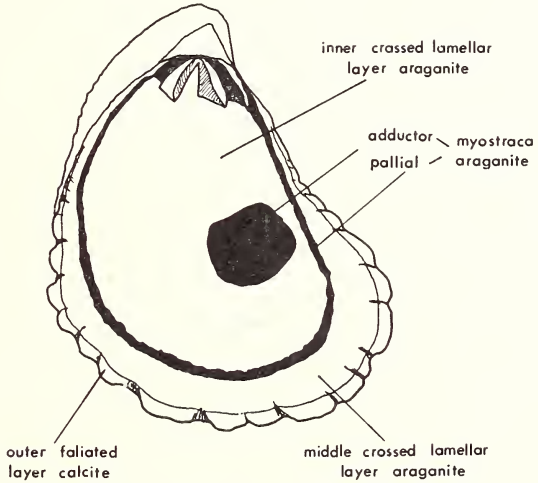

FIG. 61. Pectinacea : Plicatulidae, *Plicatula chinensis*, general view of the interior of the shell.

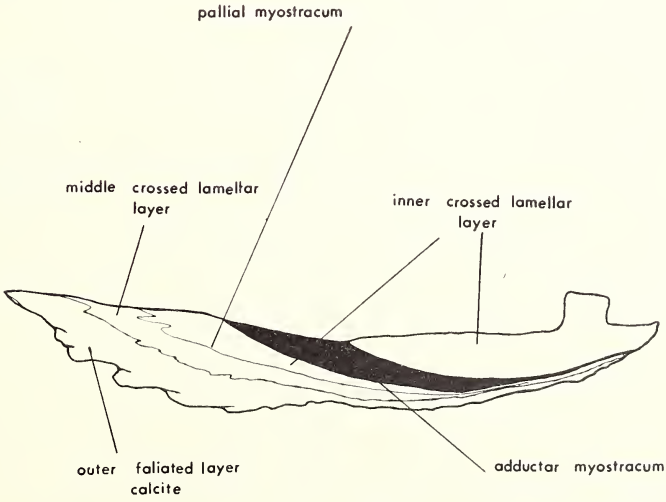

FIG. 62. Radial section of *Plicatula chinensis* showing the general distribution of the shell layers etc.

TABLE 11

PLICATULIDAE

NAME	LOCALITY	COMPOSITION	OUTER LAYER	MIDDLE LAYER	INNER LAYER	MYOSTRACA		OBSERVATIONS
						Pallial	Adductor	
Plicatula depressa Lamarck	Phillip-pines	Calcite and aragonite	Foliated calcite	Crossed-lamellar aragonite	Crossed-lamellar aragonite	Prismatic aragonite	Prismatic aragonite	
Plicatula chinensis Mörch	East Africa	Calcite and aragonite	Foliated calcite	Crossed-lamellar aragonite	Crossed-lamellar aragonite	Prismatic aragonite	Prismatic aragonite	

cut through the single adductor muscle scar show a thick pad of aragonitic myostracal prisms and a prismatic trace through the inner, crossed-lamellar layer. The crossed-lamels of the middle and inner layers of *Plicatula* show the puzzling correspondence and continuity of first order lamels across the pallial myostracum, such as we have already noted in the Spondylidae.

In the Spondylidae and Plicatulidae, as in the Pectinidae, pallial attachment is secondary, but it is closer to the shell margins than in the latter group. The detailed continuity of the middle and inner crossed-lamellar layers across the pallial myostracum may somehow be related to this condition.

Because of the phenomenon of secondary pallial attachment associated with monomyarianism, the ' inner ' and ' middle ' shell layers of the Pectinacae may not be homologous with the inner and middle layers in di- and heteromyarian bivalves. This is one of the reasons for the rejection of Oberling's (1964) shell layer terminology (see p. 7).

ANOMIACEA

(Plate 5, fig. 4 ; Pl. 6, fig. 3 ; text-figs. 63–64, 16)

Six species of Anomiacea were examined mineralogically and three optically. The shell in all cases consists of both calcite and aragonite.

Most of the shell, including the hinge and umbo in *Anomia*, consists of calcitic, foliated structure. The leaves of the folia are thin, regular and aligned approximately parallel to the shell surfaces (text-fig. 16). The inner shell layer is of aragonitic, complex crossed-lamellar structure. This layer is restricted to a small area immediately surrounding the three centrally placed muscle scars in the left

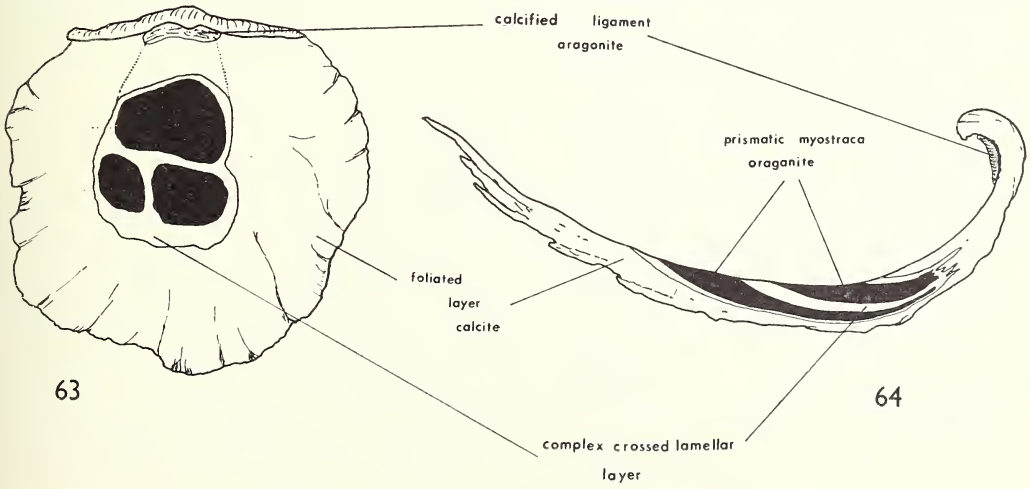

Figs. 63–64. Anomiacea : *Anomia ephippium*. Fig. 62. General view of the interior of the shell. Fig. 63. Radial section showing the general distribution of the shell layers etc.

TABLE 12

ANOMIACEA

NAME	LOCALITY	COMPOSITION	OUTER LAYER	INNER LAYER	MYOSTRACA	OBSERVATIONS
Anomia ephippium (Linnaeus)	Britain	Calcite and aragonite	Foliated calcite	Complex crossed-lamellar aragonite	Prismatic aragonite	Fibrous layer of ligament aragonitic. Three muscle scars in upper valve and one in lower.
Anomia peruviana d'Orbigny	Ecuador	Calcite and aragonite	Foliated calcite	Complex crossed-lamellar aragonite	Prismatic aragonite	Three muscle scars in upper valve, one in lower.
Placuna placenta (Linnaeus)	E. Indies	Calcite and aragonite	Foliated calcite	Absent	Prismatic aragonite	Single muscle scar in either valve.
In addition the species listed below had both calcite and aragonite in the shell.						
Anomia sp.	Mediterranean ;					
Anomia sp.	Juhn, India ;					
Enigmonia enigmatica Sowerby	Philippines					

valve, and to a thin fringe around the byssal notch in the right valve. The three muscle scars in the left valve and the single adductor scar in the right valve leave a trace of aragonitic, prismatic myostracum through the complex crossed-lamellar layer. These bands make the shell structure appear rather complicated.

Most of the members of the Anomiacea are adapted for a sedentary, attached life, and considerable modifications have taken place in the symmetry of the shell and body of the animal as a result of this adaption. The right valve is adapted for a horizontal existence against the substrate ; it is almost flat, although it usually conforms to the shape of the underlying substrate. There is also a deep embayment or byssal notch in this valve which enables the calcified byssus to be attached near the centre of the shell. As a result, there has been an enlargement of the byssal retractor muscle and the pedal muscles, and a reduction in the size of the single adductor muscle. Pallial attachment in the upper left valve is limited to a small area around the three muscle scars, and in the lower right valve to around the byssal notch and single adductor scar.

Placuna placenta is a member of the Anomiacea which has reverted to the free-living, unattached mode of life. The byssal notch, byssal retractor and pedal muscles have disappeared, and the single adductor muscle has again become enlarged. The inner complex crossed-lamellar layer has also disappeared ; the adductor myostracum is seen as an aragonitic, prismatic myostracal trace, passing through the foliated layer. The folia in *Placuna* are rather more regular than in other anomiids and the shell has a high organic content.

The calcified inner ligament of *Anomia ephippium* and *A. peruviana* is aragonitic.

Electron microscope studies were carried out on *Placuna placenta* and *Anomia ephippium*, and the results have been incorporated in the introductory sections on foliated structure. The fine structure of *Anomia lishkei* has been investigated by Wada (1963b).

LIMACEA

(Text-figs. 27, 65–67)

Seven species have been examined mineralogically and six optically. In all species the shell contains both aragonite and calcite.

In all the species examined optically there is an outer, finely foliated calcitic layer and an inner, aragonitic crossed-lamellar layer. In the crossed-lamellar layer the first order lamels have a rather simple form and are arranged concentrically. This layer extends out almost to the margins of the shell, and forms the hinge and teeth. In sections close to and through the single adductor scar, a thin, prismatic adductor myostracum can be seen running through the crossed-lamellar layer. As in the Spondylidae and Plicatulidae (p. 95) the first order lamels correspond across the myostracum.

In two species, i.e. *Lima squamosa* and *Lima rotundata* there is a restricted area of an inner, aragonitic complex crossed-lamellar layer, which is present in the centre of the shell and beneath the hinge.

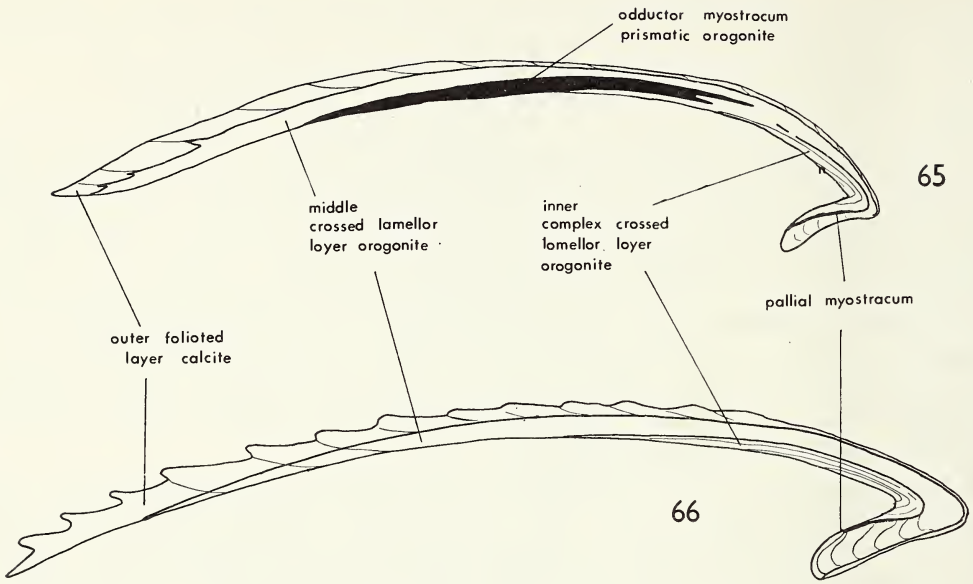

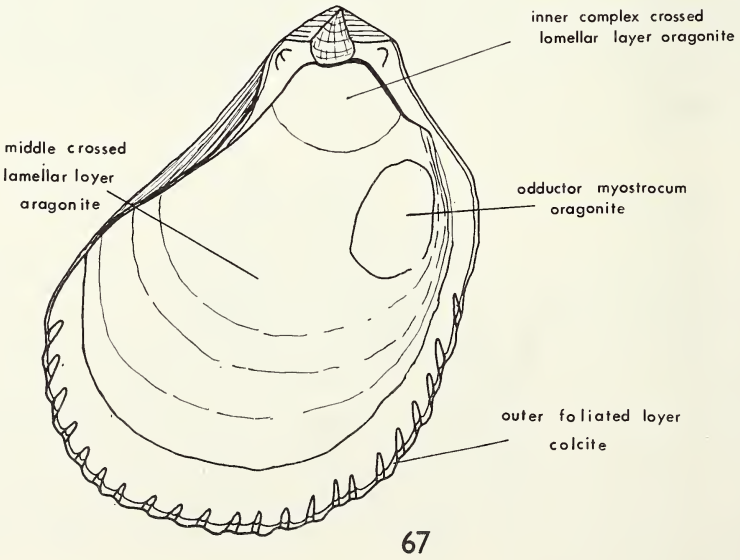

Figs. 65–67. Limacea : Radial sections of *Lima colorata* (65) and *Lima squamosa* (66) showing the general distribution of the shell layers. Fig. 67. *Lima colorata* general view of the interior of the shell.

TABLE 13

LIMACEA

NAME	LOCALITY	COMPOSITION	OUTER LAYER	MIDDLE LAYER	INNER LAYER	MYOSTRACUM		OBSERVATIONS
						Pallial	Adductor	
Lima colorata Hutton	Tertiary New Zealand	Calcite and aragonite	Finely foliated calcite	Crossed-lamellar aragonite	Complex crossed-lamellar aragonite	Prismatic aragonite	Prismatic aragonite	Pallial myostracum seen in umbo only
Lima hians Gmelin	Britain	Calcite and aragonite	Finely foliated calcite		Crossed-lamellar aragonite			
Lima inflata Lamarck	Mediter-ranean	Calcite and aragonite	Finely foliated calcite		Crossed-lamellar aragonite			
Lima d'orbignyana Matherson	Ecuador	Calcite and aragonite	Finely foliated calcite		Crossed-lamellar aragonite			
Lima rotundata Sowerby	Algoa Bay, South Africa	Calcite and aragonite	Finely foliated calcite		Crossed-lamellar			
Lima squamosa Lamarck	Australia	Calcite and aragonite	Finely foliated calcite	Crossed-lamellar aragonite	Complex crossed-lamellar aragonite	Prismatic aragonite		Pallial myostracum seen in umbo only
Promantellum stertum Iredale	S. Australia	Calcite and aragonite						

A pallial myostracum has been detected in two species only, *Lima colorata* and *L. squamosa*, as a thin prismatic band in the crossed-lamellar layer of the umbonal region. There seems little doubt that the ' middle ' crossed-lamellar layer in three-layer shells and the ' inner ' crossed-lamellar layer in two-layer shells are to be equated. The development of an inner layer of complex crossed-lamellar structure in the umbonal region, beneath the hinge, corresponds to the development of the patch of foliated structure present in the Pectinidae, and probably has the same supporting function.

The foliated and crossed-lamellar layers are roughly equal to each other in thickness in the Limacea. The crossed-lamellar structure forms internal ribs, which can be seen well in transverse sections of the shell. Compared with oysters and pectens, the folia in the Limacea are very small and fine, and they look like fine needles in some sections.

Suborder OSTREINA

OSTREACEA

(Plate 5, figs. 2–3 ; Pl. 6, figs. 1, 2, 4 ; Pl. 27, fig. 4 ; fig. 2, 8, figs. 4–5 ; text-figs. 14–15, 30, 68)

Seven species were examined mineralogically and optically. The shell consists of both calcite and aragonite.

The greater part of both valves of the oyster shell consists of calcitic foliated structure. The folia are generally arranged approximately parallel with the shell surfaces. The foliated structure is complicated by the development of ' chalky ' layers ; these consist of lenses formed of vertically arranged, irregular calcite fibres, intercalated between the folia. Chalky layers are more common in the lower valve than in the upper valve, and in older specimens. Korringa (1951) considered chalky layers to be an economy building measure by the oyster, and that their function is to smooth out irregularities on the inside of the shell. In three of the species examined by us, and probably in all species of oysters, the outermost layer of *only* the upper valve consists of simple calcitic prisms. This prismatic layer is usually seen as imbricate scales, which are usually present only near the valve margin. They are fragile, and become worn away on the earlier parts of the shell. Beneath the single adductor muscle scar there is a pad of aragonitic myostraca prisms which extends as a myostracal trace through the shell. Bøggild (1931) considered oysters to be entirely calcitic but Stenzel (1963) showed that the adductor and Quenstedt myostraca of *Crassostrea virginica* were aragonite ; we have examined myostraca in a further six species and confirmed this result.

In the Ostreacea, the radial, pallial muscles are attached to the shell around the base of the adductor muscle (Yonge 1953), and as a result the pallial myostracum is not distinct from the adductor myostracum. Apart from the prismatic layer in the upper valve, no further differentiation into shell layers could be seen in any of the species of oxyster examined, although Oberling (1964) recognises three layers within the foliated structure in this group.

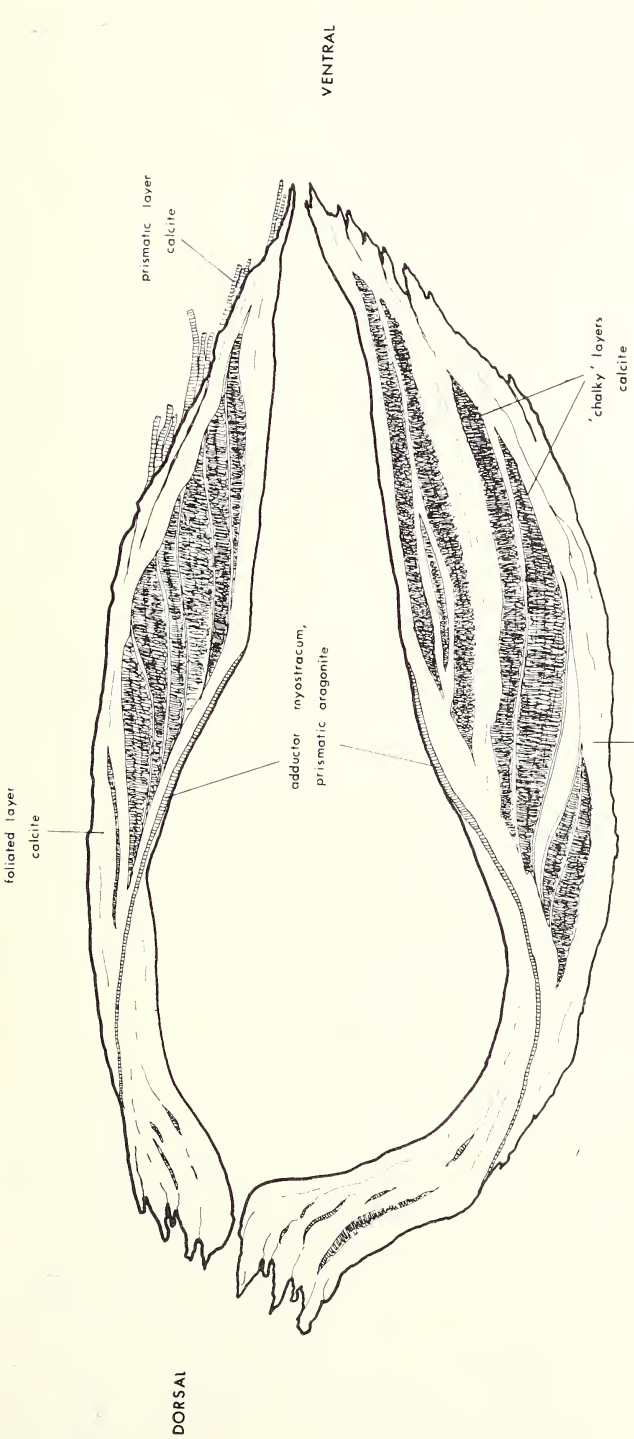

FIG. 68. Ostracea : *Ostrea edulis*, radial section showing the distribution of the shell layers, the myostracum and the chalky layers.

TABLE 14

OSTREACEA

NAME	LOCALITY	COMPOSITION	RIGHT VALVE		LEFT VALVE	ADDUCTOR MYOSTRACA	CHALKY LENSES	OBSERVATIONS
			OUTER LAYER	INNER LAYER				
Crassostrea corteziensis (Hertlein)	Ecuador	Calcite and aragonite		Foliated calcite	Foliated calcite	Prismatic aragonite	Present, calcite	
Ostrea cristagalli Linnaeus	East Indies	Calcite and aragonite		Foliated calcite	Foliated calcite	Prismatic aragonite		
Ostrea cuccullata Born	Seychelles	Calcite and aragonite	Prismatic calcite	Foliated calcite	Foliated calcite	Prismatic aragonite		
Ostrea edulis Linnaeus	Britain	Calcite and aragonite	Prismatic calcite	Foliated calcite	Foliated calcite	Prismatic aragonite	Present, calcite	Fibrous layer of ligament aragonitic
Ostrea hyotis Linnaeus	Seychelles	Calcite and aragonite		Foliated calcite	Foliated calcite	Prismatic aragonite	Present, calcite	Fibrous layer of ligament aragonitic
Ostrea irridescens Gray	Ecuador	Calcite and aragonite	Prismatic calcite	Foliated calcite	Foliated calcite	Prismatic aragonite	Present, calcite	
The following fossil oysters were examined only one of which *O. monotiscaprilis* shows any aragonite in the shell.								
Ostrea tenera (Sowerby)	Eocene, Britain ;							
Ostrea plicata (Solander)	Eocene, Dameray, France ;							
Ostrea monotiscaprilis Klipstein	U. Trias, Austria ;							
Enantiostrian spondyloides (Goldfuss)	Trias, Bavaria ;							

Stenzel (1962) found that the inner calcified part of the ligament, the resilium, in *Crassostrea virginica* was aragonitic ; this has been confirmed by us for several other species. Stenzel (1964) has also found that the prodissoconch of *C. virginica* is aragonitic ; further investigation is needed to determine if, as seems likely, there is any change in shell structure at the end of the prodissoconch stage.

A characteristic of many oysters, seen particularly in the lower left valve but occasionally in the upper, right valve is ' chambering ', i.e. the occurrence of shallow cavities within the shell which are filled with sea water, often putrefied. Orton (1937) and Korringa (1951) believe that chambering results from shrinkage of the body of the oyster, possibly caused by salinity changes ; subsequent shell secretion by the shrunken body traps sea water in cavities in the shell.

In *Ostrea cuccullata*, conchiolin patches are deposited on the inner surface of the shell, and in section it is clear that this process has been repeated several times during shell growth. As in the Unionacea (see p. 111) deposition of these conchiolin layers seems to be a reaction by the animal against excessive corrosion of the older parts of its shell. Korringa (1951) considers that similar deposits in *Ostrea edulis* are a defence against boring worms.

We have studied the fine structure of the foliated layer in three species of oyster, i.e. *Ostrea edulis*, *Ostrea irridescens* and *Pycnodonte hyotis* ; the results of this work have been discussed in the introductory section on foliated structures (p. 29). Tsujii *et al.* (1958), Watabe *et al.* (1958), and Watabe and Wilbur (1961) have described in detail the foliated layers of *Crassostrea virginica* ; organic matrix-calcium carbonate relations in the foliated layer of the same species have been described by Watabe (1965). Wada (1961b, 1963c) has briefly noted foliated structure in *Ostrea gigas*.

True oysters first appeared in the Upper Trias, and Newell (1960) considered that the ' oysterlike ' Pseudomonotidae, so common in the Upper Palaeozoic, are the most likely ancestors of the group. In 1938 Newell placed the Pseudomonotidae in the Aviculopectinidae. Previously (1937) he had recorded that ' the outer ostracum of the right valve is irregularly prismatic calcite, exactly as in Aviculopecten '.

Sub Class *PALEOHETERODONTA*
Order UNIONOIDA
UNIONACEA

(Plate 1, fig. 4 ; Pl. 2, figs. 1, 2, 4 ; Pl. 3, figs. 1, 2, 3 ; Pl. 5, fig. 1 ; Pl. 7, figs. 2, 3, 4, 5 ; Pl. 8, figs. 1, 2, 4, 5 ; Pl. 9, figs. 2–3 ; Pl. 10, figs. 1, 2, 3, 4, 5 ; Pl. 11, figs. 1, 2, 3 ; text-figs. 1, 2, 4, 5, 11–13, 17, 69–75)

Fifteen species have been examined mineralogically, and twelve optically. The shell is wholly aragonite throughout.

Two principle shell structure types, i.e. nacreous and prismatic, are present in the Unionids. The prismatic layer is thin, and is usually abraded or dissolved away in the umbonal region. In the two species of the cemented genus *Etheria*

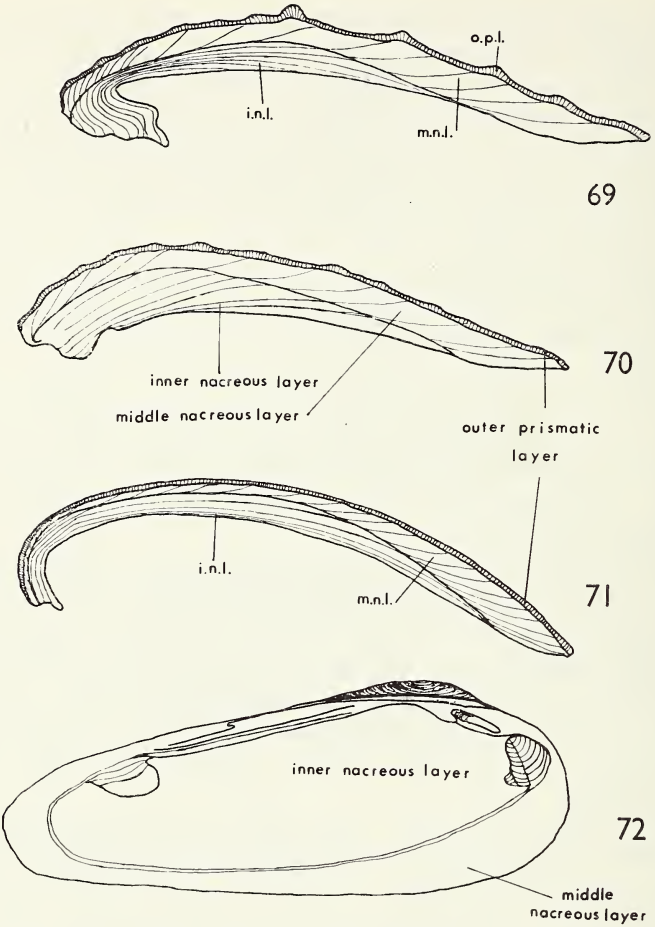

Figs. 69–72. Unionacea : Figs. 69–71. Radial sections of *Unio mytiloides* (69), *Quadrula metanevra* (70) and *Unio pictorum* (71) showing the general distribution of the shell layers. Fig. 72. *Unio pictorum*, general view of the shell interior.

that we have examined, a prismatic layer is not developed. This appears to be a primary feature of the genus. In all species where good sections of the prismatic layer were available, the prisms show a typically feathery internal structure (text-fig. 75) of downwardly diverging elements ; this is the " complex prismatic structure " of Bøggild (1930). The prisms also show prominent growth lines. The prismatic layer sometimes interdigitates with the underlying nacreous layer. Resolution of the detailed structure of nacre is largely beyond the limits of optical microscopy, although the two main types can be readily distinguished. " Sheet " nacre occurs in all the species we have examined, usually forming the innermost shell layer, while lenticular nacre forms the middle shell layer of *Anodonta anatina, A. cygnea, Potamides littoralis, Quadrula metanevra, Unio mytiloides,* and *Unio pictorum.*

A very thin, discontinuous, prismatic pallial myostracum has been observed in most of the species that we have examined. Sections through the adductor muscle scars of *Etheria* and *Margaritifera margaritifera* showed thin prismatic myostracal layers in these areas.

A striking feature of *Anodonta cygnea*, *Etheria* sp., *Etheria elliptica*, *Hyria ligatus*, *Margaritifera margaritifera* and *Unio fisherianus* is the development of thin (0·01–0·03 mm) periostracum-like, conchiolin layers within the nacre. These conchiolin sheets probably serve to preserve the frequently abraded and etched umbonal area

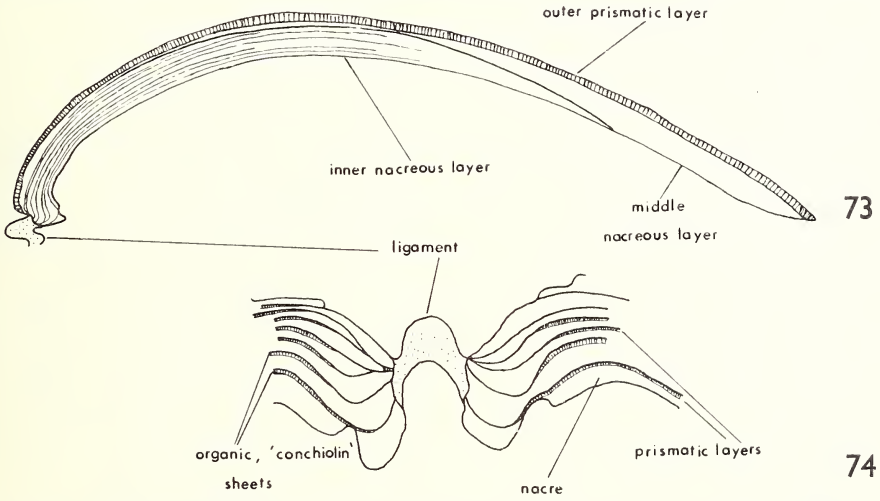

Figs. 73–74. Fig. 73. *Margaritifera margaritifera*, radial section showing the general distribution of the shell layers and the conchiolin sheets in the nacre. Fig. 74. Detail of organic ' conchiolin ' sheets and prismatic layers in the hinge area. Radial section.

against solution, and perhaps also strengthen the umbonal and hinge area, replacing the now-missing periostracum. In *M. margaritifera* these periostracum-like sheets are confined to the inner layer of the nacre and are associated with thin (0·12–0·10 mm, prismatic layers (text-figs. 73–74). Each prismatic layer lies immediately inside the adjacent conchiolin layer. It appears that these organic layers have the same structure as the periostracum, for the sequence of periostracum-prisms-nacre is the same as that occurring at the growing edge of the shell. In the umbonal region, these conchiolin bands pass through the internal ligament, although here the underlying prism band is absent. The actual stimulus for the laying down of these conchiolin layers is not known. Beedham (1965), from regeneration experiments carried out on *Anodonta cygnea*, has found that the general outer mantle surface which normally secretes only nacreous structure, can, upon injury, repair the shell with layers of periostracum, prisms and nacre in the same sequence as that found at the mantle edge, thus confirming the work of Rassbach (1912) and Rubbell (1911). During the process of regeneration the epithelial cells of the general mantle surface change their size and morphology to resemble those of the outer fold of the mantle edge. The most probable explanation of this feature, and, as already suggested,

TABLE 15

UNIONACEA

NAME	LOCALITY	COMPOSITION	OUTER LAYER	MIDDLE LAYER	INNER LAYER	MYOSTRACA		OBSERVATIONS
						Pallial	Adductor	
Anodonta anatina Lamarck	Britain	Aragonite	Prismatic	Lenticular nacre	Sheet nacre	Thin, discontinuous, prismatic		
Anodonta cygnea Bosc	Britain	Aragonite	Prismatic	Lenticular nacre	Sheet nacre	Thin, discontinuous, prismatic		Well developed conchiolin sheets in inner layer
Unio fisherianns Lea	Ohio, U.S.A.	Aragonite	Prismatic	Nacreous	Sheet nacre			Prominent conchiolin sheets in inner layer. Pallial trace separates distinctive nacres although no prismatic myostracum seen
Unio multistriata Lea	Brazil	Aragonite	Prismatic	Nacreous	Sheet nacre	Thin, prismatic		
Unio mytiloides Rafinesque	Kentucky, U.S.A.	Aragonite	Prismatic	Lenticular nacre	Sheet nacre	Thin, prismatic		
Unio pictorum Linnaeus	Britain	Aragonite	Prismatic	Lenticular nacre	Sheet nacre	Thin, prismatic		
Quadrula metanevra Rafinesque	Ohio, U.S.A.	Aragonite	Prismatic	Lenticular nacre	Sheet nacre	Thin, prismatic		
Potamides littoralis (Cuvier)	Spain	Aragonite	Prismatic	Lenticular nacre	Sheet nacre			
Margaritifera margaritifera (Linnaeus)	England	Aragonite	Prismatic	Lenticular nacre	Sheet nacre	Thin, prismatic	Thin, prismatic	Prominent conchiolin sheets in the inner layer, with associated thin prism bands
Hyria corrugatus (Lamarck)	E. Indies	Aragonite	Prismatic	Nacreous	Sheet nacre	Thin, discontinuous, prismatic		Well developed conchiolin bands in both nacreous layers. Fibrous ligament aragonitic

Name	Locality	Composition	Outer Layer	Middle Layer	Inner Layer	Myostraca		Observations
						Pallial	Adductor	
Etheria elliptica Lamarck	Nigeria	Aragonite	Nacreous		Sheet nacre	Prismatic	Prismatic	Well developed conchiolin bands in both layers. Tubes septate.
Etheria sp.	S. America	Aragonite	Nacreous		Sheet nacre	Thin, prismatic	Thin, prismatic	Well developed conchiolin bands in both layers, truncated at pallial trace.

The following species were aragonitic :

Unio mertoniana Lea	River Maranon, Peru ;
Unio cretaceus Zittel	Upper Cretaceous, Nebraska, U.S.A. ;
Unio sp.	Upper Cretaceous, Alberta.

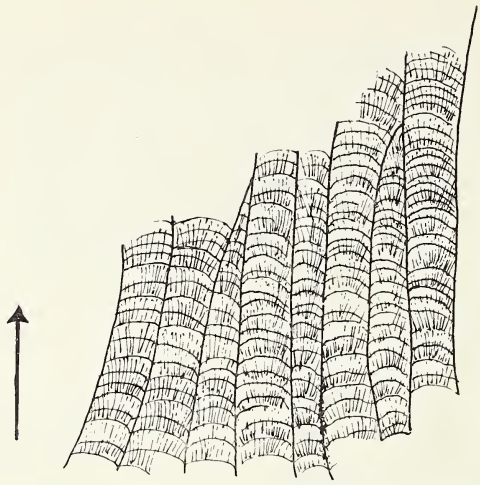

FIG. 75. Normal appearance of unionid prisms at optical level as seen in radial peels and thin sections, based on *Unio pictorum* ×250. Arrow marks direction of the interior of the shell.

of the periostracum-like layers seen in the unionids, is that it is a response by the mantle to some stimulus resulting from the abrasion and solution of the shell from the umbonal region.

The only calcified internal ligament examined, that of *Hyria corrugatus*, contained aragonite.

Perfectly preserved nacreous unionids from the Cretaceous of North America are wholly aragonitic. *Unio andersoni* Hudson (Hudson 1963) from the great Estuarine series (Jurassic, Bathonian) is also wholly aragonite, while mode of preservation of the Devonian unionid *Archandoon jukesi* (Forbes) suggests a formerly aragonitic shell.

We have examined the ultrastructure of the following unionids : *Margaritifera margaritifera, Anodonta cygnea, A. anatina, Quadrula metanevra,* and *Potamides littoralis*. Most of our observations are included in the introductory sections on nacre, prisms, myostraca, and layer boundaries (pp. 17–59). A few additional observations are noted below.

Electron microscopic studies of sections through *Margaritifera margaritifera* give additional data on the alternating periostracum-like and prismatic bands (Plate 11, figs. 1 and 2). The nacre outside the periostracum-like band (i.e. on which the band was deposited) shows no unusual features. The contact between the periostracum-like band and this nacre is relatively abrupt and regular, and usually corresponds to the interlamellar matrix of a single sheet of nacre tablets. The contact thus has the same sort of irregularities as are present between sheets of nacre. In some cases the conchiolin shows extensions out into the nacre, to a depth of several sheets of tablets. The thickness of the periostracum-like layer may vary between 1 and 3 microns in the same band, but the range of variation is probably greater. A particularly interesting feature of the periostracum-like layer is the

indication of an internal structure. This is seen on our pictures as a series of very fine, subparallel, sinuous lines which run almost normal to the inner and outer surfaces of the conchiolin sheet, thus dividing it up into bands 0·2–0·5 microns wide. Sometimes these lines branch, so that the bands are divided up into smaller units. The significance of these bands is quite unknown, as there appears to be no other work on the ultrastructure of the bivalve periostracum.

The inner boundary of the periostracum-like layer is in the form of shallow, rounded embayments (Plate 11, fig. 1), between inwardly projecting conchiolin wedges. These wedges form the walls of the underlying layer of prisms. These prisms, unlike those of the outer prismatic shell layer, are not always parallel, but converge and join to produce distinctive patterns. The prisms are small, with apparent diameters being between 5 and 10 microns, while apparent heights are between 6 and 10 microns. The surface of the section of each prism has a scaly appearance which is due to the outcropping of many thin membranes of intracrystalline organic matrix within each prism. Thus each prism is built up of smaller blocks like those forming the prisms of the outer shell layer. These small prisms pass down into quite normal nacre, with a characteristic poorly ordered transitional zone between the two structures. The sequence in the bands thus parallels that of the whole shell layering in miniature, even at the finest structural level.

The inner surface of the innermost shell layer of *M. margaritifera* shows some features not previously recorded in nacreous structure. The tablets building up the sheet nacre in this layer have irregular or rounded outlines and are frequently arranged into rosette-like patterns. Thus one tablet occupies a central position and up to ten other tablets are arranged around it, each having a radial elongation (Plate 5, fig. 1). Quite large areas of the inner surface of the inner layer are covered in a mosaic of these rosettes, the significance of which is as yet unexplained. The arrangement may be merely the configuration resulting from growth of nacre tablets together, but if this is so, it is surprising that this feature has not yet been recognised in any other species of nacreous mollusc.

TRIGONACEA

(Plate 1, figs. 1–3 ; Pl. 28, fig. 1 ; Pl. 13, figs. 1–3 ; text-figs. 76–77)

Three species were examined mineralogically and two optically. The shell is entirely aragonitic.

The outer shell layer, which forms the ribs and tubercles, is prismatic. In the spaces that separate ribs or tubercles the prisms are more or less regularly polygonal and columnar, with a conchiolin wall between each prism. The prisms have conspicuous downward divergent striations, representing the joins between their constituent crystallites. These striations are more conspicuous than in any other group of bivalves that we have studied. Prisms may be strongly reclined towards the shell margin. The outer portion of each prism bears a small boss or mamelon,

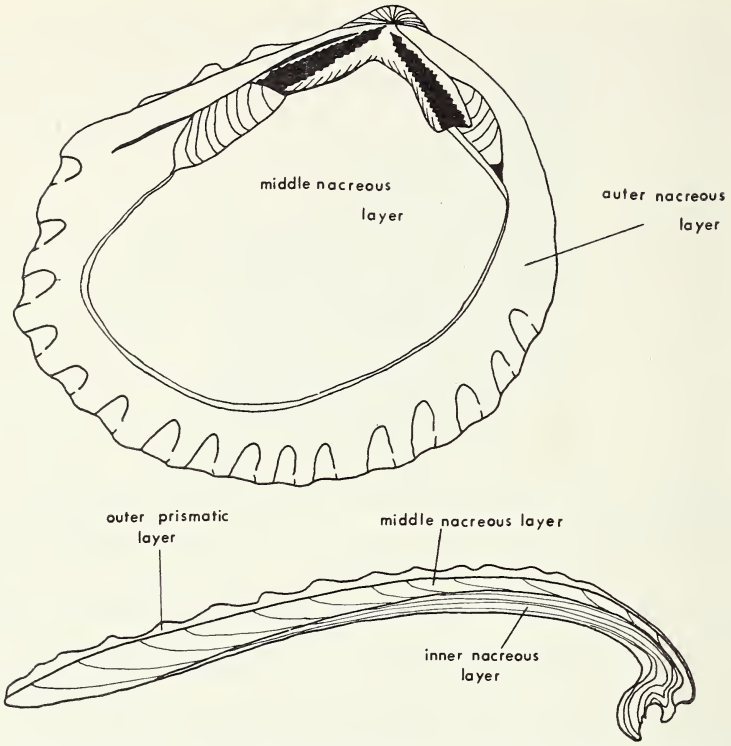

FIGS. 76–77. Trigonacea : *Neotrigonia margaritacea* interior of the shell (76) and radial section (77) showing the general distribution of the shell layers.

with a sharp shoulder joining it to the rest of the prism, with which it is in continuity. This boss may show concentric striations. The outer ends of each prism are separated from each other by a wedge of periostracum (Plate 13, figs. 1–2). The boss represents the initial spherulite from which each prism has developed, on the inner surface of the periostracum. In the ribs and tubercles, however, the prisms lose their regularity, and become very much smaller, so that obvious prismatic structure disappears, and the layer is formed in these regions of irregularly imbricating layers of small granules. In section this structure appears dark grey, with a finely granular appearance.

Between the outer prismatic layer and the pallial line there is a middle, aragonitic layer of lenticular nacre. The middle nacreous layer is separated from an inner layer of sheet nacre by a structural discontinuity marking the trace of the pallial myostracum. Prisms are only locally present but there is a definite unconformity of growth layers on either side of the trace of the pallial line.

Detailed electron microscope studies were carried out on *Neotrigonia dubia* and *N. pectinata*.

The mode of preservation of fossil trigoniids from the Jurassic onwards suggests that these were originally aragonitic, as does the preservation of Triassic species of *Myophoria* that we have examined.

TABLE 16

TRIGONACEA

NAME	LOCALITY	COMPOSITION	OUTER LAYER	MIDDLE LAYER	INNER LAYER	MYOSTRACA		OBSERVATIONS
						Pallial	Adductor	
Neotrigonia dubia (Sowerby)	Port Jackson, Australia	Aragonite	Prismatic	Lenticular nacre	Sheet nacre	Prismatic, thin		Fibrous layer of ligament aragonitic
Neotrigonia margaritacea (Lamarck)	Australia	Aragonite	Prismatic	Lenticular nacre	Sheet nacre	Prismatic, thin		
Eotrigonia semiundulata (MacCoy)	Oligocene, Victoria	Aragonite	Prismatic	Lenticular nacre	Sheet nacre			

REFERENCES

Abolinš-Krogis, A. 1958. The morphological and chemical characteristics of organic crystals in the regenerating shell of *Helix pomatia*. *Acta zool.* (Stockholm), **39** : 19–38, 15 figs.

—— 1961. The histochemistry of the hepatopancreas of *Helix pomatia* (L.) in relation to the regeneration of the shell. *Ark. zool.*, Stockholm, 13, 159–202, pls. 1–9, 1 fig.

—— 1963. The histochemistry of the mantle of *Helix pomatia* (L.) in relation to the repair of the damaged shell. *Ark. zool.*, Stockholm, **15** : 461–474.

Barker, R. M. 1964. Microtextural variation in pelecypod shells. *Malacologia*, Ann Arbor, **2** (1) : 69–86, 4 figs.

Bauer, E. 1964. Growth of oriented films on amorphous surfaces. pp. 43–67, figs. 1–16 *in* : *Single crystal films*, Edited Francombe, M. H. and Sato, H., pp. 420, Oxford.

Beedham, G. E. 1958a. Observations on the mantle of the Lamellibranchia. *Quart. J. micr. Sci.*, Oxford, **99** : 181–197, pls. 1–2, 2 figs.

—— 1958b. Observations on the non-calcareous component of the shell of the Lamellibranchia. *Quart. J. micr. Sci.*, Oxford, **99** : 341–357, 3 figs.

—— 1965. Repair of the shell in species of *Anodonta*. *Proc. Zool. Soc. Lond.*, **145** (1) : 107–124, pls. 1–2.

—— & Owen, G. 1965. The mantle and shell of *Solemya parkinsoni* (Protobranchia : Bivalvia). *Proc. Zool. Soc. Lond.*, **145** (3) : 405–430, 1 pl., figs. 1–12.

—— & Trueman, E. R. 1967. The relationship of the mantle and shell of the Polyplacophora in comparison with that of other Mollusca. *J. Zool.*, London, 151, 215–231, 6 figs.

Biedermann, W. 1901. Untersuchungen über Bau und Entstehung der Molluskenschalen. *Jena Z. Naturw.*, **36** : 1–164, pls. 1–6.

Bøggild, O. B. 1930. The shell structure of the mollusks. *K. danske Vidensk. Selsk. Skr.*, Copenhagen, **2** : 232–325, pls. 1–15, 10 figs.

Borradaile, L. A., Eastham, L. E. S., Potts, F. A. & Saunders, J. T. 1963. *The Invertebrata*. 4th edition, xvii + 820 pp., 523 + 11 figs. Cambridge.

Buchsbaum, R. 1951. *Animals without backbones*. 400 pp., pls., figs. Penguin Books, London.

Buckley, H. E. 1951. *Crystal Growth*. xv + 571 pp., pls. 1–88, 169 figs. New York.

Carpenter, W. B. 1844. On the microscopic structure of shells. *Rep. Brit. Ass. Adv. Sci.* (for 1844) London : 1–24, pls. 1–20.

—— 1848. Report on the microscopic structure of shells, pt. 2. *Rep. Brit. Ass. Adv. Sci.*, (for 1847) London : 93–134, pls. 1–20.

Chave, K. E. 1954. Aspects of the biogeochemistry of magnesium. 1. Calcareous marine organisms. *J. Geol.*, Chicago, **62** : 266–283, 16 figs.

Christyakov, Yu. D. & Lainer, B. D. 1966. Oriented overgrowth (Epitaxis) of crystalline materials. *In : Growth of crystals* (English transl. Consultants Bureau New York) ed. Shubinov, A. V. & Sheftal, N. N. **4** : 171–179.

Clarke, F. W. & Wheeler, W. C. 1922. The inorganic constituents of marine invertebrates. *U.S. Geol. Survey Prof. Paper*, Washington, 124, 62 pp.

Cornish, V. & Kendall, F. K. 1888. On the mineralogical constitution of calcareous organisms. *Geol. Mag.*, London (Dec. 3), **5** : 66–73.

Cox, L. R. 1959. The gelogical history of the Protobranchia and the dual origin of taxodont Lamellibranchia. *Proc. Malac. Soc.* London, **33** (5) : 200–209, 5 figs.

—— 1960. General characteristics of gastropods. *In : Treatise on Invertebrate Palaeontology Part I. Mollusca 1.* (Ed. R. C. Moore) : 84–169, 37 figs.

Deer, W. A., R. A. Howie & J. Zussman 1962. *Rock forming minerals*. Vol. 5, non-Silicates. ix + 1–370 figs. Longmans, London.

Degens, E. T. 1965. *Geochemistry of sediments : a brief survey*. ix + 342 pp., illustr. Englewood Cliffs, New Jersey.

Degens, E. T., Spencer, D. W. & Parker, R. H 1967. Palaeobiochemistry of molluscan shell proteins. *Comp. biochem. physiol.*, London, **20** : 553–579, tables 1–14, 1 fig.
Dekeyser, W. & Amelinckx, S. 1955. *Les Dislocations et la Croissance des Cristaux.* 168 pp., pls. 1–57, figs. Paris.
Dodd, J. R. 1963. Palaeoecological implications of shell mineralogy in two pelecypod species. *J. Geol.*, Chicago, **71** : 1–11, 8 figs.
—— 1964. Environmentally controlled variation in the shell structure of a pelecypod species. *J. Paleont.*, Tulsa, **38** : 1065–1071, 1 pl., 6 figs.
—— 1965. Environmental control of strontium and magnesium in *Mytilus*. *Geochim. et Cosmochim. Acta*, 29, 385–398.
—— 1966a. The influence of salinity on mollusk shell mineralogy ; a discussion. *J. Geol.*, Chicago, **74** : 85–89, 4 figs.
—— 1966b. Processes of conversion of aragonite to calcite with examples from the Cretaceous of Texas. *J. sed. petrology*, Tulsa, **36** : 733–741, 3 figs.
Dunachie, J. F. 1963. The periostracum of *Mytilus edulis*. *Trans. Roy. Soc. Edinb.*, **65** (15) : 383–411, 1 pl.
Easton, W. H. 1960. *Invertebrate Palaeontology*, 701 pp., figs. New York.
Ehrenbaum, E. von. 1885. Untersuchungen über die Struktur und Bildung der Schale der in der Kieler Bucht hanftig vorkommenden Muscheln : *Z. wiss. Zool.*, Leipzig, **41** : 1–47, pls. 1–2.
Eisma, D. 1966. The influence of salinity on mollusk shell mineralogy : a discussion. *J. Geol.*, Chicago, **74** (1) : 89–94, 5 figs.
Epstein, S. & Lowenstam, H. A. 1953. Temperature-shell-growth relations of recent and interglacial Pleistocene shoal-water biota from Bermuda. *J. Geol.*, Chicago, **61** : 424–438.
Forty, A. J. 1954. Direct observations of dislocations in crystals. *Adv. Phys.*, London, **3** : 1–25.
Frank, F. C. 1952. Crystal growth and dislocations. *Adv. Phys.*, London, **1** : 91–110.
Fulman, R. L. 1955. The growth of crystals. *Sci. Amer.*, New York.
Glimcher, M. J. 1960. Specificity of the molecular structure of organic matrices in mineralisation. *In :* Calcification in Biological Systems (R. F. Sognnaes, ed., *Am. Assoc. Advance Sci.*, Washington, D.C., Publ. **64** : 421–487, 20 figs.
Gordetsky, A. F. & Saratovkin, D. D. 1958. Dendritic form of crystals produced in antiskeletal growth. *Repts. 1st. Conf. on Crystal Growth, U.S.S.R.* (Engl. transl. Consultants Bureau, New York) : 151–158, 12 figs.
Grégoire, C. 1957. Topography of the organic components in mother-of-pearl. *J. biophys. biochem. Cytol.*, Baltimore, **3** : 797–808, 1 fig.
—— 1959. A study of the remains of organic components in fossil mother-of-pearl. *Bull. Inst. Sci. nat. Belg.*, Brussels, **35** (13) : 1–14, pls. 1–8.
—— 1960. Further studies on structure of the organic components in mother-of-pearl, especially in pelecypods (Part I). *Bull. Inst. Sci. nat. Belg.*, Brussels, **36** (23) : 1–22.
—— 1961a. Structure of the conchiolin cases of the prisms in *Mytilus edulis* Linne *J. biophys. biochem. Cytol.*, Baltimore, **9** : 395–400, 9 figs.
—— 1961b. Sur la structure submicroscopique de la conchioline associée aux prismes de coquilles de mollusques. *Bull. Inst. Sci. nat. Belg.*, Brussels, **37** (3) : 1–34, pls. 1–10.
—— 1962. On submicroscopic structure of the *Nautilus* shell. *Bull. Inst. Sci. nat. Belg.*, Brussels, **38** (49) : 1–71 pls. 1–24, 8 figs.
—— 1964. Thermal changes in the *Nautilus* shell. *Nature*, London, 203 (4947) : 868–869.
& Telheus, C. 1965. Conchiolin membranes in shell and cameral deposits of Pennsylvanian cephalapods, Oklahoma. *Oklahoma Geological Notes*, **25** : 175–201.
—— Duchateau, G. & Florkin, M. 1955. La trame protidique des nacres et des perles. *Ann. Inst. océanogr.*, Paris, **31** : 1–36, pls. 1–23.
Grigor'ev, D. P. 1965. *Ontogeny of minerals.* v + 250 pp., 195 figs., Jerusalem.
Haas, F. 1929–35. Bivalvia. *In :* Bronn, H. G., *Klassen und ordnungen des Tierreichs*, Band 3, Abt. 3, Teil 1, xii + 984 pp., 562 figs.

HALL, A. & KENNEDY, W. J. 1967. Aragonite in fossils. *Proc. Roy. Soc.* London. B 168, 377–412.

HARE, P. E. 1963. Amino acids in the proteins from aragonite and calcite in the shells of *Mytilus californianus*. *Science*, New York, **139** : 216–217.

—— & ABELSON, P. H. 1964. Proteins in Mollusk shells. *Rep. Dir. geophys. Lab. Carnegie Instn.*, Washington, **63** : 267–270.

—— 1965. Amino acid composition of some calcified proteins. *Rep. Dir. geophys. Lab. Carnegie Instn.*, Washington, **64** : 223—232.

HUBENDICK, B. 1958. On the molluscan adhesive epithelium. *Ark. Zool.*, Stockholm, 2nd ser. **2** : 31–36, pls. 1–3, 1 fig.

HUDSON, J. D. 1962. Pseudopleochroic calcite in recrystallised shell limestones. *Geol. Mag.*, London, **99** : 492–500, pl. 21.

—— 1963. The ecology and stratigraphical distribution of the invertebrate fauna of the Great Estuarine Series. *Palaeontology*, London, **6** : 327–348, 1 pl., 3 figs.

—— 1968. The microstructive and mineralogy of the shell of a Jurassic mytilid (Bivalvia). *Palaeontology*, London, **11** : 163–182, pls. 31–35, 5 figs.

JACKSON, R. T. 1890. Phylogeny of the Pelecypoda, the Aviculidae and their allies. *Boston Soc. Hat. Hist. Mem.*, **4** : 277–400 pls. 23–30, 53 figs.

JAMESON, L. H. 1912. Studies on pearl-oysters and pearls. I. The structure of the shell and pearls of the Ceylon Pearl-oyster (*Margaritifera vulgaris* Schumacher) with an examination of the Cestode theory of Pearl production. *Proc. Zool. Soc. London*, **1912**, 260–358.

KADO, Y. 1953. On the scheme of the shell structure of lamellibranchs. *J. sci. Horishima Univ.* Ser. B, div. 1, **14** : 243–254, pls. 1–2, 3 figs.

KAWAGUTI, S. & IKEMOTO, N. 1962a. Electron microscopy on the mantle of the bivalved gastropod. *Biol. J. Okayama Univ.* **8** : 1–20, 24 figs.

—— 1962b. Electron microscopy on the mantle of a bivalve, *Fabulina nitidula*. *Biol. J. Okayama Univ.* **8** (1–2) : 21–30, 11 figs.

—— 1962c. Electron microscopy on the mantle of a bivalve, *Musculus sentousia* during regeneration of the shell. *Biol. J. Okayama Univ.* **8** (1–2) : 31–42, 17 figs.

KAYE, D. 1961. *Techniques for electron microscopy*. xvii + 331 pp., text-figs. 1–138. Blackwell Scientific Publications, Oxford.

KEITH, M. L., ANDERSON, G. M. & EICHLER, R. 1964. Carbon and oxygen isotopic composition of mollusk shells from marine and freshwater environments. *Geochim. et Cosmochim. Acta*, 28, 1757–1786.

—— & PARKER, R. H. 1965. Local variation of ^{13}C and ^{18}O content of mollusk shells and the relatively minor temperature effect in marginal marine environments. *Marine Geol.*, 3, 115–129, 2 figs.

KELLEY, A. 1901. Beiträge zur mineralogischen Kenntnis der Kalkausscheidungen im Tierreich. *Jena Z. Naturw.* **35** : 431–494, pls. 15, 2 figs.

KENNEDY, W. J. & HALL, A. 1967. The influence of organic matter on the preservation of aragonite in fossils. *Proc. Geol. Soc., London*, no. 1643, 253–255.

—— & TAYLOR, J. D. 1968. Aragonite in rudists. *Proc. Geol. Soc., London*, no. 1645, 325–331.

KESSEL, E. 1944. Über Periostracum-Bildung. *Z. Morph. Oköl. Tiere.*, Berlin, **40** (3) : 348–360, pls. 1–7.

KITANO, Y. & HOOD, D. W. 1965. The influence of organic material on the polymorphic crystallisation of calcium carbonate. *Geochim. et Cosmochim. Acta*, 29, 29–42.

KLASSEN-NEKLYUDOVA, M. V. 1964. *Mechanical twinning of crystals*. (Engl. transl., Consultants Bureau, New York, xiv + 212 pp., figs.

KOBAYASHI, I. 1964. Microscopical observations on the shell structure of Bivalvia—part 1, *Barbatia obtusoides* (Nyst.). *Sci. Rep. Tokyo Kyoiku Daig.* Sec. C, **8** (82) : 295–301, pls. 1–3.

KOBAYASHI, S. 1961. ' Personal communication '. *In : Physiology of Mollusca* vol. 1 (ed. Wilbur, K. M. & Yonge, C. M. (1964) : 243–282, London.

KOBAYASHI, S. 1964. Studies on shell formation. A study of the proteins of the extra-pallial fluid in some molluscan species. *Biol. Bull. mar. biol. Lab.* Woods Hole, **126** : 414–422, 2 figs.

KORRINGA, P. 1951. On the nature and function of ' chalky ' deposits in the shell of *Ostrea edulis*. *Proc. Calif. Acad. Sci.*, San Francisco, Ser. 4, **27** (5) : 133–158, 2 figs.

KUMMEL, B. & RAUP, D. M. 1965. *Handbook of Paelaeontological techniques*. xiii + 852 pp., figs. San Francisco and London.

LERMAN, A. 1965a. Palaeoecological problems of Mg and Sr in biogenic calcites in light of recent thermodynamic data. *Geochim. et Cosmochim. Acta*, 29, 977–1002.

—— 1965b. Strontium and magnesium in water and in *Crassostrea* calcite. *Science*, 150, 745–751, 2 figs.

LEUTWEIN, F. 1963. Spurenelemente in rezenten cardien verschiedener Foundorte : *Fortschr. geol. Rheinld. Westf.*, Krefeld, **10** : 283–292.

—— & WASKOWIAK, R. 1962. Geochemische untersuchungen antezenten marinen Molluskenschalen. *Neues Jb. Miner. Geol. Palaeont.*, Stuttgart, **99** : 45–78.

LLOYD, R. M. 1964. Variations in the oxygen and carbon isotope ratios of Florida Bay mollusks and their environmental significance. *J. Geol.*, 72, 84–111, 19 figs.

LOPPENS, K. 1920. Note sur la composition chimique et la formation des coquilles chez les mollusques. *Annals Soc. r. zool. malacol. Belg.*, Brussels, **51** : 75–90.

LOWENSTAM, H. A. 1954a. Environmental relations of modification compositions of certain carbonate-secreting marine invertebrates. *Proc. natn. Acad. Sci.*, **40** : 39–48, 3 figs.

—— 1954b. Factors affecting the aragonite : calcite ratios in carbonate-secreting marine organisms. *J. Geol.*, Chicago, **62** : 284–322, 15 figs. 2 tbls.

—— 1963. Biologic problems relating to the composition and diagenesis of sediments. *In : The Earth Sciences : Problems and Progress in Current Research :* 138–195, 14 figs. Chicago.

—— 1964. Coexisting calcites and aragonites from skeletal carbonates of marine organisms and their strontium and magesium contents. *In : Recent Researches in the Fields of Hydrosphere Atmosphere and Nuclear Geochemistry*, 373–404, 5 figs. Tokyo.

MACCLINTOCK, C. 1963. Reclassification of gastropod *Proscutum* Fischer based on muscle scars and shell structure. *J. Palaeont.*, Tulsa, **37** : 141–156, pl. 20, 31 figs.

—— 1967. Shell structure of patelloid and bellerophontoid gastropods (Mollusca). *Bull. Peabody Mus. nat. Hist.*, New Haven, **22** : 1–140, pls. 1–32, 128 figs.

MACKAY, I. H. 1952. The shell structure of the modern molluscs. *Colo. Sch. Mines. Q.*, **47** (2) : 1–27, pls. 1–6, 1 fig.

MANIGAULT, P. 1960. Coquille des mollusques : structure et formation : 1823–1844, 13 figs. *In : Traite de zoologie* (ed. Grasse, P. P.) V. Paris.

MAYER, F. K. 1931. Rontgenographische Untersuchung en Gastrophoden Schalen. *Jena Z. Naturw.* **65** : 487–512, pl. 2, 8 figs.

—— & WEINECK, E. 1932. Die Verbreitung des Kalziumkarbonates in Tierreich unter besonderer Berücksichtigung der Wirbellosen. *Jena Z. Naturw.* **66** : 199–222.

MERRILL, A. S., POSGAY, J. A. & NICHY, F. E. 1966. Annual marks on shell and ligament of sea scallop (*Placopecten magellanicus*). *Fish. Bull. U.S.*, Washington, **65** : 299–311, 12 figs.

MOORE, R. C., LALICKER, C. G. & FISHER, A. G. 1952. *Invertebrate Fossils*. 766 pp., figs. New York.

MUTVEI, H. 1964. On the shells of *Nautilus* and *Spirula* with notes on the shell secretions in non-cephalopod molluscs. *Ark. Zool.*, Stockholm, **16** : 221–278, pls. 1–22.

NATHUSIUS-KÖNIGSBORN, W. 1877. *Untersuchungen über nicht cellulare organismen namentlich Crustacean-panzer, Molluskenschalen und Eihüllen*. 144 pp., figs. Berlin.

NEVILLE, C. H. 1967. Daily growth layers in plants and animals. *Biol. Rev.*, Cambridge, **42 :** 421–439

NEWELL, N. D. 1937. Late Palaeozoic pelecypods : Pectinacea. *State Geol. Surv. Kansas*, Lawrence, **10** : 1–123, pls. 1–20, 42 figs.

—— 1960. The origin of the oysters. *Rept. 21st Internat. Geol. Congr.*, Oslo, **22** : 81–86.

—— 1965. Classification of the Bivalvia. *Amer. Mus. Novit.*, no. 2206, 25 pp.

Oberling, J. J. 1964. Observations on some structural features of the pelecypod shell. *Mitt. naturf. Ges. Bern.* **20** : 1–63, pls. 1–6, 3 figs.

Odum, H. T. 1951. Notes on the strontium content of seawater, celestite radiolaria and strontianite snail shells. *Science*, New York, **114** : 211–213.

Omori, M., Kobayashi, I. & Shibata, M. 1962. Preliminary report on the shell structure of *Glycimeris vestita* (Dunker) with special reference to the newly found structural patterns like to ' Punctum ' in the shell of Brachiopoda. *Sci. Repts. Tokyo Kyoiku Diagaku.* **8** : 197–202, pls. 1–3, 3 figs.

Orton, J. H. 1937. *Oyster biology and oyster culture.* 211 pp., figs., London.

Owen, G., Trueman, E. R. & Yonge, C. M. 1953. The ligament in the Lamellibranchia. *Nature*, London, **171** : 73–75, 5 figs.

Petrov, D. A. & Kolachev, B. A. 1958. Impurity redistribution during crystallisation and the way this appears in the crystal structure. *Repts. 1st Conf. on Crystal Growth, U.S.S.R.* (Engl. Transl.), Consultants Bureau, New York, 126–134, figs. 1–16.

Ranson, G. 1952. Les huîtres et le calcaire. Calcaire et substratum organique chez les mollusques et quelques autres invértebrès marins. *C.r. hebd. Séanc. Acad. Sci.*, Paris, **234** : 1485–1487.

Rassbach, R. 1912. Beiträge zur Kenntnis der Schale in der Schalenregeneration von *Anodonta cellensis* Schröt. *Z. wiss. Zool.* Lepizig, **103** : 363–448, 64 figs.

Raup, D. M. 1966. Geometric analysis of shell coiling : general problems. *J. Paleont.* Tulsa, **40** : 1178–1190, figs. 1–10.

Read, W. T. 1953. *Dislocations in Crystals.* xvii + 228 pp., figs. New York.

Roche, J., Ranson, B. & Eysseric-Lafon, M. 1951. Sur la composition des scléroprotéines des coquilles des mollusques (conchiolines). *C.r. Séanc. Soc. Biol.*, Paris, **145** : 147–1477.

Rose, G. 1858. Über die heteromorphen Zustände der Kohlensauren Kalkerde. II : Vorkommen des Aragonits und Kalkspaths in der organischen natur. *Abhand. der Kön. Akad. Wissen, Berlin*, 1858 : 63–111, pls. 1–3.

Rubbel, A. 1911. Über Perlen und Perbildung bei *Margaritana margaritifera* nebst Beitragen zur Kenntnis ihrer Schalenstruktur. *Zool. Jb. Anat. Abt., Jena*, **32** : 287–366, pls. 1–2, 60 figs.

Schenk, H. G. 1934. Literature on the shell structure of Pelecypods. *Bull. Mus. r. Hist. nat. Belg.*, Brussels, **10** (34) : 1–20.

Schmidt, W. J. 1921. Bau und Bildung der Perlmuttermasse. *Verh. dt. zool. Ges., Leipzig*, **26** : 59–60.

—— 1922. Über den aufbau der Schale von *Nucula*. *Arch. mikr. Anat.*, **96** : 171–181, 7 pls.

—— 1923. Bau and Bildung der Perlmuttermasse. *Zool. Jb. Anat. Abt. Jena*, **45** : 1–148, pls. 1–5, figs.

—— 1924. *Die Bausteine des Tierkörpers in polarisiertem Licht.* 528 pp., 230 figs., Bonn.

—— 1925. Bau and Bildung der Prismen in den Muschelschalen. *Mikrocosmos*, Stuttgart, **18** : 49–54, 73–76, figs.

—— 1959. Bemerkungen zur Schalenstruktur von *Neopilina galathea*. Galathea rept. **3** : 73–77, 2 pls.

Schröder, O. 1907. Beiträge zur Histologie des Mantels von *Calyculina* (Cyclas) *lacustris* Muller. *Zool. Anz.*, Leipzig, **31** : 506–510, 2 figs.

Sheftal, N. N. 1958. Real crystal formation. *Repts. 1st Conf. on Crystal Growth, U.S.S.R.* (Engl. transl. Consultants Bureau, New York) : 5–27, 25 figs.

Shrock, R. R. & Twenhofel, W. H. 1953. *Principles of invertebrate palaeontology.* 2nd ed. 816 pp. figs. New York.

Simkiss, K. 1960. Some properties of the organic matrix of the shell of the cockle (*Cardium edule*). *Proc. Malac. Soc., London*, **34** (2) : 89–95, figs. 1–2.

—— 1964. The inhibitory effects of some metabolites on the precipitation of calcium carbonate from artifical and natural sea water. *J. du Conseil Internat, expl. de la mer*, Copenhagen, **29** : 6–18, 4 figs.

Simkiss, K. 1965. The organic matrix of the oyster shell. *Comp. biochem. physiol.*, London, **16** : 427–435, 3 figs.
Sorby, H. C. 1879. Address on the structure and origin of limestones. *Quart. J. Geol. Soc.*, London, **35** : 56–95, 11 figs.
Stegemann, H. 1961. Über die Skleroprotide der Mollusken. *Naturwissenschaften*, Berlin, **48** : 501.
—— 1963. Proteine (Conchagene) und Chitin im Stützbewebe von Tintenfischen. *Hoppe-Seyler's Z. physiol. Chem.*, Strassburg, **331** : 269–279.
Stenzel, H. B. 1962. Aragonite in the resilium of oysters. *Science*, New York, **136** : 1121–1122.
—— 1963. Aragonite and calcite as constituents of adult oyster shells. *Science*, New York **142** : 232–233, 1 fig.
—— 1964. Oysters : composition of the larval shell. *Science*, New York, **145** : 155–6, 2 figs.
Stolkowski, J. 1951. Essai sur le déterminisme des formes minéralogiques du calcaire chez les êtres vivants (calcaires coquilliers). *Ann. Inst. oceanogr.*, Paris, **26** : 1–113.
Tanaka, S., Hatano, H. & Itasaka, O. 1960. Biochemical studies on pearl. IX. Amino acid composition of conchiolin in pearl and shell. *Bull. chem. Soc. Japan*, **33** : 543–545.
Thiele, J. 1893. Beiträge zur Kenntnis der Mollusken. II. Über die Molluskenschale. *Z. wiss. Zool.*, Leipzig, **55** : 220–251, pl. 11.
Togari, K. & Togari, S. 1959. Conditions controlling the crystal form of calcium carbonate minerals. (2). Mineralogical study of Molluska. *Hokkaido Univ. Fac. Sci. J.* (Ser. 4), **10** : 447–456, figs.
Towe, K. M. & Hamilton, G. H. 1968. Ultramicrotome-induced deformation artifacts in densely calcified material. *J. ultrastructure research*, **22**, 274–281.
Trueman, E. R. 1949. The ligament of *Tellina tenuis*. *Proc. Zool. Soc. Lond.*, **119** : 717–742, 17 figs.
—— 1953a. The ligament of *Pecten*. *Quart. J. micr. Sci.*, Oxford, **94** : 193–202, 5 figs.
—— 1953b. Observations on certain mechanical properties of the ligament of *Pecten*. *J. experimental Biol.*, Cambridge, **30** : 453–467, 10 figs.
Tsujii, T. 1960. Studies on the mechanism of shell- and pearl-formation of Mollusca. *J. Fac. Fisheries Prefect. Univ. Mie.*, **5** : 2–70, pls. 1–13, 21 figs.
—— Sharp, D. G. & Wilbur, K. M. 1958. Studies on shell formation VII. The submicroscopic structure of the shell of the oyster *Crassostrea virginica*. *J. biophys. biochem. Cytol.*, Baltimore, **4** : 275–279, pls. 148–151, 1 fig.
Tullberg, T. 1882. Studien über den Bau und das Wachstum des Hummerpanzers und der Molluskenschalen. *K. svenska vetecsk-Akad.* Handl., Stockholm, **19** : 1–57, pls. 1–12.
Turekian, K. K. & Armstrong, R. L. 1960. Magnesium, strontium and barium concentrations and calcite-aragonite ratios of some recent molluscan shells. *J. mar. Res.* New Haven, **18** : 133–151, New Haven.
Vinogradov, A. P. 1953. The elementary chemical composition of marine organisms. Sears Foundation for Marine Research, Memoir 2, 647 pp.
Voll, G. 1960. New work of petrofabrics. *L'pool Manchr. geol. J.*, **2** (3) : 503–567, pls. 23, 24, 22 figs.
Wada, K. 1957. Laminary structures of cultured pearls observed with electron microscope–1. Nacreous layer pearl. *Bull. Jap. Soc. Scient. Fish.*, Tokyo, **23** : 320–305, 4 figs. (In Japanese).
—— 1958. The crystalline structure of the nacre of Pearl Oyster shell. *Bull. Jap. Soc. Scient. Fish.*, Tokyo, **24** : 422–427, 4 figs.
—— 1959. On the arrangement of crystals in the inner layer of nacre. *Bull. Jap. Soc. Scient. Fish.*, Tokyo, **25** : 342–345, 3 figs.
—— 1960a. Crystal growth on the inner shell surface of *Pinctada martensii* (Dunker) I. *J. Electron Microscop.*, Tokyo, **9** : 21–23, 5 figs.

WADA, K. 1960b. The relation between the crystalline structure of the cultured pearls and the elongation of the transplanted tissue in the process of pearl-sac formation. *Bull. Jap. Soc. Scient. Fish.*, Tokyo, **26** : 459–553, 3 figs.

—— 1961a. On the relationship between shell growth and crystal arrangement of the nacre in some Pelecypoda. *Venus*, Tokyo, **2** : 204–211, 2 figs. (In Japanese).

—— 1961b. Crystal growth of molluscan shells. *Bull. Natn. Pearl Res. Lab.*, Kashikojima, **7** : 703–828, 20 t. figs., 149 figs.

—— 1963a. On the relationship between shell growth and crystal arrangement of the sub-nacreous layer in some Pelecypoda—II. *Venus*, Tokyo, **22** : 281–289, 4 figs.

—— 1963b. On the spiral growth of the inner surface of the calcitic shell *Anomia lischkei*—I. *Bull. Jap. Soc. Scient. Fish.*, Tokyo, **29** : 320–324, 3 figs.

—— 1963c. On the spiral growth of the inner surface of the calcitic shell *Ostrea gigas*—II *Bull. Jap. Soc. Scient. Fish.*, Tokyo, **29** : 447–451, 4 figs.

—— 1963d. Laminary structure of cultured pearls observed with electron microscope—II. Direct observation on ultra thin sections of a nacreous layer pearl by using a diamond knife. *Bull. Jap. Soc. Scient. Fish.*, Tokyo, **29** : 658–661, 1 fig.

—— 1963e. Studies on the mineralisation of the calcified tissue in Molluscs—VI. Crystal structure of the calcite growing on the inner surface of Calcitostracum. *J. Electron Microscop.*, Tokyo, **12** : 224–227, 2 figs.

—— 1964a. On the spiral growth on the inner surface of the calcitic shell *Chlamys nobilis*—III. *Bull. Jap. Soc. Scient. Fish.*, Tokyo, **30** : 127–131, 5 figs.

—— 1964b. Studies on the mineralisation of the calcified tissue in molluscs—I. Relations among mantle and its products. *Bull. Jap. Soc. Scient. Fish.*, Tokyo, **30** : 319–324, 5 figs.

—— 1964c. Studies on the mineralisation of the calcified tissue in molluscs—II. Experiments by the administration of Tetracycline on the mineralisation of shell. *Bull. Jap. Soc. Scient. Fish.*, Tokyo, **30** : 326–330, 6 figs.

—— 1964d. Studies on the mineralisation of the calcified tissue in molluscs—III. Localisation and distribution of ^{45}Ca in the mantle tissue and on the growing shell surface in several marine bivalves by radiography. *Bull. Jap. Soc. Scient. Fish.*, Tokyo, **30** : 385–392, 3 figs.

—— 1964e. On the spiral growth of the calcite shell—IV. The crystal structure of calcite. *Bull. Jap. Soc. Scient. Fish.*, Tokyo, **30** : 132–136, 2 figs.

—— 1964f. Studies on the mineralisation of the calcified tissue in molluscs—V. Radiautographic investigation on the patterns of layer formation. *Bull. Jap. Soc. Scient. Fish.*, Tokyo, **30** : 465–471, 4 figs.

—— 1964g. Studies on the mineralisation of the calcified tissue in molluscs—VI. Selective fixation of ^{45}Ca into or onto the metachromatic matter in the process of shell mineralisation. *Bull. Jap. Soc. Scient. Fish.*, Tokyo, **30** : 393–399, 5 figs.

—— 1964h. Studies on mineralisation of the calcified tissue in molluscs—VII. Histological and histochemical studies of organic matrices in shells. *Bull. Natu. Pearl Res. Lab.*, Kashikojima, **9** : 1079–1086, 1 table.

—— 1964i. Studies on the mineralisation of the calcified tissue in molluscs—VIII. Behaviour of eosinophile granules and of organic crystals in the process of mineralisation of secreted organic matrices in glass coverslip preparation. *Bull. Natu. Pearl Res. Lab.*, Kashikojima, **9** : 1087–1098, 12 figs.

—— 1964j. Studies on the mineralisation of the calcified tissue in molluscs—X. Histochemical determination of the nature of acid mucopolysaccharide in organic crystals. *Bull. Jap. Soc. Scient. Fish.*, Tokyo, **30** : 993–998, 4 figs., 1 table.

—— 1966. Spiral growth of nacre. *Nature*, London, **211** : 1427, 1 fig.

WAELE, A. DE. 1930. Le sang d'*Anodonta cygnea* et la formation de la coquille. *Mem. acad. roy. Belg. Cl. Sci.* (2), **10**, fasc. 3 ; 1–51.

WASKOWIAK, R. 1962. Geochemische Untersuchungen an rezenten Molluskenschalen mariner Herkunft. *Freiberger Forsch.-H.*, C 136, 7–155.

WATABE, N. 1955. The observation of the surface structure of the cultured pearls relating to colour and luster. *Rept. Fac. Fish. Prefect. Univ. Mie*, **2** : 18–26, pls. 1–3, 1 fig.
—— 1956. Dahllite identified as a constituent of Prodissoconch of *Pinctada martensii* (Dunker). *Science*, New York, **124** : 630.
—— 1963. Decalcification of thin sections for electron microscope studies of crystal-matrix relationship in mollusc shell. *J. Cell. Biol.*, Baltimore, **18** : 701–703, 2 figs.
—— 1965. Studies on shell formation—XI. Crystal-matrix relationships in the inner layers of mollusc shells. *J. Ultrastruct. Res.*, New York, **12** : 351–370, 16 figs.
WATABE, N. & KOBAYASHI, S. 1961. mentioned in K. M. Wilbur, 1964.
—— SHARP, D. G. & WILBUR, K. M. 1958. Studies on shell formation—VIII. Electron microscopy of crystal growth of the nacreous layer of the oyster *Crassostrea virginica*. *J. biophys. biochem. Cytol.*, Baltimore, **4** : 281–286, pls. 152–156.
—— & WADA, K. 1956. On the shell structures of the Japanese pearl oyster *Pinctada martensii*(Dunker). (I). Prismatic layer I. *Rep. Fac. Fish. prefect. Univ. Mie*, **2** : 227–232, pls. 1–2, 7 figs.
—— & WILBUR, K. M. 1960. Influence of the organic matrix on crystal type in Molluscs. *Nature*, London, **188** : 334.
—— 1961. Studies on shell formation—IX. An electron microcope study of crystal layer formation in the oyster. *J. biophys. biochem. Cytol.*, Baltimore, **9** : 761–772, 18 figs.
WILBUR, K. M. 1964. Shell formation and regeneration. *In : Physiology of Mollusca* (ed. Wilbur, K. M. & Yonge, C. M.) vol. 1 : 243–282, 14 figs.
—— & OWEN, G. 1964. Growth. Chapter 7 in : *Physiology of Mollusca* (ed. K. M. Wilbur & C. M. Yonge), vol. 1, 211–242, Acadmic Press, New York and London.
—— & WATABE, N. 1963. Experimental studies on calcification in molluscs and the alga *Coccolithus huxleyi*. *Ann. N.Y. Acad. Sci.*, **109** : 82–112, 19 figs.
WILLIAMS, A. 1956. The calcareous shell of the Brachiopoda and its importance to their classification. *Biol. Rev.*, Cambridge, **31** : 243–287, 7 figs.
—— 1965. *Treatise on Invertebrate Palaeontology* (ed. R. C. Moore) *Part H—Brachiopoda*. 2 vols. xxxii + 1–927, illustr., Kansas.
YONGE, C. M. 1953a. The monomyarian condition in the Lamellibranchia. *Trans. Roy. Soc. Edinb.*, **62** : 421–478, 13 figs.
—— 1953b. Form and habit in *Pinna carnea* Gmelin. *Phil. Trans. R. Soc.*, London, (B), **238** : 335–374, 19 figs.
ZITTEL, K. A. VON. 1915. *Grundzüge der Paläontolgie* 1 Abt. Invertebrata, 4th Auflage. xi + 694 pp., illustr. Munchen & Berlin.

Dr. J. D. TAYLOR, B.Sc., Ph.D.
Department of Zoology
BRITISH MUSEUM (NATURAL HISTORY)
CROMWELL ROAD, LONDON, S.W.7

Dr. W. J. KENNEDY
Department of Geology and Mineralogy
THE UNIVERSITY OF OXFORD
PARKS ROAD, OXFORD

Dr. A. HALL
Department of Geology
UNIVERSITY OF LONDON
KING'S COLLEGE
STRAND, LONDON, W.C.2

PLATES

PLATE 1

FIG. 1. Replica of a surface of the inner, sheet nacre layer of *Neotrigonia dubia* showing an almost complete sheet of nacre tablets ; outlines of individual tablets can be seen. The significance of the longitudinal ridges on the tablets is not known. × 5700.

FIG. 2. Inner surface of the middle nacreous layer of *Pinctada margaritifera* showing rounded nacre tablets. × 4500.

FIG. 3. Surface of the inner nacreous layer of *Neotrigonia dubia* showing seed tablets of nacre, growing all over the surface of the underlying sheet of tablets. × 9200.

FIG. 4. Heavily decalcified radial section of the middle nacreous layer of *Margaritifera margaritifera*. Inter-lamellar and inter-crystalline organic matrix are very clearly visible. Discontinuities in the organic matrix between the tablets indicate that tablets in successive layers are sometimes in contact. Polished and etched (1% HCl). × 8000.


1

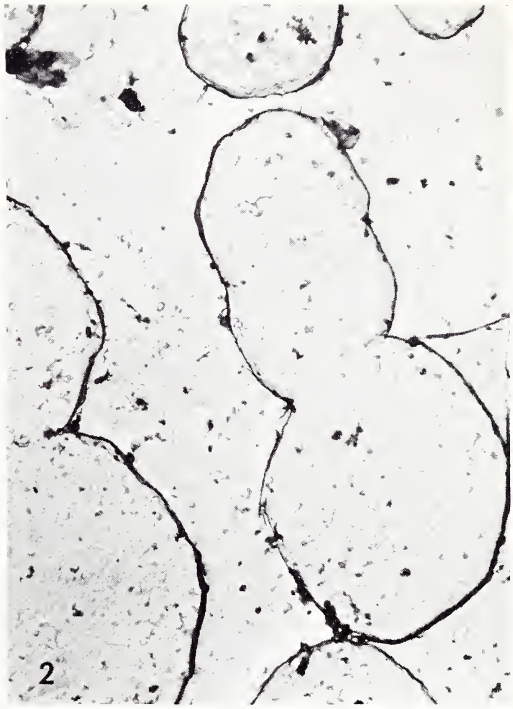
2


3


4

PLATE 2

FIG. 1. Inner surface of the inner sheet nacre layer of *Margaritifera margaritifera,* showing the rosette-like arrangement of irregular nacre tablets found in this species. ×4050.

FIG. 2. Inner surface of the middle nacreous layer of *Margaritifera margaritifera* showing a spiral growth hill, made up of irregular nacre tablets. × 4050.

FIG. 3. Spiral growth hills on the surface of middle nacreous layer of *Isognomon ephippium.* Acetate peel. × 50.

FIG. 4. Inner surface of the inner nacreous layer of *Margaritifera margaritifera* showing very irregular nacre tablets, possibly the result of natural dissolution. × 4050.


1

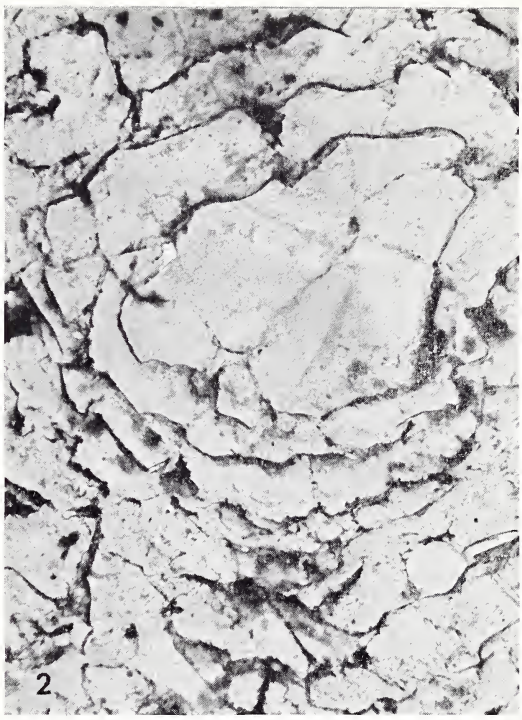
2

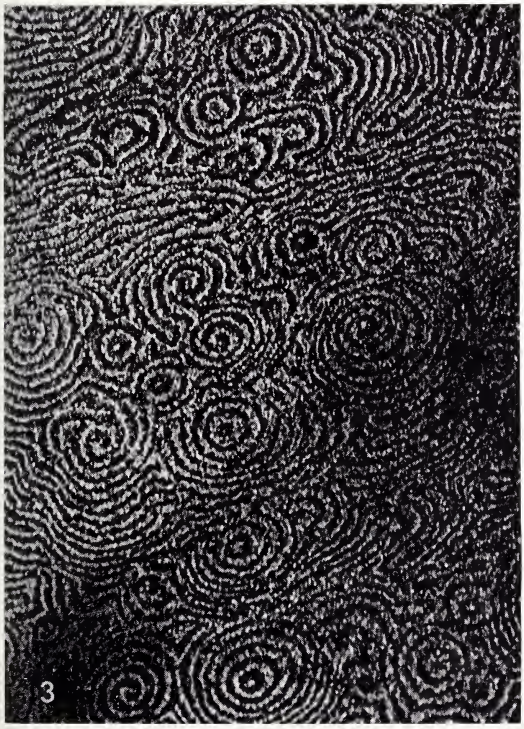
3


4

PLATE 3

FIG. 1. Radial section of inner nacreous layer of *Quadrula metanevra* showing the fenestrate organic matrix where parts of nacre tablets have been pulled out during sectioning. Replica of polished EDTA-etched section. × 7500.

FIG. 2. Inner surface of the inner nacreous layer of *Margaritifera margaritifera* showing a completed sheet of nacre, with the boundaries between the tablets clearly visible. × 3750.

FIG. 3. Replica of the inner surface of the middle lenticular nacre layer of *Anodonta cygnea*, with nacre tablets piled one on top of each other. The edges of the nacre tablets show fine terracing. Many small crystal seeds are also present. × 9500.

FIG. 4. Fractured section of the middle nacreous layer of *Nucula sulcata* showing the curvature of the layers of nacre parallel to the growth lines. Scanning electron micrograph. × 720.


1

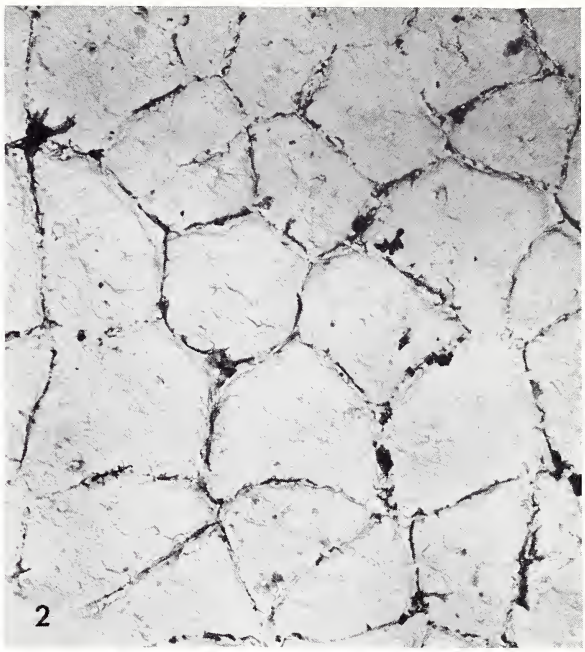
2


3


4

PLATE 4

FIG. 1. Radial section of *Spondylus calcifer* showing the outer foliated calcitic layer (top), middle aragonitic crossed-lamellar layer, thin band of prismatic pallial myostracum, inner aragonitic crossed-lamellar layer, and prismatic, aragonitic adductor myostracum. Acetate peel. × 25.

FIG. 2. Radial section of the foliated outer layer of *Chlamys varia* in the umbonal region. Acetate peel. × 100.

FIG. 3. Radial section of the foliated outer layer of *Chlamys varia* showing the dendritic arrangement of folia. Acetate peel. × 100.

FIG. 4. Radial section of the middle lenticular nacreous layer of *Quadrula metanevra*. Acetate peel. × 157.

FIG. 5. Radial section of the middle lenticular nacreous layer of *Unio mytiloides*. Acetate peel. × 157.

FIG. 6. Oblique section of the outer foliated layer of *Pecten maximus* cut almost parallel to the folia, showing the laterally-joined laths building up the layer. × 157.

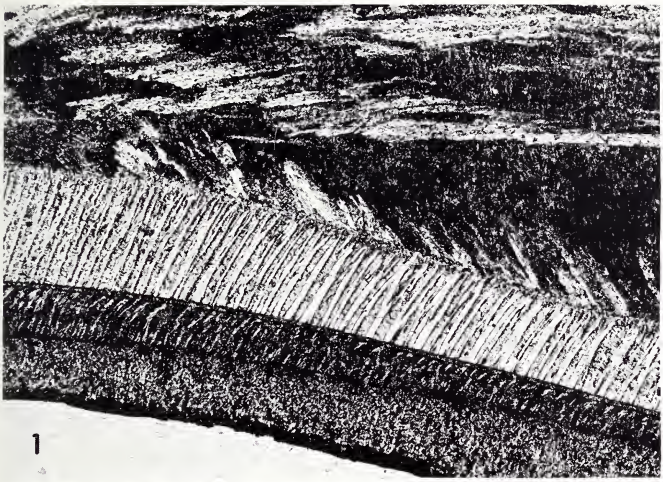
1

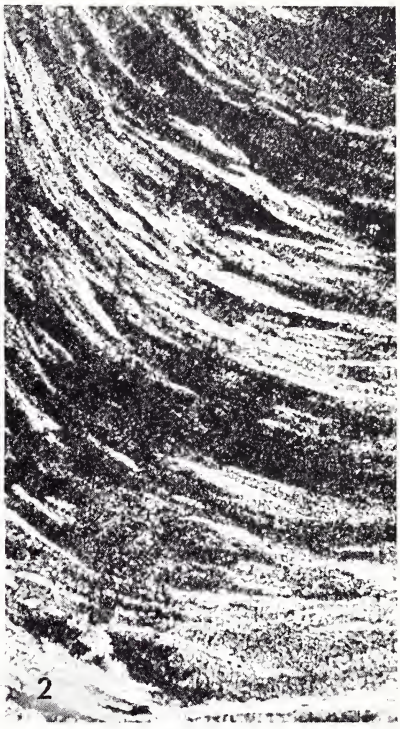
2

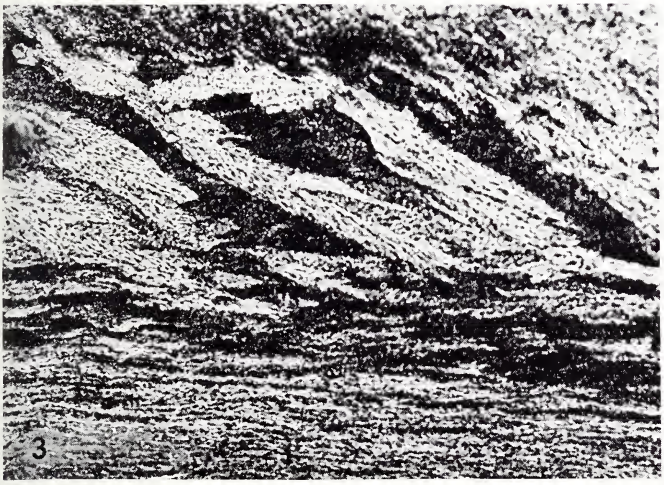
3

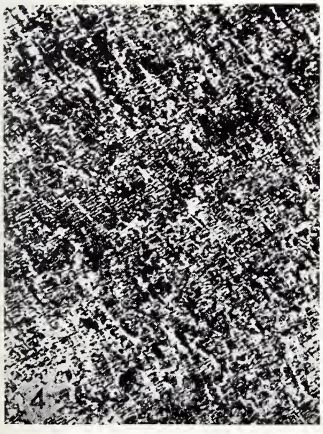
4

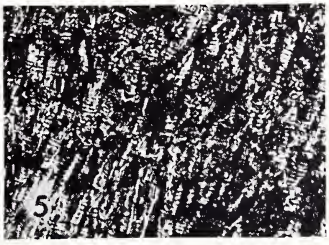
5

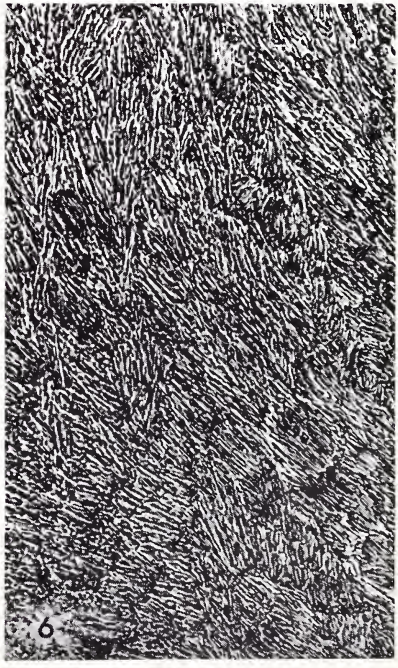
6

PLATE 5

FIG. 1. Radial section of the middle lenticular nacreous layer of *Quadrula metanevra*, showing nacre tablets stacked into columns. Interlamellar and intercrystalline matrix clearly shown. Replica of polished, EDTA-etched section. Faint horizontal lines are artifacts. × 3000.

FIG. 2. Replica of the inner surface of the foliated layer of *Ostrea hyotis* showing the surface of the calcite laths covered in a lace-like fenestrate sheet of intercrystalline organic matrix. × 23,800.

FIG. 3. A fractured section of the foliated layer of *Ostrea edulis* scanning electron micrograph. × 850.

FIG. 4. Replica of inner surface of foliated layer of *Placuna placenta* with overlapping sheets of laths in side to side contact, direction of growth towards bottom right corner. Note smooth surface of laths. × 3900.


1

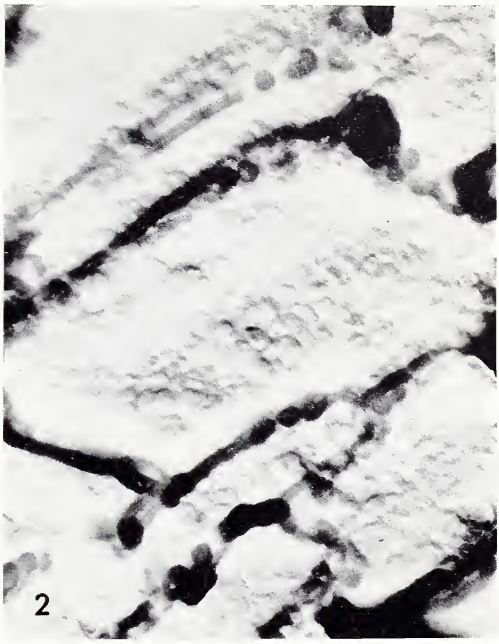
2


3

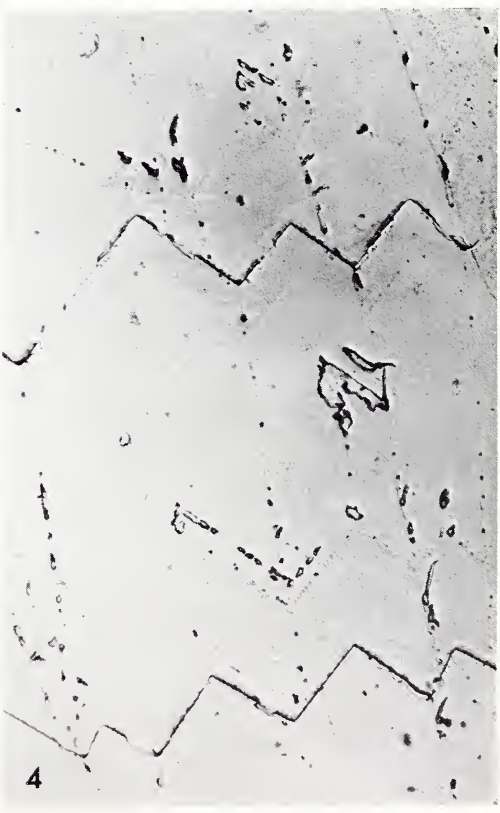
4

PLATE 6

FIG. 1. Replica of the inner surface of the foliated layer of *Ostrea hyotis* showing a change in orientation of successive layers of laths. × 8400.

FIG. 2. Replica of the inner surface of the foliated layer of *Ostrea hyotis* showing rounded seed crystallites developing on an undulating surface which is probably an organic membrane. × 900.

FIG. 3. Replica of the inner surface of the foliated layer of *Anomia ephippium* showing areas of non-deposition within a lath, which are aligned parallel to the growing face. The direction of growth of the laths is towards the top right-hand corner of the page. Note the smooth surface of the laths. × 6000.

FIG. 4. Replica of the inner surface of the foliated layer of *Ostrea hyotis* showing the overlapping sheets of calcite crystals. × 10,000.


1

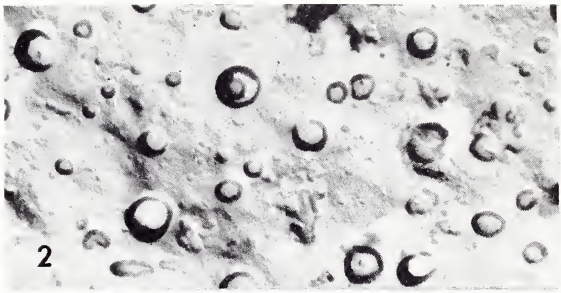
2

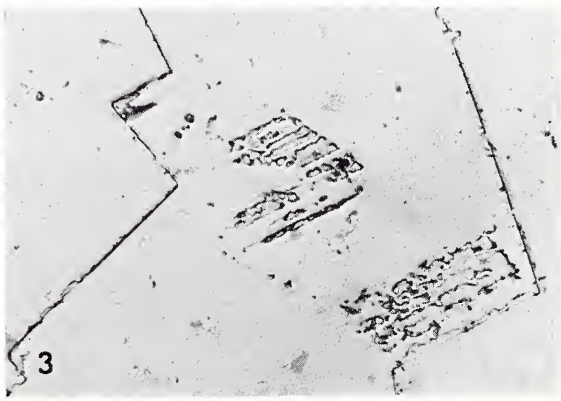
3

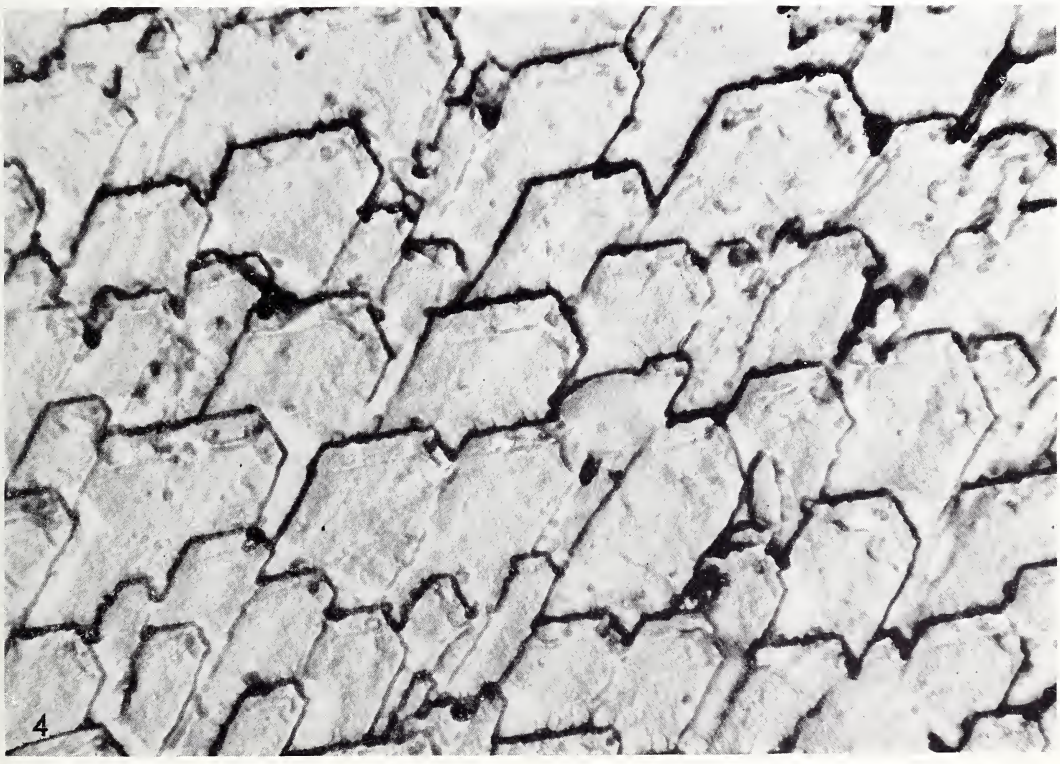
4

PLATE 7

FIG. 1. Oblique section through the outer calcitic prismatic layer of *Electroma alacorvi* showing the conspicuous interprismatic conchiolin walls. Faint horizontal lines are growth banding cut obliquely. Acetate peel. × 157.

FIG. 2. Radial section of the prismatic layer of *Margaritifera margaritifera* showing geometric selection near the periostracum and the meniscus-shaped accretion lines within the prisms. Thin section. × 100.

FIG. 3. Screw dislocation on a nacre tablet on the inner surface of *Potamides littoralis*. × 3000.

FIG. 4. Slightly oblique radial section of the prismatic layer and the middle nacreous layer of *Anodonta cygnea*, showing the interprismatic walls and downward diverging striations and meniscus-shaped accretion lines within the prisms. Acetate peel. × 100.

FIG. 5. Radial section of the prismatic layer of *Margaritifera margaritifera* showing geometric selection of prisms near the periostracum. Thin section. × 100.

FIG. 6. Oblique section through the calcitic prismatic layer of *Pinctada margaritifera* showing the thick interprismatic walls and the transverse accretion lines within the prisms. Acetate peel. × 100.

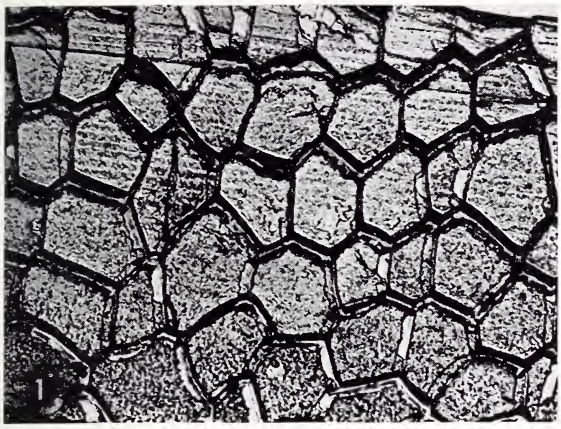
1

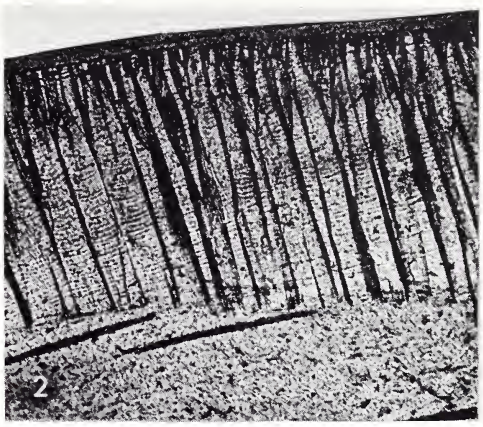
2


3


4

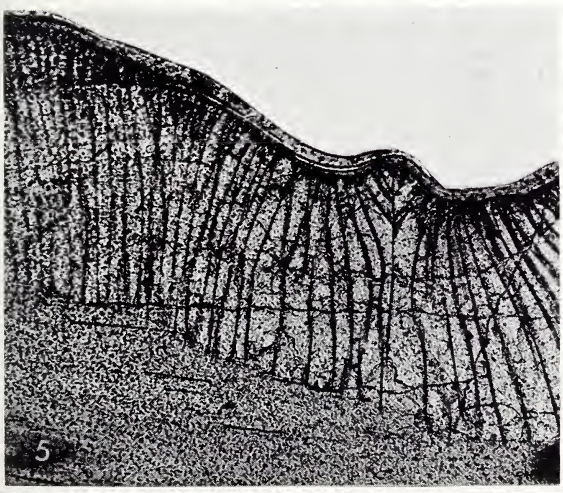
5

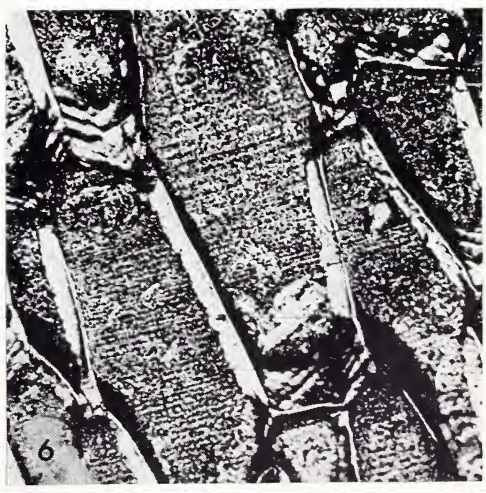
6

PLATE 8

FIG. 1. An early growth stage of the prismatic layer of *Anodonta cygnea* as seen on the inner surface of the margin of the periostracum. × 252.

FIG. 2. Contact between the outer prismatic layer and the middle nacreous layer of *Margaritifera margaritifera*, showing the conchiolin interprismatic wall, and the transition zone between the prismatic and nacreous layers, with the gradual development of the interlamellar organic matrix. Radial, polished, EDTA-etched section. × 3600.

FIG. 3. Radial section of the outer calcitic prismatic layer of *Atrina vexillum*, showing prominent transverse accretion lines within prisms. Acetate peel. × 158.

FIG. 4. Inner surface of the outer prismatic layer of *Anodonta cygnea* on a detached periostracum fragment from near the margin of the shell. × 150.

FIG. 5. Early growth stages of aragonite prisms on the inner surface of the periostracum edge of *Anodonta cygnea*. × 400.

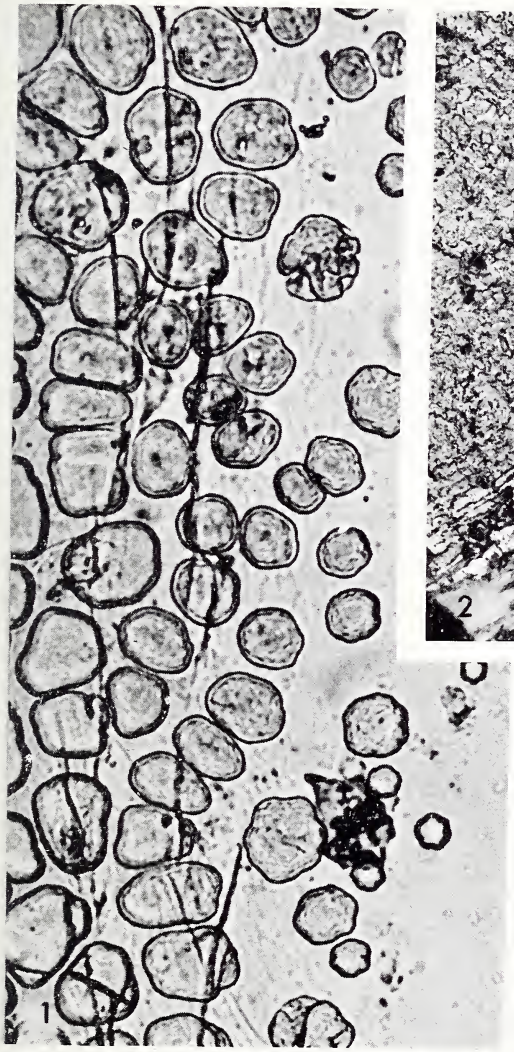
1

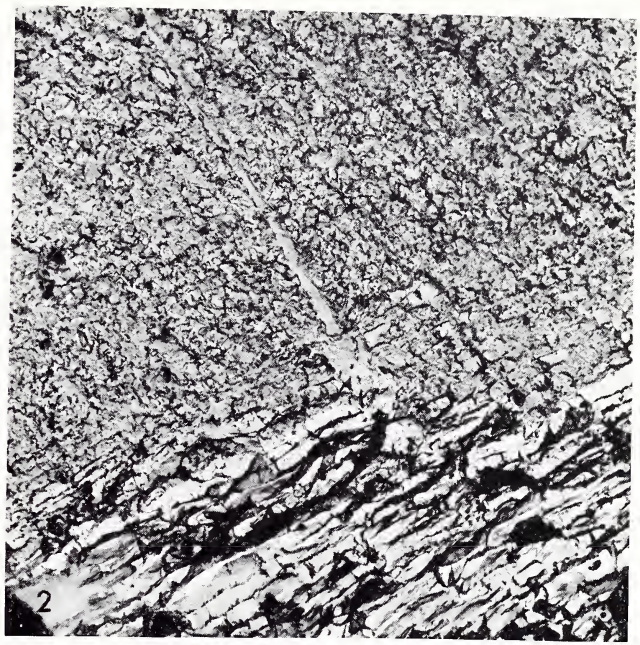
2


3

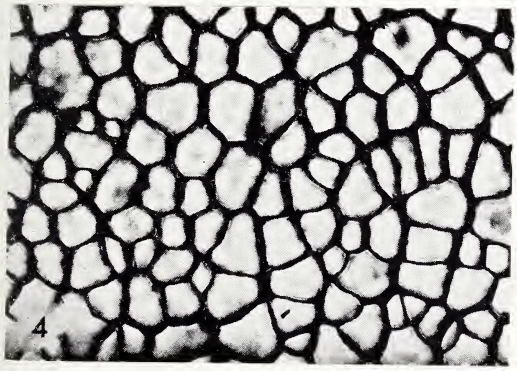
4

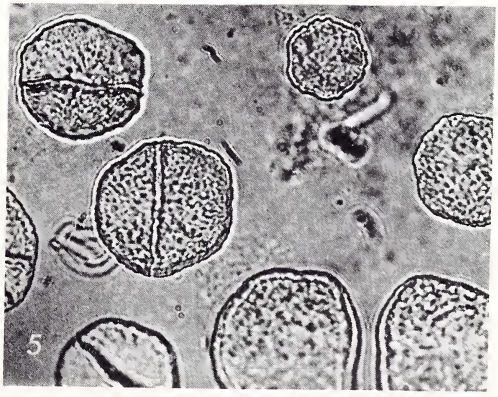
5

PLATE 9

FIG. 1. Scanning electron micrograph of the inner surface of the prismatic layer of *Pinctada margaritifera*. The interprismatic conchiolin walls are conspicuous, standing out from the surface. × 2000.

FIG. 2. Replica of the inner surface of the prismatic layer of *Anodonta cygnea* showing the interprismatic conchiolin walls and the scale-like crystallites on the surface of the prisms. × 4500.

FIG. 3. Replica of the inner surface of the prismatic layer of *Anodonta cygnea*, with an elongate extension of a conchiolin wall into a prism with a flange-like termination. × 3000.


1

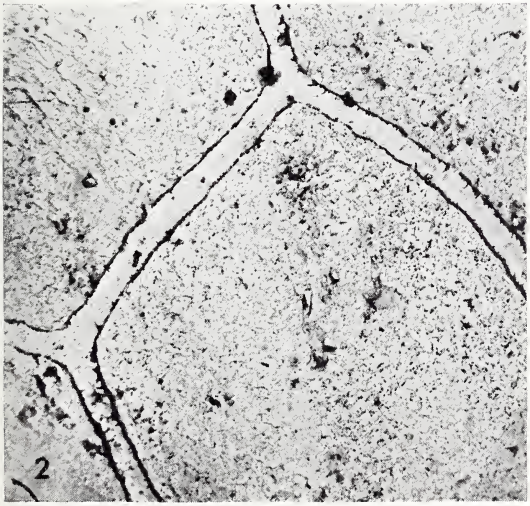
2


3

PLATE 10

FIG. 1. Radial section of the outer aragonitic prismatic layer of *Unio pictorum* showing the transverse meniscus-shaped accretion lines and the downwardly diverging feathery structure within the prisms. Acetate peel. × 157.

FIG. 2. Radial section of *Margaritifera margaritifera* showing outer prismatic layer (top) and fine periostracum-like conchiolin sheets within the inner nacreous layer. Each sheet has a thin band of prisms beneath it. The pallial myostracum, seen hear top of micrograph separates two different nacre layers. Thin section. × 25.

FIG. 3. Section of *Margaritifera margaritifera* showing one of the thin prismatic bands and its associated conchiolin sheet. Detail of fig. 2. Thin section. × 157.

FIG. 4. Oblique section through a conchiolin sheet and prism band of *Margaritifera margaritifera* showing the irregular shape of the prisms. Thin section. × 157.

FIG. 5. Radial section of *Margaritifera margaritifera* showing three bands of conchiolin and prisms. Acetate peel. × 100.

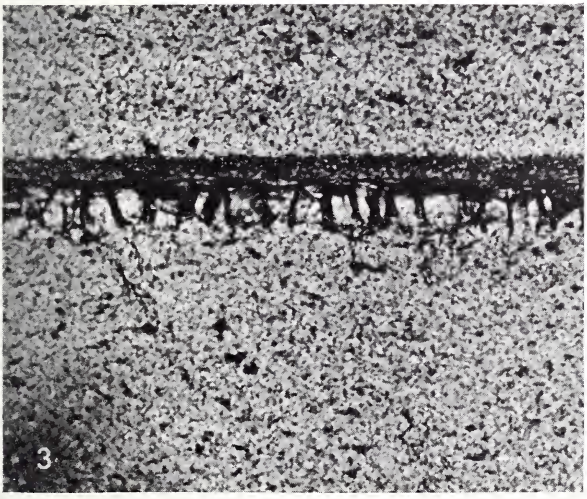

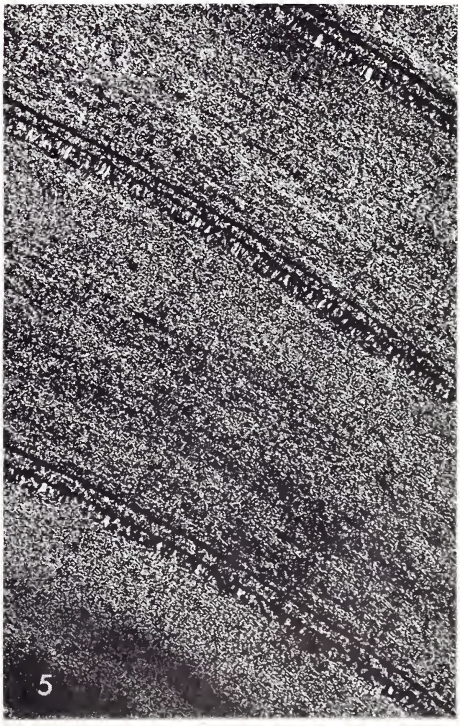

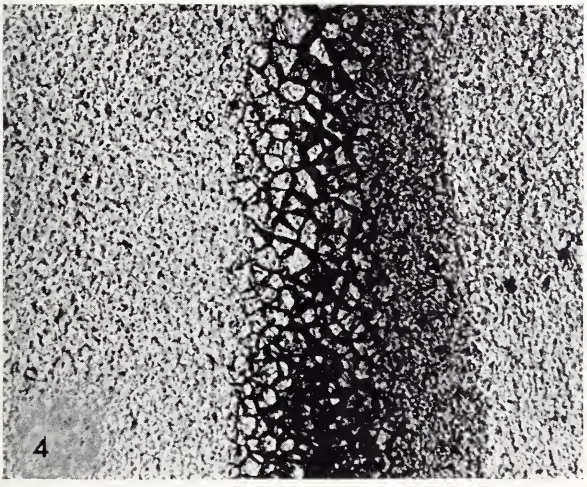

PLATE 11

FIG. 1. Radial section of *Margaritifera margaritifera* cut through a conchiolin sheet and an associated underlying thin prismatic layer. Part of the enclosing inner nacreous layer is seen at the top. The conchiolin shows traces of internal structure, and projects downwards as the inter-prismatic walls. × 3000.

FIG. 2. Replica of polished, EDTA-etched section of *Margaritifera margaritifera* showing one of the periostracum-like conchiolin bands developed in the inner nacreous layer (top left). A thin prismatic band underlies the conchiolin layer, which projects inwards as the interprismatic walls. × 8100.

FIG. 3. Replica of polished, etched (1% HCl) section of the prismatic layer of *Margaritifera margaritifera* showing the thick conchiolin wall (top left) and intracrystalline organic matrix within the aragonite. × 5100.

FIG. 4. Replica of polished, etched (EDTA) section of the contact between the composite prismatic layer (top) and the middle crossed-lamellar layer of *Codakia punctata*. × 5400.

FIG. 5. Tangential section of the contact between the composite prismatic layer and the underlying middle lenticular nacreous layer of *Nucula placentina*. The downward projections of the prisms are the trace of the marginal denticles. Acetate peel. × 100.

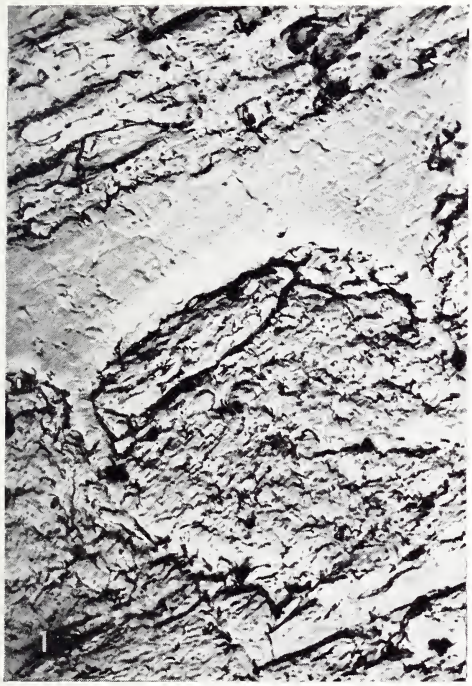
1


2

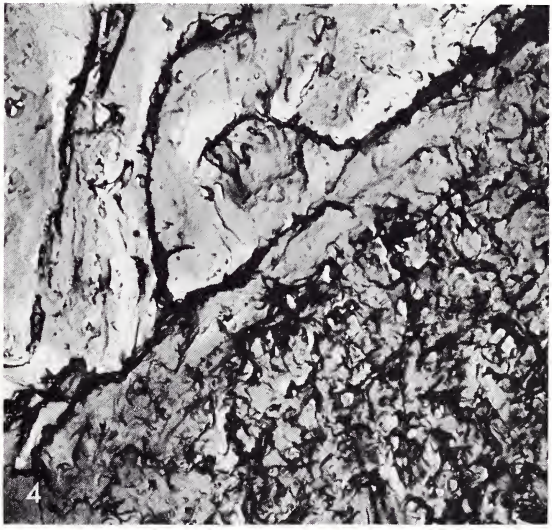
4

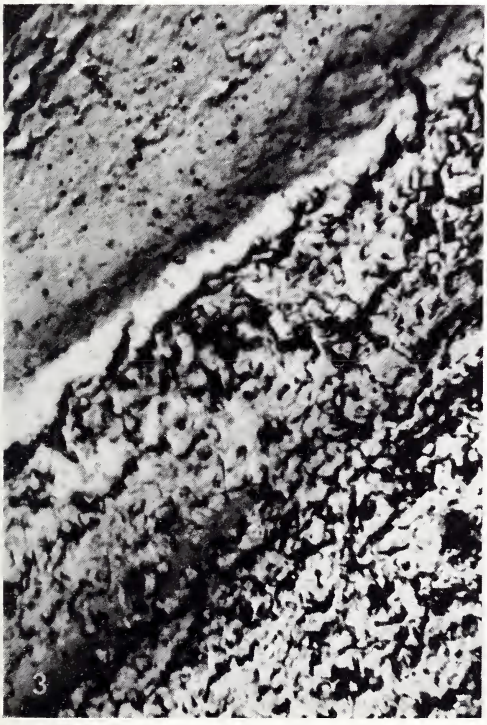
3

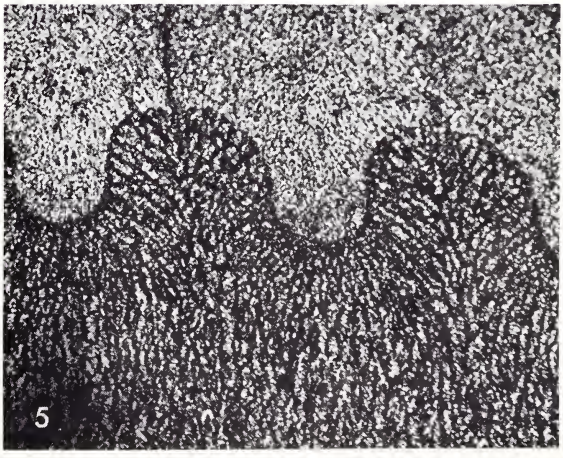
5

PLATE 12

FIG. 1. Scanning electron micrograph of the inner surface of the prismatic layer of *Soleyma australis* showing the thick interprismatic conchiolin walls, and the irregular plates of aragonite within them. × 500.

FIG. 2. Scanning electron micrograph of the inner surface of the prismatic layer of *Solemya australis* showing the irregular outlines of the prisms. × 200.

FIG. 3. Scanning electron micrograph of the contact between the outer prismatic layer and the inner homogeneous layer of *Solemya australis*. × 120.

FIG. 4. Scanning electron micrograph of a fractured section of the prismatic layer of *Solemya australis*. × 65.

FIG. 5. Acetate peel of an area of the inner surface of the prismatic layer of *Solemya australis*, in which the prism outlines are very regular. × 120.


1

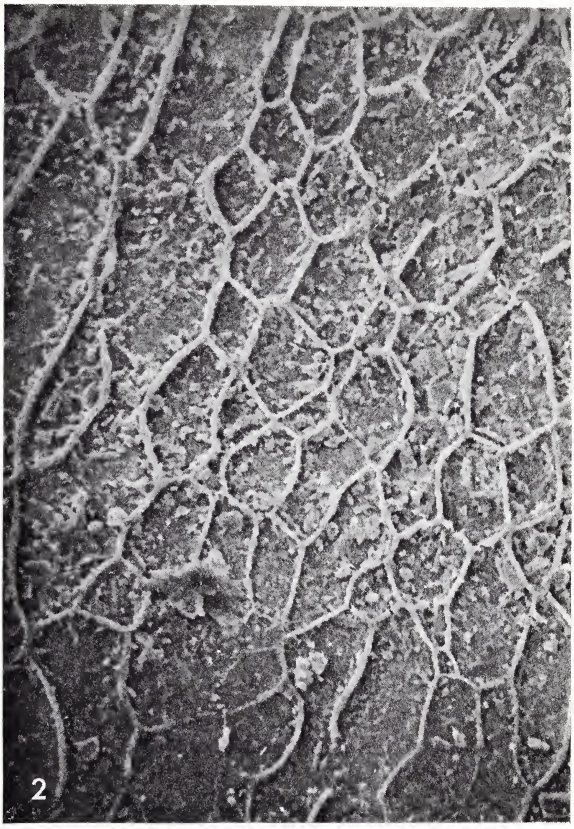
2


3

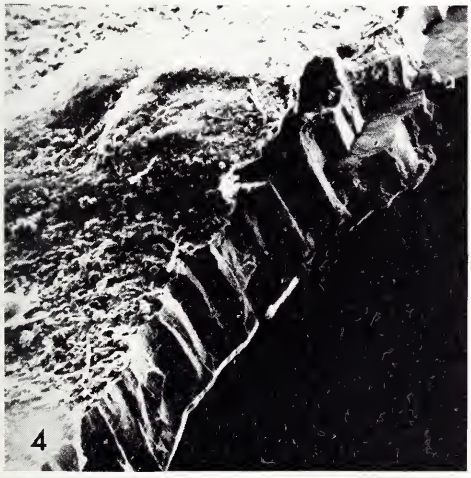
4

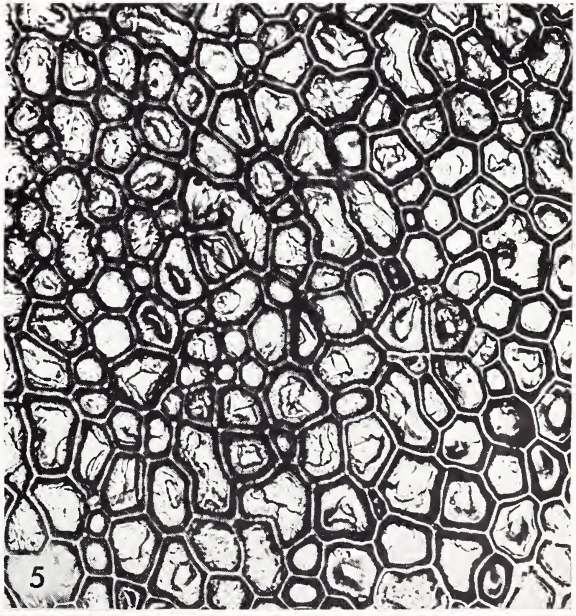
5

PLATE 13

All scanning electron micrographs.

FIG. 1. Periostracum and outer surface of the prismatic layer of *Neotrigonia margaritacea*, showing the polygonal shape of the prisms and the hemispherical cavity left beneath the periostracum indicating the site of the initial spherulite. × 410.

FIG. 2. Periostracum and outer surface of the prismatic layer of *Neotrigonia margaritacea*. Part of the periostracum is folded back, revealing the spaces which were occupied by initial seeds of the spherulites from which the prisms have developed. × 240.

FIG. 3. Outer surface of the periostracum of *Neotrigonia margaritacea* showing the perforations above the terminal bosses of the prsims in prismatic layer. × 240.

FIG. 4. Radial section through the outer, composite prismatic layer of *Codakia punctata* The small prism units are cut transversely, and each is surrounded by a sheath of organic matrix, while traces of intracrystalline organic matrix are also visible. Polished, EDTA-etched section. × 3600.

FIG. 5. Radial section of the outer, composite prismatic layer of *Codakia punctata* showing the small prism units cut longitudinally. Each is separated by a conspicuous sheet of organic matrix. Polished, EDTA-etched section. × 2900.


1

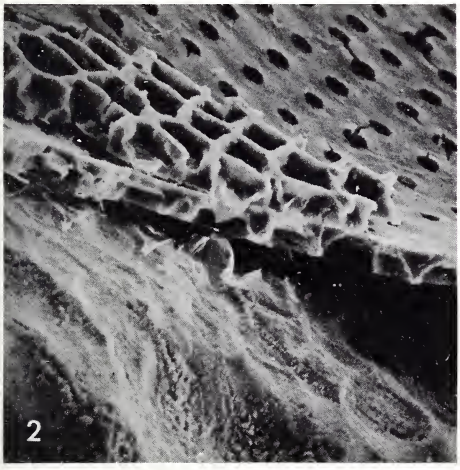
2

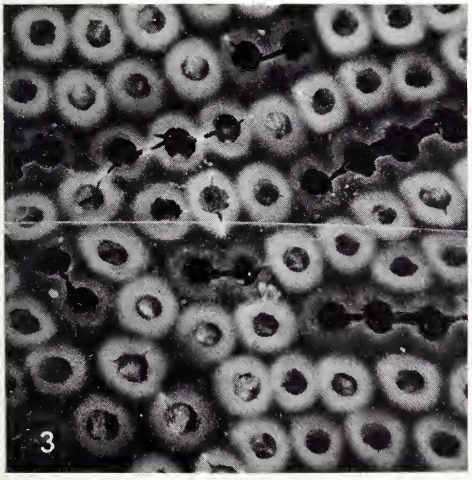
3


4

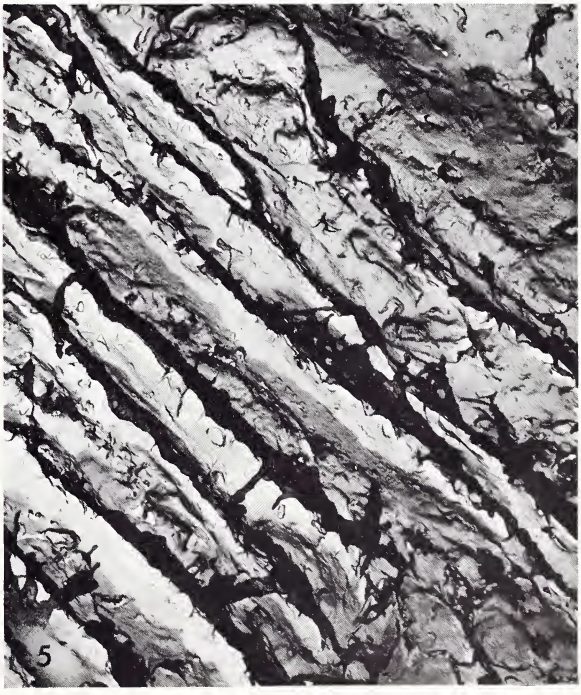
5

PLATE 14

FIG. 1. Radial section through the adductor myostracum of *Trigonocardita guanocostense*. The first order lamels of the crossed-lamellar layer are cut obliquely (top), and below this is the irregularly prismatic aragonitic adductor myostracum. Acetate peel. × 157.

FIG. 2. Contact between the prismatic adductor myostracum and the crossed-lamellar layer in *Spondylys nicobaricus*. Note the fine banding in the myostracum. × 100.

FIG. 3. Radial section through the umbonal region of *Hippopus hippopus* showing the contact between the crossed-lamellar layer and the complex crossed-lamellar layer. Note the regular banding of the complex crossed-lamellar layer. Acetate peel. × 25.

FIG. 4. Section of the crossed-lamellar layer of *Glycimeris glycimeris* showing several tubules cut obliquely. Acetate peel. × 157.

FIG. 5. Radial section of the crossed lamellar layer of *Hippopus hippopus*. Acetate peel. × 157.

FIG. 6. Radial section of *Spondylus calcifer* showing the crossed lamellar layer (bottom), the prismatic pallial myostracum, the foliated outer layer, and tubules. Acetate peel. × 100.

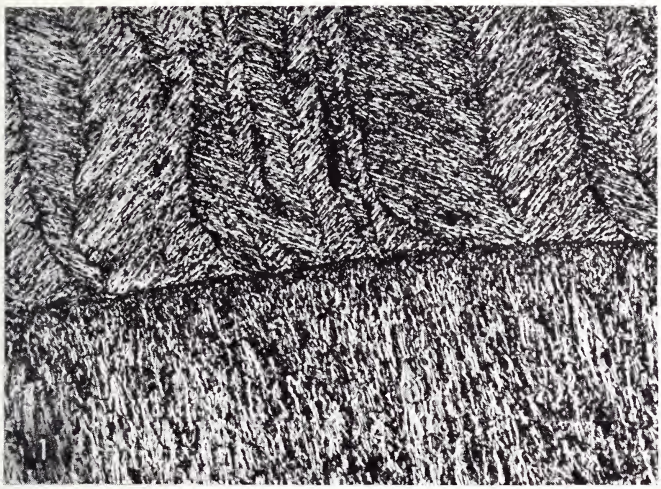
1


2

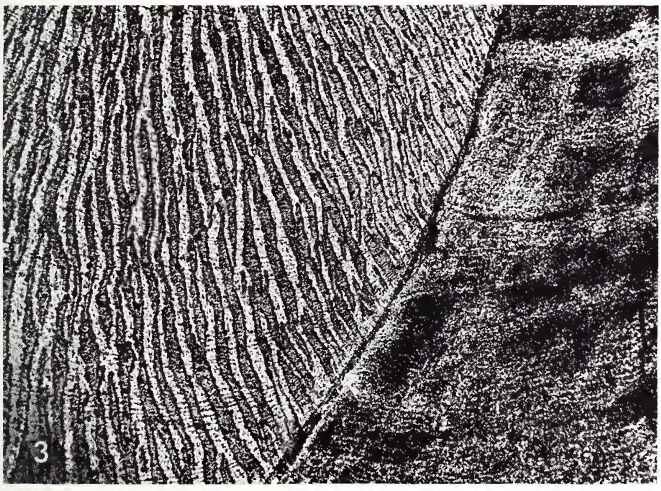
3

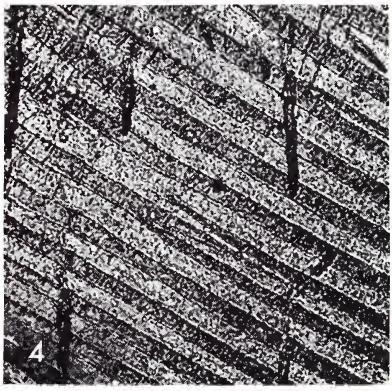
4


5

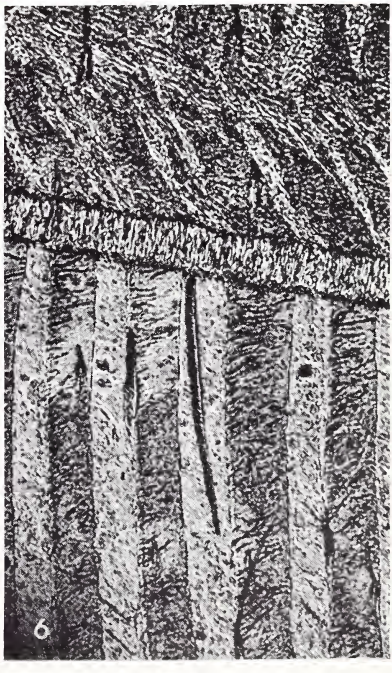
6

PLATE 15

FIG. 1. Radial section of the umbonal region of *Trisidos tortuosa* showing the characteristic divergence of the first order lamels in this region. Acetate peel. × 157.

FIG. 2. Radial section of the umbonal region of *Hippopus hippopus* showing the contact of the crossed-lamellar and complex crossed-lamellar layers. Acetate peel. × 100.

FIG. 3. Radial section of the crossed-lamellar structure of *Hippopus hippopus* showing the contact between adjacent first order lamels and the laths making up second order lamels, as seen in cross- and longitudinal section. The organic matrix separating the lamels is clearly seen in upper part of the picture. Polished, etched (1% HCl) section. × 12,000.

FIG. 4. Inset—detail of an area similar to that seen in figure 3, showing a fenestrate network of intercrystalline organic matrix on the surface of the laths building up the second order lamels. × 18,000.

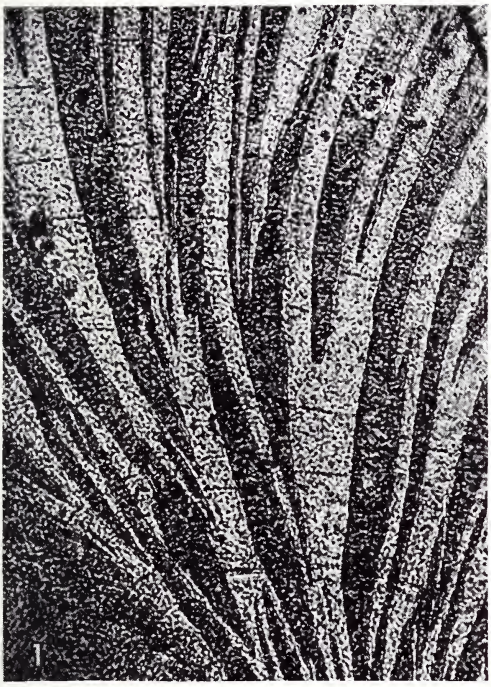
1

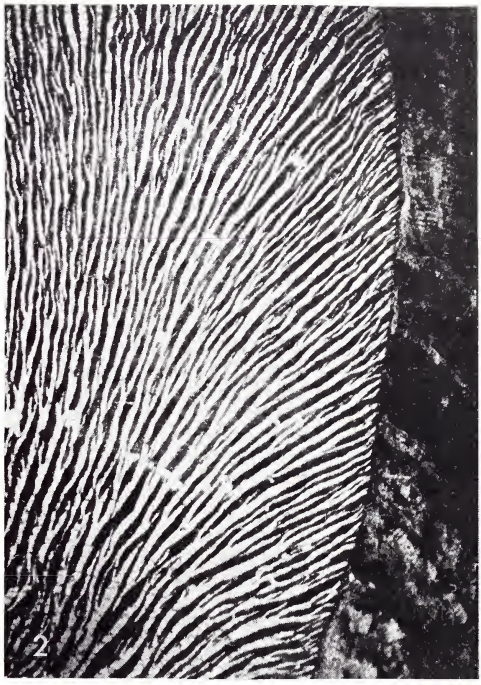
2

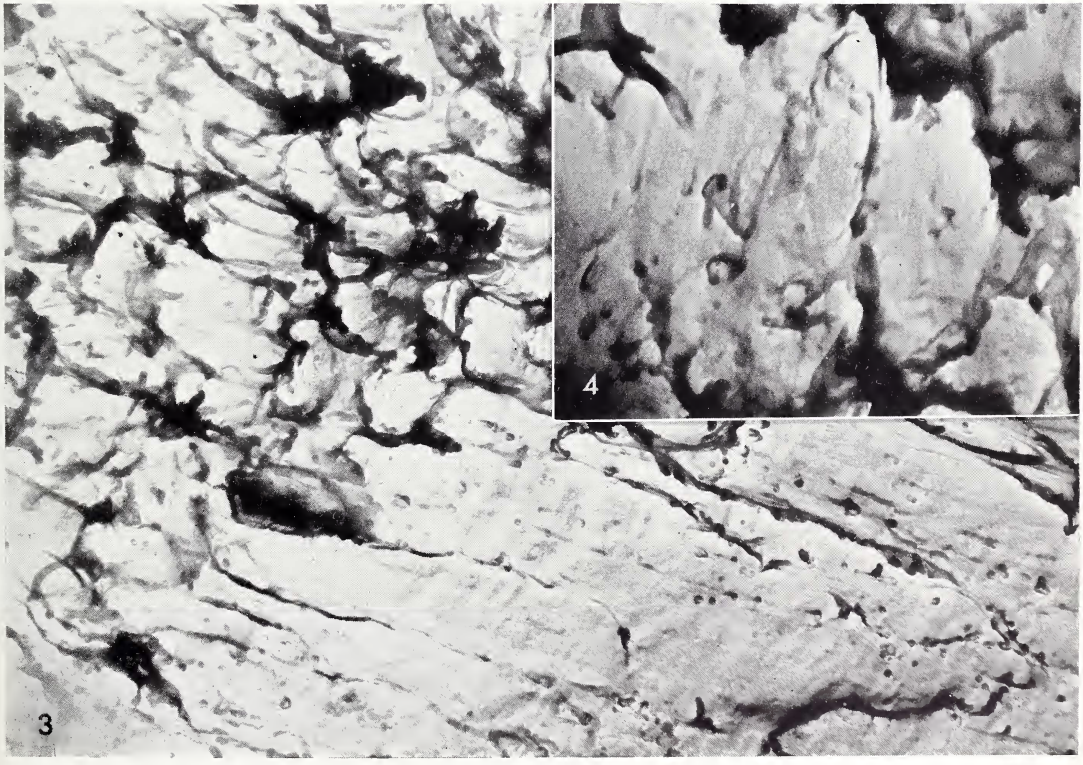
3
4

PLATE 16

FIG. 1. Replica of the inner surface of the crossed-lamellar layer of *Tridacna maxima* showing a change in the orientation and attitude of outcrop of second order lamels at the contact between adjacent first order lamels. × 7400.

FIG. 2. Replica of the inner surface of the crossed-lamellar layer of *Tridacna maxima* showing successively outcropping second order lamels, with irregular growth fronts. Each second order lamel is in turn made up of laths, joined together in side-to-side contact. × 5250.

FIG. 3. Radial section of the crossed-lamellar layer of *Hippopus hippopus* showing five adjacent first order lamels. The second order lamels making up the first order lamels have obviously differing orientations. The section through second order lamels is almost transverse to their length and thus exposes a greater area of the interlamellar and intercrystalline matrix (darker bands) than in other sections almost along their lengths. Replica of a polished, etched (1% HCl), radial section. × 3700.

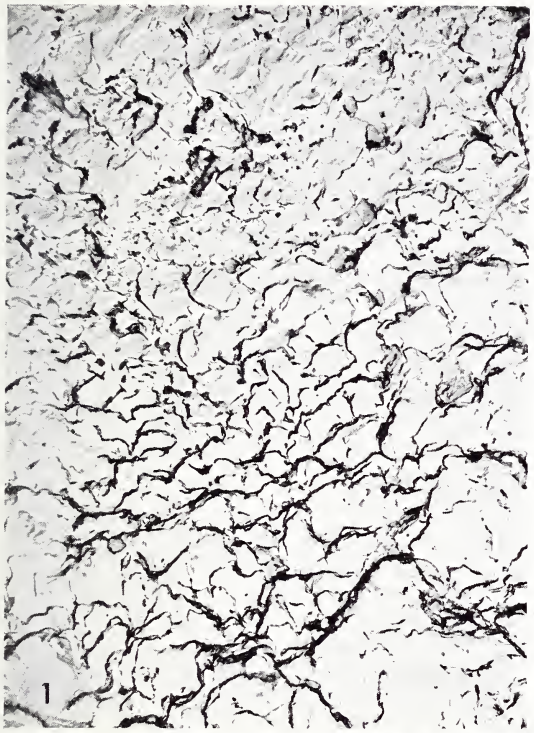
1

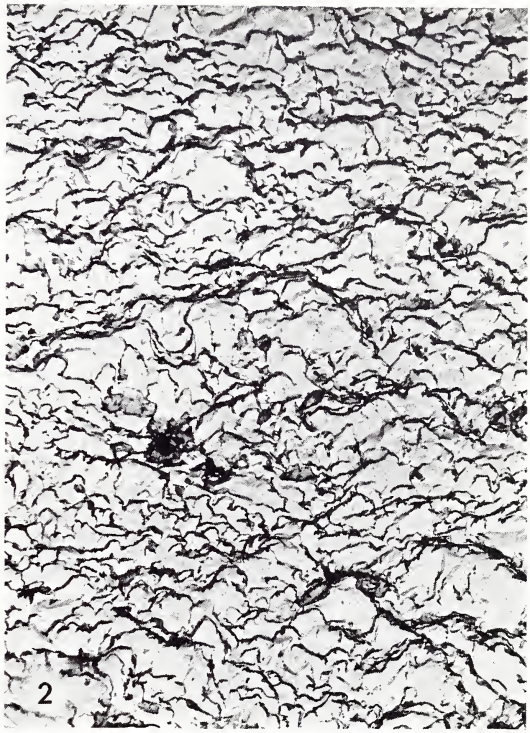
2

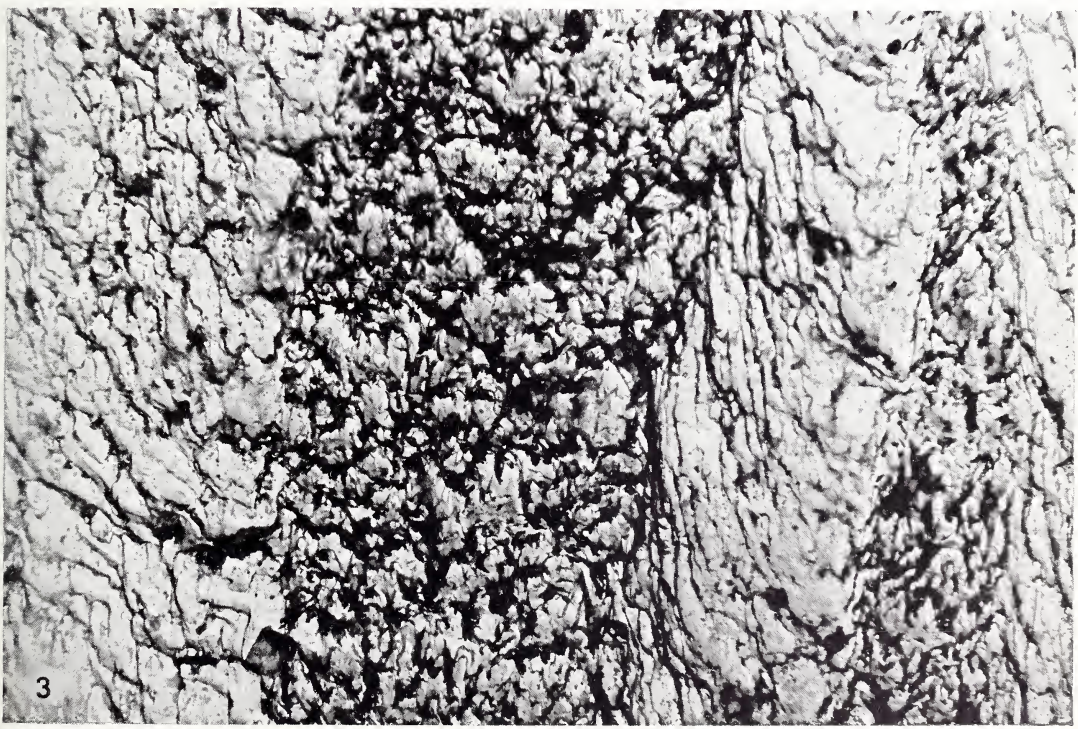
3

PLATE 17

FIG. 1. Replica of a polished, etched (1% HCl) radial section cut near the posterior adductor scar of *Trachycardium consors* showing crossed-lamellar structure and the boundary between adjacent first order lamels and the intersection of 2nd order lamels along this boundary. × 4500.

FIG. 2. Section showing the intersection of adjacent first order lamels in the crossed-lamellar layer of *Trachycardium consors*. Replica of a polished, EDTA-etched radial section. × 5250.

FIG. 3. Radial section of the crossed-lamellar layer of *Trachycardium consors*, showing three first order lamels with second order lamels inclined in opposite directions. Section polished and EDTA-etched. × 4500.

FIG. 4. Radial section of the crossed-lamellar layer of *Trachycardium consors* cut almost parallel to the second order lamels of one first order lamel. Polished, EDTA-etched. × 2200.

FIG. 5. Replica of the inner surface of the inner, complex crossed-lamellar layer of *Trisidos tortuosa*, showing the laths building up second order lamels. × 5000.


1

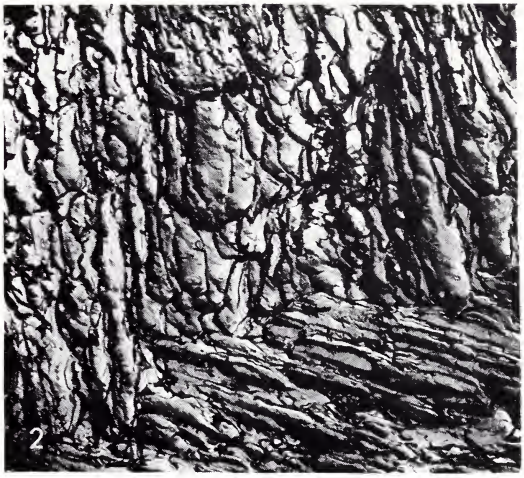
2

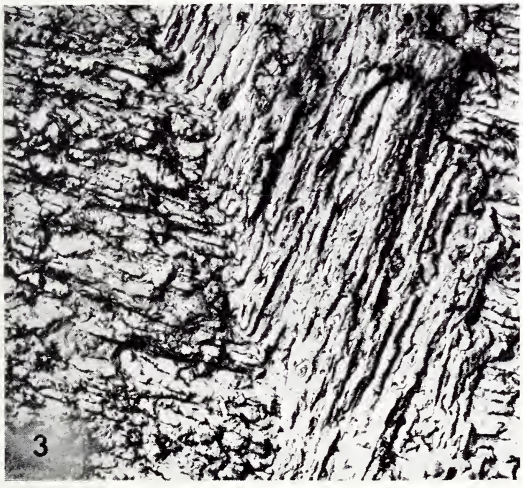
3

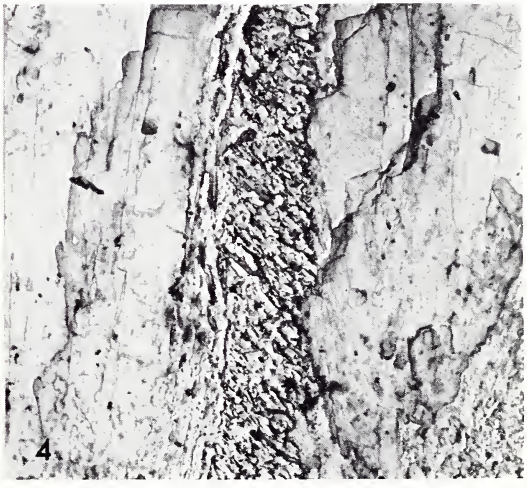
4

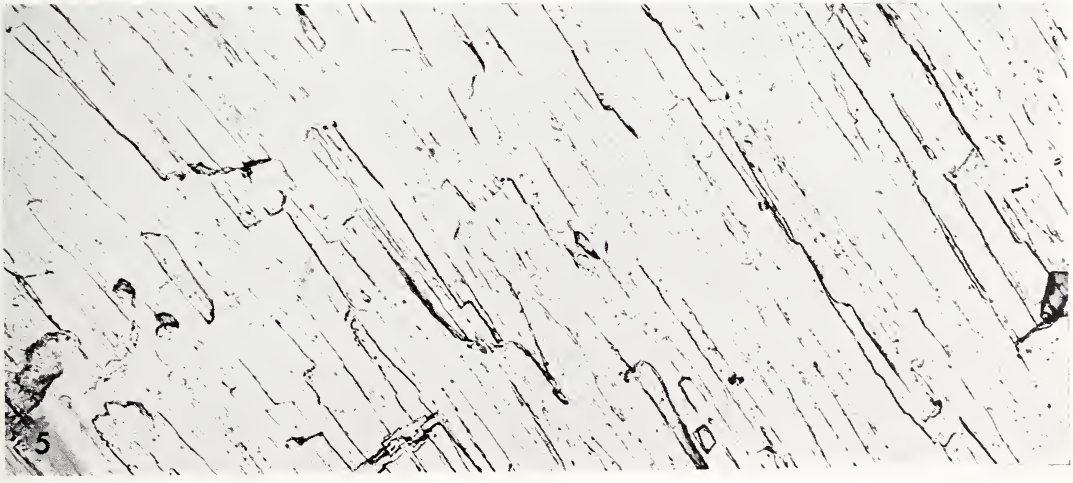
5

PLATE 18

FIG. 1. Fractured section of the outer crossed-lamellar layer of *Barbatia helblingi* showing first order lamels and constituent laths. × 1200.

FIG. 2. Fractured section of the inner 'homogeneous' layer of *Ensis siliqua* showing that it is in fact built of complex crossed-lamellar structure with sheets of myostracal prisms. × 800.

FIG. 3. Fractured section of the outer crossed-lamellar layer of *Chama macerophylla*. × 450.

FIG. 4. Etched section of the crossed-lamellar layer of *Scutarcopagia scobinata* showing organic matrix strands surrounding the constituent laths of the structure. × 1800.

All figures are scanning electronmicrographs.


1


2


3


4

PLATE 19

FIG. 1. Radial section of the inner complex crossed-lamellar layer of *Polymesoda anomalata*. Acetate peel. × 100.

FIG. 2. Radial section of the inner complex crossed-lamellar layer of *Glycimeris glycimeris* showing the arrangement of second order lamels into broad columns, and tubules. Acetate peel. × 80.

FIG. 3. Radial section of *Anadara antiquata* showing the contact between the crossed-lamellar outer layer (top) and the complex crossed-lamellar inner layer. Note the difference in orientation of the block of second order lamels in the complex crossed-lamellar layer, and the prominent tubles. Acetate peel. × 100.

FIG. 4. Tangenital section of *Anadara antiquata* showing the contact between the crossed-lamellar layer (top right) and the complex crossed-lamellar layer. Note that although the section is at right angles to that shown in fig. 3, the structure is similar. A few tubules are visible. Acetate peel. × 80.

FIG. 5. Radial section of *Anadara grandis* showing the inner complex crossed-lamellar layer and tubules. Acetate peel. × 100.

FIG. 6. Tangenital section of the inner complex crossed-lamellar layer of *Glycimeris glycimeris*. Note the banding and tubules. Acetate peel. × 100.

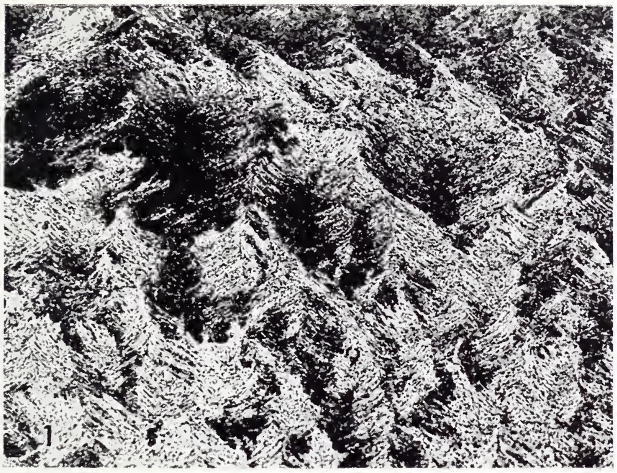
1

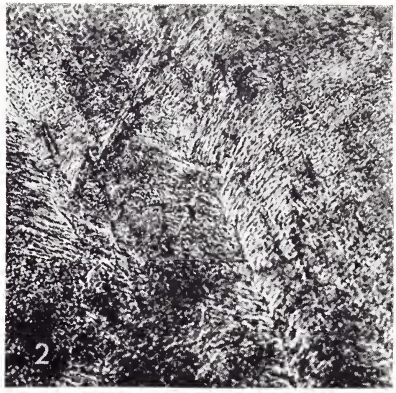
2

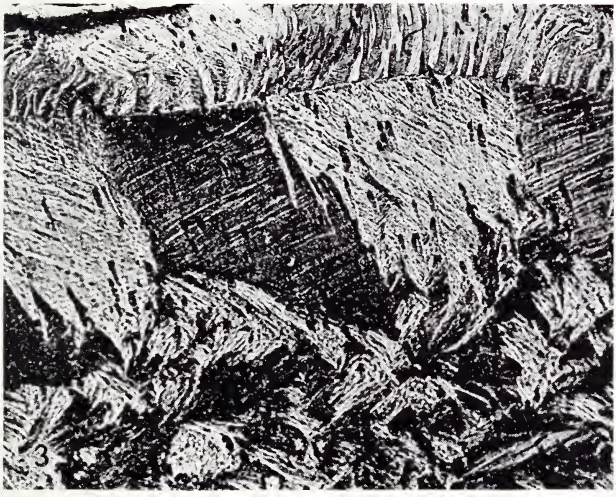
3

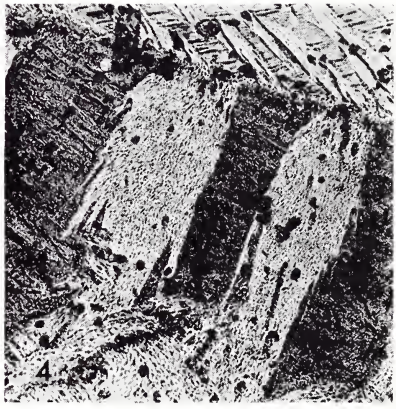
4

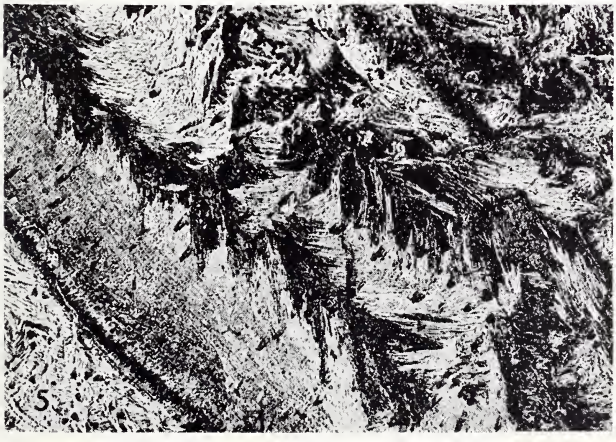
5

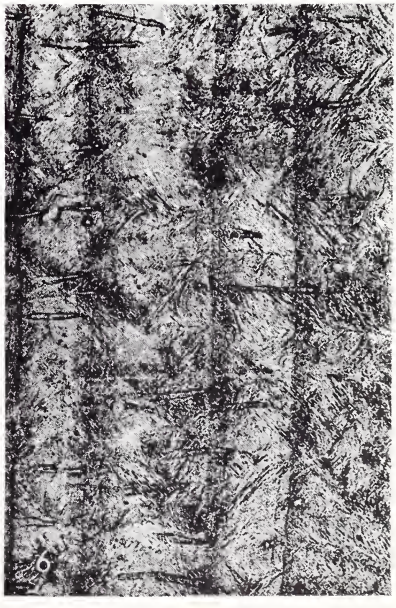
6

PLATE 20

FIG. 1. Replica of the inner surface of the type of inner complex crossed-lamellar structure found in *Stavelia horrida* showing the outcrop of laths with different orientations in adjacent blocks. Dark filamentous structures are replicas of tubules. × 3000.

FIG. 2. Replica of the inner surface of the complex crossed-lamellar layer of *Stavelia horrida* showing details of laths in side to side contact. × 10,500.

FIG. 3. Radial section of *Cyclinella saccata* showing the contact between the outer crossed-lamellar layer (top left) and the inner complex crossed-lamellar layer. A thin prismatic pallial myostracum separates the two layers, and several sheets of myostracal-type prisms are present within the complex crossed-lamellar layer. Acetate peel. × 100.

FIG. 4. Radial section of the complex crossed-lamellar layer, with prismatic bands, in *Cyclinella saccata*. Acetate peel. × 100.

FIG. 5. Radial section of *Stavelia horrida* showing the inner complex crossed-lamellar layer and the middle nacreous layer. Note the interdigitating contact between the layers. Acetate peel. × 100.

FIG. 6. Radial section of the inner complex crossed-lamellar layer of *Polymesoda anomalata*. Acetate peel. × 100.


1


2

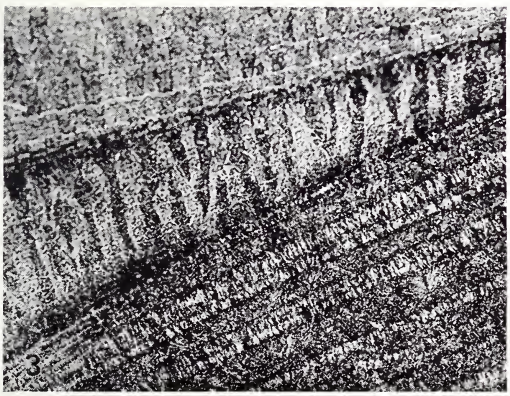
3

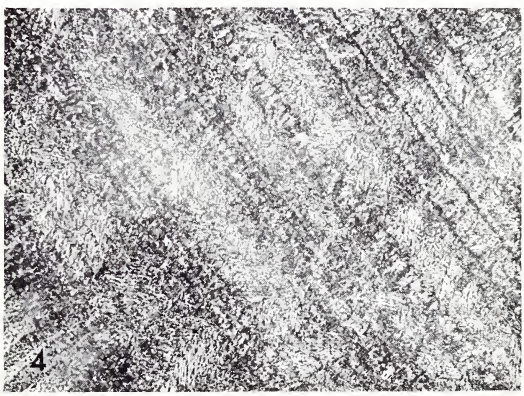
4

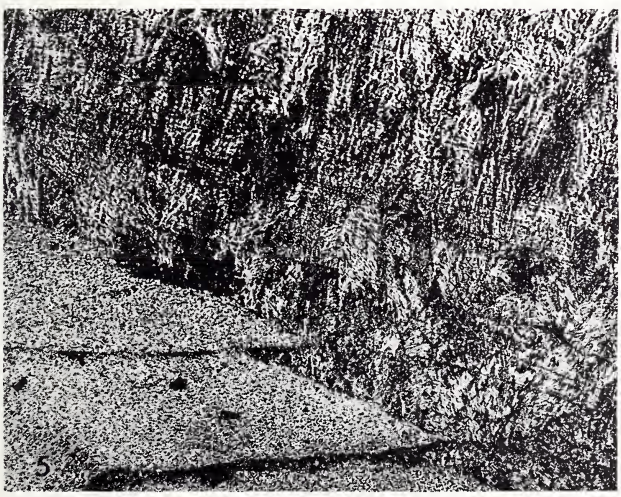
5


6

PLATE 21

FIG. 1. Inner surface of the inner complex crossed-lamellar layer of *Caryocorbula amethystina* showing the several orientations of groups of laths. Scanning electron micrograph. × 1160.

FIG. 2 Scanning electron-micrograph of a fractured section of the inner, complex crossed-lamellar layer of *Pholas dactylus*. × 600.

FIG. 3. Radial section of the complex crossed-lamellar layer of *Codakia punctata*. Polished, EDTA-etched section. × 3600.

FIG. 4. Inner surface of the complex crossed-lamellar layer of *Anadara antiquata* showing the euhedral lath terminations of the laths which build up the second order lamels. × 14,400.

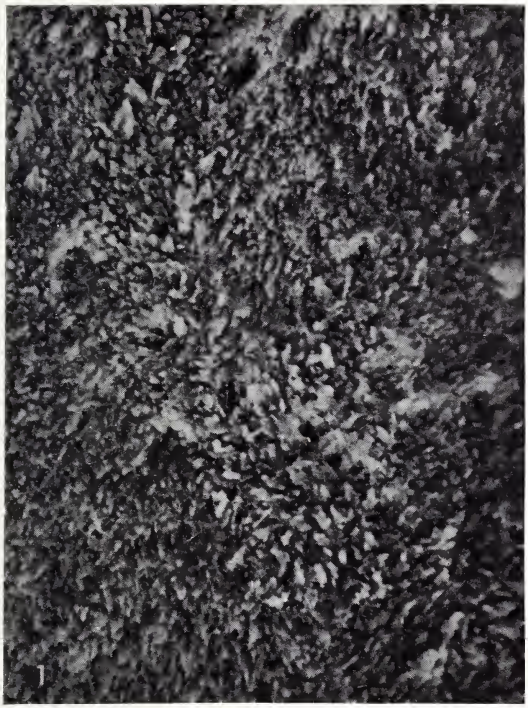
1

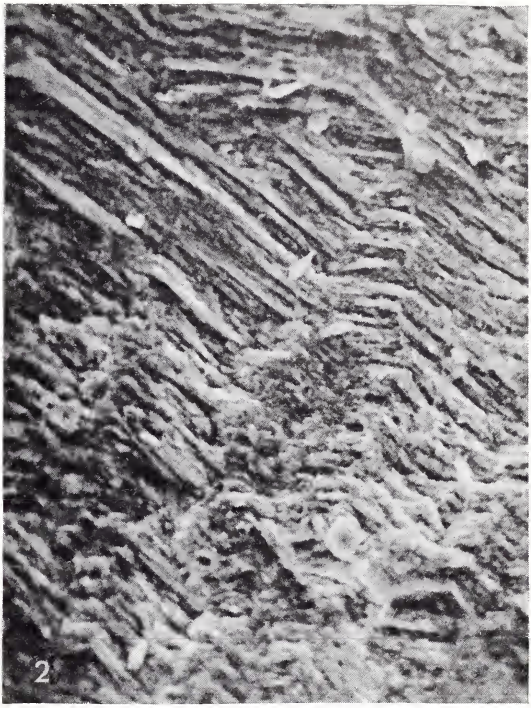
2


3

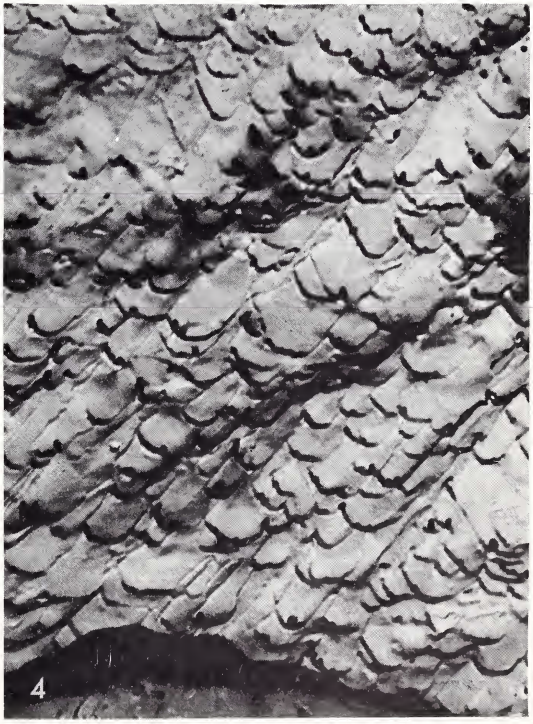
4

PLATE 22

FIG. 1. Replica of the surface of the inner, complex crossed-lamellar layer of *Anadara antiquata* showing the laths making up the second order lamels arranged in ridges ; the ventral margin of the shell is towards bottom right of the page. × 4500.

FIG. 2. Inner surface of the complex crossed-lamellar layer of *Barbatia fusca* showing the longitudinal ridges corresponding to those seen in fig. 1 on the surface of the blocks of second order lamels. Note the openings of several tubules. Scanning electron micrograph. × 500.

FIG. 3. Radial section of the complex crossed-lamellar layer of *Codakia punctata* showing the contact between the blocks of second order lamels building up the layer. Section polished and EDTA-etched. × 3600.

FIG. 4. Inner surface of the complex crossed-lamellar layer of *Modiolus auriculatus*. Note that this picture is taken at higher magnification than other figures of this structure, reflecting the minute size of the units in this species. × 20,000.

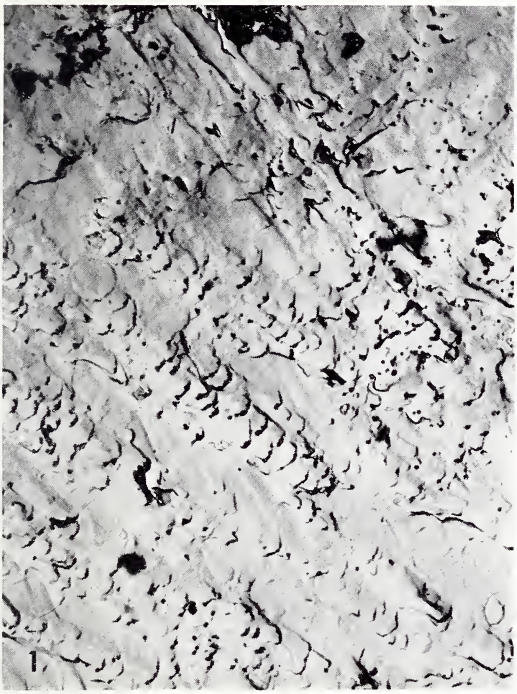
1


2

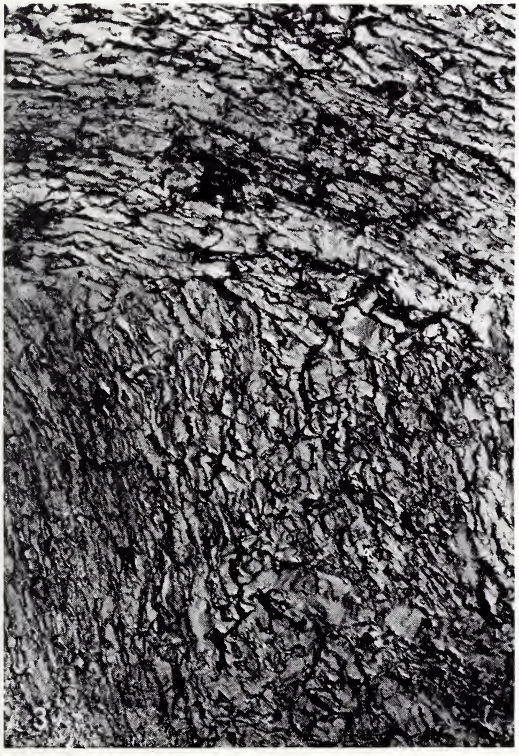

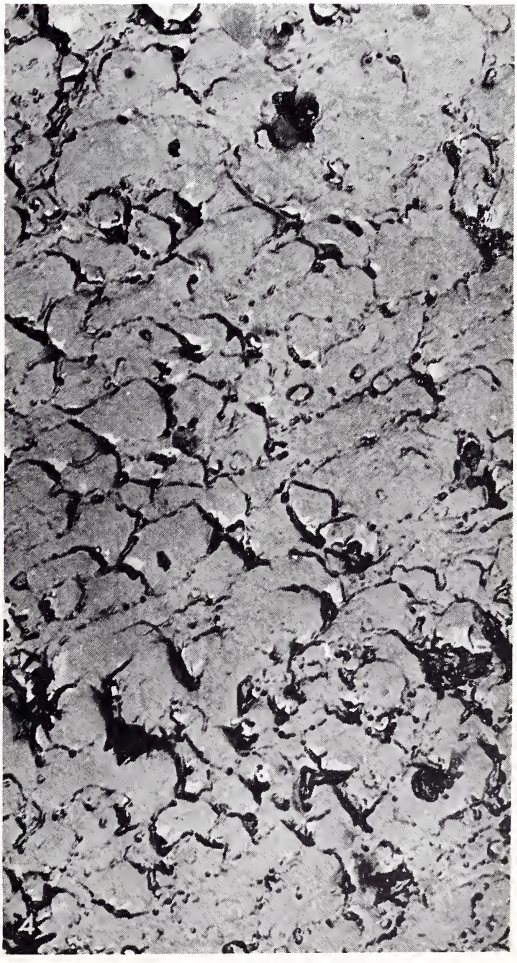
4

PLATE 23

FIG. 1. Radial section of the inner homogeneous layer of *Arctica islandica ;* note the banding, and the arrangement of granules into horizontal sheets and vertical rows. Thin section. × 40.

FIG. 2. Radial section of the umbonal region of *Arctica islandica* showing the homogeneous structure, with details as above. Thin section. × 40.

FIG. 3. Fractured section of the umbonal region of *Arctica islandica* showing the granular nature of the homogeneous structure and rhomboidal arrangement of the granules. × 1800.

FIG. 4. Radial section of the inner homogeneous layer of *Nuculana oblongoides.* Note the banding. Acetate peel. × 100.


1


2


3


4

PLATE 24

FIG. 1. Inner surface of the inner homogeneous layer of *Arctica islandica* showing the obscure arrangement of the aragonite granules in sheets (lower left) and the associated organic matrix envelopes. × 10,000.

FIG. 2. Scanning electron micrograph of the inner surface of the homogeneous tube of *Clavagella* sp., showing the irregular, flattened granules building the structure. × 5500.

FIG. 3. Inner surface of the inner homogeneous layer of *Thracia phaseolina*. Scanning electron micrograph. × 6500.

FIG. 4. Radial section of the inner, homogeneous layer of *Arctica islandica*, polished and EDTA-etched, showing the organic matrix around the aragonite granules and indications of organic matrix within these granules. × 9000.


1

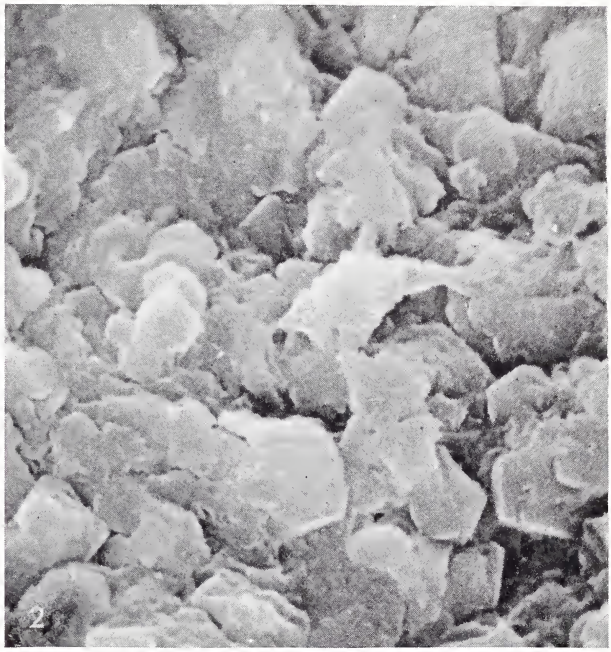
2

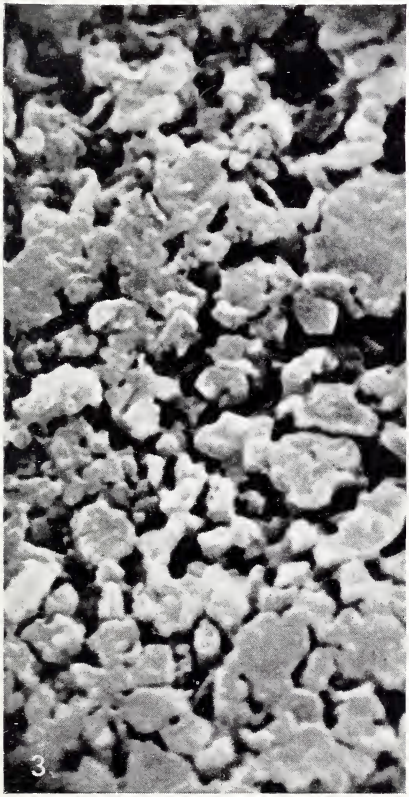
3


4

PLATE 25

FIG. 1. Radial section of *Chama nubea* showing pillars of myostracal prisms, within the complex crossed-lamellar layer, outcropping as bosses on the inner surface of the shell. Note the fine banding in the pillars. Acetate peel. × 100.

FIG. 2. Radial section of *Modiolus modiolus* showing the alternation of sheets of myostracal prisms and nacre. Acetate peel. × 100.

FIG. 3. Planar section through the adductor myostracum of *Chama lazarus* showing the highly irregular outlines of the prisms. Acetate peel. × 125.

FIG. 4. Radial section of *Pecten maximus* showing the trace of the prismatic adductor myostracum. Acetate peel. × 100.

FIG. 5. Radial section of *Chama iostoma* showing the myostracal pillars in the inner complex crossed-lamellar layer. Acetate peel. × 100.


1

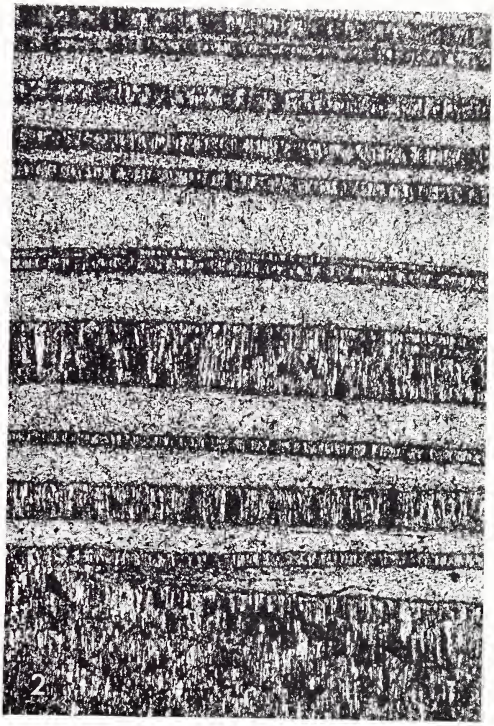
2

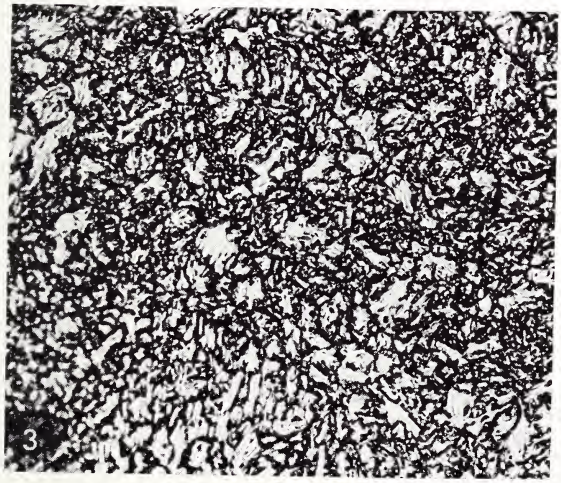
3

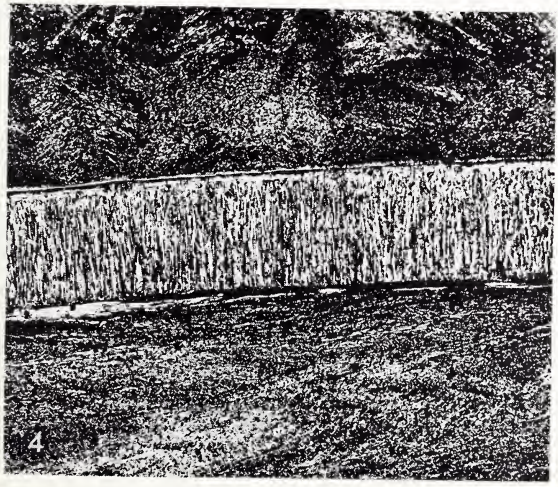
4

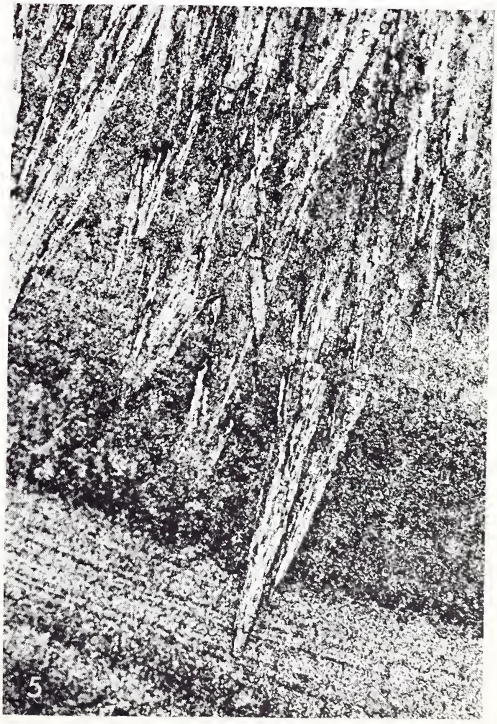
5

PLATE 26

FIG. 1. Slightly oblique radial section through the adductor myostracum of *Trachycardium consors*. Irregular prisms of aragonite are surrounded by a sheath of organic matrix. Replica of polished, etched (1% HCl) section. × 5400.

FIG. 2. Replica of a radial section of the adductor myostracum in *Trachycardium consors*. × 4500.

FIG. 3. Radial section of *Trachycardium consors* showing the prismatic pallial myostracum separating the complex crossed-lamellar layer (above) and the crossed-lamellar below. Replica of polished, EDTA-etched section. × 3000.

FIG. 4. Radial section of *Trachycardium consors* cut through the contact between the crossed-lamellar layer (bottom) and the prismatic adductor myostracum. Negative print of replica of polished EDTA-etched section. × 3600.

FIG. 5. Scanning electron micrograph of the inner surface of the marginal region of *Nucula sulcata*, showing the marginal denticles, the periostracum (lower) and the dimpled inner surface of the composite prismatic layer. × 300.


1

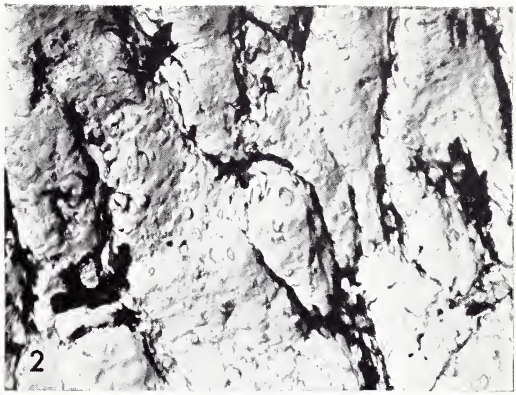
2

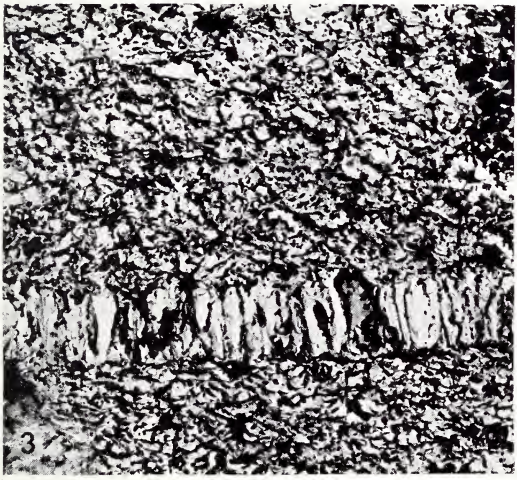
3


4

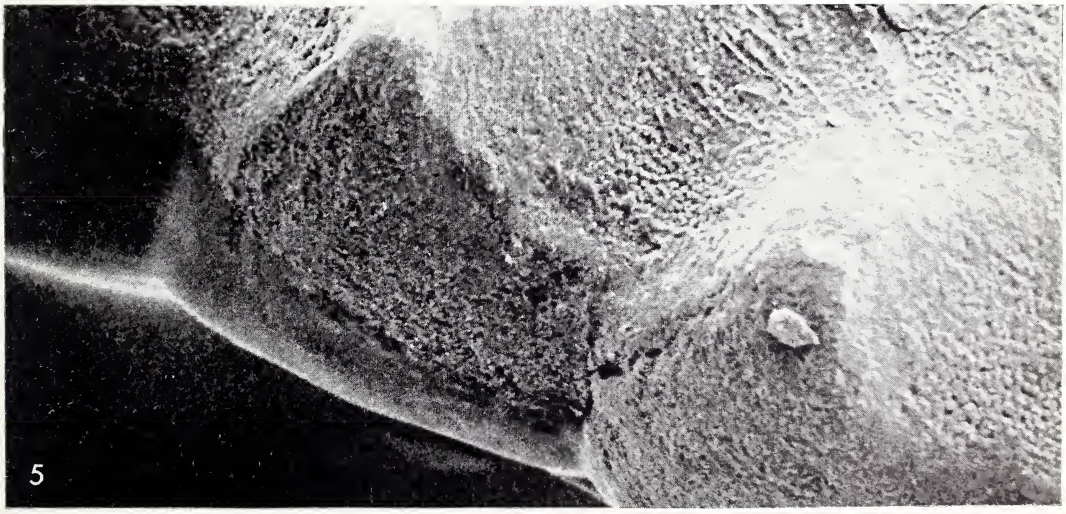
5

PLATE 27

FIG. 1. Replica of the inner surface of the adductor myostracum of *Arctica islandica* showing the irregular shape and surface structure of the myostracal prisms and the thin sheath of organic matrix surrounding them. Note parallelism of structure within 'cells' and the 'ring-like' conchiolin processes. × 5000.

FIG. 2. Replica of the inner surface of the adductor myostracum of *Ostrea irridescens* showing the irregular outline and surface structure of the myostracal prisms and the sheath of intercrystalline organic matrix surrounding each prism. × 5000.

FIG. 3. Replica of the surface of the adductor myostracum of *Arctica islandica* showing details of the intercrystalline organic matrix and surface structure of the myostracal prisms. × 25,000.

FIG. 4. Replica of the surface of the adductor myostracum of a gerontic specimen of *Ostrea hyotis* showing the granular surface, penetrated by 'filaments'. It is uncertain whether these projecting filaments are actual structures or replicas of the inside of tubular perforations in the shell. × 11,760.

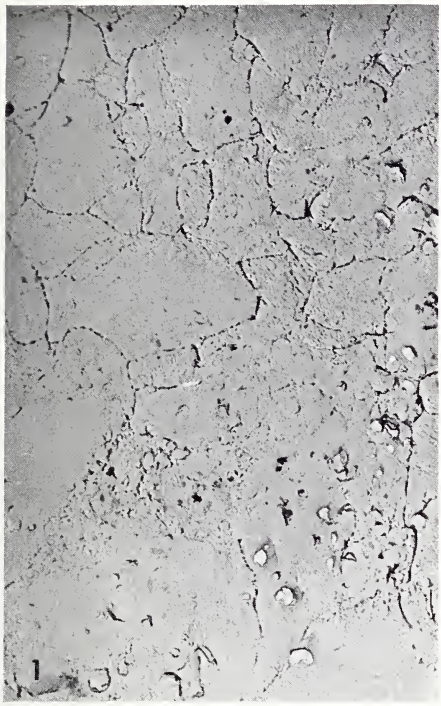
1

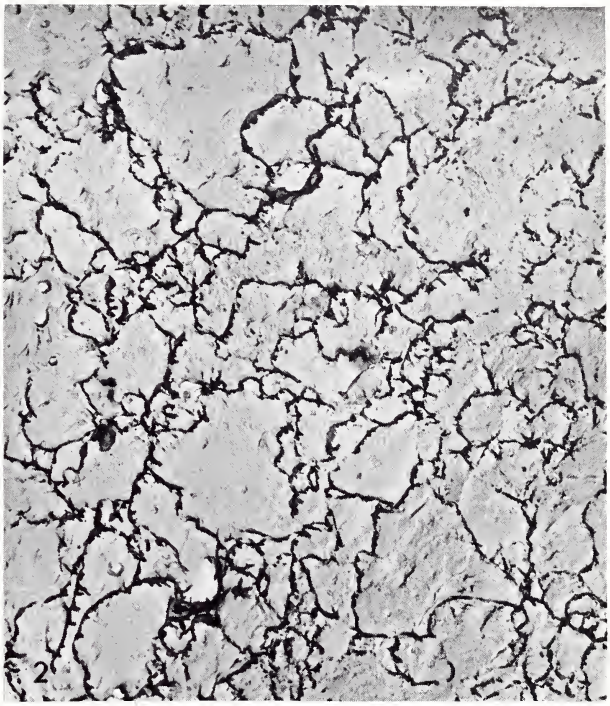
2


3

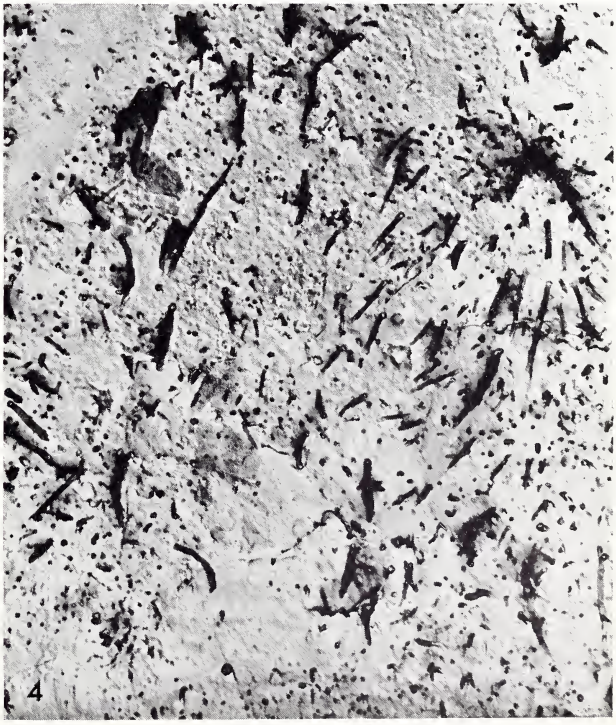
4

PLATE 28

FIG. 1. Scanning electron micrograph of the inner ligament or resilium of *Chlamys senatoria* the valves having been removed. The fibrous calcified layer is uppermost, with organic lamellar layer beneath. Note the banding. × 16.

FIG. 2. Part of the calcified area seen in fig. 1 at a higher magnification, showing the outcrop of fibres of aragonite. Scanning electron micrograph. × 30.

FIG. 3. Radial section of the calcified layer of the inner ligament or resilium of *Chlamys senatoria* showing the fibrous nature and the conspicuous banding. Acetate peel. × 160.

FIG. 4. Scanning electron micrograph of a fractured surface of a ' chalky layer ' in *Ostrea edulis*. × 350.

FIG. 5. Scanning electron micrograph of a fractured section of a ' chalky layer ' in *Ostrea edulis*. × 800.


1

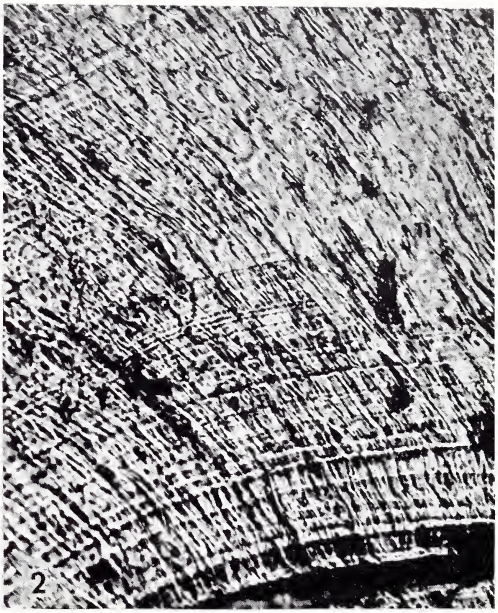
2


3

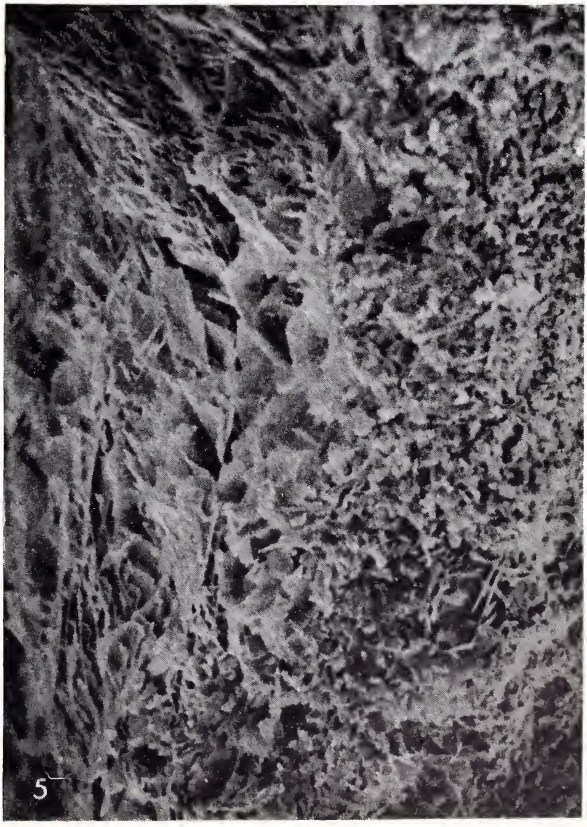
5


4

PLATE 29

FIG. 1. Radial section of *Arca avellana* showing the high density of tubules. Thin section. × 100.

FIG. 2. Radial section of the complex crossed-lamellar layer of *Scapharca subcrenata* showing oblique sections through tubules. Acetate peel. × 160.

FIG. 3. Inner surface of the inner complex crossed-lamellar layer of *Barbatia fusca* showing the density and irregular distribution of tubules. Scanning electron micrograph. × 200.

FIG. 4. Scanning electron-micrograph of a fractured section of *Barbatia fusca* showing a tubule passing through the crossed-lamellar layer. Notice the sharp terminations of laths against the side of the tubule. × 1600.

FIG. 5. Enlargement of the above. × 8000.


1

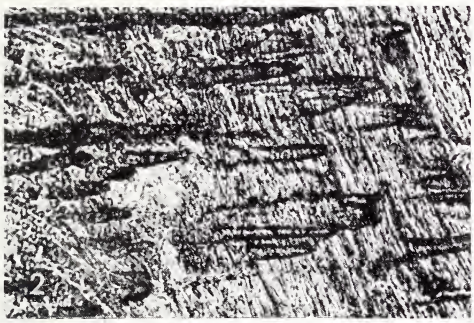
2


3

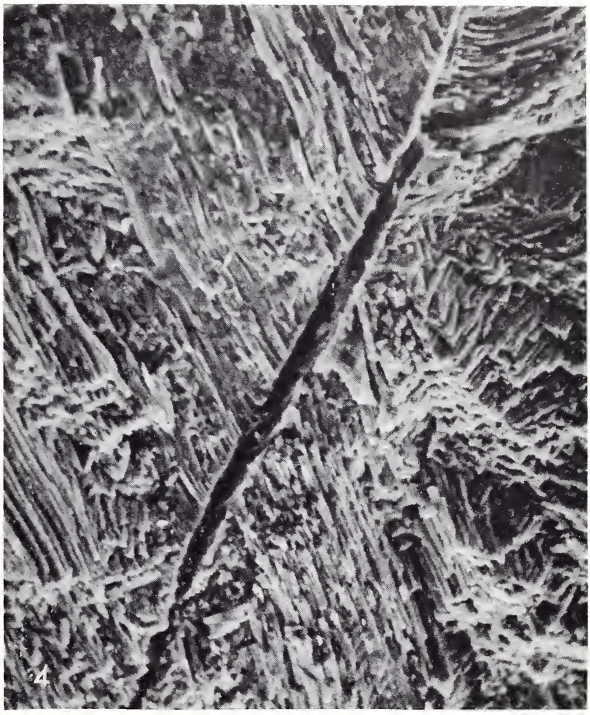
4


5